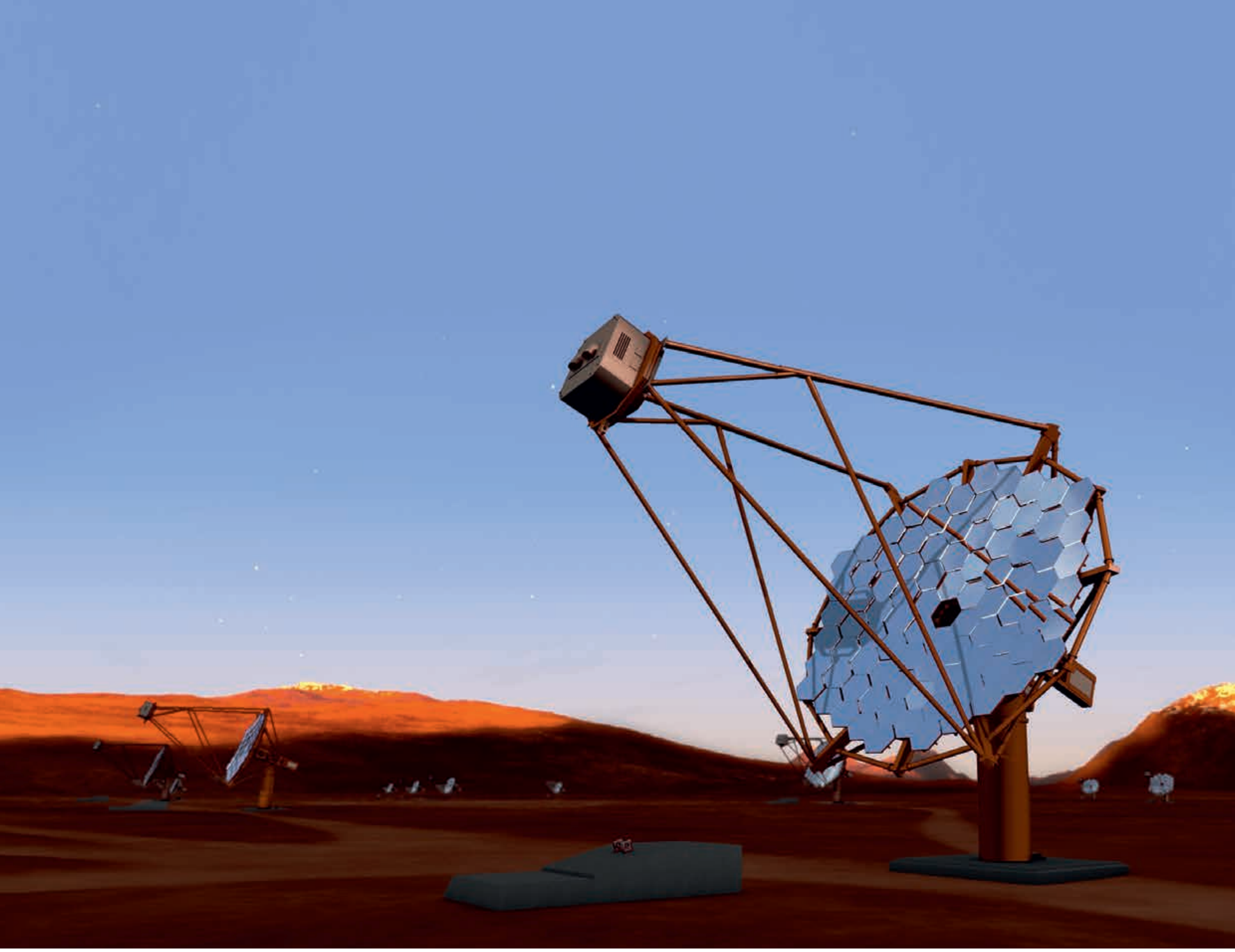

PARTICLE PHYSICS 2013.

Highlights and Annual Report

Accelerators | Photon Science | Particle Physics

Deutsches Elektronen-Synchrotron
A Research Centre of the Helmholtz Association

Cover

A possible design of CTA, the Cherenkov Telescope Array.
(Credit: G. Pérez, IAC)

PARTICLE PHYSICS 2013.

Highlights and
Annual Report

Contents

The year 2013 at DESY.

Chairman's foreword

2013 was very busy for DESY. In the last years, DESY has most successfully brought about many new projects, such as the European XFEL X-ray laser, the new FLASH II free-electron laser facility and the extensions of the experimental hall of the PETRA III synchrotron radiation source. In parallel to the development of new user facilities, new research centres are being established at DESY that exploit the unique properties of the DESY light sources, such as the interdisciplinary Centre for Structural Systems Biology (CSSB). All these projects are now under construction, shaping the current picture of the DESY campus.

The construction of the European XFEL X-ray free-electron laser is DESY's top-priority endeavour. DESY contributes significant resources to this international prestige project. The superconducting niobium cavities devised by DESY are at the heart of the facility, and the successful implementation of their industrial series production once again underlines DESY's competence in accelerator R&D. Cavity performance tests at DESY proved that the required technical specifications were met or even exceeded, which is also an interesting technological achievement for future linear accelerator and collider projects. The European XFEL will emit first laser light in 2016.

2013 was also a very successful year in particle and astroparticle physics. The clear highlight of the year was the discovery of the first high-energy extragalactic neutrinos by the IceCube neutrino telescope at the South Pole. The much-acclaimed discovery is a marvellous success in neutrino astrophysics, celebrated worldwide as a scientific breakthrough of the year 2013. DESY is a very visible partner in the IceCube consortium and very

DESY's expertise is essential to the IceCube neutrino telescope at the South Pole, whose discovery of extragalactic neutrinos was selected by *Physics World* as breakthrough of the year 2013.

The underground construction for the European XFEL X-ray laser was completed in June 2013. From left to right: Helmut Dosch (DESY), Stephan Hebgen (ARGE Tunnel XFEL), Dorothee Stapelfeldt (Senator for Science Hamburg), Christian Scherf (DESY), Beatrix Vierkorn-Rudolph (Head of the Directorate for Large Facilities and Basic Research, BMBF), Claudia Burger (European XFEL) and Massimo Altarelli (European XFEL).

proud of this scientific achievement. In the field of gamma astronomy, DESY is currently devoting considerable efforts to get the new Cherenkov Telescope Array (CTA) up and running, an international gamma-ray observatory that will provide novel insights into the depth of the non-thermal high-energy universe. High-energy gamma radiation is produced during cosmic events of tremendous violence, such as supernova explosions. This new observatory will enable the investigation of largely unexplored energy ranges from 100 GeV to some 10 TeV with unprecedented sensitivity. Focusing the scientific programme of DESY in Zeuthen on this large-scale international project bears fruits in the potential privilege to host the CTA headquarters.

The Nobel Committee awarded the 2013 Nobel Prize in Physics to François Englert and Peter Higgs for their theory explaining the mass of elementary particles. In the prize announcement, the ATLAS and CMS experiments at the Large Hadron Collider (LHC) at CERN near Geneva, Switzerland, were explicitly mentioned for their significant contributions to the understanding of the origin of mass and in particular for their discovery of the Higgs boson. DESY was involved at several points in this discovery, among others with several junior research groups. Right now, preparations are under way also at DESY for the restart of LHC operation in spring 2015. Moreover, DESY is currently preparing components for installation in the coming years and in particular during the next long LHC shutdown in 2018. In parallel, several DESY groups are carrying out intensive R&D work for major upgrades of the detectors for the high-luminosity phase of the LHC.

Along with other Helmholtz centres within the research field “Structure of Matter”, DESY has been very busy in 2013 formulating its research plans for the upcoming Helmholtz funding period 2015-2019, which will enable DESY to continue all its ambitious activities. I am confident that we will convince the international reviewers of the outstanding quality of our programme.

Helmut Dosch
Chairman of the DESY Board of Directors

Particle and astroparticle physics at DESY.

Introduction

The year 2013 was remarkably eventful for particle and astroparticle physics at DESY. The new particle discovered in 2012 at CERN's Large Hadron Collider (LHC) was identified as a Higgs boson, and consequently the fathers of the Higgs mechanism, Francois Englert and Peter Higgs, were awarded the 2013 Nobel Prize in Physics. Other projects in particle physics, like the planned International Linear Collider (ILC) or the Belle II experiment at the SuperKEKB collider in Japan, reached major milestones and received considerable attention. In astroparticle physics, the confirmation of extragalactic neutrinos, as discovered by the IceCube neutrino telescope at the South Pole, presented a major achievement. In parallel to all the work leading up to these physics successes, DESY has been preparing for the next five-year funding period of the Helmholtz Association, which will start in 2015.

Francois Englert and Peter Higgs, Nobel laureates in physics 2013, together with the Swedish Royal family during the prize ceremony (Courtesy: © Nobel Media AB 2013, Photo: Alex Ljungdahl)

In May 2013, at a special meeting at the European Commission in Brussels, the CERN Council adopted the updated European Strategy for Particle Physics. This strategy defines a clear path into the future, with the full exploitation of the LHC, including the high-luminosity phase reaching into the 2030s, and the ILC among the highest-priority projects. This strategy is fully in line with DESY's plans for particle physics as laid down in the proposal "Fundamental Particles and Forces" for the third period of the Helmholtz Association's Programme-Oriented Funding starting in 2015. This proposal rests on a triangle formed by DESY's main activities: the LHC, experiments at electron–positron colliders (ILC and Belle II) and a strong theory group.

With the discovery of a Higgs boson, the LHC has taken but its first step. Although so far all measurements of the new particle's properties indicate its compatibility with the Higgs boson of the Standard Model of particle physics, more data and higher centre-of-mass energies are needed to fully establish the character of the particle. To this end, DESY scientists and technicians are working tirelessly with their colleagues in the LHC collaborations on preparations for the LHC Run 2, which will begin in spring 2015, and on the necessary detector upgrades. Preparations for the upgrades for the high-luminosity LHC also play a special role: together with German universities and international partners, DESY has developed plans to build tracker end-caps for both ATLAS and CMS. These plans have been presented to our funding agencies and we are working eagerly to secure the necessary technical and financial basis for such a major endeavour.

The data and the knowledge acquired at DESY's former HERA collider on the proton structure prove more and more important for LHC analyses. We are therefore happy to see eminent progress in combining the corresponding efforts at both colliders. The completion of the HERA data analysis is progressing well, and several key measurements were published. Particular emphasis is now on the combination of the results from the H1 and ZEUS experiments. The HERA collaborations are preparing to preserve their data in a way to enable analysis of their unique data set also in the future.

The ILC saw two major achievements in 2013. First, the technical design report for this next large-scale project in particle physics was published – a step with which the mandate of the Global Design Effort ended. The GDE is succeeded by the Linear Collider Collaboration, which combines under its roof all efforts worldwide towards the realisation of an electron–positron linear collider. DESY scientists are playing leading roles in this global effort. Also in 2013, the Japanese high-energy physics community selected a potential construction site for the ILC, thus facilitating as next steps the site-specific studies necessary to make the ILC in Japan a reality. Meanwhile, DESY is further advancing the technical basis for the ILC – in particular the superconducting radio-frequency cavities. The accelerating gradient of these cavities, and their industrial production, is the subject of dedicated research, and much has already been learned from the manufacturing process of the cavities for the European XFEL currently under construction in Hamburg. In many aspects, the European XFEL is a very valuable accelerator prototype for the ILC. Also, the experience gained with the electronic data management system used for the European XFEL construction will help DESY to become a lead player in the construction of the ILC.

Theory is the third building block of the DESY particle physics strategy. Theory makes the high-precision predictions necessary for the experiments to compare their data to; it guides the experimentalists in their measurements, suggests new experiments and measurements, and – a very important aspect after the Higgs discovery and on the verge of LHC data taking at unprecedentedly high centre-of-mass energies – it interprets the experimental findings in the light of models of new physics beyond the Standard Model. The DESY theory department with its broad and outstanding range of topics – particle phenomenology, cosmology, lattice gauge theory and string theory – is working at the forefront of research and clearly shapes the field in Germany and beyond. The Wolfgang Pauli Centre, which was recently founded by DESY and the University of Hamburg, will further increase the impact of theory “made in Hamburg”.

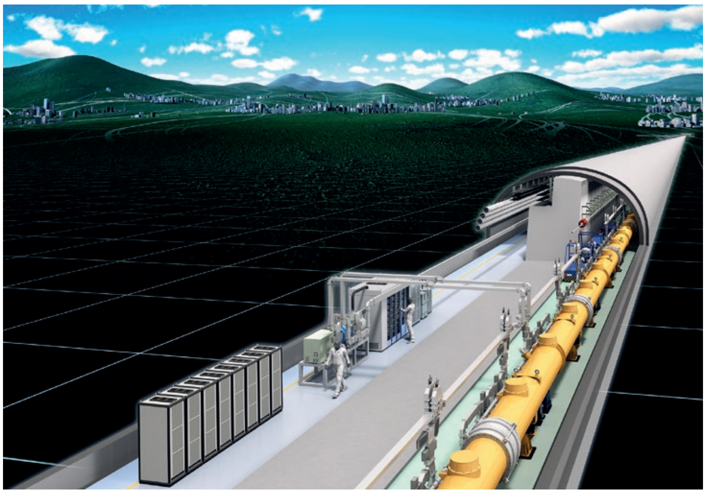

Artist’s view of the planned ILC in the Kitakami mountain region in Japan

DESY’s involvement in the Belle II experiment in Japan is progressing well. In late 2013, the vertex detector, to which DESY, the MPI for Physics in Munich, the MPG Semiconductor Lab and seven German university partners are contributing the conceptually new pixel detector, successfully passed a crucial beam test at DESY. The DESY physicists and technicians are now eager to finalise the hardware developments and see the results of their efforts at work at the SuperKEKB collider, which will go into operation in 2016.

Another facility reached the end of its lifetime in 2013: the DORIS electron–positron storage ring was finally shut down on 2 January 2013, after almost 40 years of operation. This day also marked the end of data taking for the OLYMPUS experiment at DORIS. The collaboration is now performing the very demanding

Impression of IceCube’s digital optical modules, arranged in strings

analysis to achieve unprecedented precision in the measurement of low-energy electron (positron)–proton scattering.

Also for astroparticle physics, 2013 was a highly successful year. After the IceCube discovery of two very high-energy neutrino events in 2012, more of these extraordinary signals were observed in 2013. The experiment thus could establish the extragalactic origin of high-energy neutrinos. Meanwhile, the plans for upgrades of the IceCube neutrino telescope are maturing, and more spectacular physics can be expected.

The same is true for the planned CTA gamma-ray observatory, in which DESY is a driving force with many responsibilities. Currently, the site selection process on both the northern and the southern hemisphere is in progress, and DESY is working towards becoming a central laboratory for the operation and scientific exploitation of CTA.

In summary, we believe that DESY is well prepared to shape the future of our field, and we hope to further strengthen our standing by the appointments of several professors and leading scientists, in particular in the framework of the Helmholtz recruiting initiative. We hope to have all appointment procedures finalised by the end of 2014.

This report describes in more detail several of the activities and contributions of DESY in the field of particle and astroparticle physics in 2013. I wish you an enjoyable reading.

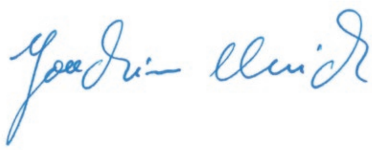

Joachim Mnich
Director in charge of Particle Physics
and Astroparticle Physics

Helmholtz Alliance.

Physics at the Terascale

After the end of its original funding in December 2012, the Helmholtz Alliance "Physics at the Terascale" continues to connect its 21 partner institutions and shape high-energy particle physics in Germany. This was demonstrated at the annual workshop of the Alliance in Karlsruhe in December 2013, which was again attended by close to 250 physicists. Meanwhile, discussions about the future of the Terascale Alliance in a changing Helmholtz Association environment are ongoing.

The Helmholtz Alliance "Physics at the Terascale" is a research network comprising the Helmholtz centres DESY and KIT, 18 German universities and the MPI for Physics in Munich. It represents close to 1000 physicists working on the LHC, on the preparations for the planned ILC, in theoretical particle physics and on numerous other projects. The goal of the Terascale Alliance is to strengthen, also in the long term, the international role of German particle physics. For this purpose, structures were developed and collaborations established that go beyond single sites and experiments – and reach across experiment and theory – and thus facilitate fruitful exchange and communication as well as the definition and exploitation of synergies. In its original setup, the Alliance had four pillars: physics analysis, Grid computing, detector development and accelerator physics.

The original Alliance funding from the Helmholtz Association's "Initiative and Networking Fund" (IVF) consisted of 5 million euro per year, which was supplemented by significant funds from the partner universities, mainly in the form of positions. This IVF funding came to an end in December 2012, and for the years 2013/14, a reduced funding of 0.5 million euro per year has been granted. This amount is supplemented by about 1 million euro from DESY base funding (used mainly for Alliance-relevant positions, computing infrastructures etc.) and by a similar amount from the university partners, mainly for the continuation of positions.

Despite the reduced funding, the Terascale Alliance continues to form the high-energy physics landscape in Germany in

Some of the participants of the 2013 annual workshop of the Terascale Alliance, held from 2 to 4 December 2013 at KIT in Karlsruhe, Germany

Potpourri of poster advertisements for Alliance events in 2013

several ways. Eminent examples are three projects that were selected for a funding of together 380 000 euro per year: The project “Enabling Technologies for Silicon Microstrip Tracking Detectors at the HL-LHC” connects six partners; it aims at developing novel detector technologies that can stand the challenging environment at the high-luminosity LHC. The project “Inclusive and Semi-inclusive Constraints on the Parton Distributions at the LHC and the Study of Hard Processes” also unites six Alliance partner institutions. The goal of the project is to achieve a new level of precision in the knowledge of the nucleon structure and of other central QCD parameters. Finally, the computing project “Performance Optimisation for the Present and Next-generation HEP Data Analysis on the Grid” with its six partners wants to prepare physicists at the LHC and elsewhere for the data challenges to come. All three projects have started off exceedingly well and are producing new insights and results, which were reported at the annual meeting and at dedicated workshops.

Another important building block of the Alliance is the highly esteemed school and workshop programme. This programme was continued in 2013, with again many hundreds of physicists at all career levels participating in discussions, training events and scientific exchange. Of particular interest to the community is the large “hands-on” fraction of training events, which often involves real data and real problems, thus directly engaging the participants in present-day research questions. In addition, the ability of the Alliance and the Alliance Forum to flexibly and on short notice organise small-scale expert discussions and topical workshops is highly appreciated by the community.

The seventh annual workshop of the Terascale Alliance took place in December 2013 in Karlsruhe with about 250 participants, thus demonstrating the continued strong interest of the Alliance community in common discussions and activities. After the discovery of a Higgs boson and the awarding of the 2013 Nobel Prize in Physics for the theoretical development of the Higgs mechanism, one focus naturally was on the respective achievements of the LHC and in particular on the interpretation of this new particle in the Standard Model and in theories beyond. (Alliance partners were involved in several central places in the Higgs discovery and in the current understanding of its properties and role.) A further important aspect was the interesting development of the ILC project, which saw its technical design report published and a construction site selected in 2013. For both topics, eminent speakers could be attracted (among others the former CMS spokesperson Tejinder Virdee, theorist Marcela Carena and the chair of the Linear Collider Board, Sachio Komamiya).

With the introduction of the new programme “Matter and the Universe” in the Helmholtz research field “Structure of Matter”, the challenges and opportunities for the Helmholtz Alliances in the three programme topics are changing: the Terascale Alliance (topic “Fundamental Particles and Forces”), the Helmholtz Alliance for Astroparticle Physics (topic “Matter and Radiation from the Universe”) and the ExtreMe Matter Institute EMMI (topic “Cosmic Matter in the Laboratory”) have been asked to provide a concept that addresses the commonalities – there is considerable overlap in the fundamental research questions between the three programme topics – while maintaining the individual structural elements that were a major reason for the universities to support the Helmholtz Alliance concept.

All in all, the Terascale Alliance is very much “alive and kicking”, and the structures and instruments that were built up during the past six years continue to assist German particle physicists in their scientific activities at the LHC and elsewhere.

Contact:

Ties Behnke, ties.behnk@desy.de
Klaus Desch, klaus.desch@desy.de
Thomas Schörner-Sadenius, thomas.schoerner@desy.de

References:

http://www.terascale.de

News and events.

News and events.

A busy year 2013

January

Administrative Council reappoints directors

In January 2013, DESY's Administrative Council extended the term of office of Helmut Dosch, Chairman of the DESY Board of Directors, for another five years until the end of February 2018. The Council also confirmed in office, as of 2014, both Joachim Mnich, DESY Director in charge of Particle Physics and Astroparticle Physics, and Edgar Weckert, DESY Director in charge of Photon Science, for another five years.

The DESY Board of Directors (left to right): Edgar Weckert, Christian Scherf, Helmut Dosch, Christian Stegmann, Reinhard Brinkmann and Joachim Mnich

OLYMPUS successfully concludes data taking

On 2 January, the nuclear-physics experiment OLYMPUS at the DORIS storage ring successfully concluded its second data-taking phase. In a final two-month period, the OLYMPUS team had collected 4 fb^{-1} of electron–proton and positron–proton collisions. After the final shutdown of DORIS, the scientists recorded cosmic tracks for one additional month in order to precisely determine the alignment of the detector components. After the data taking, the detector was optically measured once more and its inhomogeneous magnetic field was mapped.

The OLYMPUS experiment was set up at DORIS to determine the contribution of multiphoton exchange to electron–proton scattering. In their final data analysis, the OLYMPUS scientists hope to obtain results with an uncertainty of less than 1%.

February

Physics Olympiad at DESY

From 27 January to 2 February, DESY hosted the German national selection round for the International Physics Olympiad 2013. During this week, 51 pupils had the opportunity to showcase their skills in solving theoretical and experimental physics tasks, and thereby come a step closer to one of the coveted tickets for the German national team. In addition, participants gained many interesting insights into the work of the research centre.

Participants in the German national selection round for the International Physics Olympiad 2013

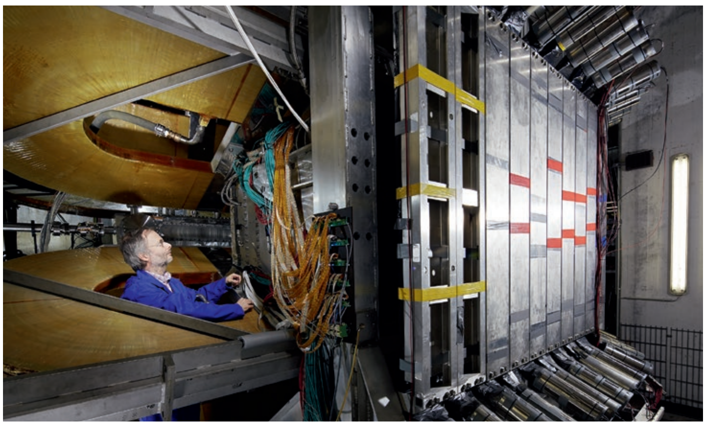

The OLYMPUS detector at the DORIS storage ring

Regional winners of youth science competition selected at DESY

In mid-February, nearly 100 pupils presented their research projects to the jury of the regional youth science and experiments competition, which took place at the DESY school lab in Hamburg. The results were impressive: 34 contributions were selected, 12 of which qualified for the next competition round.

Presentations spanned a fascinating spectrum of subjects from the working world, biology, chemistry, earth and space sciences, mathematics, computer sciences, physics and technology. The youngest participants were fourth-graders, the oldest secondary-level pupils. More than half of the ideas submitted to the competition came from pupils younger than 15 years of age.

Pupils at the regional youth science and experiments competition, which took place at the DESY school lab in Hamburg

DESY continues management of "Netzwerk Teilchenwelt" project

The particle world network "Netzwerk Teilchenwelt", a successful collaboration of 24 German research institutes and CERN in Geneva, will be funded for three additional years by the German Federal Ministry of Education and Research (BMBF). DESY in Zeuthen will thus continue to ensure the management and scientific coordination of the network's "cosmic" project, with additional support from the Helmholtz Alliance for Astroparticle Physics.

The German "Netzwerk Teilchenphysik" network aims to communicate the fascination of particle and astroparticle physics to young people and teachers. In the new funding period, the network will give young people the opportunity to evaluate original data from CERN, including true Higgs particle candidates. Interested youths can also use detectors developed by the network to measure cosmic particles and thus collect their own data.

New Linear Collider Collaboration

From now on, two next-generation accelerator projects will operate under one roof. The Linear Collider Collaboration, LCC for short, was established in Vancouver, Canada, at the end of February. The LCC unites the linear accelerator projects ILC and CLIC, which could one day complement the Large Hadron Collider (LHC). Both projects will continue to exist; the LCC will coordinate the research and development work for the accelerators and detectors. LCC director is the former LHC project manager Lyn Evans. The Linear Collider Board, a supervisory board that was established at the same time, is headed by Sachio Komamiya from the University of Tokyo.

March

Shakti P. Duggal Award for DESY scientist Rolf Bühler

DESY scientist Rolf Bühler received the 2013 Shakti P. Duggal Award for astroparticle physics. Every two years, this prestigious prize is presented to young scientists not older than 36 years of age for outstanding contributions in the field of cosmic-ray and astroparticle physics research.

Bühler was honoured for his ingenious work based on data from the Fermi Gamma-Ray Space Telescope and the H.E.S.S. gamma-ray observatory. In addition, Bühler measured, for the first time, the density of the extragalactic background light over cosmological distances. All these analyses required an outstanding intuition of the detectors used for the measurements, and Bühler played a leading role in the analyses and their publication. His work provided important results, the influence of which extends well beyond astroparticle physics.

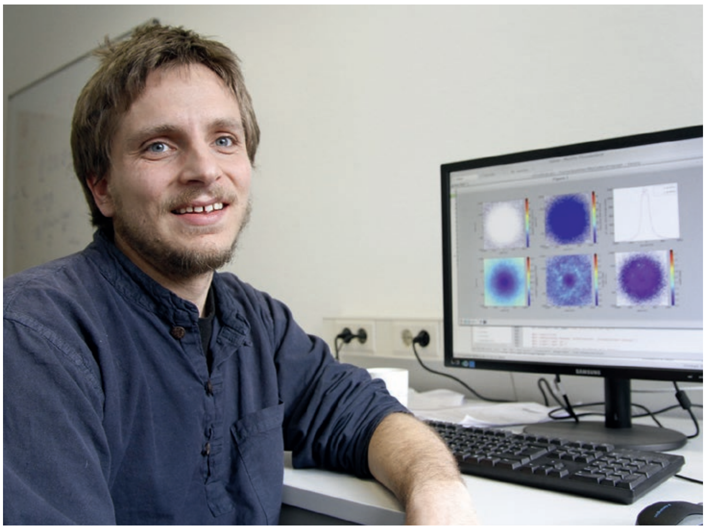

Rolf Bühler

April

Theoretical physics with international reputation

DESY and the University of Hamburg jointly established the Wolfgang Pauli Centre (WPC) for theoretical physics, which was inaugurated with a symposium at DESY on 17 April. “The close cooperation of the theory groups at the university and DESY has made Hamburg a key region for theoretical physics with international reach,” WPC spokesman Wilfried Buchmüller pointed out. “The aim of the Wolfgang Pauli Centre is to expand these joint activities and make them widely visible.”

The new research and educational centre is part of the strategic Partnership for Innovation, Education and Research (PIER) between the University of Hamburg and DESY. The WPC will extend the long-standing cooperation of the two institutions in theoretical high-energy physics to include solid-state physics and quantum optics. Altogether, some 160 scientists will work within the centre.

Wolfgang Pauli during a lecture in the 1920s

Clearing the way for the CTA gamma-ray observatory

The German Federal Ministry of Education and Research (BMBF) included the Cherenkov Telescope Array (CTA), a planned observatory for cosmic high-energy gamma rays, as one of three projects into its roadmap for large-scale research infrastructures. “This paves the way for clarifying the open questions regarding content and funding,” German federal research minister Johanna Wanka pointed out in a letter to Christian Stegmann, head of DESY in Zeuthen.

The CTA observatory will consist of three telescope types of different sizes. DESY is responsible for the design and construction of the mid-sized telescopes. In May 2013, a prototype took up test operation at the Berlin Science Park Adlershof.

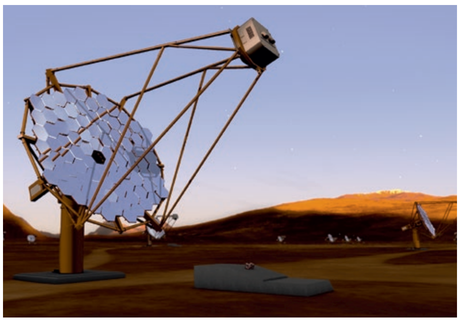

DESY is developing and building the mid-sized telescopes for the CTA observatory.

May

DORIS days

At a symposium on 14 May, several hundred guests from science, politics and business celebrated the outstanding performance of DESY's venerable DORIS accelerator. The DORIS storage ring was switched off in early January 2013 after nearly 40 years of operation for particle physics, accelerator development and research with synchrotron radiation. Only a few large-scale research facilities throughout the world have such a long and successful history of science.

Celebrating the retirement of DESY's DORIS accelerator after nearly 40 years of successful operation

ATLAS and CMS receive EPS prize

The teams of the ATLAS and CMS experiments at the Large Hadron Collider (LHC) at CERN were awarded the prestigious High Energy and Particle Physics Prize 2013 of the European Physical Society (EPS). Together with the three experimental physicists Michel Della Negra (Imperial College London), Peter Jenni (CERN and University of Freiburg) and Tejinder Virdee (Imperial College London), the collaborations were honoured for the discovery of a new heavy particle with the properties of the long-sought Higgs particle.

"DESY is one of the largest institutions participating in the LHC experiments ATLAS and CMS, and one of the few institutes in the world contributing to both experiments. We are very honoured and glad to receive this renowned research prize from the European Physical Society," said Joachim Mnich, DESY Director in charge of Particle Physics and Astroparticle Physics.

In total, more than 700 German scientists participate in the LHC experiments ATLAS and CMS, including 400 young scientists.150 DESY scientists are involved in the two experiments, and DESY operates completely equipped control rooms for both of these huge particle detectors.

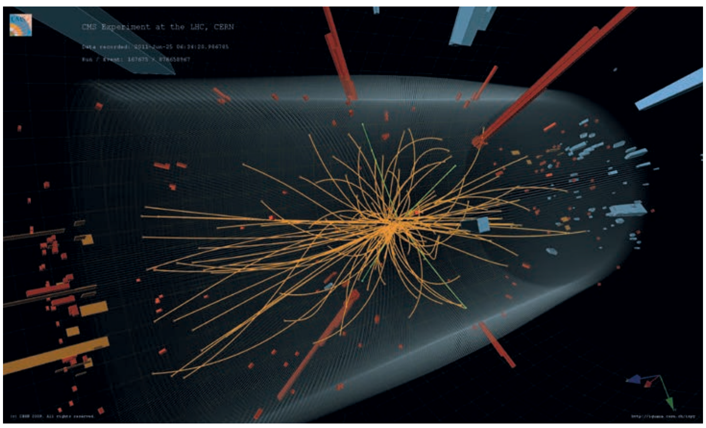

Higgs event in the CMS detector

European Strategy for Particle Physics adopted

At a special meeting hosted by the European Commission in Brussels on 30 May, the CERN Council formally adopted the update of the European Strategy for Particle Physics. This strategy sets the course for the future of particle physics in Europe, making recommendations for future projects and research fields. Particle physicists from all European countries, together with colleagues from Asia and America, participated in the development of the European Strategy.

"The central building blocks of the European strategy, the LHC and the ILC, are completely in accordance with the long-term particle physics strategy of DESY," said Joachim Mnich, DESY Director for Particle Physics and Astroparticle Physics, who participated in the development of the strategy as a member of the international European Strategy Group.

European Strategy Update

May

ECFA LC2013 workshop at DESY

The European Linear Collider Workshop ECFA LC2013 took place at DESY from 27 to 31 May. The meeting coincided with many events and results relevant to the linear collider project, such as the discovery of the Higgs boson and the completion of the technical design report for the ILC accelerator and the detailed baseline design for the ILC detectors.

In coincidence with the workshop, the organisational structure that had led the project to the present status finished its mandate. The excellent work and leadership of Jonathan Bagger as Chairman of the ILC Steering Committee, Barry Barish as Director of the Global Design Effort and Sakue Yamada as the Research Director were well recognised and thanked for. The next step was the transition to the new Linear Collider Collaboration (LCC), led by Lyn Evans.

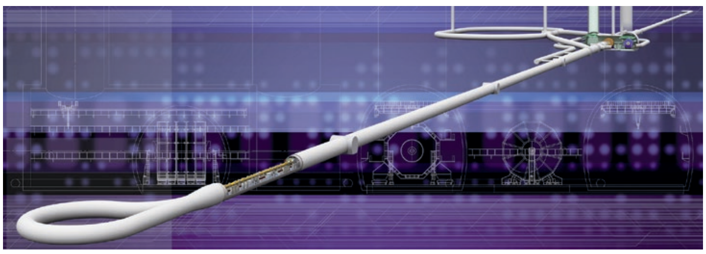

The two linear accelerators at the heart of the ILC will be built using the superconducting TESLA technology originally developed at DESY.

June

CMS prepares for high-luminosity LHC

From 3 to 7 June, almost 250 members of the CMS collaboration visited DESY to participate in the CMS Upgrade Week and prepare for the high-luminosity era of the LHC (HL-LHC). From 2023 onward, the HL-LHC is expected to deliver an instantaneous luminosity of 5 x 10^{34} $cm^{-2}s^{-1}$, which is a factor five higher than the LHC design luminosity. The resulting increase in track density requires an upgrade of several detector components, including a completely new tracker, faster readout systems and an improved trigger.

The DESY CMS group is involved in the design of the future CMS tracker and takes a leading role in the development of detector modules and the support structures for the tracker end-caps. The CMS Upgrade Week comprised a comprehensive review of all ongoing R&D activities and set the scope for the upgrades towards the HL-LHC. A first milestone will be the technical proposal to be published by the end of 2014.

ILC technical design report published

The technical design report (TDR) for the International Linear Collider (ILC), a next-generation particle collider to complement and advance beyond the physics of the LHC at CERN, was published on 12 June. In three consecutive ceremonies in Asia, Europe and the Americas, the authors officially handed over the report to the international oversight board for projects in particle physics, the International Committee for Future Accelerators (ICFA). The TDR presents the latest, most technologically advanced and most thoroughly scrutinised design for the ILC. The centrepieces of the ILC, two linear accelerators for electrons and positrons, are based on the superconducting TESLA technology, which was, for years, the subject of intensive research and further improvements at DESY, among others.

July

Kerstin Borras elected CMS deputy spokesperson

DESY particle physicist Kerstin Borras was elected deputy spokesperson of the CMS experiment at the LHC. As of January 2014, the head of the CMS group at DESY will assume the office for two years, together with Paris Sphicas from the University of Athens, Greece. The new spokesperson will be Tiziano Camporesi from CERN.

Kerstin Borras, head of the CMS group at DESY

DESY welcomes more than 100 summer students from 32 nations

More than 100 students from 32 countries on five continents gained research experience at DESY in Hamburg and Zeuthen during the eight-week DESY summer student programme, which started on 17 July. The practical work in various projects of accelerator, particle and astroparticle physics and in research with X-ray radiation was complemented by a comprehensive lecture programme.

The DESY summer student programme is very popular among students, not only because of the opportunity to gain practical experience in genuine research projects but also because of its internationality. In 2013, more than 500 students applied for the programme; 112 were invited to DESY in Hamburg or Zeuthen.

DESY summer students 2013

August

ILC candidate site in Japan announced

The ILC site evaluation committee of Japan announced the result of the assessment on the two candidate sites in Japan in a press conference held at the University of Tokyo on 23 August 2013. As a location, they recommended the Kitakami mountains in the Iwate and Miyagi prefectures. The search for an appropriate candidate site for the construction of International Linear Collider in Japan has been ongoing since 1999. More than ten candidate sites were announced in 2003. In 2010, the list was further reduced to two with Kitakami in north-east of main-island of Japan, and Sefuri in Kyushu, the south-west island.

A process to make the assessment on these two remaining candidates was started in January this year in order to narrow them down, from scientific point of views. Within Japan, a site evaluation committee of eight members was formed and additional two sub-committees of sixteen technical experts and twelve socio-environmental experts were separately created to provide expertise on issues such as the geological conditions, the environmental impact, the possible problems during construction and the social infrastructure of each candidate site

After more than 300 hours of meetings, the site evaluation committee made a tentative choice in early July. This choice was then submitted and reviewed by an international review committee. The international review committee recognized that the process to choose the site which to be reviewed had been conducted with great care, and the presented site has excellent geological conditions for tunneling and stability.

September

New Helmholtz Young Investigator Group at DESY

María Aldaya Martín

In the present funding period, DESY will again establish a new Helmholtz Young Investigator Group. Particle physicist María Aldaya Martín, who was selected in a rigorous international peer review process, will be supported by the Helmholtz Association and DESY in the creation of her own Young Investigator Group. Martín and her group, which will be established in collaboration with the Karlsruhe Institute of Technology (KIT) and the University of Hamburg, will work at the CMS experiment at the LHC to carry out precision measurements of top quarks and use these to search for new physics.

Highest Austrian doctoral degree for Clemens Raab

Clemens Gunter Raab from the theory group at DESY in Zeuthen completed his doctoral studies with distinction in 2012 within the graduate school "Computational Mathematics" at the Research Institute for Symbolic Computation of Johannes Kepler University Linz, Austria. On 13 September 2013, he was awarded the doctoral degree "Promotio sub auspiciis Praesidentis rei publicae" by the President of the Republic of Austria, Heinz Fischer, for his achievements. Clemens Raab also received the honorary prize of the Austrian Ministry for Science and Research.

The President of Austria, Heinz Fischer, congratulates Clemens Raab.

"Teilchenzoo" – interactive exhibition inaugurated

On 27 September, DESY and the Universum Bremen science centre inaugurated the interactive exhibition "Teilchenzoo" (particle zoo), which aims to convey the fascination of particle physics by motivating visitors to hunt for Higgs bosons, quarks and other particles.

Right at the beginning of the exhibition, a catchy personality test prompts the visitors to find out their particle counterpart by comparing their own character with the physical properties of the elementary particles. The subsequent exhibits then provide more information about the different particles, their discovery and the ways they influence both science and our daily lives. Various hands-on experimental stations enable the visitors to explore the underlying scientific principles for themselves.

DESY contributed its theoretical expertise and several hands-on contributions to the "Teilchenzoo" exhibition, which will be on display until 30 June 2014 at the Bremen science centre.

October

DESY mourns Gustav-Adolf Voss

Gustav-Adolf Voss, Director of the Accelerator Division at DESY from 1973 to 1994, passed away on 5 October in Hamburg at the age of 84. Voss greatly influenced the development of particle accelerators worldwide. He was highly respected throughout the world and a lifelong advocate of international cooperation in science.

With the death of Gustav-Adolf Voss, DESY has lost one of its most influential figures. His charismatic leadership, expert skills and foresight have greatly contributed to DESY's current standing as an internationally leading accelerator laboratory.

Gustav-Adolf Voss

DESY congratulates Englert and Higgs on Nobel Prize in Physics

On 8 October, the Nobel Committee awarded the 2013 Nobel Prize in Physics to François Englert and Peter Higgs for their theory explaining the mass of elementary particles. DESY congratulated the Nobel laureates on this important recognition of their work.

The theory, which has since become known as the "Higgs mechanism", explains the mass of elementary particles through the ubiquitous interaction with a scalar Higgs field. With the discovery of the associated Higgs particle at the LHC at CERN in July 2012, the mechanism was finally confirmed after 48 years of searching. Numerous German researchers were involved in the discovery.

François Englert (left) and Peter Higgs at CERN
Photo: Maximilien Brice (CERN)

PhD thesis award 2013

The PhD thesis award 2013 of the Association of the Friends and Sponsors of DESY (VFFD) was shared by Johannes Hauk and Andrej Singer. The association presents the prize every year for one or two outstanding PhD theses from the two previous university terms. The award ceremony took place on 30 October in conjunction with the Jentschke Lecture in Hamburg.

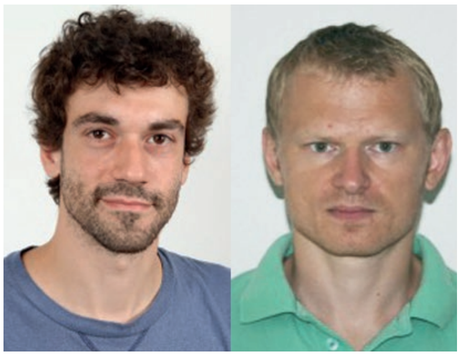

Johannes Hauk and Andrej Singer

In his PhD thesis "Measurement of associated Z^0 boson and b-jet production in proton-proton collisions with the CMS experiment", Hauk presented outstanding contributions to particle physics.

Singer studied coherence and statistical properties of radiation at new X-ray sources, documented in his thesis "Coherence properties of third and fourth generation X-ray sources – theory and experiment".

November

Record number of visitors at DESY Open Day

Particle physics detector exhibit on the DESY Open Day

The traditional DESY Open Day, which took place on 2 November in conjunction with the fifth Hamburg Science Night, attracted a record number of 18 674 visitors. In more than 100 attractions, lectures and hands-on activities, the DESY staff, guests and partner institutions presented their work on the DESY campus. Within experimental halls, laboratories, workshops, engineering departments and the DESY school lab, more than 1000 voluntary helpers – another record in the history of the Open Day – tirelessly answered innumerable questions and demonstrated what characterises a major research centre.

December

New injection concept for plasma acceleration

A team around DESY's plasma acceleration researcher Jens Osterhoff developed a new concept to improve electron-beam-powered plasma accelerators. Simulations suggest that their idea should enable the acceleration of very high-quality particle bunches. The DESY researchers published the results of their studies in *Physical Review Letters*.

As the next step, the researchers plan to test their gas cell under real conditions at the FACET facility at SLAC in the USA. Starting in 2016, they will use a 10 cm long plasma cell in the FLASHForward experiment at DESY's FLASH free-electron laser facility to both accelerate particles from the plasma itself and push particle bunches from FLASH to higher energies.

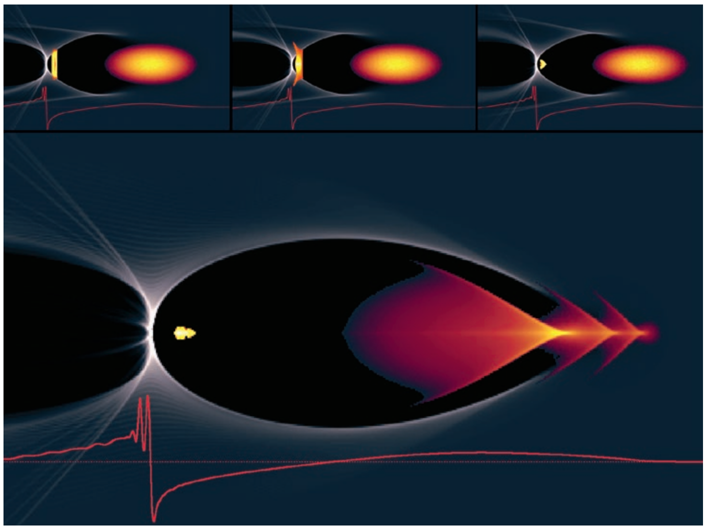

Simulation of a compact and ultrarelativistic electron beam propagating through a hydrogen plasma

IceCube's discovery of extragalactic neutrinos was selected by *Physics World* as breakthrough of the year 2013.

IceCube discovery selected as breakthrough of the year

The renowned British science magazine *Physics World* selected the IceCube collaboration's discovery of the first high-energy cosmic neutrinos as the most significant scientific breakthrough in 2013. Between May 2010 and May 2012, using their one cubic kilometre detector at the South Pole, the IceCube scientists successfully managed to capture a total of 28 neutrinos with energies greater than 30 TeV, among them two with an energy of more than 1000 TeV. DESY is strongly involved in the IceCube collaboration, which had published this first evidence of highest-energy astrophysical neutrinos only a few weeks earlier in the journal *Science*.

Research topics.

Virtual reality at HERA.

What virtual quarks can tell us about gluons in the proton

More than three decades after their discovery at DESY's PETRA electron–positron collider, gluons, the carriers of the strong interaction, continue to be objects of great interest in the theory of quantum chromodynamics (QCD). The kinetic energy of the gluons and quarks inside protons and neutrons is responsible for nearly 95% of the mass of a human being, of the solar system and of the visible matter in the universe. More than half of this kinetic energy is associated with gluons. However, direct knowledge of the distribution of gluons inside the proton is difficult to come by. A unique view of the gluon distribution can nonetheless be achieved through measurements of the deep-inelastic scattering of electrons on protons at DESY's former HERA collider. But a trick is needed since electrons can only directly "see" the proton's electrically charged quarks and not the electrically neutral gluons. The trick is to measure the scattering of electrons on the virtual quarks that arise from the splitting of initial-state quasi-real gluons. Such a measurement, expressed in terms of the longitudinal structure function, F_L, was achieved from dedicated runs at HERA in 2007.

Deep-inelastic scattering (DIS) of electrons on protons at the HERA collider (Fig. 1) is well suited to study the properties of strong interactions. Such scattering occurs mainly through the exchange of virtual photons, which interact with the electrically charged quarks in the proton. When the energy transferred from the electron to the quark in an interaction – or more precisely the four-momentum transfer squared Q^2 – is significantly larger than the proton mass squared, the quarks inside the proton can usually be treated as quasi-real and nearly massless. Virtual photons can have transversely and longitudinally polarised components. Due to helicity conservation for massless particles, scattering by quasi-real massless quarks can only proceed through transversely polarised photons. In contrast, longitudinally polarised photons can only interact with virtual quarks, i.e. quarks whose effective masses strongly deviate from their nominal (almost vanishing) mass. Such virtual quarks can arise as fluctuations, e.g. from the splitting of quasi-real initial-state gluons; they have a lifetime limited by the Heisenberg uncertainty relation. Thus, some light can be shed on the distribution of gluons inside the proton by separating the electron–proton scattering cross section into contributions from transversely and longitudinally polarised photons.

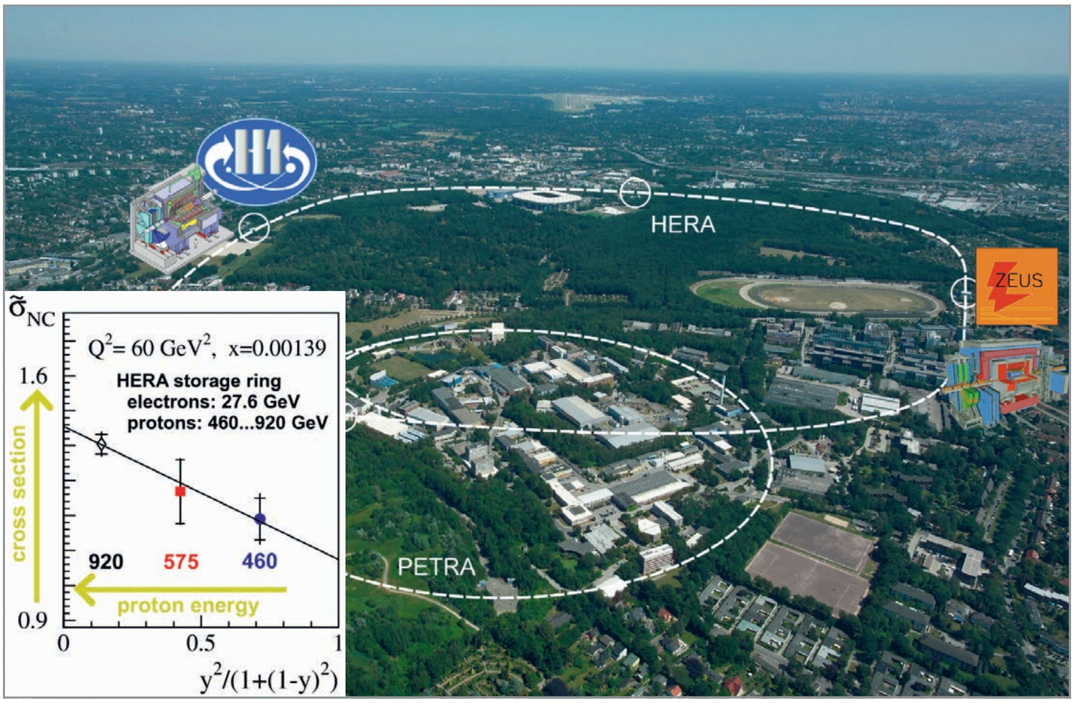

Figure 1

Aerial view of DESY with the HERA electron–proton collider and the locations of the H1 and ZEUS experiments. The inset shows an example from recently finalised H1 measurements of so-called Rosenbluth plots of the reduced electron–proton cross section for different proton beam energies, from dedicated runs taken in 2007. The slope directly measures the proton structure function F_L.

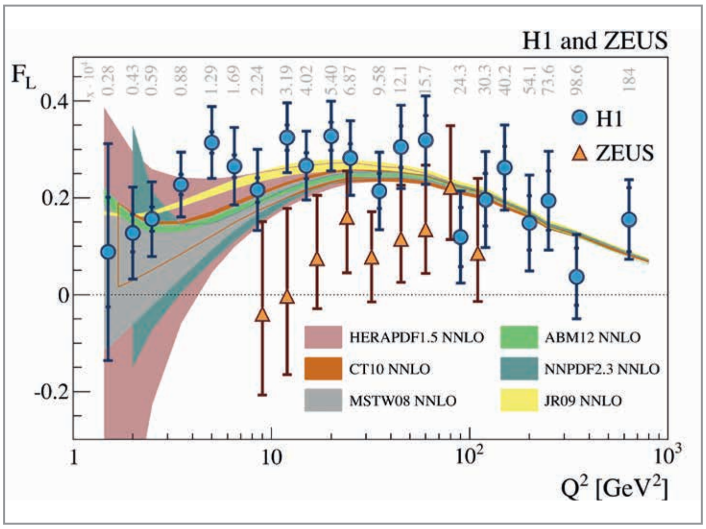

Figure 2

F_L as a function of Q^2 for the recent final measurements of H1 and ZEUS, compared to several QCD predictions at next-to-next-to leading order (NNLO)

Traditionally, the cross section for electron–proton scattering is expressed in terms of the proton structure functions F_2 and F_L. While F_2 is sensitive to all photons, the longitudinal structure function F_L is exclusively sensitive to longitudinally polarised photons. The two structure functions can be distinguished experimentally by the fact that the scattering-angle dependence of the corresponding cross section contributions differ. DIS cross sections can be parameterised in terms of the inelasticity y, which is related to the fraction of the incoming electron momentum transferred to the exchanged virtual photon; i.e. the value of y ranges between 0 and 1. The cross section contribution from F_L is particularly strong at large values of y. Since y depends on the proton beam energy, the F_L contribution can be extracted directly by measuring the same cross section at several proton beam energies. From such measurements, a Rosenbluth plot such as the one shown in Fig. 1 can be made. The slope of the curve shown in the plot directly yields the value of F_L and thus reveals the gluon distribution of the proton through the mechanism explained above.

Figure 2 shows the final results for F_L obtained by the H1 and ZEUS collaborations using the procedure outlined above. For both data sets, parts of the uncertainties are correlated between the data points, and the measurements are consistent with each other within these uncertainties. The H1 data cover a larger kinematic range since the detector was somewhat better suited for this kind of measurement. As also shown in the figure, QCD predictions based on different parameterisations of the proton's gluon distribution are consistent with the measurements. The two data sets are now being combined to further improve the experimental precision.

The H1 collaboration has also used their data to extract an explicit measurement of the gluon distribution. The result is shown in Fig. 3. This directly extracted gluon distribution is well described by predictions (shown as curves in Fig. 3) based on more indirect measurements from other data. This is an important test of the self-consistency of the behaviour of gluons inside the proton and therefore of the validity of QCD.

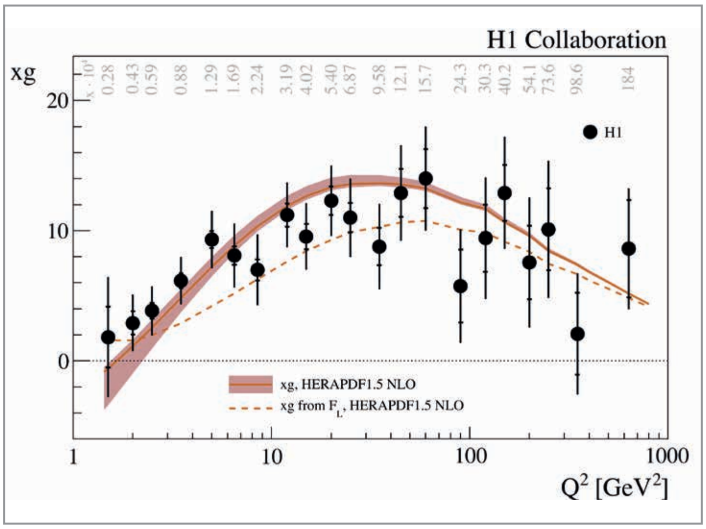

Figure 3

Average gluon density $xg(x,Q^2)$ extracted from the H1 data in Fig. 2, where x is the fraction of the proton momentum carried by the gluon

Contact:

Stefan Schmitt, stefan.schmitt@desy.de
Achim Geiser, achim.geiser@desy.de

References:

H1 Collaboration, DESY-13-211 [arXiv:1312.4821], accepted by EPJ C
ZEUS Collaboration, DESY-14-053 [arXiv:1404.6376]

Charm fragmentation fractions at HERA.

Supporting the picture of universality

Millions of charm quarks have been produced in high-energy electron–proton (*ep*) collisions at DESY's HERA collider. Because of the "confinement" property of strong interactions, their so-called "colour charge" prevents quarks from being observed as free particles. However, charm quarks can still be detected: After their production they fragment into observable bound states – the charmed hadrons – that contain in addition one or two lighter quarks. The ZEUS experiment at HERA has recently completed a precise measurement of the relative abundances of the most copiously produced "charmed" hadronic states and compared them to other experiments to test the common assumption that the fragmentation process is independent of the production process (i.e., that it is "universal").

The study of charm-quark production at DESY's former *ep* collider HERA provides unique insights into the dynamics of strong interactions, as described by quantum chromodynamics (QCD). The production proceeds mainly via the fusion of a gluon (g) from the proton with a virtual photon (γ^*) radiated from the electron to produce a charm–anticharm quark pair (c and $\bar{c}$), as shown in Fig. 1.

The subsequent fragmentation process, during which quark–antiquark pairs are produced from the vacuum and colourless bound states are formed, comprises as its final stage the hadronisation phase, which culminates in the formation of hadrons – bound states of either two (mesons) or three quarks (baryons). In this process, the charm quark can bind

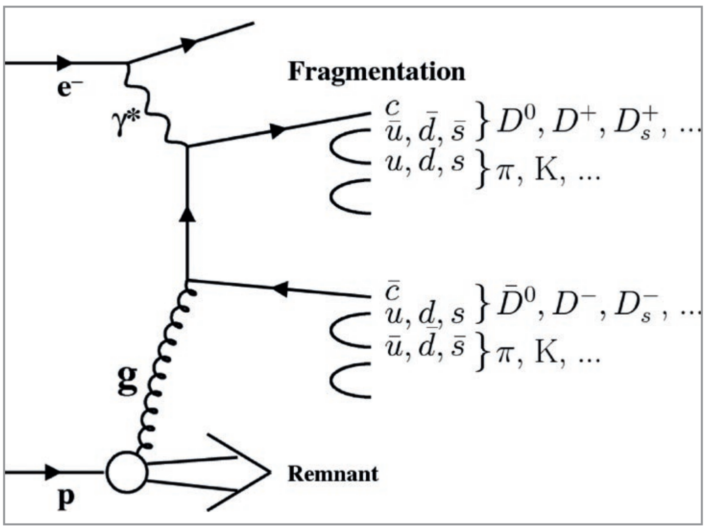

Figure 1

Charm production at HERA and subsequent fragmentation

to one light antiquark, either of up, down or strange type, to form a pseudoscalar D^0, D^+ or D_s^+ meson when the spins of the two quarks add up to zero. When they add up to one, they can form vector mesons such as the D^{*+} (vector mesons are marked with an asterisk). Baryons, such as the Λ_c, which consists of a charm, an up and a down quark, can also be formed. However, QCD cannot yet predict the fractions of charm quarks fragmenting into specific hadrons (the "charm fragmentation fractions").

In the phenomenological string fragmentation model, the formation of hadrons proceeds through strings – narrow tubes of strong colour fields connecting quarks with antiquarks that carry complementary colours (e.g. red and anti-red). However, in *ep* collisions, the charm and the anticharm quarks inherit non-complementary colours from the gluons in the proton. The charm quark might, for example, carry red and the anticharm anti-green colour. Thus, according to the string fragmentation picture, the charm and anticharm quark cannot form a string between them; instead, they form separate strings to complementarily coloured particle systems in the proton remnant. The situation is different at electron–positron (e^+e^-) colliders, where a virtual photon or Z boson originating from the e^+e^- annihilation can directly produce a colourless charm–anticharm pair. Despite this difference, it is usually assumed that the charm fragmentation fractions are universal, although this has not been rigorously proven.

The ZEUS experiment has measured the relative production rates of the most copiously produced charm states in the large data sample collected during the HERA II run: D^0, D^+, D_s^+ and D^{*+} mesons as well as Λ_c baryons. The measurement was performed in the photoproduction kinematic region, where the photon emitted from the electron (Fig. 1) is quasi-real, i.e. nearly massless. The charmed hadrons were fully reconstructed via their decays into charged particles. For the D^+ meson, for instance, the decay mode $D^+ \rightarrow K\pi\pi$ into one kaon (K) and two pions (π) was investigated. The trajectories and momenta of the charged particles are accurately measured with the ZEUS tracking detector and used to calculate the invariant mass of the $K\pi\pi$ three-body system. Figure 2 shows the invariant-mass

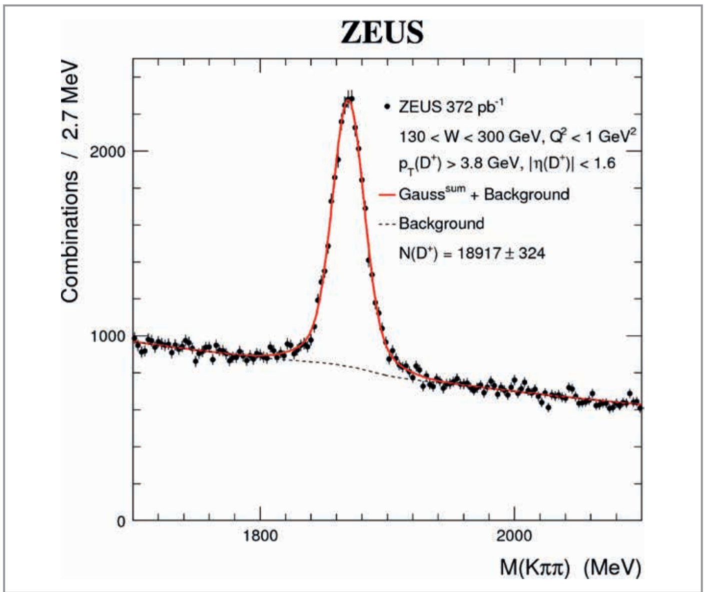

Figure 2

Observed $K\pi\pi$ mass distribution and D^+ signal and background estimated from a fit

spectrum resulting from an analysis of the entire data sample. A clear signal peak is visible at the nominal mass of the D^+ meson at 1870 MeV; the total number of reconstructed D^+ mesons is 18 917 ± 324. The fragmentation fractions were determined by comparing the individual production yields of each of the investigated channels to the sum of all yields. The result is shown in the first column of Fig. 3.

For comparison, the older HERA I results from H1 and ZEUS and the fragmentation fractions for charm production in e^+e^- annihilations are also shown in Fig. 3. The precision of the new measurement alone is competitive with the e^+e^- result. The various measurements from e^+e^- and from ep collisions are in agreement with each other. In the future, the new results can be used to improve the precision of the world average values. This will, in turn, be helpful for interpreting charm production results from the LHC at CERN or other colliders.

What can we learn from the magnitude of the fragmentation fractions? We find, for instance, that meson production dominates over baryon production. This agrees with the intuition that it is more laborious to produce and bind two light quarks to the charm quark compared to one light antiquark. A further observation is the suppression of the production of the D_s^+ meson (which contains a strange quark) compared to the other mesons. This can be explained by the mass of the strange quark, which is large compared to the up- and down-quark masses.

Thus, a wealth of interesting observations have been obtained, which reveal details of the charm fragmentation process and significantly improve the precision of the charm fragmentation fractions.

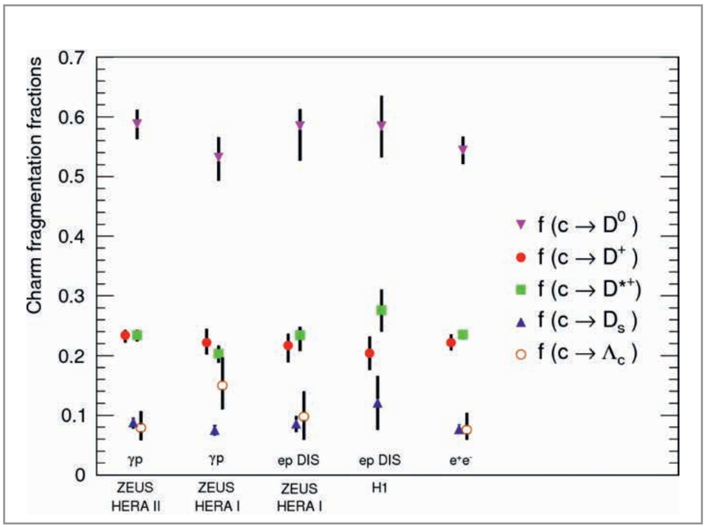

Figure 3

Charm fragmentation fractions obtained from various experiments. The new ZEUS results are shown in the first column.

Contact:
Olaf Behnke, olaf.behnke@desy.de

References:
ZEUS Collaboration, DESY-13-106, JHEP 09 (2013) 058

Elastic J/ψ photoproduction at HERA.

Probing the gluon density of the proton

The elastic production of J/ψ mesons in collisions between photons and protons is a unique probe of the gluon content of the proton. At DESY's former HERA collider, J/ψ mesons were produced in electron–proton collisions. In elastic J/ψ production, the electron first radiates a photon, which then collides with the proton to produce a J/ψ meson and nothing else. A similar process takes place in proton–proton collisions: one of the protons will sometimes emit a photon, which can then collide with the other proton to produce a J/ψ meson. For this reason, the J/ψ data from HERA can be directly compared to data collected in proton–proton collisions at the LHC at CERN.

The J/ψ meson was discovered in 1974 by two independent experimental groups. One of the groups named it J, the other named it ψ, and it has been called J/ψ ever since. The J/ψ – which is a bound state of a charm quark and an anticharm quark – is not a stable particle, but rather decays almost instantly into other particles. In about 20% of all cases, it decays into a pair of leptons – either a pair of muons or an electron–positron pair. At the HERA electron–proton collider, the J/ψ was sometimes produced “elastically”, i.e. in a collision that left the proton intact. Figure 1 shows an event display of an elastically produced J/ψ decaying into a pair of muons. The detector is otherwise empty, a distinctive signature of an elastic collision. Both of the beam particles, the proton and the electron, escape along the beam direction and remain undetected.

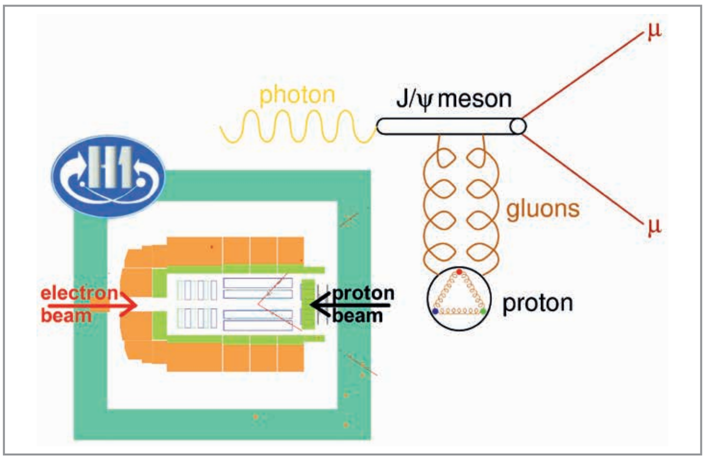

Figure 1

J/ψ production at HERA. The two thin red lines in the event display show the muons produced in the J/ψ decay. The drawing illustrates how the J/ψ is produced in elastic photon–proton collisions.

However, a solitary lepton pair can also arise from processes other than J/ψ production. For a measurement of J/ψ production, it is therefore not enough to just count elastic lepton pair production events. Fortunately, the J/ψ meson has a very well known mass, which can be calculated from the momenta measured for the two leptons. The invariant-mass distributions of electron–positron pairs and of muon pairs measured at HERA are shown in Fig. 2. The distinct peak at an invariant mass near 3.1 GeV is due to J/ψ mesons and can be used to separate J/ψ production from other processes. Compared to the J/ψ peak in the distribution of muon pairs, the peak in the electron–positron pair distribution broadens towards lower mass values due to photons radiating off the outgoing electrons and positrons. In both distributions, some residual background from other processes is visible and must be subtracted to obtain an accurate estimate of the total number of produced J/ψ mesons.

With the knowledge of the total number of produced J/ψ mesons, the more fundamental question of the J/ψ production mechanism in elastic photon–proton collisions can be addressed. The proton consists of quarks and gluons. These particles carry special charges, analogous to electric charges, called colour charges. There are three such colour charges, which are commonly called “red”, “green” and “blue”. If the three colours are mixed in equal parts, they neutralise each other. This is similar to a computer screen where a pixel perceived as being white is actually composed of three coloured pixels: red, green and blue. In the theory of the strong interaction (quantum chromodynamics, QCD), which is responsible for J/ψ production, reactions of particles are explained by the exchange of coloured gluons. Because the colours of the quarks and gluons inside the proton are balanced, the proton as a whole is colour-neutral, like the

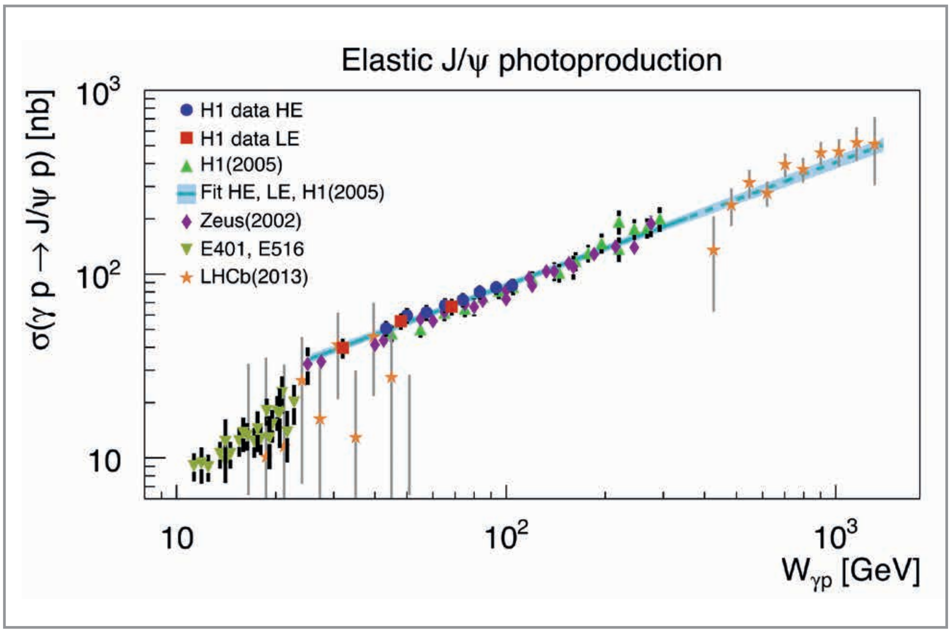

Figure 3

Cross section for elastic J/ψ production as a function of the centre-of-mass energy, *W*. The recent H1 measurements, labeled "H1 data HE" and "H1 data LE", were performed at two different settings of the HERA proton beam energy: high energy (HE, 920 GeV) and low energy (460 GeV, LE). Measurements of other experiments are also shown.

white pixel on the computer screen. In an elastic reaction, in which the proton stays intact, the proton's colour neutrality is preserved, and therefore at least two gluons that together are colour-neutral must participate in the collision. For this reason, the number of J/ψ mesons produced elastically at HERA is particularly sensitive to the proton's gluon content. The exchange of two gluons between the J/ψ meson and the proton is illustrated in Fig. 1.

In order to understand the dynamics of this reaction in greater detail, the cross section for J/ψ production is studied as a function of the centre-of-mass energy, *W*, of the photon–proton system. For large *W*, the gluons taken from the incoming proton carry only a small fraction, denoted *x*, of the proton momentum. On the other hand, if *W* is small, *x* is large. The cross section of elastically produced J/ψ mesons measured at HERA is shown for different values of *W* (and thus *x*) in Fig. 3. Measurements by other experiments (also shown) complement the HERA measurements by extending the measured range in *W*; they are in excellent agreement. The data from the LHCb experiment were measured in proton–proton collisions, in which one of the protons takes over the task of the initial-state electron of the HERA process by radiating a photon that then interacts with the other proton. (More precise results from LHCb, which show the same excellent agreement with the HERA measurements, have recently become available, see references.)

When used in a QCD analysis, the J/ψ data have the potential to constrain the gluon density $g(x)$ in the proton. The extraction of $g(x)$ from the J/ψ data is complementary to the determination of the gluon density from measurements of the inclusive structure functions F_2 and F_L. Measurements of F_L are described in another article of this report.

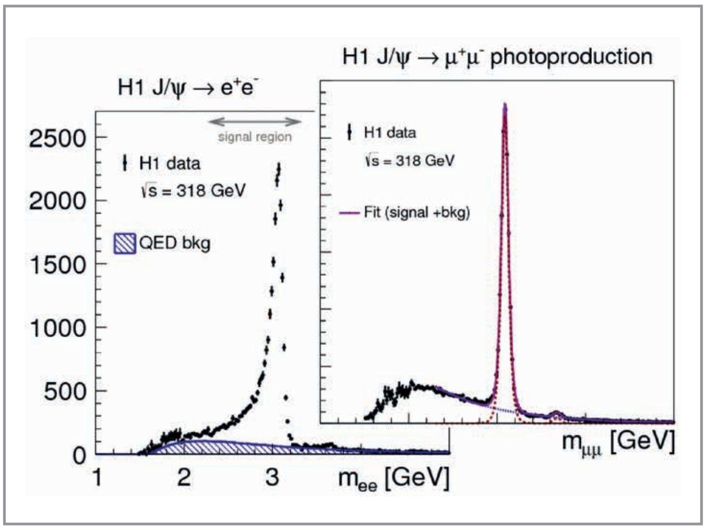

Figure 2

Invariant-mass distribution of elastically produced J/ψ mesons

Contact:

Michel Sauter, michel.sauter@desy.de
Stefan Schmitt, stefan.schmitt@desy.de

References:

H1 Collaboration, EPJC 73 (2013) 2466
ZEUS Collaboration, EPJC 24 (2002) 345
LHCb Collaboration, arXiv:1402.3288
S.P. Jones et al., JHEP 1311 (2013) 085

Adding a touch of flavour to hadronisation.

Hadron production in lepton scattering from unpolarised protons and deuterons

High-energy particle collisions frequently produce collimated jets of particles in their final states, which can be traced to the "hadronisation" of energetic quarks involved in the collision process. The hadronisation process cannot be described by a fundamental theory without considerable input from experiments. The HERMES experiment used the 27.6 GeV electron and positron beams of DESY's former HERA collider to provide data that will refine the current understanding of this hadronisation process and, in particular, shed light on the role of "flavour" in hadronisation.

Hadronisation and parton fragmentation functions

The development of the model of the nucleon – the basic building block of nuclear matter – in terms of partons, i.e. quarks and gluons, is one of the great triumphs of 20th-century particle physics. Deep-inelastic scattering (DIS) of electrons or other high-energy leptons by protons was a prominent contributor to this effort and remains one of the most productive probes of the partonic structure of the nucleon.

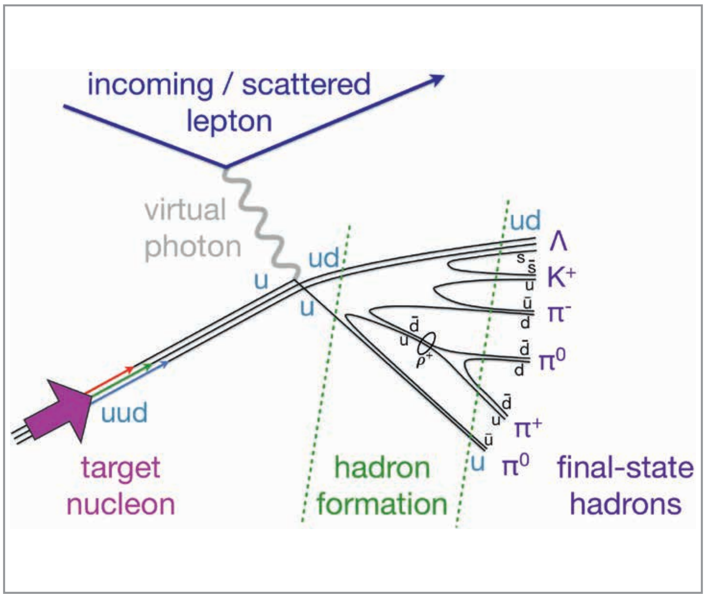

Figure 1

Diagram of the semi-inclusive DIS process. The incoming lepton emits a virtual photon, which is absorbed by one of the quarks in the nucleon. In the case depicted, the struck quark fragments into a pion in the final state. In semi-inclusive processes, the scattered lepton and part of the hadronic final state are detected in coincidence.

The DIS process can be thought of as the emission of a virtual photon by an incoming lepton (Fig. 1), which kicks a charged quark or antiquark that then attempts to escape the nucleon. However, isolated quarks have never been observed in nature. Instead, as the kicked quark or antiquark tries to escape from the bound state of quarks and gluons that constitutes the nucleon, a shower, or "jet", of hadrons develops.

A number of models are available that describe this showering process. In all of them, the final stage is the generation of several "colour singlet" hadrons, that is, hadrons in which quarks appear only in combinations that neutralise the strong colour fields of the quarks, such as pions and kaons. The modelling of hadronisation is essential for a complete picture of the strong interaction of quarks and gluons. The hadronisation models are expressed in terms of polarisation-averaged "fragmentation functions" (FF), which give the number density of particular hadron types produced by the fragmentation of a struck quark or antiquark of a given flavour.

Hadron multiplicities in semi-inclusive DIS

A complete description of the DIS process also requires a parameterisation of the proton structure in terms of quarks of different flavours (up, down and strange), i.e. a "parton distribution function" (PDF). While the knowledge of PDFs is

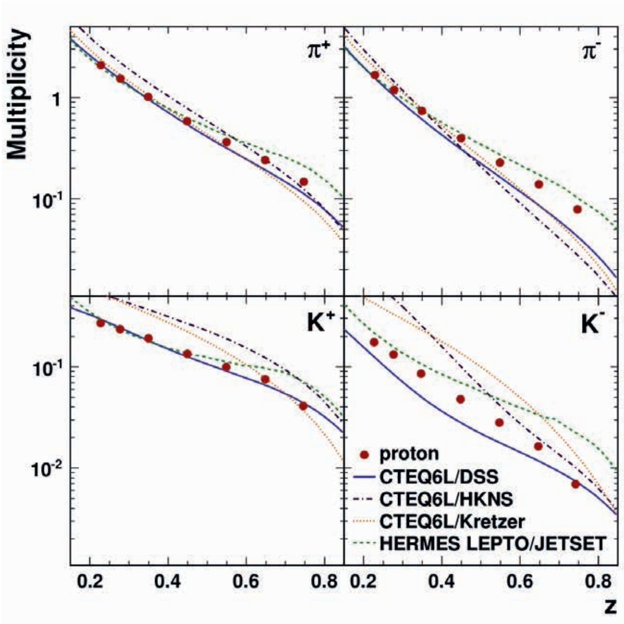

Figure 2

Pion and kaon multiplicities in semi-inclusive DIS from a proton target as a function of the fractional virtual-photon energy carried by the hadron produced, compared to leading-order calculations using various parton distribution and fragmentation function parameterisations. The statistical error bars on the experimental points are too small to be visible.

highly developed, the amount of data available for constraining FFs is much more limited, particularly for the "disfavoured" fragmentation modes in which struck quarks of a given flavour hadronise into final-state hadrons that do not have a significant component of this particular flavour. The FFs provide the database of the phenomenology of the hadronisation process and are therefore central to models of hadronisation as well as to the description of hadron production in any high-energy scattering process. The measurement of normalised yields of specific hadrons in the final states of semi-inclusive DIS events, i.e. particle multiplicities, provides a powerful means of extracting FFs.

The HERMES experiment with its highly developed particle identification system and pure gas targets was ideally suited for such measurements. Before the end of the last HERA run in 2007, the collaboration was able to collect a high-statistics data set produced by semi-inclusive DIS for proton and deuteron targets. These data are used to study the multidimensional dependences of the multiplicities, including their kinematic dependence on the component of the hadron momentum transverse to the momentum transfer, $P_{h\perp}$. Thus, these data reach beyond the usual standard collinear factorisation and probe the transverse-momentum dependence (TMD) of the fragmentation process. The extraction of multiplicities of pions and kaons separately for positive and negative charges provides sensitivity to the individual quark and antiquark flavours in the fragmentation process, quite in contrast to what can be learned from electron–positron annihilation into hadrons.

The HERMES collaboration has tabulated its data in several multidimensional decompositions and produced a number of kinematic projections of particular interest. Some of the latter are plotted in Fig. 2 as a function of z, the fractional virtual-photon energy carried by the produced hadron, and compared to various predictions based on the previous knowledge of fragmentation functions. While the data for pions agree fairly well with the predictions, significant discrepancies can be seen in the predictions of the kaon distributions. These data thus provide unique information on the fragmentation of quarks into final-state hadrons and will contribute valuable input for the extraction of flavour-dependent fragmentation functions using quantum chromodynamics (QCD) fits. The multiplicities measured as a function of $P_{h\perp}$ will provide constraints on models of the motion of quarks in the nucleon in the transverse plane of momentum space as well as on the models of the fragmentation process. They will also serve as a powerful ingredient to test the so-called TMD factorisation hypothesis.

Contact:

G. Schnell, gunar.schnell@desy.de

References:

HERMES Collaboration, *Multiplicities of charged pions and kaons from semi-inclusive deep-inelastic scattering by the proton and the deuteron,* Phys. Rev. D87 (2013) 074029
http://www-hermes.desy.de/multiplicities

The Nobel particle.

As Englert and Higgs receive highest honours, more secrets of their boson are revealed

Within only one year, the paradigm in Higgs boson physics shifted from discovery to precise measurement of properties. After in-depth analysis of the Run I data of the LHC collider at CERN, the ATLAS and CMS experiments confirmed that the particle whose discovery they announced in July 2012 is indeed a Higgs boson. The couplings of this particle to bosons and fermions, as well as its spin and parity, are being studied, and all are found to be compatible with the Standard Model expectations. Recently, direct evidence for fermionic decays has been established, and the first differential cross sections have been measured. This highly exciting year for Higgs boson physics was crowned by the 2013 Nobel Prize in Physics being awarded to François Englert and Peter Higgs, the fathers of the Higgs mechanism.

Discovery and Nobel Prize

In July 2012, the ATLAS and CMS experiments announced the discovery of a particle resembling the long-sought-after Higgs boson. After the completion of LHC Run I, the full recorded data set has been analysed, and in March 2013, in the light of the updated ATLAS and CMS results, CERN announced that the properties of the new particle are indeed those of a Higgs boson.

In recognition of their ground-breaking theoretical work, crowned by this outstanding discovery, the 2013 Nobel Prize in Physics was awarded jointly to François Englert and Peter Higgs for "the theoretical discovery of a mechanism that contributes to our understanding of the origin of mass of subatomic particles, and which recently was confirmed through the discovery of the predicted fundamental particle, by the ATLAS and CMS experiments at CERN's Large Hadron Collider". In his Nobel banquet speech, Higgs thanked the ATLAS and CMS scientists and underlined that the discovery of this boson "was a great achievement by all the people involved, and [they] are grateful to them for enabling [them] to be here today."

The conclusion that the discovered particle is a Higgs boson derives from the analysis of its quantum numbers, like spin and parity, and from its interaction with other particles.

Increasing significance

The Higgs boson is unstable; it decays immediately after its production into pairs of either bosons (photons, Z bosons, W bosons) or fermions (τ leptons or b quarks). The Higgs signal was first observed in the bosonic decay channels. At the time of the discovery, a significance of 5σ had been reached (meaning that the probability that the signal had been faked by a statistical fluctuation is $6{\cdot}10^{-7}$). In the meantime, using the full data set and refined analysis techniques, the significance of the observation has grown enormously in both experiments, and significant signals have been established in individual decay channels.

In all cases, the number of observed signal events is compatible with the predictions of the Standard Model. For example, the ATLAS di-photon measurement alone, to which DESY is strongly contributing, has now reached a significance of 7.4σ, and the signal strength relative to Standard Model expectations is $1.55^{+0.33}_{-0.28}$, in agreement with the prediction within 1.9 standard deviations. Very recently, ATLAS and CMS have established direct evidence for Higgs decays into fermions. Figure 1 shows the result of the CMS combination of the $\tau\tau$ channel, to

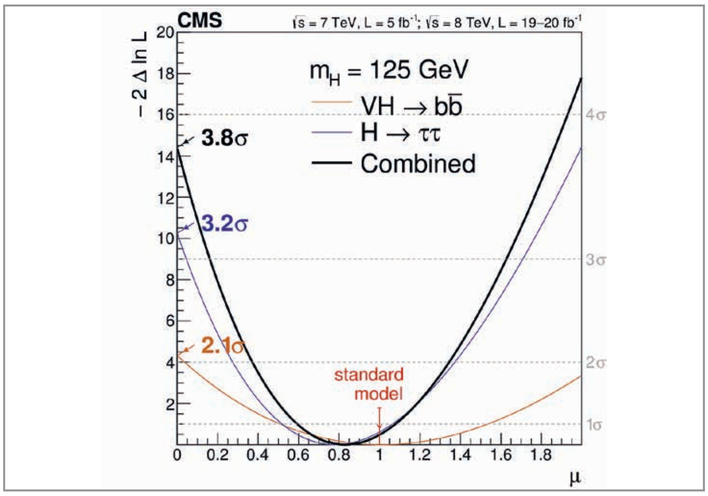

Figure 1

Likelihood scans as a function of signal strength, showing the significance of Higgs signals in the $b\bar{b}$ and $\tau\tau$ channels

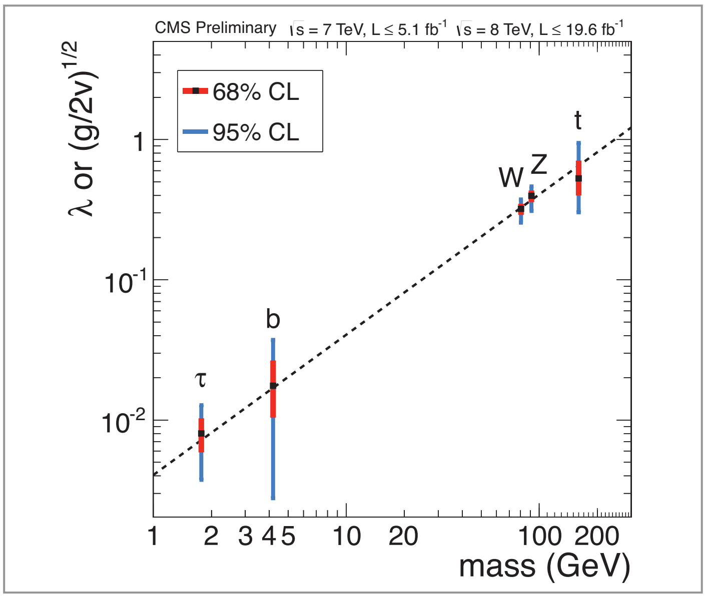

Figure 2

Coupling parameters of the Higgs boson as a function of the mass of the corresponding bosons and fermions

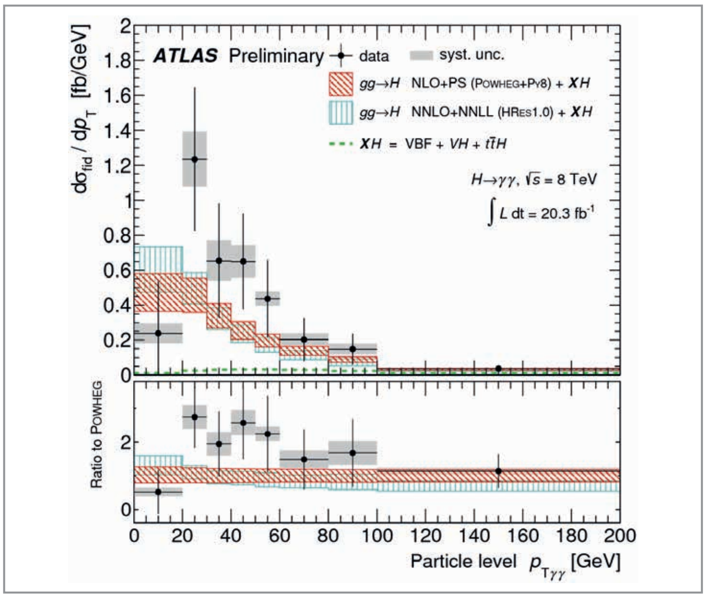

Figure 3

Differential cross section of the di-photon transverse momentum for two photons coming from a Higgs boson

which the DESY CMS group strongly contributed, with the $b\bar{b}$ channel [1]. The total observed significance for fermionic decays is 3.8σ, and the signal strength is 0.83 ± 0.24, in full accord with the Standard Model prediction.

Couplings

Since both the production and the studied decays of the Higgs boson involve the couplings to τ, *b*, *W*, *Z* and *t*, the couplings of these particles to the Higgs boson can be derived. Both ATLAS and CMS find that the measured couplings agree with the Standard Model expectation within two standard deviations. Figure 2 shows that the respective coupling parameters are in excellent agreement with a linear dependence on the mass, a direct fingerprint of the Higgs mechanism at work [2].

Spin and parity

Other properties of the Higgs boson are its spin – it is postulated to have spin 0 – and its parity (a measure of how its mirror image behaves), which should be positive. ATLAS and CMS tested this hypothesis and several others with three decays channels of the Higgs boson – two photons, two *Z* bosons and two *W* bosons – separately and also combined. It was shown that the data are compatible with the Standard Model 0^+ quantum numbers for the Higgs boson, whereas all alternative hypotheses, namely some specific 0^-, 1^+ , 1^- and 2^+ models, are excluded at confidence levels above 97.8% – a very strong indication that the assignment spin 0 and positive parity is preferred.

Differential cross sections

The study of the Higgs boson entered a new phase with the first successful differential cross section measurements of the Higgs boson, to which DESY contributed significantly. The number of Higgs boson candidates decaying via the di-photon channel has grown to some several hundred, a large enough sample to allow measurements of the underlying kinematic properties of Higgs boson production and decay [3].

Several di-photon and jet distributions were measured and compared to model expectations. The transverse-momentum distribution of the di-photon pair is shown in Fig. 3. The Higgs boson is expected to be produced with non-zero transverse momentum because of the radiation of quarks and gluons from the initial-state partons. This distribution is thus sensitive to the QCD description of Higgs boson production in gluon fusion. Such measurements, although currently still limited by statistics, will help enormously to improve the description of Higgs boson kinematics by simulation.

Contact:

Rainer Mankel, rainer.mankel@desy.de
Elisabeth Petit, elisabeth.petit@desy.de

References:

[1] CMS Collaboration, arXiv:1401.6527
[2] CMS Collaboration, CMS-PAS-HIG-13-005
https://twiki.cern.ch/twiki/bin/view/CMSPublic/Hig13005TWiki
[3] ATLAS Collaboration, ATLAS-CONF-2013-072

Physics beyond the Standard Model.

Searching for electroweak production of gauginos and sleptons in di-lepton final states

Following the observation of a Higgs boson in 2012, the search for physics beyond the Standard Model of particle physics has become arguably the hottest topic in high-energy physics at the LHC collider at CERN. Scientists from the DESY ATLAS group play a leading role in many of these searches, including searches for the electroweak particles predicted by supersymmetry models.

While the predictions of the Standard Model (SM) of particle physics have been repeatedly verified, several mysteries remain – notably, the particle responsible for dark matter has not been found. Supersymmetry (SUSY) may be the answer. SUSY postulates that each SM particle is paired with an additional (as yet undiscovered) particle with the same properties apart from spin and mass. If the lightest of these SUSY particles is stable, it is a viable dark-matter candidate. Since this “lightest supersymmetric particle” (LSP) is also electrically neutral, it would escape direct detection, but if it is produced in a collision of two particles, its presence can be inferred by summing for all detected particles in the final state, the momentum components transverse to the beam direction. A large value for the summed transverse momentum would imply, by momentum conservation, that one or more particles, possibly including an LSP, had been produced. The LSP could be either a neutralino or a gravitino. (The SUSY partners, or superpartners, of the SM electroweak bosons are known as charginos and neutralinos, or collectively as gauginos. The SM leptons, neutrinos, quarks and gluons are paired with sleptons, sneutrinos, squarks and gluinos, respectively.)

During the first years of LHC running, most SUSY searches focused on processes with large predicted cross sections, such as the strong production of gluinos and squarks. These studies found no evidence for the existence of such particles for masses up to about 1 TeV. Initially, the possible electroweak production of SUSY had not received much attention since the predicted cross sections are smaller and thus the study is more difficult. However, in some scenarios, it is the dominant superparticle production process and thus merits attention.

One promising electroweak SUSY channel is the direct production of slepton pairs followed by their decays into leptons and the LSP (in this case a neutralino: the neutralino1). Other possible electroweak modes are the direct production of chargino pairs or the pair production of a chargino with a next-to-lightest neutralino (neutralino2).

To further complicate matters, two different chargino decay modes might exist: if sleptons and sneutrinos are light, the

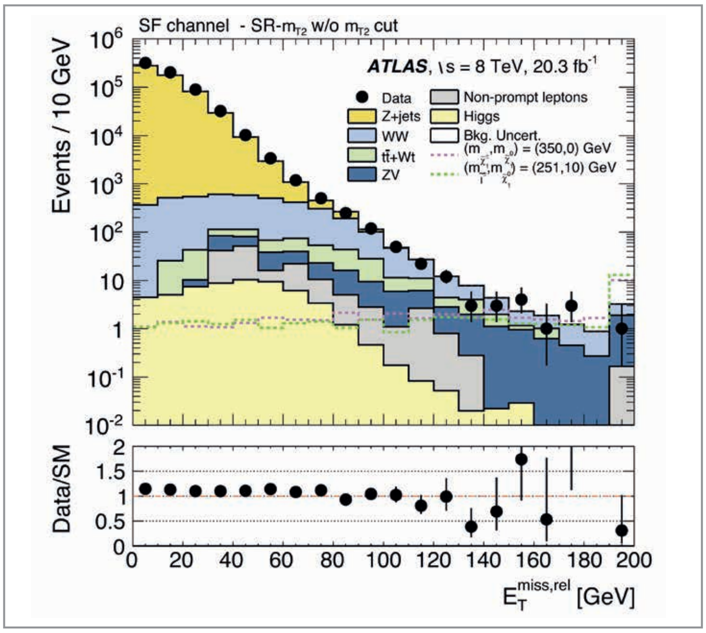

Figure 1

Distribution of $E_T^{miss,rel}$ in the like-flavour channel after applying most of the selection cuts. The hashed regions represent the total uncertainties on the background estimates; the right-most bin includes the overflow.

decay proceeds through intermediate sleptons and sneutrinos, but if sleptons and sneutrinos are heavy, the electroweak gauginos decay to either a *W* or *Z* boson and a neutralino1, with subsequent boson decay into quarks or leptons.

The final states of all of these production channels include two isolated, oppositely charged leptons and substantial missing transverse energy, E_T^{miss}, mainly from the two LSPs. These are all viable signatures for experimental searches. Based on them, search regions for final states with two like- or unlike-flavour leptons (e^+e^-, $\mu^+\mu^-$ or $e\mu$), no *Z* candidate and no jets were defined. In addition, to target decay modes with hadronically decaying *W* bosons, a search region consisting of two like-flavour leptons, two jets, E_T^{miss} together with a *Z* candidate was added. Figure 1 shows the relative E_T^{miss} distribution in the like-flavour channels after applying most of the selection cuts. The major SM backgrounds are from *WW* di-boson, *ZW*, *ZZ* and top pair production. The strengths of these backgrounds are estimated in dedicated control regions. Other backgrounds due to leptons from heavy-flavour decays or photon conversion, or from hadronic jets mis-identified as signal leptons, are estimated in a fully data-driven way. Minor backgrounds such as that from Higgs boson decays are estimated from predictions.

The analysis of the full $\sqrt{s}$ = 8 TeV ATLAS data set has been recently completed and the results are found to agree well with the SM predictions. They thus indicate the absence of a SUSY signal. Given this agreement, the next step is to derive model-independent upper limits on production cross sections that take into account all possible error sources and statistical uncertainties. The results are also interpreted in the context of simplified models with SUSY-like topologies, which assume single specific decay chains. For example, Fig. 2 shows the expected and observed exclusion limits on the chargino mass in a SUSY model that includes only chargino pair production followed by *W*-mediated decay. For a massless neutralino, chargino masses between 100–105 GeV, 120–135 GeV and 145–160 GeV are excluded. This is the first direct limit on chargino masses in this scenario obtained at a hadron collider. Further limits are set on the masses of the lightest chargino, next-to-lightest neutralino and sleptons for several masses of the lightest neutralino.

The DESY ATLAS group has been strongly involved in these SUSY searches and is currently working on combining the di-lepton SUSY analysis with other electroweak searches. In parallel, preparations for the future challenge of even higher interaction rates and a near doubling of the LHC centre-of-mass energy are under way.

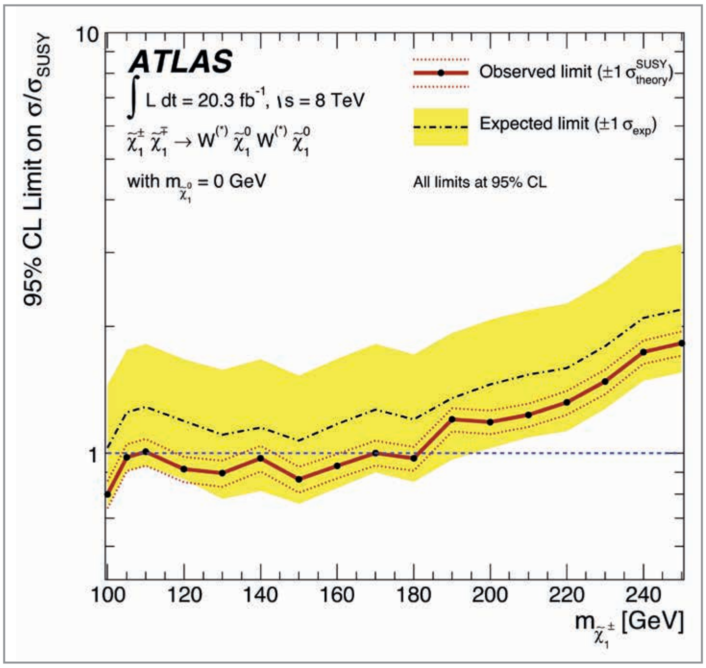

Figure 2

Observed and expected 95% CL upper limits on the cross section normalised by the simplified-model prediction as a function of the chargino mass for a massless LSP

Contact:

Janet Dietrich, janet.dietrich@desy.de

References:

ATLAS Collaboration, CERN-PH-EP-2014-037

DESY ATLAS group prepares for high luminosity.

Low-mass detectors for high-mass discoveries

An ambitious target: the assembly and testing of a full silicon strip end-cap. This is the planned DESY contribution to the high-luminosity LHC (HL-LHC) upgrade of the ATLAS detector. R&D is progressing fast, and the plans for the full tracker replacement, which is due to be installed in 2023, are taking shape.

LHC and ATLAS upgrade

Exploring the Higgs sector and extending the search for new high-mass states are the main goals of the high-luminosity upgrade of the LHC (HL-LHC). However, the enormous radiation doses and the huge number of tracks per event expected at the HL-LHC would overwhelm the present ATLAS detector. Furthermore, by the time of the LHC upgrade in 2023, the current tracker will have accumulated a radiation dose large enough to compromise its performance. Current plans call for replacing it with a new, all-silicon tracker consisting of a barrel constructed from five layers of “staves” and two end-caps, each made up of seven disks built from “petals” (Fig. 1). The sensitive elements of the staves and petals will be silicon strip detector modules with several rows of n-in-p strip sensors, as shown in Fig. 2.

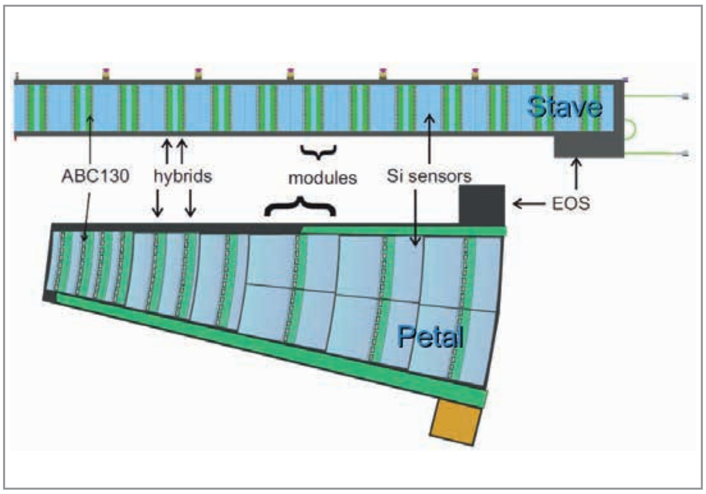

Figure 1

Stave and petal – base structures with silicon sensor modules for the new ATLAS tracker

The main DESY contribution to the upgraded ATLAS detector will be the module assembly and the full assembly of one of the two end-caps. The end-cap will be equipped with modules produced in Valencia (IFIC, Spain), Freiburg (University of Freiburg) and at DESY in Zeuthen (together with Humboldt University Berlin). All modules will be collected at DESY in Hamburg and mounted on petals, which will then be inserted into the detector frame. Finally, the completed end-cap will be shipped to CERN near Geneva, Switzerland.

R&D at DESY

The necessary R&D is being carried out by a collaboration of more than 30 institutes worldwide. The DESY ATLAS group is laying the groundwork needed to evaluate the current baseline design and possible improvements by developing techniques to measure detector properties (e.g. detector resolution, charge collection efficiency, material thickness) and by exploring alternative materials and detector construction methods. One important R&D project now under way is the construction and characterisation of small-scale prototypes, called petalets. Petalet components, including very thin titanium cooling tubes for CO_2 cooling, carbon fibre support cores, electrical tapes and full silicon strip modules, are being developed. After assembly, the petalets will be operated in a variety of environments, including test beams, to spot pitfalls of the design and ultimately establish full HL-LHC compliance.

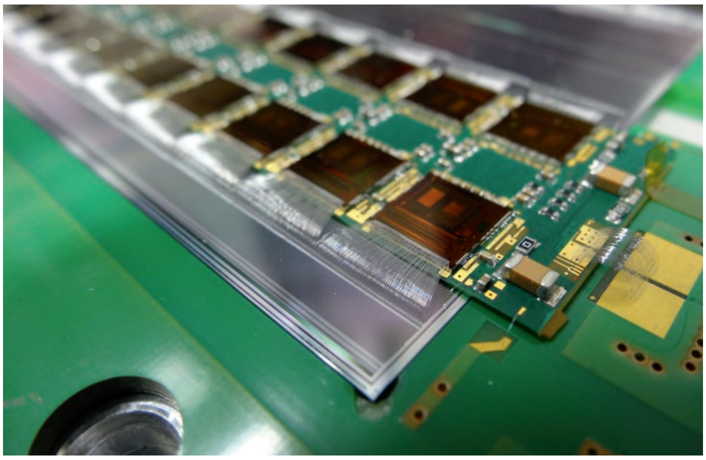

Figure 2

Upgrade module prototype

The test beam facility at DESY in Hamburg plays an essential supporting role. An important part of the test beam infrastructure is a high-precision pixel telescope that was developed and built at DESY. This telescope is being employed in a setup used to make maps of material thickness (in terms of radiation lengths) by measuring the average amount of multiple scattering in large samples of test beam events. Figure 3 shows a thickness map of a calibration structure made with this technique.

A similar test stand, which also includes a powerful magnet (1 T), was developed to study the charge collection efficiency of irradiated sensors. The results of the study (Fig. 4) are the first charge collection efficiency measurements made with high-energy particles in a test beam; they agree well with previous measurements made with other techniques. The same test setup is now being used to study an important effect of radiation damage on the observed signal, as characterised by the Lorentz angle. These newly developed setups can be exploited to study the impact of the choice of materials for components of strip detector modules on the detector performance.

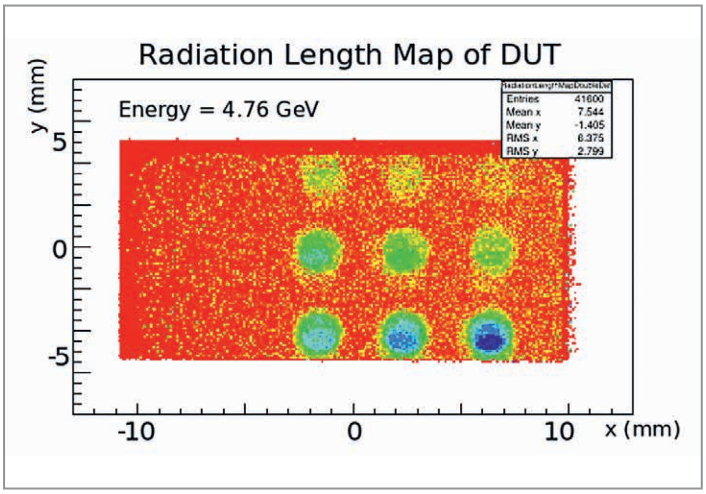

Figure 3

Measured distribution of material thickness (in units of radiation length, X_0) across a test structure consisting of a stack of aluminium plates in which an array of holes of varying thickness has been drilled

In parallel, a large-scale search for adhesives for module assembly is yielding first results. Traditionally, two-component silver-loaded epoxy glue has been used to bond readout chips to the readout flex boards since it possesses good electrical and thermal properties and is also radiation-tolerant. However, this type of glue has the disadvantages of a rather short radiation length and a long curing time, and it also raises health concerns. As an alternative, we are exploring a wide range of UV-curing adhesives, which offer fast curing times, long shelf times and long radiation lengths. Tests are showing encouraging thermal and mechanical properties even after thermal cycling and irradiation.

Armed with the knowledge gained from the petalet programme, we will begin the construction and characterisation of a full petal.

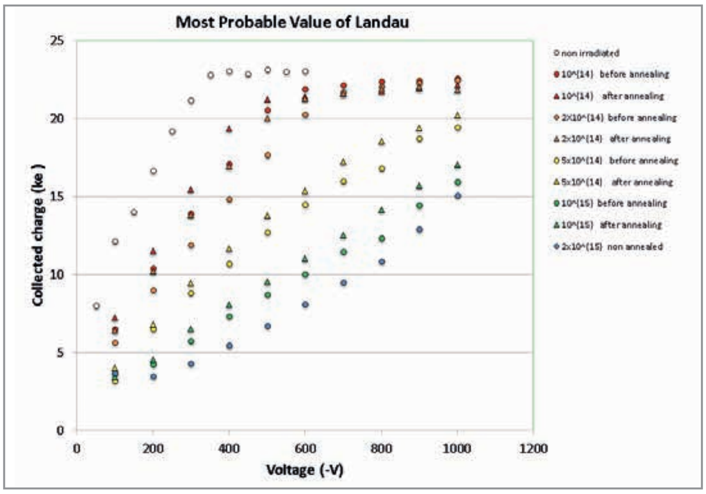

Figure 4

Reduction of charge collection efficiency with increased irradiation of a sensor. The amount of collected charge is plotted as a function of the bias voltage for sensors, before and after irradiation.

Contact:

Ingo Bloch, ingo.bloch@desy.de
Ingrid-Maria Gregor, ingrid.gregor@desy.de

Higgs bosons on the test-bench.

Probing Higgs couplings to fermions at the LHC

Since the discovery of a new boson in July 2012, the ATLAS and CMS collaborations have performed crucial measurements of the bosonic decay modes, which show that the properties of the new particle are consistent with those expected for the Standard Model Higgs boson. However, it became clear only recently that the new particle also couples to fermions. In December 2013, the CMS collaboration reported the observation of Higgs boson decays into pairs of τ leptons and thus confirmed that the new boson does indeed couple to the heaviest lepton, as expected. In parallel, CMS continues to search for heavy resonances decaying into pairs of *b* quarks, in the hope of finding evidence for the extended Higgs sector expected in supersymmetric models.

Evidence for Higgs decays into τ lepton pairs

The measurement of the coupling strength of the Higgs boson to fermions is eagerly awaited in the particle physics community since it would extend our knowledge of the mechanism that generates the masses of the elementary particles. At present, the measurement can only be made in the τ lepton pair and *b* quark pair decay channels of the Higgs boson.

The DESY CMS group has made significant contributions to a recently published CMS analysis of its full data set on one of these channels: τ lepton pairs. It is an extraordinarily difficult measurement, which explores about 30 different topologies, exploiting minute differences in events between various Higgs production modes and τ lepton decay channels. The resonance decaying into τ leptons is searched for in a wide mass range from 90 to 160 GeV. After combining all the channels, the CMS collaboration observed evidence for Higgs boson decays into τ leptons with a statistical significance of 3.2 standard deviations, meaning that the probability of having observed a fake signal is of the order of one permille.

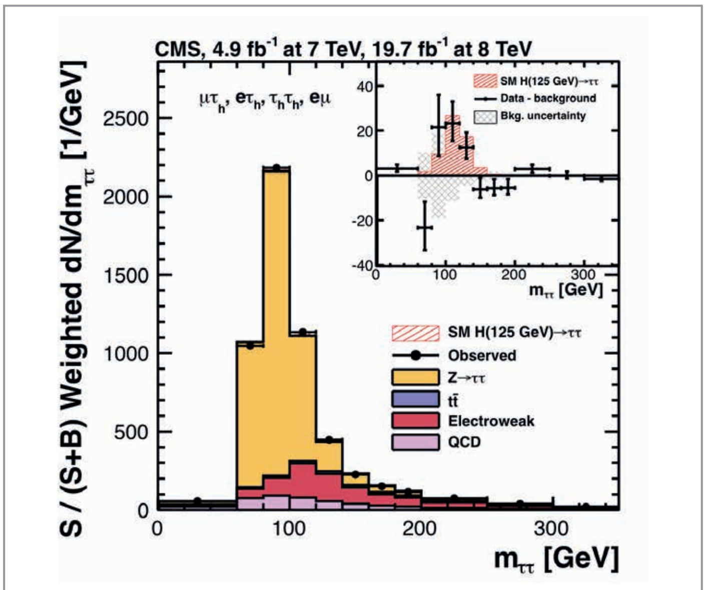

Figure 1

Combined observed and predicted $m_{\tau\tau}$ distributions in the μ+τ_h, e+τ_h, τ_h+τ_h and e+μ decay modes of τ lepton pairs. Here τ_h denotes semi-hadronic τ lepton decays.

Figure 1 illustrates the signal observed in the CMS data, which is compatible with the production of the Higgs boson with a mass near 125 GeV. Shown is the distribution of the mass of the Higgs candidates as reconstructed from the two τ leptons, $m_{\tau\tau}$. Figure 2 presents the signal strength μ, i.e. the ratio of the probed $H \to \tau\tau$ rate relative to the value predicted in the Standard Model, as measured in various analysed channels.

The measurements are consistent with each other and with the value $\mu = 1$, expected in the Standard Model. The combination of all analysed channels yields the measured value of $\mu = 0.78 \pm 0.27$. The Higgs boson mass measured by CMS in the $\tau\tau$ channel, $m_H = 122 \pm 7$ GeV/c^2, is consistent with earlier measurements performed in the $H \to \gamma\gamma$ and $H \to ZZ \to$ 4-lepton decay modes. The fact that the decay of the Higgs boson into τ leptons has been observed, but not that into pairs of muons or electrons, indicates that – as predicted by the Higgs mechanism – the coupling of the new particle to leptons is not universal.

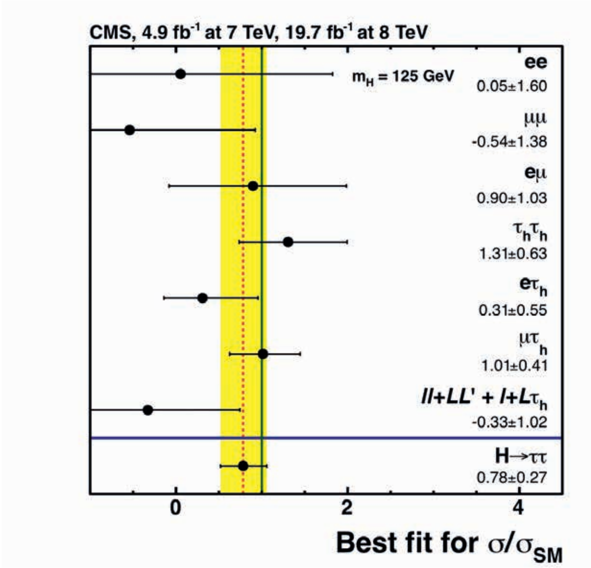

Figure 2

Values of the signal strength μ measured by CMS from various channels. Also shown is the value obtained by combining all the analysed channels.

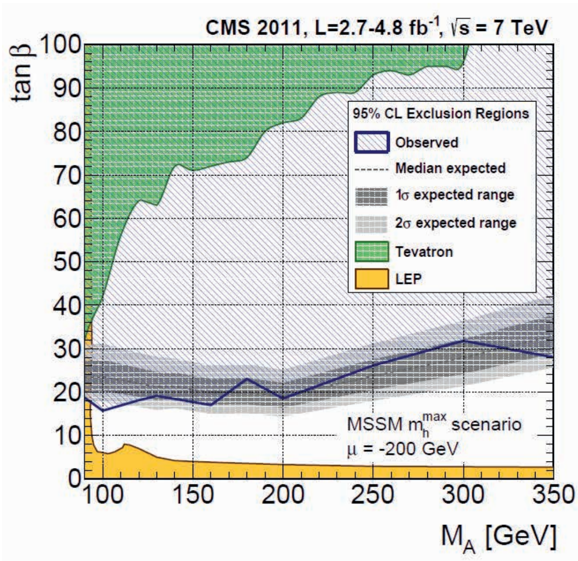

Figure 3

Observed and expected 95% confidence exclusion contours in the ($\tan\beta$, m_A) parameter plane in the m_h^{max} MSSM benchmark scenario. Results from CMS are compared with those from the Tevatron experiments.

Search for supersymmetric Higgs bosons in decays to *b* quarks

The study of fermionic Higgs decays is also crucial in searches for additional Higgs states, expected in theories with an extended Higgs sector. One example is the Minimal Supersymmetric Standard Model (MSSM), which predicts five physical Higgs states: two neutral scalars (*h* and *H*), one pseudo-scalar (*A*) and two charged bosons ($H^{\pm}$).

The DESY CMS group plays a leading role in the analysis searching for heavy neutral MSSM Higgs bosons produced in association with *b* quarks and decaying into a pair of *b* quarks. The rate of this process is enhanced at large values of $\tan\beta$, the ratio of vacuum expectation values of the two Higgs doublets in the MSSM, making this channel very attractive for MSSM Higgs boson searches. The overwhelming background from QCD processes and an efficient triggering of the signal events present major challenges for this study. Members of the DESY CMS group together with collaborators from INFN Padova in Italy have developed dedicated triggers that record events with multiple *b* quark jets. The analysis, designed by the DESY CMS group, searches for a resonant structure in the invariant-mass spectrum of the two leading *b* jets in the sample of selected events with one additional spectator *b* jet. The QCD multijet background is measured from data using a sample of events with at least three jets, out of which two jets are identified as *b* jets. Extrapolation of the background prediction to the triple *b* jet sample is then done by modelling the tagging of the third untagged jet. The study, performed in a data sample of about 4 fb^{-1} collected by CMS at 7 TeV, revealed no signal.

The sensitivity of the search for MSSM Higgs bosons decaying to *b* quarks has been significantly improved by combining results obtained by the DESY CMS group with the analysis performed by collaborators from INFN Padova. The latter study employed a trigger that records multijet events with signatures of muonic *b* hadron decays. No evidence of a signal is found in the combination of the two analyses, and the results of the search are translated into constraints on MSSM parameters. Figure 3 shows the upper 95% confidence level limit on $\tan(\beta)$ as a function of the CP-odd Higgs boson mass, m_A. The sensitivity of the search significantly surpasses the sensitivity of similar searches by the D0 and CDF experiments at the Tevatron collider of Fermilab near Chicago. This is the first time this kind of measurement is performed at the LHC.

Since its publication of MSSM Higgs boson searches in decays to *b* quarks using the LHC data at a centre-of-mass energy of 7 TeV, CMS has collected an additional 20 fb^{-1} at 8 TeV. With this data, the CMS collaboration continues its hunt for heavy supersymmetric Higgs bosons in fermionic decay modes, $H/A \to b\bar{b}/\tau\tau/\mu\mu$.

Contact:

Rainer Mankel, rainer.mankel@desy.de
Alexei Raspereza, alexei.raspereza@desy.de

References:

CMS Collaboration, "Evidence for 125 GeV Higgs boson decaying to a pair of tau leptons", arXiv:1401.5041, submitted to JHEP

CMS Collaboration, "Search for a Higgs boson decaying into a b-quark pair and produced in association with b-quarks in proton-proton collisions at 7 TeV", Phys. Lett. B722 (2013) 207

CMS tracker upgrade for high-luminosity LHC.

Investigating potential module designs and sensor materials

The CMS experiment at CERN's LHC collider has started an intensive R&D programme targeted at the upgrade of its tracker for the high-luminosity LHC (HL-LHC), which is planned to start in 2023. The HL-LHC is expected to deliver an instantaneous luminosity of 5 x 10^{34} $cm^{-2}s^{-1}$, which is a factor five more than the LHC design luminosity. Accordingly, radiation levels will also increase – a fact that has to be taken into account in the design of the tracker and the choice of its materials. In addition, radiation-harder sensors have to be used.

DESY and the University of Hamburg are collaborating on research activities that investigate potential sensor materials and layouts to be used under HL-LHC conditions. Technology CAD simulations of structures, including bulk radiation damage, are used to interpret measurement results. Irradiated and non-irradiated mini-sensors manufactured from epitaxial silicon material were tested in the DESY II test beam facility using the DESY test beam telescope beam telescope, and data are being analysed.

The higher track densities expected in the HL-LHC era demand a new tracker with higher granularity, in order to keep the occupancy at a reasonably low level and maintain the excellent tracking performance of the current detector. To achieve this, the new detector modules will have significantly shorter strips and a smaller pitch. Even with radiation-hard sensor material, the detector modules will be operated at -20°C to minimise the leakage current after irradiation and ensure good performance up to the end of the HL-LHC running.

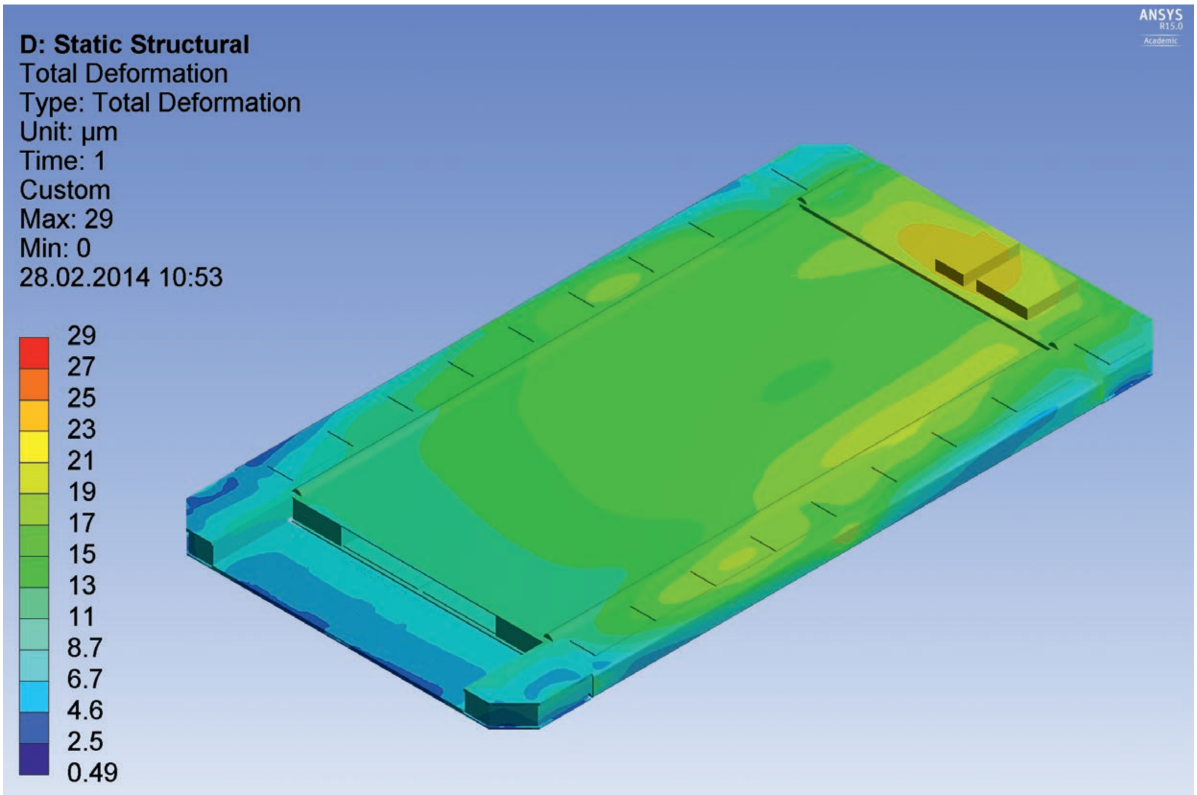

Figure 1

Mechanical finite element analysis of a pixelated trigger module

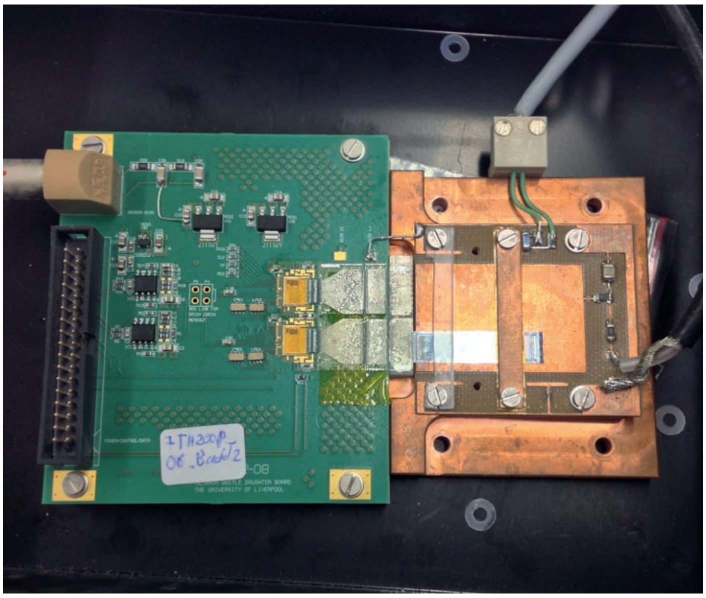

Figure 2

A highly irradiated mini-strip sensor wire-bonded to a readout board, ready for insertion into the DESY test beam telescope

It is also foreseen that the future tracker provides information to the CMS Level 1 trigger to ensure efficient triggering also under HL-LHC conditions. To achieve this, each detector module will consist of a sandwich of two sensors whose signals will be correlated by the front-end electronics already on the module. With the strong magnetic field of CMS, this allows for an on-module determination of the transverse momentum of particles and for the provision of a trigger signal for tracks with high transverse momentum. The modules are designed and optimised for their thermal and mechanical properties and a minimum amount of passive material at the same time. Two different module types are foreseen for the new tracker.

Above a radius of 60 cm, the utilised modules will consist of two silicon strip sensors with an active area of 10 cm x 10 cm and a strip length of 5 cm (“2S modules”). First prototype modules equipped with two novel front-end ASICs were characterised at the DESY test beam in November 2013. Based on the data obtained during this test beam campaign, the trigger efficiency of the modules was measured and the novel module concept could be confirmed.

At the inner radii, the tracker will be equipped with so-called PS modules, which are sandwiches made of a pixelated sensor and a strip sensor. The active area is 9 cm x 5 cm with a pixel size of 1.4 mm x 100 µm and a corresponding strip length of 2.5 cm. The DESY CMS group is heavily involved in the design and optimisation of this module type by performing thermal and mechanical analyses. Figure 1 shows the deformation of a PS module when operated at a temperature of -25°C. First parts for a mechanical prototype of the PS module are available. Their mechanical and thermal performance will be tested using the infrastructure available at DESY.

The new CMS tracker will be equipped with about 8000 PS and 7000 2S modules. Design work has started on the mechanical structures, with strong involvement of DESY in the design and production of small-scale prototype support and cooling structures.

Contact:

Andreas Mussgiller, andreas.mussgiller@desy.de

Doris Eckstein, doris.eckstein@desy.de

Anticipating plasma accelerators.

HiPACE: a novel, efficient quasi-static particle-in-cell code

In the rapidly developing field of plasma-based accelerators, particle-in-cell (PIC) simulations play an integral role. Indeed, they may be regarded as the major catalyst for the recent progress in the theoretical description of such accelerators. In addition, PIC simulations are used for the preparation and analysis of experimental wakefield studies. However, in many cases, full 3D PIC simulations are computationally too expensive, even on today's supercomputer infrastructure. The new PIC code HiPACE, jointly developed by DESY and LBNL in Berkeley, California, exploits the quasi-static approximation to significantly enhance the efficiency of simulations of plasma wakefield accelerators (PWFAs) while retaining the physical fidelity for a variety of scenarios.

Introduction

The experimental production of GeV-scale electron beams in plasma targets with lengths of a few centimetres and the energy doubling of 40 GeV electrons within a distance of less than a metre have promoted plasma acceleration to a promising technology candidate for future accelerators. Along with this experimental progress, numerical techniques are becoming more versatile and efficient and now allow for the study of non-linear and kinetic phenomena in plasma accelerators. The PIC technique is a well-established and indispensable pillar of plasma-based accelerator research: not only does it connect theory to experiment, it also substantially drives innovations in the field.

When executed on modern supercomputers, massively parallelised PIC codes allow for full 3D modelling of relativistic laser or charged-particle beam interactions with plasmas. However, a typical 3D simulation of a beam-driven plasma accelerator with a centimetre-scale plasma target at a density of about 10^{17} cm^{-3}, and with an energy gain in the GeV range, requires 10^4–10^5 core hours when simulated with a conventional full PIC code. Such excessive computational costs strictly constrain its usability for parameter scans, modelling of metre-scale propagation or comprehensive analyses of other typical issues in plasma-based acceleration.

Quasi-static method in HiPACE

Dynamics in plasma-based accelerators span a large range of time scales. For instance, a plasma evolves on a time scale that is given by the inverse plasma frequency, $\tau_p \sim \omega_p^{-1}$, while the beam evolves on a time scale of the order of the inverse betatron frequency, $\tau_\beta \sim \omega_\beta^{-1} \simeq (2\gamma)^{1/2}\, \omega_p^{-1}$, where γ is the beam energy. Thus, $\tau_p << \tau_\beta$ for highly relativistic ($\gamma >> 1$) beams. The disparity between these two scales is used to formulate the quasi-static approximation. Pictorially, the beam can be assumed to be rigid during the passage of a plasma electron. This approximation is used in the electromagnetic, relativistic, 3D and parallel quasi-static PIC code HiPACE (Highly Efficient Plasma Accelerator Emulation) to decouple the treatment of the plasma from that of the particle beam and thus enable a time step size that can be much greater than those in full PIC codes.

A simulation in HiPACE starts by depositing beam currents onto the computational lattice. The beam current distribution is then held static while plasma macro-particles and fields are advanced from the initial, unperturbed state. This implies that

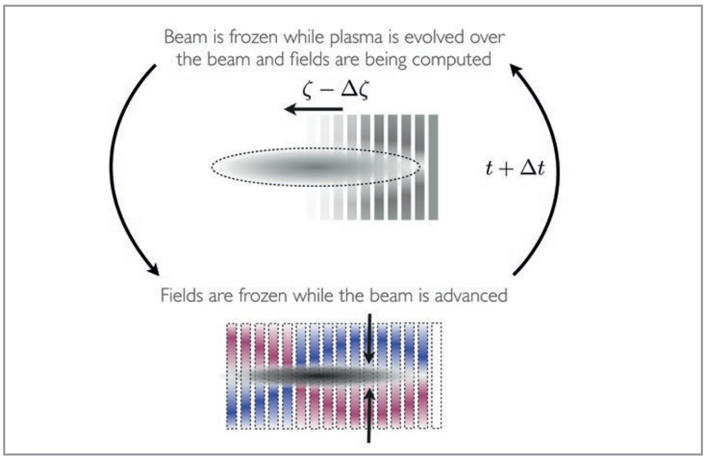

Figure 1

Basic cycle followed in the HiPACE calculation: the beam current distribution is frozen while the plasma is evolved. Subsequently, the plasma is assumed static while the beam is propagated.

the plasma and field integration starts from co-moving positions $\zeta = z - t$ ahead of the beam and evolves in the negative ζ direction (here, the time t is normalised to ω_p^{-1}; the z coordinate – the propagation direction – is normalised to $c\omega_p^{-1}$, where c is the speed of light). In a second step, the fields and the plasma are held static while the beam macro-particles are advanced in t. This time-staggered scheme is depicted in Fig. 1. In this scheme, the fields must be solved on a set of transverse 2D slices. Fortunately, in the quasi-static approximation, the Maxwell equations reduce to Poisson-type equations, which are efficiently solved by means of fast Fourier transforms.

The simulation domain in HiPACE is distributed over many processors with individual memories. Interprocessor communication is handled by the standardised message passing interface (MPI), which, when rigorously employed, allows an efficient distribution of the computational load.

Comparison to the full PIC code OSIRIS

In order to illustrate the capability of HiPACE to simulate common plasma acceleration problems consistently, we compare the results from a HiPACE simulation with those of a simulation of the same physical process by the full PIC code OSIRIS [1]. Specifically, we consider a highly relativistic 3D Gaussian electron beam with peak density $n_b/n_0 = 1.0$, where n_0 is the ambient plasma density, propagating through a homogeneous plasma.

Apart from the time step size, exactly the same physical and numerical simulation parameters are used for the two simulations. The time step in OSIRIS is constrained by the cell size through the Courant–Friedrichs–Lewy condition (here to $\Delta t = 0.0072$). The time step in HiPACE resolves the betatron motion of the beam (here $\Delta t = 4.21$). The results are compared in Figs. 2 and 3.

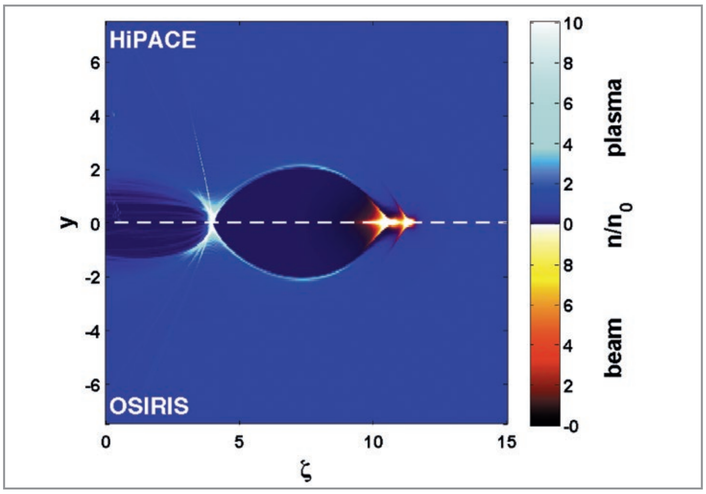

Figure 2

Comparison of simulation results from HiPACE (top half) and the fully explicit PIC code OSIRIS (bottom half). Depicted is a central slice of the plasma electron (blue) and beam particle (red) distribution. The variable y is the normalised transverse coordinate.

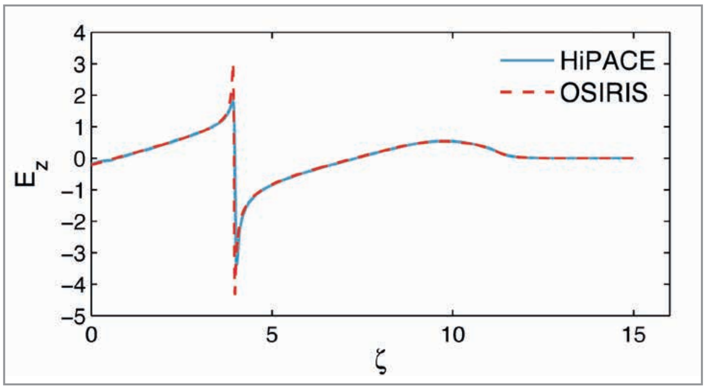

Figure 3

Comparison of the normalised on-axis longitudinal field in a HiPACE and OSIRIS simulation

Figure 2 shows a qualitative comparison of a central slice of the plasma and beam densities after a distance of $z = 450$ of beam propagation. The beam density distributions and plasma wave structure of the HiPACE results are qualitatively close to those of OSIRIS.

Figure 3 depicts the longitudinal field values, normalised to the wave-breaking field E_0, on the propagation axis. The curves coincide, apart from a significant deviation at the crest of the plasma wave, where a large number of plasma macro-particle trajectories cross and generate a spike in the longitudinal field. Of high importance, however, is the significant difference in the simulation run times. While OSIRIS needed 19 968 core hours to simulate this problem up to a distance of $z = 450$, HiPACE needed only 474 core hours for the same propagation distance, implying a speed-up by a factor of 42.

Conclusion

The PIC code HiPACE exploits the quasi-static approximation to decouple beam and plasma evolution in PWFA simulations and thus enables time steps that can be orders of magnitude larger than those in explicit PIC codes. It thereby makes simulations of a variety of problems in PWFA highly efficient. The speed-up is particularly interesting for studies of the possible use of PWFAs in high-energy physics applications. Comparisons with results obtained from OSIRIS indicate the capability of HiPACE to simulate a variety of plasma acceleration problems at significantly lower computational costs while retaining physical fidelity. This is achieved through the quasi-static numerical scheme, an efficient computational implementation and a parallelisation in all three dimensions.

Contact:

Timon Mehrling, timon.mehrling@desy.de
Jens Osterhoff, jens.osterhoff@desy.de

References:

[1] R.A. Fonseca et al., 2002 Proceedings of ICCS, Lecture Notes in Computer Science 2331 (2002); R.A. Fonseca et al., Plasma Phys. Control. Fusion 50 124034 (2008)

Strict synchrony.

Synchronisation to better than the X-ray pulse duration is demonstrated at FLASH

X-ray free-electron lasers (FELs) generate intense pulses with durations of a few tens of femtoseconds or even less – as short as atomic time scales. However, full exploitation of these light sources in experiments on atomic time scales is limited by insufficient synchronisation between all accelerator subsystems and independent optical lasers. Ideally, to obviate the need for additional arrival time measurements, the synchronisation accuracy should be smaller than the pulse duration. Although synchronisation is most often considered in the context of pump–probe experiments, this is merely part of a more fundamental issue for the overall performance and capability of generating stable X-ray pulses. At DESY's FLASH facility, this issue has been successfully addressed.

The level of synchronisation between a photon pulse generated by the FEL and an optical laser pulse severely affects the time resolution achievable in pump–probe experiments, in which one pulse is used to initiate dynamics in a specimen, while the other probes its development. A second limit is given by the duration of an individual pulse.

Although it is possible to measure the durations and the relative arrival time of the pulse pairs and use them to time-sort the acquired experimental data afterwards, these techniques can interfere with the actual pump–probe experiment and are inefficient, since most pulses occur outside their proper temporal overlap. Therefore, it is desirable to provide synchronisation accuracy to better than the pulse duration and thus overcome the need for additional arrival time measurements. Furthermore, such a level of synchronisation would improve the internal operation of the accelerator and thus FEL photon pulse generation.

Lastly, improved synchronisation is required for the development of next-generation seeded FEL light sources. Depending on the scheme used, FEL emission is initiated by an external laser and FEL pulses are generated at the seeding wavelength or a harmonic of it. Synchronisation is crucial for consistent temporal overlap of the electron bunch and the optical laser pulse.

To achieve the necessary level of synchronisation, a reference signal whose stability is beyond the capabilities of traditional

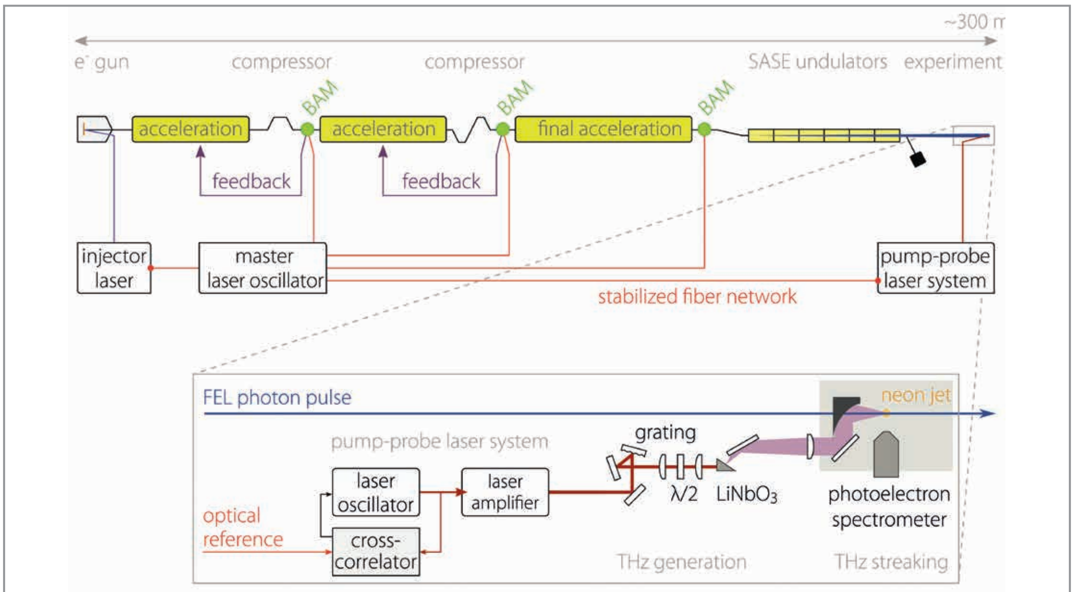

Figure 1

FLASH free-electron laser facility with laser-based femtosecond precision synchronisation system (top) and experimental geometry to evaluate the facility-wide synchronisation accuracy (bottom)

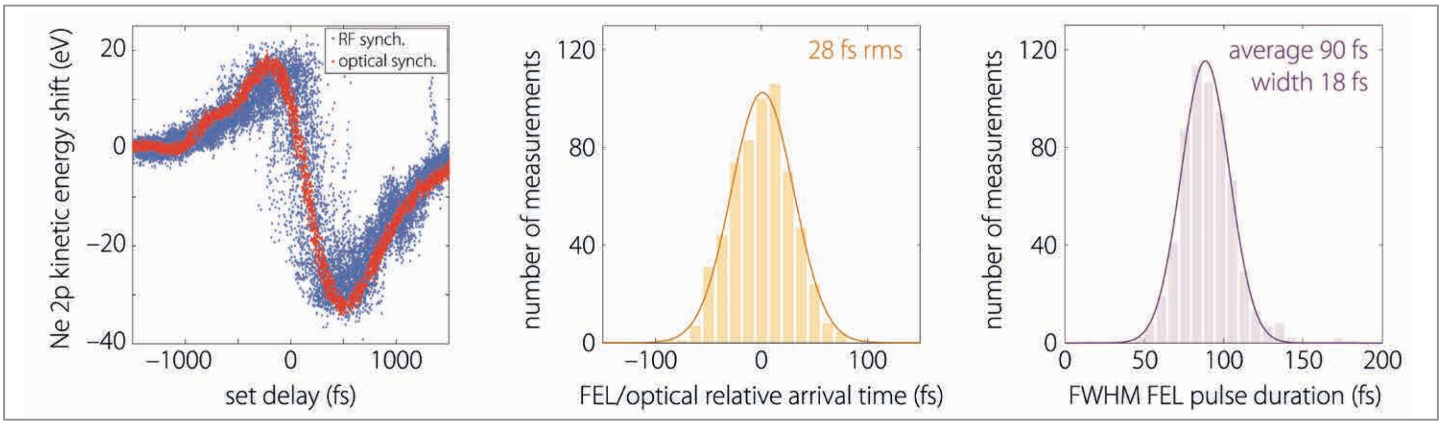

Figure 2

Results from THz photoelectron spectroscopy. Left: Streaking map comparison between traditional, RF-based synchronisation of the accelerator and the new, all-optical scheme. Centre: Relative timing fluctuation between the FEL and the optical laser pulses. Right: Distribution of FEL pulse durations reconstructed simultaneously with the timing jitter.

radio-frequency-based distribution systems is required. Consequently, an optical-laser-based synchronisation system, based on a low-noise mode-locked femtosecond optical oscillator, is being developed and implemented for both FLASH and the European XFEL. The system, depicted in Fig. 1, augments the existing radio-frequency distribution (see also [1]). The laser pulses, serving as clock signal, are distributed along the accelerator to all critical subsystems on optical fibres that are length-stabilized to a few hundred nanometres, and hence the laser pulse arrival time at the end of a fibre is stable to better than 1 fs (rms).

The reference pulses can be used to lock any external laser system, such as the FLASH pump–probe laser, to the optical clock by means of a novel optical cross-correlator, in which pulses of the external laser and the reference are directly mixed in a non-linear crystal. The relative timing fluctuation between the laser oscillator and the reference is found to be a small, but finite, 5 fs (rms), which is a major improvement of almost one order of magnitude over the traditional RF system.

To provide a basis for accelerator stabilisation, the arrival time of the electron bunches is measured by mixing optical reference pulses with the transient electric fields of the bunches [2]. This beam-based information is included in the feedback that regulates the accelerating fields in order to minimise arrival time fluctuation across pulse trains [3]. An electron bunch arrival time jitter of 19 fs (rms) was thereby achieved.

Single-shot terahertz (THz) photoelectron spectroscopy [4] is used to evaluate the performance of the facility-wide all-optical synchronisation infrastructure. In the experiment sketched in the lower part of Fig. 1, the FEL photon pulse ionises neon gas, thus producing a burst of photoelectrons that replicates the pulse's temporal shape. At the same time, a THz pulse that, depending on the relative timing, modifies the final kinetic energy of the photoelectrons is overlapped. When the timing is set such that overlap occurs on the streaking ramp of the THz vector potential, as shown in the left panel in Fig. 2, and the FEL pulse is shorter than the length of the ramp, the relative arrival time of the two pulses and the FEL pulse profile can be reconstructed. Since the THz pulse is generated by optical rectification, which is inherently synchronised to its drive pulse, the streaking measurement is equivalent to an arrival time measurement between the FEL and the optical laser pulses. The total timing fluctuation is finally found to be only 28 fs (Fig. 2), as a measure for the overall performance of the facility.

In addition to the retrieval of the arrival time jitter, the FEL photon pulse duration can simultaneously be reconstructed from the acquired photoelectron spectra, providing context for the observed timing jitter. For the given machine operation parameters, an average pulse duration of 90 fs FWHM (corresponding to 38 fs rms, Fig. 2, right panel) is observed, with an 18 fs width of the distribution.

In summary, this work demonstrates for the first time the interplay of all crucial components of the optical synchronisation system. Furthermore, an analysis of the uncorrelated jitter contributions suggests that the synchronisation accuracy scales with the FEL photon pulse duration and that the existing infrastructure can support sub-10 fs synchronisation accuracy, when shorter pulses are delivered. This level of performance, previously only available in table-top laser systems, is now within reach for kilometre-scale accelerator-based X-ray light sources such as FLASH and the upcoming European XFEL.

Contact:

Sebastian Schulz, seb.schulz@desy.de
Holger Schlarb, holger.schlarb@desy.de
Adrian Cavalieri, adrian.cavalieri@mpsd.mpg.de
Bernhard Schmidt, bernhard.schmidt@desy.de

References:

[1] S. Schulz et al. "Past, present and future aspects of laser-based synchronization at FLASH", Proc. IBIC2013, 753-756 (2013)

[2] M. K. Bock et al. "Benchmarking the performance of the present bunch arrival time monitors at FLASH", Proc. DIPAC11, 365-367 (2011)

[3] S. Pfeiffer et al. "Design of an optimal and robust controller for a free-electron laser exploiting symmetries of the RF system", Proc. CDC2012, 4253-4258 (2012)

[4] I. Grguraš et al. "Ultrafast X-ray pulse characterization at free-electron lasers", Nature Photon. 6, 852-857 (2012)

Cavities – stonewashed.

Exploring an alternative surface treatment for superconducting radio-frequency cavities

While the manufacture of superconducting radio-frequency (RF) cavities for the European XFEL X-ray laser is in full swing, particle physicists are striving to increase the cavities' maximum sustainable accelerating field to benefit the International Linear Collider (ILC), an electron–positron collider currently being planned by the Linear Collider Collaboration. To this end, an adaptation of a well-known technique in garment treatment is being explored: stone washing, in which abrasive materials of varying granularities are used to polish the inner surface of the cavities. Meanwhile, Japan is making big strides towards becoming the host of the ILC facility at a site in northern Japan in the Iwate prefecture. While the political decision-making process of the Japanese government is moving forward, DESY is preparing to bring its technical expertise to the table.

Cavities for the International Linear Collider

The public release of the technical design report (TDR) for the ILC [1], in a world-spanning event in June 2013, concluded the effort of hundreds of physicists to prepare a comprehensive design. The multivolume report documents the physics case and the plans for the accelerator and the detectors. The publication is timely: the recent discovery of a Higgs particle at the LHC at CERN calls for further precise exploration. Furthermore, Japanese physicists have declared that the ILC is their highest priority, and the Japanese government is currently examining the impact of such a project in preparation for a decision on whether or not to support it as host nation. A site has already been selected: the Iwate prefecture is ideally suited to host a linear collider of up to 50 km in length.

According to the TDR, the linear accelerators of the ILC will be based on the technology of 1.3 GHz superconducting niobium cavities similar to those that are currently being installed at the European XFEL in Hamburg. The experience gained by preparing the European XFEL has given Europe a unique position in the field of advanced cavity development.

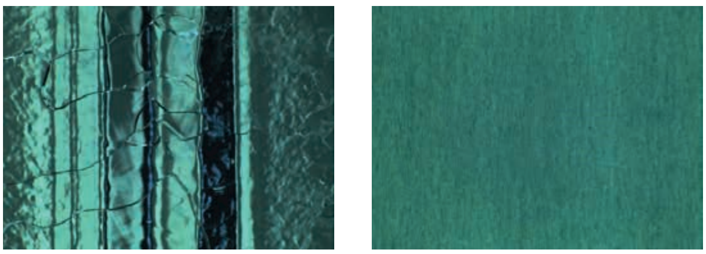

Figure 1

Left: Cavity welding seam after electropolishing.

Right: Same seam after centrifugal barrel polishing with successively finer abrasive materials.

To progress even further, 24 cavities specifically earmarked for ILC-related studies are being produced in parallel with the 800 cavities for the European XFEL. The goal of these detailed dedicated studies is to achieve an accelerating field strength suitable for use at the ILC. The additional production is supported by the ILC-HiGrade [2] grant of the Framework Programme 7 of the European Commission.

The cavities, consisting of nine cells, are manufactured from individual half-cells, which are then electron-beam welded. The welding is one of the most delicate steps in the manufacture since the weld is required to fully penetrate the niobium and yet not protrude at the seam. Subsequent chemical treatment with an aggressive acid augmented by an electrical current is used to smooth the surface, including the seam. This electropolishing procedure is well established and yields fields of 35 MV/m and more. It has been adopted as the "standard recipe" for ILC cavities in the TDR [1]. An image of a seam after electropolishing is shown in Fig. 1 (left).

An emerging alternative to electropolishing is centrifugal barrel polishing of the cavity inner surface with successively finer abrasive materials [3], of which a selection is shown in Fig. 2. Initially, the cavity is filled with a mix of stones, and subsequently with finer materials such as hardwood or polymer in a liquid environment. The effect on the same welding seam after an intermediate polishing step is shown in Fig. 1 (right).

Figure 3 shows a cavity being lowered into the housing of the polishing apparatus. When operated, the cavity rotates around its longitudinal axis and the whole assembly rotates around the centre axis of the polishing machine. A counterweight balances

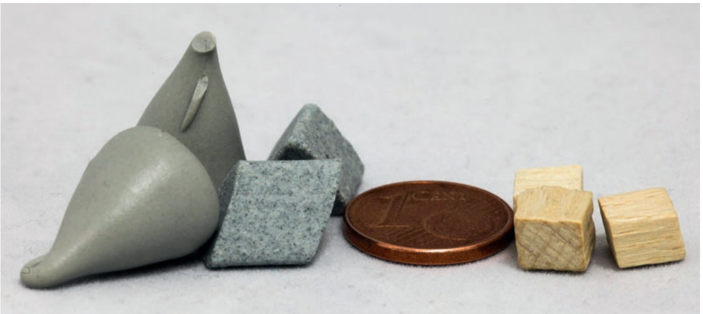

Figure 2

Abrasive materials used for “stone washing” the cavities

the weight of the cavity. A typical polishing step lasts from one to several days, depending on the amount of material to be removed and the granularity of the polishing medium. With coarse stones, the material removal rate is about 10 μm/h, and much less when finer abrasives are used. Between the polishing steps, the cavity is rinsed and cleaned in an ultrasonic bath. Figure 4 shows a scanning electron microscope (SEM) image of a small surface area cut-out after an intermediate polishing step using aluminium oxide on a wooden carrier: scratches and grooves from the abrasive process can be detected. The final step produces a mirror-like surface finish.

Figure 3

Cavity being lowered into the housing of the polishing apparatus

At present, the whole procedure is being commissioned in a controlled fashion for two applications: The polishing of cavities with coarse materials in order to remove a thickness of several hundred micrometres is being considered as a replacement for the bulk electropolishing step. The polishing of cavities with fine materials could also serve as a post-processing step for cavities with small surface irregularities. The mechanical polishing process has the added advantage that it can remove protruding materials irrespective of their chemical composition.

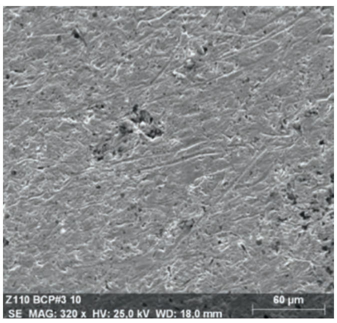

Figure 4

SEM image of a small surface area cut-out after an intermediate polishing step using aluminium oxide on a wooden carrier. The image reveals scratches and grooves from the abrasive process.

Finally, possible improvements in the imaging of the inner surfaces of cavities are being investigated. The inner surface of a nine-cell cavity is difficult to inspect. One method is to insert a special, remotely operated camera [4] into the cavity assembly to provide high-resolution images. However, the visual appearance of a surface region depends on illumination. To obtain a better understanding of the 3D surface structure, a silicone imprint can be taken as shown in Fig. 5. A two-component silicone compound is poured into the cavity in the region of interest and completely removed after hardening. The resulting silicone is a “negative” replica of the same region, which can be measured in all details.

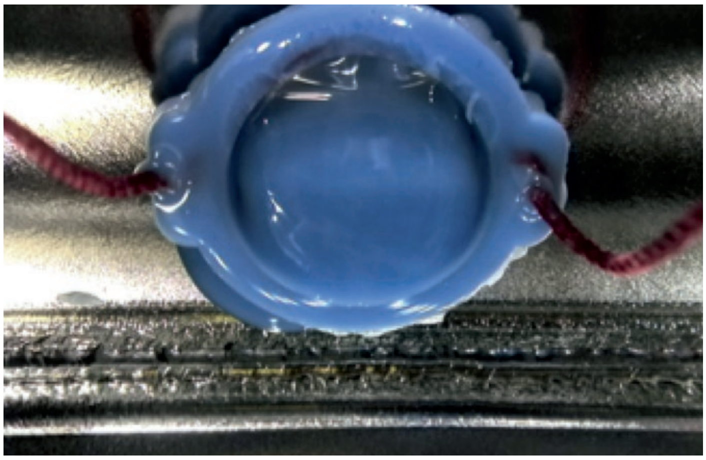

Figure 5

Two-component silicone compound used to take an imprint of the cavity 3D surface structure

The proposed techniques may contribute to optimising the manufacture and performance of the cavities for the ILC and will be further evaluated.

Contact:

Eckhard Elsen, eckhard.elsen@desy.de

References:

[1] C. Adolphsen et al., editor. *The International Linear Collider Technical Design Report – Volume 3.I: Accelerator R&D in the Technical Design Phase* and ibid, *Volume 3.II: Accelerator Baseline Design,* DESY-13-062

[2] A. Navitski et al., *ILC HiGrade cavities as a tool of quality control for European XFEL,* 16th International Conference on RF Superconductivity, SRF 2013, Paris, France, Sep. 23-27, MOP043. See also: ilc-higrade.eu

[3] C.A. Cooper and L.D. Cooley, *Mirror-smooth surfaces and repair of defects in superconducting RF cavities by mechanical polishing,* Supercond. Sci. Technol. 26 (2013) 015011

[4] A. Navitski et al., *R&D on cavity treatments at DESY towards the ILC performance goal,* SRF 2013, Paris, France, Sep. 23-27, MOP053

ILC technical design documentation.

Maintaining a complete, consistent and correct design of the International Linear Collider

The technical design documentation of the International Linear Collider (ILC) comprises the complete set of documents produced in the course of the engineering work conducted by the Global Design Effort (GDE). Through its engineering data management system (EDMS), DESY is hosting this documentation and playing a leading role in the design integration activities.

Providing the basis for the TDR

The year 2013 was pivotal for the ILC: it saw the GDE complete its mission with the publication of the technical design report (TDR) for the ILC facility after seven years of R&D (Fig. 1) and hand it over to the newly founded Linear Collider Collaboration (LCC). The TDR describes the baseline design for a future electron–positron linear collider with a centre-of-mass energy of 200 to 500 GeV and an upgrade option to 1 TeV. The design is based on the superconducting technology initially developed at DESY for the TESLA project and now utilised for the European XFEL X-ray free-electron laser.

However, even the 566 pages of the two TDR volumes that describe the accelerator are not enough to present all of the R&D and engineering work that went so far into the planning of this 31 km long machine. Fortunately, the development of the TDR benefited from a hard lesson learned from the ILC's reference design report (RDR) published in 2007: only a few years after the release of the RDR, it was realised that many of the design calculations, specifications, CAD drawings and 3D models were scattered over web pages or, worse, over individual hard disks in the many institutes around the world that had contributed to the RDR. As a consequence, it was decided that all data relevant to the TDR would be collected and maintained as a single, coherent body of documentation: the technical design documentation (TDD). Storage and maintenance of the TDD are being provided as an in-kind contribution by DESY through its web-based EDMS system.

Providing the basis for the cost estimate

Compared to other science projects, the cost of the ILC accelerator is large: according to the estimate of the TDR, it amounts to 7.78 billion US dollars in 2012 prices, plus 22.6 million person–hours of work. The credibility of any organisation – including the ILC – that prepares a project of this enormous scale depends in no small part on its ability to present a thorough, justifiable and stable cost estimate that withstands expert scrutiny. The same goals that apply to the design of the facility must also apply to its cost estimate, namely, it should be correct, complete and consistent with the engineering design. This is easier said than done.

Modern project management revolves around the work breakdown structure (WBS), which defines the scope of the overall project and all its parts. In this spirit, the TDD itself was organised along the lines of a WBS, with design documents for the numerous parts of the accelerator as deliverables. This structure, and the fact that all the

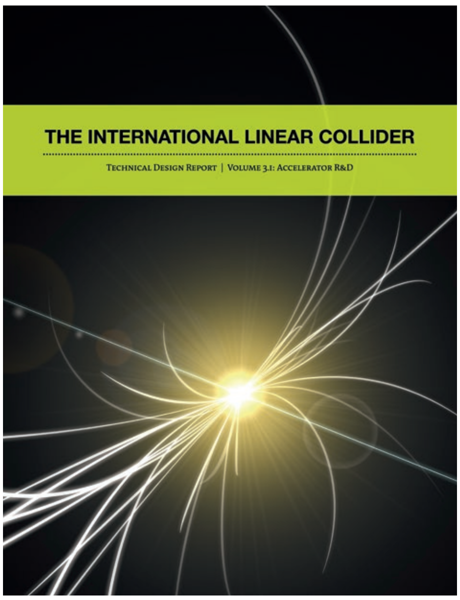

Figure 1

Cover of the ILC TDR

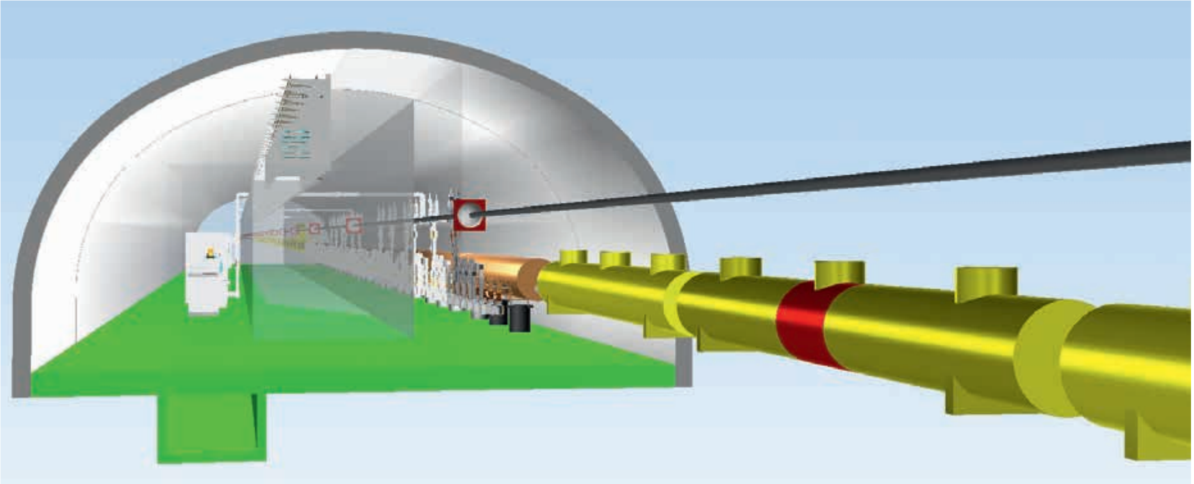

Figure 2

View of the Japanese "Kamaboko" (fishcake)-shape tunnel design, combined with a simpler visualisation of the main linear accelerator and return line (RTML) lattice

documents are available from a single source, namely the DESY EDMS, allows all cost estimates to be linked to more detailed estimates as well as to the engineering designs on which they are based. This makes the overall cost estimate traceable all the way back to the fully detailed design, and establishes the consistency of both.

Establishing consistency and completeness

Not only must the cost estimate be consistent with the engineering design, the design must also be internally consistent. The experience gained with large accelerator projects such as the European XFEL and PETRA III has allowed DESY to contribute to the integration of the ILC design, with the result of a complete and consistent lattice for the whole accelerator, which serves as the basis for the planning of the underground tunnels with their more than 70 km of beamlines and caverns (Fig. 2). Since the lattice elements are mapped to existing designs of components such as magnets or cryomodules (Fig. 3), it is possible to check that the component specifications correspond to the lattice design parameters (such as field strengths and apertures) and to generate the accurate component counts needed to estimate the costs and plan accordingly. With reference to the TDD, the cost review committee wrote: "An integrated lattice file, facilitating end-to-end optics simulation and CAD layout of components to check tunnel and component geometries, interferences, etc. has recently been compiled," and went on to add: "Congratulations! An absolutely essential feature!"

Preparing for change: traceability

In August 2013, Japan expressed interest in hosting the ILC, and the Japanese ILC site selection committee followed up by selecting a site in the Kitakami mountains of the Iwate prefecture in northern Japan. Starting with the Linear Collider Workshop held in Tokyo in November, activities are now under way to find the best placement for the accelerator in the region, to check whether the existing baseline design is suitable for the local circumstances and to identify where it can be, or must be, adapted and optimised. In the site-dependent design phase now under way, the design will inevitably change in many places. Maintaining its integrity and consistency so that all stakeholders have reliable and up-to-date information at hand at any time requires careful change management. The ILC TDD in EDMS captures dependencies between design documents with links that show which documents may need revision after another document has been updated. This traceability is an essential prerequisite for propagating the looming design changes through the whole design.

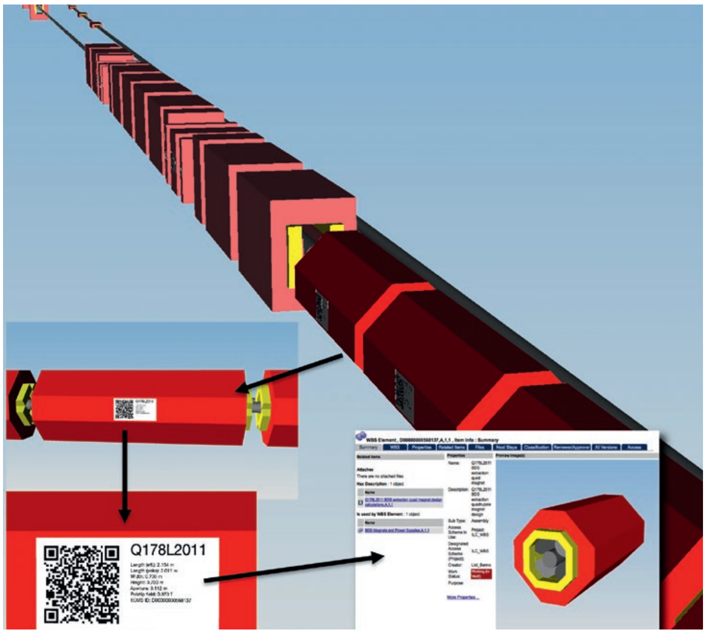

Figure 3

Part of the visualisation of the beamlines in the beam delivery system (BDS). The magnets in the visualisation are labelled with their type and key specifications and have a link to the component description in EMDS.

Contact:

Lars Hagge, lars.hagge@desy.de
Benno List, benno.list@desy.de

ILD detector performance.

Optimising a detector for the next big project in particle physics

The International Linear Collider (ILC) is a proposed electron–positron collider with a centre-of-mass energy ranging from 250 to 500 GeV and with an option to upgrade to 1 TeV. The ILC technical design report (TDR) describes the physics opportunities the facility will offer in light of the recent results from the LHC collider at CERN, as well as the technical design of its accelerator systems and particle detectors. The ILD is one of two detector designs developed for the ILC. It is optimised for precise impact parameter measurements and for "particle flow" event reconstruction, which requires highly granular calorimeters and excellent track momentum resolution. A realistic simulation model with an engineering level of detail, supplemented by sophisticated reconstruction algorithms, is used to study the performance of the future detector and its physics capabilities.

Physics requirements

The rich and unique physics programme planned for the ILC is imposing challenging requirements on the performance of a particle detector. For example, a prime goal of the physics programme is a model-independent measurement of the Higgs mass and cross section using so-called Higgs-Strahlung events, in which a *Z* boson radiates a Higgs boson and subsequently decays into a lepton pair (Fig. 1); a meaningful Higgs mass measurement would demand that the decay leptons of the *Z* boson be measured with the unprecedented momentum resolution of $2 \cdot 10^{-5}$ GeV^{-1} [1]. Other physics goals demand that the *W* and *Z* bosons that decay into two jets be recognised and distinguished from each other; this, in turn, demands excellent jet energy resolution. Excellent impact parameter resolution is also needed to pick out decays of hadrons containing *b* quarks and thus tag the flavour of jets; this is essential for many studies, for example the accurate measurements of the Higgs branching ratios.

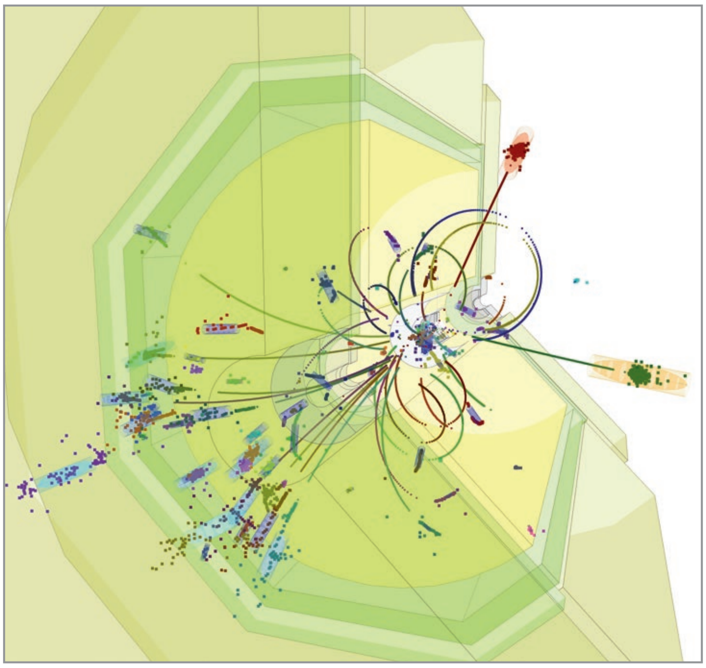

Figure 1

Simulated Higgs-Strahlung event ($e^+e^- \rightarrow HZ, Z \rightarrow \mu^+\mu^-$) in the ILD detector at 250 GeV

The required detector performance can only be reached by combining intense detector R&D with novel technologies and the development of sophisticated reconstruction algorithms. The relatively high event multiplicities and the high energy of the produced particles at 1 TeV centre-of-mass energy pose additional challenges to the detector as well as to the reconstruction algorithms.

Simulation and reconstruction software

To understand and optimise the detector performance, the ILD concept group created a detailed simulation model in Geant4 that follows very closely the existing engineering models (Fig. 2). Particular attention was paid to the proper modelling of detector imperfections, such as gaps and dead areas, as well as to the material added by cabling and supply infrastructures [3].

A large set of reconstruction algorithms addresses pattern recognition (needed to find charged-particle tracks), calorimeter shower identification and flavour tagging based on multivariate techniques. Of particular importance for the measurement of

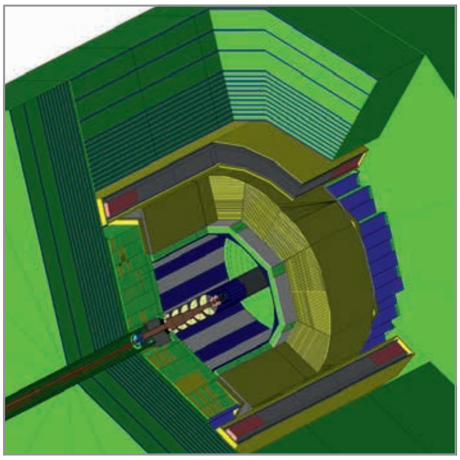

Figure 2

Detailed simulation model of the ILD detector used for the detector performance studies in the TDR

the energy of hadronic particle jets is the particle flow algorithm, which tries to identify every single particle created in the interaction, both charged and neutral, by combining reconstructed tracks and calorimeter clusters.

Detector performance

Many tens of millions of Monte Carlo events have been produced on the Grid and are being used to estimate the achievable performance of the ILD detector and to demonstrate its physics capabilities by analysing a set of carefully chosen physics benchmark reactions. Among the key performance indicators studied in the TDR [3] are the momentum resolution of charged particles and the jet energy resolution. Figure 3 shows the resolution of the inverse transverse momentum of muons as a function of momentum for a range of polar angles. The lines show the design goal for ILD based on the Higgs mass measurement mentioned above.

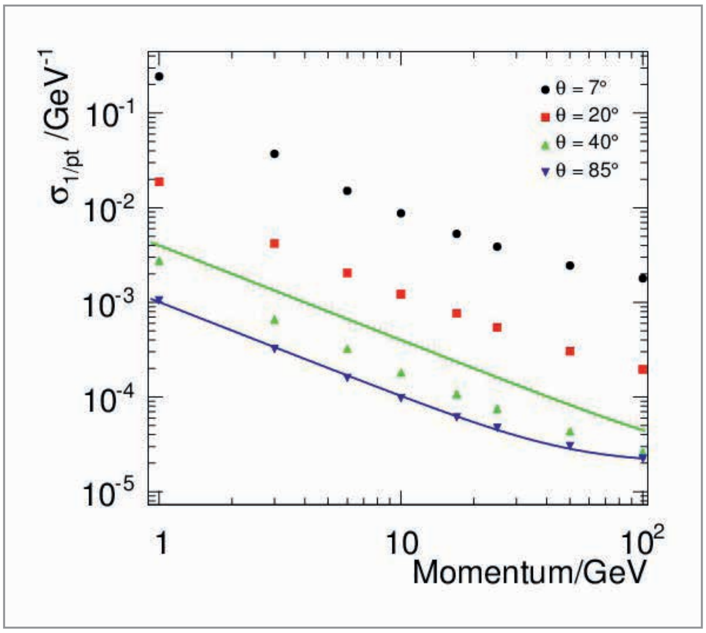

Figure 3

Resolution of the inverse transverse momentum for the ILD tracking system. The lines show a parameterisation of the design goal.

The relative jet energy resolution as a function of polar angle (cos θ) is shown in Fig. 4 for a few selected jet energies. The achieved resolution of ~4% or better for most of the kinematic range will allow *W* and *Z* boson decays to be separated.

These and other results from the TDR show that the design of the ILD detector has now reached maturity, and they clearly demonstrate that the detector will meet its design goals for the whole range of centre-of-mass energies from 250 to 1000 GeV.

Further detector optimisation

The TDR marks a milestone for the ILD detector but not the end of the road for R&D. An interesting question remains: is it possible to find an alternative detector design that performs equally well but at lower cost? The main cost drivers are the large calorimeters inside the magnetic field and the surrounding coil. The ILD collaboration has started a new programme of detector optimisation that focuses on understanding the impact of reducing detector size on performance. A number of expert groups are now attempting to find significant cost reductions through the further optimisation of their detector components, and already some interesting possibilities that entail only minor performance compromises are emerging. This refinement process will surely continue for years to come.

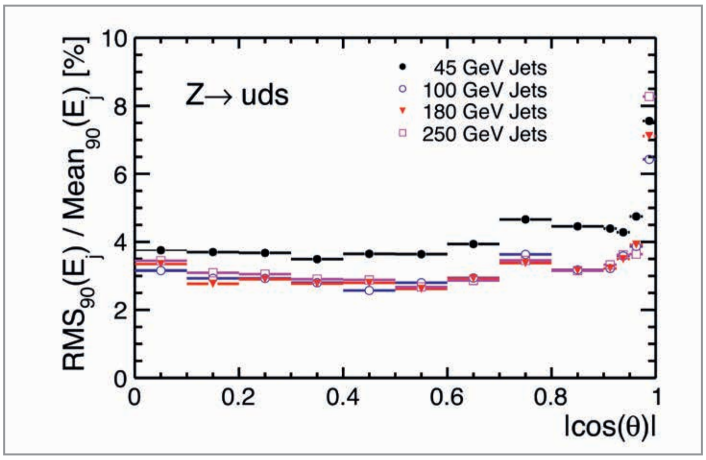

Figure 4

Jet energy resolution as a function of polar angle for the ILD simulation model

Contact:

Frank Gaede, frank.gaede@desy.de
Ties Behnke, ties.behnke@desy.de

References:

[1] T. Barklow, "Physics Impact of Detector Performance", Presented at International Linear Collider Workshop, LCWS 2005

[2] S. Agostinelli et al., "GEANT4: A Simulation toolkit", Nucl. Instrum. Meth. A506 (2003) 250–303

[3] T. Behnke, J. E. Brau, P. N. Burrows, J. Fuster, M. Peskin, M. Stanitzki, Y. Sugimoto, S. Yamada et al., "The International Linear Collider Technical Design Report – Volume 4: Detectors", arXiv:1306.6329 [physics.ins-det]

The new look of hadron showers.

Measuring and modelling hadron showers with unprecedented granularity

The energy reconstruction of particles and jets, as well as the detectors they rely on, must fulfil ambitious goals at the International Linear Collider (ILC). ILC jet reconstruction will require the use of particle flow algorithms that reconstruct individual particles in the detector component, providing the best precision for every particle type. This demands that particles in hadron showers be resolved from each other, which, in turn, requires unprecedented detector granularity, especially in the hadron calorimeters. The CALICE collaboration has developed large prototype calorimeters with volumes up to a cubic metre with the required granularity. Beam tests have not only demonstrated their feasibility for the ILC, but also provided detailed input for modelling hadron showers in simulation programs.

Simulation of hadron showers

Simulating hadron shower evolution is challenging since no single physics model is able to describe hadronic interactions over the full energy range, which extends from the first hard interaction at up to several TeV down to the MeV range of nuclear binding effects. Therefore, different approaches must be combined and transition regions must be bridged. The first simulation codes were based on phenomenological parameterisations of the interaction and aimed at reproducing average shower properties. In the past decade, significant progress has been made in replacing these empirical parameterisations by more fundamental, theory-driven models within the Geant4 framework [1]. The new models are not tuned to calorimetric measurements since the latter provide at best indirect guidance for adjusting model parameters; rather they rely on knowledge of the differential cross sections of hadron scattering by nuclei. Calorimeter data are nonetheless essential for validation.

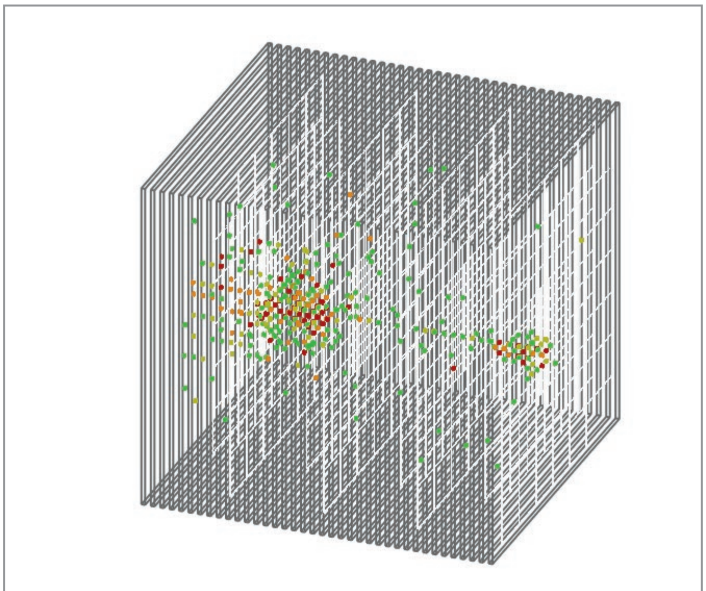

Figure 1

Shower produced by an 80 GeV pion in the CALICE scintillator–tungsten hadron calorimeter. The pion enters from the right. The colours denote small (green), medium (yellow) and large (red) energy depositions.

The development of the theory-driven models was strongly motivated by the needs of the LHC experiments and, more recently, also by the demands of particle flow calorimetry. The models focus on the internal shower structure, particle composition and even time evolution. Major revisions, guided by detailed comparisons with LHC test beam data, have resulted in a good description of LHC test beam data. However, given the much higher granularity of the CALICE prototypes, a more stringent test would be a detailed comparison with CALICE test beam data. Such a comparison would also serve as an essential basis to validate the concept of particle flow calorimetry. In addition, the fine granularity of the prototypes gives access to new observables related to the internal shower structure, such as its charged track multiplicity.

Track multiplicities in hadron showers

The cascade evolution of a hadron shower leads to a tree-like structure, with both visible and invisible branches. For illustration, an 80 GeV pion shower measured in the CALICE scintillator–tungsten hadron calorimeter is shown in Fig. 1. Centres of dense activity, due either to electromagnetic sub-showers or the short-ranged nuclear evaporation products that surround hard interactions, can be seen. In between are

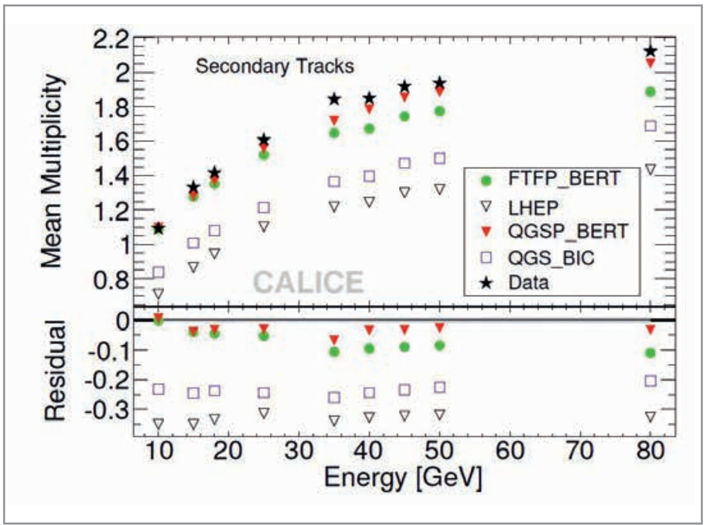

Figure 2

Dependence of the mean track multiplicity in a hadron shower on the shower energy. Modern, theory-driven shower models (QGSP_BERT, FTFP_BERT) agree with the data, while older parameterisations (LHEP, also used in QGSP-BIC) fail to reproduce the showers at this level of detail.

regions in which leading interaction products travel distances of the order of a nuclear interaction length, leaving at most a track signature, or possibly no trace at all. Particle flow algorithms exploit these fine-grain measurements of the shower substructure, for example by using the pointing information of tracks to or from clusters of energy deposition, to improve the precision of shower parameter measurements. It is thus highly important to understand whether the corresponding effects are adequately modelled in the simulations.

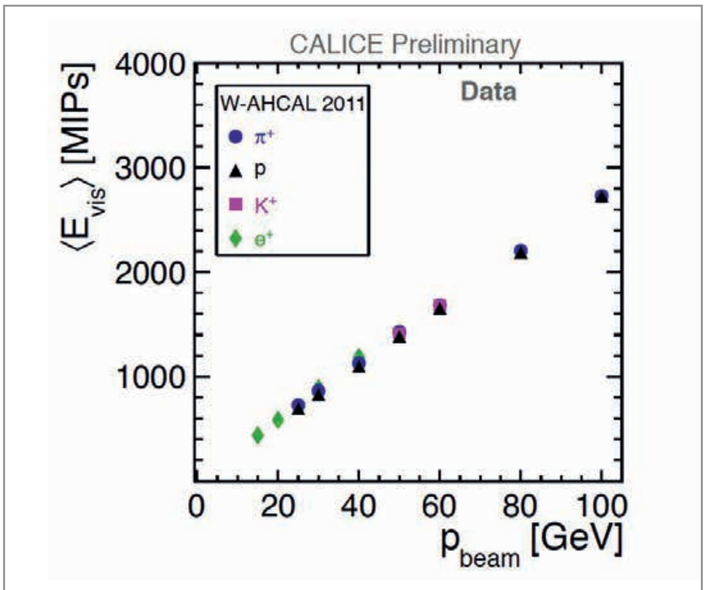

Figure 3

Dependence of the mean visible energy in a tungsten sampling calorimeter on the beam energy for electrons, pions and protons

To illustrate the level of detail that the CALICE data provide, Fig. 2 displays the dependence of the mean track multiplicity of a hadron shower on its shower energy (the primary track of the incoming hadron has been excluded). The multiplicity is well reproduced by recent versions of Geant4, e.g. FTFP_BERT, while the older parameterisations like LHEP fail. Although not fully perfect, the level of agreement achieved is a triumph for the modern, theory-driven shower models.

Hadron calorimetry with tungsten absorber

Interest in the use of tungsten as an absorber material instead of the more usual steel has recently increased since it would allow for a more compact detector. The nuclear interaction length (which determines the length of hadronic cascades) of tungsten is nearly half that of steel. However, in tungsten, neutrons are expected to play a larger role in the shower development, and their treatment requires special care in the simulations. In order to test the suitability of tungsten absorbers for a particle flow calorimeter, CALICE also studied hadron calorimeter prototypes built with tungsten absorbers in both electron and hadron beams. The calorimeter response for electrons, pions, protons and kaons for beam energies up to 100 GeV is shown in Fig. 3. While most sampling calorimeters with steel absorbers differ in their response to hadrons and electrons of the same energy, the combination of tungsten absorber and scintillator responds to electrons and hadrons in a very similar way. This behaviour is well reproduced by a Geant4 simulation supplemented by a detailed modelling of the interaction and capture of neutrons with energies below 20 MeV.

Summary

Particle flow reconstruction uses shower topology information in great detail and therefore requires highly granular calorimetry. Test beam data, recorded with fine-grained CALICE prototypes, were used to probe shower simulation algorithms in much more detail than previously possible. The results confirm the recent progress made in improving the theory-motivated shower models implemented in the Geant4 framework, and provide a basis for further refinements. Overall, the more recent hadron shower models reproduce the details of the shower evolution, such as the multiplicity of charged track segments, with an accuracy of a few percent. Comparisons of data from the CALICE tungsten prototype with simulation show that the shower models are also valid for modelling heavier materials.

Contact:

Felix Sefkow, felix.sefkow@desy.de
Katja Krüger, katja.krueger@desy.de

References:

[1] S. Agostinelli et al., "GEANT4: A Simulation toolkit", Nucl. Instrum. Meth. A506 (2003) 250–303

[2] C. Adloff et al. (CALICE Collaboration), "Track segments in hadronic showers in a highly granular scintillator-steel hadron calorimeter", JINST 8 P09001 (2013)

[3] CALICE Collaboration, "Shower development of particles with momenta from 10 to 100 GeV in the CALICE scintillator-tungsten HCAL", CALICE Analysis Note CAN-044

Spin tracking at the ILC.

Understanding systematic effects for high-precision polarimetry

The International Linear Collider (ILC) foresees the collision of beams with polarisations as high as 80% for electrons and 30% for positrons. Precisely measuring the polarisation needed by the ILC physics programme requires upstream and downstream polarimeters and a thorough understanding of the effects on polarisation of the beam delivery system and in the interaction region.

Polarimetry challenge

Selecting different values for the longitudinal polarisation P_z at the ILC collision point can enhance or suppress cross sections of signal and background processes, and thus increase sensitivities in many measurements.

Some measurements planned for the ILC require that the polarisation be known precisely, for example, $dP/P < 0.25\%$ for measurements of parity-violating asymmetries and $dP/P < 0.1\%$ for a possible high-statistics runs at the Z boson mass [1]. Such a precise measurement requires the use of dedicated Compton polarimeters positioned upstream and downstream of the interaction region (Fig. 1).

Spin tracking in the beam delivery system

While the polarimeters are designed to achieve measurements with a sub-percent precision, they do not supply the value of the polarisation at the interaction point, which must therefore be inferred by interpolation. Understanding the systematics of the interpolation is crucial for understanding the systematic uncertainties of the measurement. To do so, detailed simulations with particle tracking code, which also includes the depolarising effects of collisions, have been carried out [2]. Figure 2 shows that the resulting longitudinal polarisation before the collision differs from the downstream polarisation by more than 0.5%, much more than the needed precision. The result emphasises the importance of the spin tracking studies.

The beam–beam interactions change not only the polarisation of the particle bunches, but also the bunch shapes and energy distributions. This must also be taken into account at the downstream polarimeter, where the laser beam samples only a part of the bunch area. Figure 2 shows simulated polarisation measurement values at the downstream Compton polarimeter for several laser spot sizes.

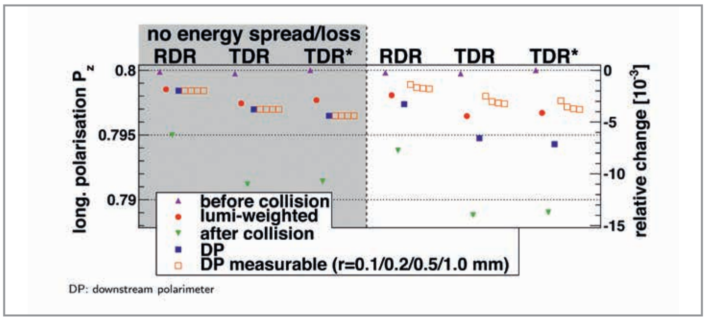

Figure 2

Longitudinal polarisation after the collision, at the downstream polarimeter and luminosity-weighted [3]. Results for the ILC TDR beam parameters are labelled TDR. The open squares illustrate the effect of different laser properties for the downstream polarimeter.

Conclusion

The ILC physics programme requires the beam polarisation to be measured to high precision. Simulations show that the depolarising effects of the beam–beam interactions and spin precession are large compared to the needed precision and thus need to be understood in detail.

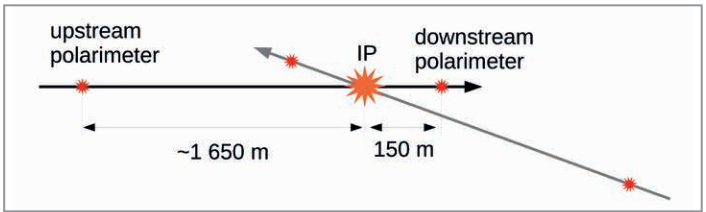

Figure 1

Compton polarimeters in the beam delivery system of the ILD, one of the two detectors proposed for the ILC. IP denotes the ILD interaction point [2].

Contact:

Jenny List, jenny.list@desy.de

References:

[1] T. Behnke, J. E. Brau, P. N. Burrows, J. Fuster, M. Peskin, M. Stanitzki, Y. Sugimoto and S. Yamada et al., The International Linear Collider Technical Design Report – Volume 4: Detectors", arXiv:1306.6329 [physics.ins-det]

[2] M. Beckmann, Spin Transport at the International Linear Collider and its Impact on the Measurement of Polarization, DESY-THESIS-13-053

[3] M. Beckmann, Challenges for Polarimetry at the ILC, EUCARD Workshop, Mainz, 2014

Detectors for polarimetry at the ILC.

Cherenkov detectors and calibration systems for high-precision polarimetry

The International Linear Collider (ILC) requires Compton polarimetry at least a factor 2 more precise than at any previous collider. Two different R&D approaches for measuring the Compton-scattered electrons promise to achieve the necessary reduction of systematic uncertainties to $dP/P < 0.25\%$. The limiting source of uncertainty is the calibration of the photon detectors that measure the Cherenkov light emitted by the Compton-scattered beam electrons in the radiator medium. To keep the precision of the polarisation measurement below 0.1%, the non-linearity of the photon detectors must not exceed 0.5%.

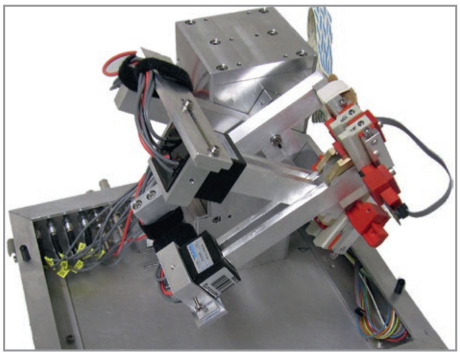

Figure 2

Prototype of the quartz Cherenkov detector operated in the DESY test beam [3]

Permille-level calibration system

Permille-level measurements of photon detector non-linearities are extremely challenging. A promising technique exploits the difference between the response to a variable base light pulse alone and the combined response to the base pulse and a small but very reproducible add-on. In case of perfect linearity, the response difference is independent of the intensity of the base pulse. An observed variation of the differential response can be used to linearise the response of the detector, provided the required precision can be reached.

Figure 1 shows the LED driver board that has been developed to provide 10 ns short light pulses matching the specific requirements for polarimetry in terms of stability, dynamic range and applicability of the detector [1], along with a sketch of the setup used to successfully demonstrate that the precision goal can be reached [2].

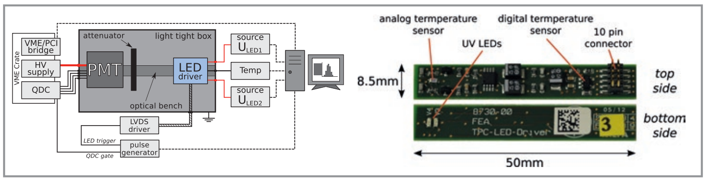

Figure 1

Schematics of the test setup (left) and the LED driver (right) developed for the polarimeter calibration system

Self-calibrating detector

For small light yield, a detector channel shows a broad signal response, corresponding to the average number of Compton electrons. For a substantially larger light yield, individual peaks, superimposed on the expected Poisson distribution of the actual Compton electrons, can be resolved. The measurement of the distance between the peaks will lead to an *in situ* linearity calibration [3].

A prototype detector based on quartz as Cherenkov medium (Fig. 2) was built and successfully operated in the DESY test beam with single electrons. The observed single-electron response implies that signals of up to 20 electrons can be resolved. We plan to confirm this result soon by checking the response to a multielectron beam.

Conclusion

The ILC requires the polarisation of both beams to be measured to better than 0.25%. This entails permille-level calibration of the detectors employed in the Compton polarimeters. Two complementary approaches have been investigated in test setups and at the DESY test beam. Results indicate that the precision goal can be achieved by both approaches. A full evaluation and comparison of both schemes is planned as a next step.

Contact:
Jenny List, jenny.list@desy.de

References:

[1] C. Bartels, J. Ebert, A. Hartin, C. Helebrant, D. Kafer and J. List, Design and Construction of a Cherenkov Detector for Compton Polarimetry at the IIC, JINST 7 (2012) P01019
[2] B. Vormwald, From Neutrino Physics to Beam Polarisation – a High Precision Story at the ILC, DESY-THESIS-2014-006
[3] A. Vauth, A Quartz Cherenkov Detector for Polarimetry at the ILC, EUCARD Workshop, Mainz, 2014

Positrons for a Higgs factory.

ILC positron source design for low-energy operation

The ILC will collide electrons and positrons at centre-of-mass energies of up to 500 GeV or possibly higher. In light of the Higgs boson discovery at the LHC in 2012, it is planned to start the ILC as a 250 GeV Higgs factory before moving on to higher energies. To this end, special optimisation studies were needed to prove that the ILC baseline positron source is suited to deliver enough positrons at this low energy and thus avoid an expensive alternative.

Positron generation and capture

In the ILC baseline design [1], the electron beam is used to create positrons: before colliding, the electron beam passes a helical undulator, which generates circularly polarized multi-MeV photons that then impinge on a thin target to generate electron–positron pairs. The positrons are then focused by a pulsed magnetic focusing device called a flux concentrator (FC), captured and accelerated in radio-frequency (RF) cavities. The undulator parameters were optimized to cover a centre-of-mass energy range starting from 350 GeV. For an electron beam of 120 GeV, however, fewer photons are created, which are also less energetic. Less photon energy implies lower efficiency for conversion into electron–positron pairs. It was not clear whether the baseline source could supply the needed flux. To get around this problem, the ILC technical design report suggests that an additional electron beam with higher energy, alternating with the electron beam used for physics collisions, could be used to create the positrons. However, since such a scheme is technically demanding and power hungry, a detailed study was undertaken to see if the baseline positron source design itself could also be made to work at low energies.

A Geant4-based code [2] was used to simulate the positron source and evaluate its performance at low energy. The study found that the use of the full effective length of the undulator would improve positron yield by 35%. It was also shown that optimising positron capture in the FC would result in further gains. The effective FC aperture was found to be the parameter with the biggest effect on positron yield. Increasing the aperture from about 6 mm to 8.5 mm improved the positron yield by about 14%, as shown in Fig. 2. The larger aperture would not result in an increase in heat load and stress compared to higher energies.

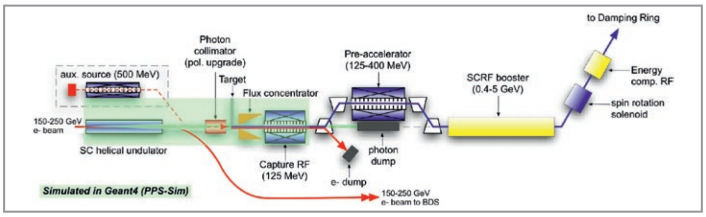

Figure 1

Scheme of the undulator-based positron source for Higgs boson production, including the elements up to the damping ring [1]

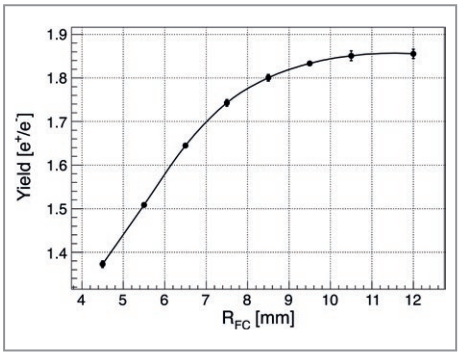

Figure 2

Positron yield as function of FC aperture radius

Conclusion

The baseline design of the ILC positron source has been shown to also be suitable for a 250 GeV Higgs factory. The required number of positrons, including the 50% safety margin stipulated in the ILC design, can be generated if the full undulator length is used and the aperture of the flux concentrator is increased to a radius of 8.5 mm [2]. The polarisation of the positron beam in this scenario is about 30%.

Contact:

Sabine Riemann, sabine.riemann@desy.de

Andriy Ushakov, andriy.ushakov@desy.de

References:

[1] C. Adolphsen et al., The International Linear Collider Technical Design Report – Volume 3: Accelerator, arXiv:1306.6353 and arXiv:1306.6328 [physics.acc-ph]

[2] A. Ushakov et al., LC Note LC-REP-2013-019, May 2013

Emerging detector technologies.

New sensors for applications in harsh radiation environment

Detectors near the beams of accelerators and colliders may experience large and rapidly varying radiation doses. For example, when the electron and positron bunches in the planned International Linear Collider (ILC) are brought to collision, a very large number of energetic photons (termed collectively as beamstrahlung) are emitted in the very forward region due to the high charge and energy of the bunches. Thus, any detector positioned near the beam must be extremely radiation-tolerant. The FCAL collaboration has studied several potentially applicable sensor materials. Recently, for the first time, a detector based on sapphire sensors was investigated in the DESY test beam, with surprisingly good results. These detectors are also interesting options for beam condition monitors at the European XFEL and the LHC.

Sensors made of sapphire

Single-crystal sapphire wafers are commercially available. For our purpose, we cut samples of 1 cm^2 size and 500 µm thickness, which were then metallised on both sides with pads made of thin Al/Pt/Au layers, as shown in Fig. 1.
The leakage current of the sensors was measured on a probe station and found to be in the picoampere range.

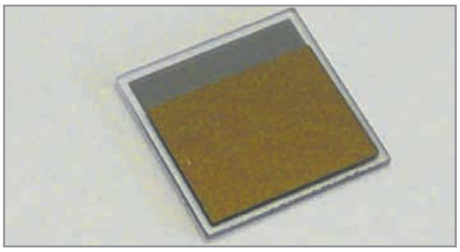

Figure 1
Sapphire sensor prepared for assembly

Radiation hardness studies

Several sensors were exposed to a high-intensity electron beam at the linear accelerator of TU Darmstadt, Germany. The beam energy was set to 10 MeV, in the expected range for beamstrahlung at the ILC. The signal current as a function of the absorbed dose is shown in Fig. 2 for two sensor samples. As can be seen, the signal size degrades to about 30% after a dose of 10 MGy, corresponding to 10 years of operation at the ILC.

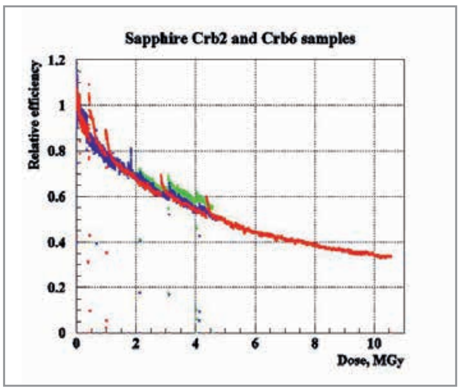

Figure 2
Signal current as a function of the absorbed dose for two sapphire sensor samples

Results at the DESY test beam

A stack of eight sensors, as shown in Fig. 3, was prepared for measurements in the test beam at DESY II. Every second pad was connected to high voltage, and the pads in between were read out with a charge-sensitive amplifier. The signal size was measured as a function of the voltage. We found a signal size of 22 000 electrons per crossing particle, corresponding to a charge collection efficiency (CCE) of 10% at 1000 V.
In comparison to other extremely radiation-hard sensors, such as diamond, sapphire is relatively cheap and hence a promising alternative for applications where other sensors would fail due to the high radiation field.

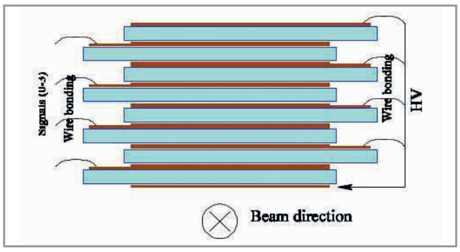

Figure 3
Sketch of sapphire cube prepared for test beam

Contact:
Olena Karacheban, olena.karacheban@desy.de
Wolfgang Lange, wolfgang.lange@desy.de
Wolfgang Lohmann, wolfgang.lohmann@desy.de
Sergej Schuwalow, sergej.shuwalow@desy.de

OLYMPUS.

Detector performance and data analysis

The goal of the OLYMPUS experiment is to quantify the effect of two-photon exchange in electron–proton scattering by making a precise measurement of the ratio of the positron–proton and electron–proton elastic-scattering cross sections. The experiment was performed using the intense beams of electrons and positrons stored in the DORIS ring at DESY, an unpolarised internal hydrogen gas target and the former BLAST detector of the MIT Bates Linear Accelerator Center, USA. The data taking for the measurement started in 2012 and finished in early January 2013. Since then, several studies have been done to improve the understanding of the detector performance in the main data-taking period. The focus of the collaboration has now shifted to the analysis of the data and the derivation of final results.

The goal of the OLYMPUS collaboration is to determine the contribution of multiphoton exchange processes to electron–proton scattering. This is accomplished by measuring the ratio of the elastic-scattering cross section of positrons with protons to that of electrons with protons. The motivation for the measurement is the surprising deviation from unity in the electric-to-magnetic form factor ratio of the proton as determined in polarisation transfer measurements observed at Jefferson Lab, USA. This measurement is in apparent contradiction with measurements made using the Rosenbluth separation technique. However, since the Rosenbluth formula assumes that only the one-photon exchange between the electron and proton is important, higher-order radiative corrections, in particular multiphoton exchanges, could be the source of the discrepancy. Thus, a precise determination of the multiphoton exchange cross section could reconcile the two measurements or point to something more interesting.

The OLYMPUS collaboration employed the former MIT BLAST detector, which was shipped from MIT to DESY and re-assembled at the DORIS storage ring. A very successful data-taking run with the detector, beginning in 2012 and finishing in early January 2013, collected a total integrated luminosity of 4.1 fb^{-1}, substantially more than the original goal for the experiment of 3.6 fb^{-1}.

Since the end of data taking, several studies, aimed at improving the understanding of parameters needed for precise analysis of the data, have been performed. This includes a one-month cosmic-ray run, a complete geometric survey of the detector components and a full remapping of the magnetic field. In addition, the beam position monitors, which were mounted up- and downstream of the target chamber, were calibrated since a precise knowledge of the beam position is essential for luminosity determination with the symmetric Møller/Bhabha monitor. The simulation of the detector components has also been improved. Monte Carlo generators for radiative corrections and pion electro-production have been developed to study the detector acceptance and efficiency and determine the background.

Now, armed with the new geometric survey, improved magnetic field map and improved detector calibration and simulation, the collaboration is focusing on the analysis of the data. At

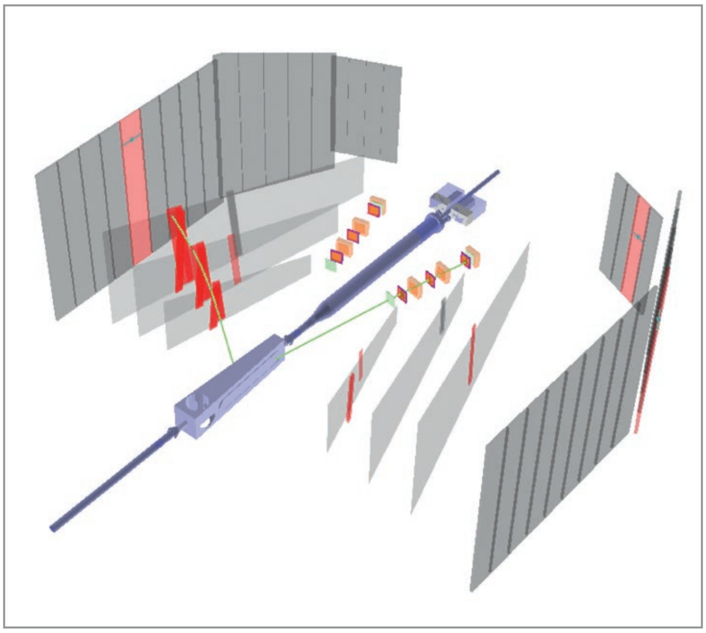

Figure 1

Elastic event candidate in the 12-degree luminosity telescope. The green track in the forward direction is the electron, and the track going to the left with the large red entries in the detector chambers is the recoil proton.

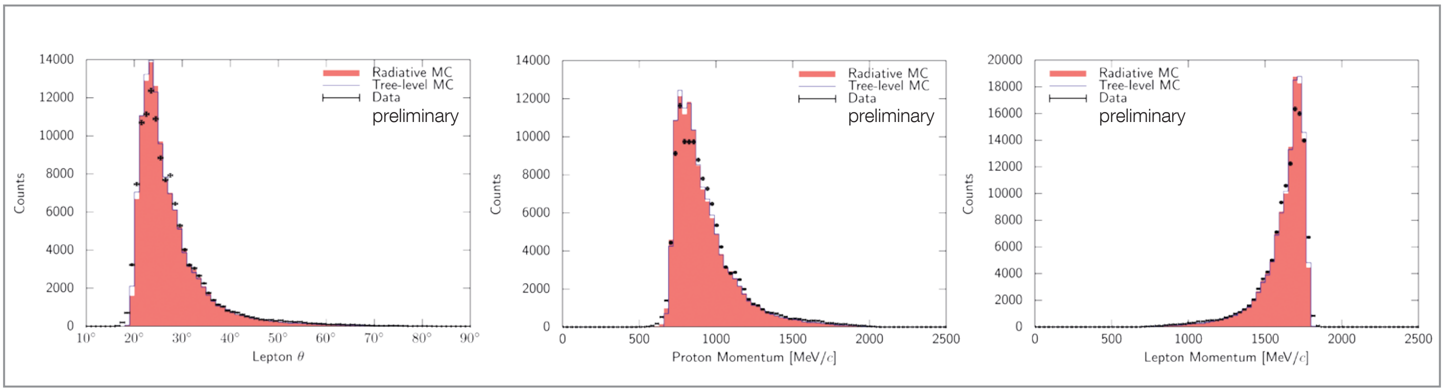

Figure 3

Olympus data compared with simulations

present, the track reconstruction algorithms for the wire chambers are being finalised along with the detector alignment constants, particle identification code and event selection. In parallel, a precise determination of the total luminosity accumulated during the run is in progress. The luminosity is initially determined by three independent methods. The first is based on a record of measurements of the beam current, the gas flow in the target and the target temperature, made during the run. The second method uses measurements of the Møller/Bhabha scattering of incident electrons (or positrons) by the electrons in the hydrogen atoms of the target. The last method is the measurement of elastic scattering at low angles (where the two-photon exchange cross section is negligible) of incident electrons or positrons by the protons that constitute the hydrogen nuclei. Møller/Bhabha scattering and lepton–proton scattering via one-photon exchange are very well-understood processes whose cross sections can be precisely calculated. After checking for consistency, the three methods will be combined to increase the precision of the overall luminosity measurement.

Once this work is completed, the two-photon exchange cross section will be determined (in rough outline) by counting the number of elastic-scattering events as a function of the scattering angle for incident electrons and also for incident positrons, normalising them to their respective luminosities and then calculating their ratio. This ratio will be compared with Monte Carlo studies that account for radiative corrections and the performance of the detector. Before this can happen, the detector acceptances and efficiencies and the luminosity must be understood at the 1% level. By relying on the ratio measurement, we are able to significantly reduce potential measurement biases that affect the electron and positron results in similar ways. This is an important feature of the experiment's design.

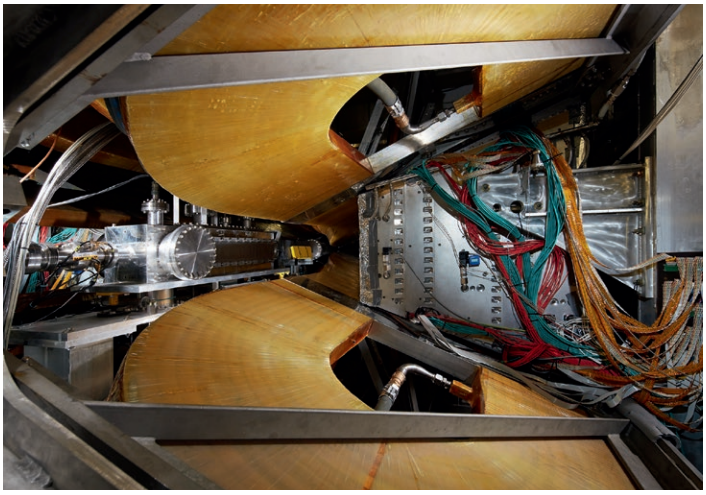

Figure 2

Picture of the OLYMPUS detector, showing the target chamber in the beamline, one of the drift chambers and part of the toroidal magnet

Contact:

Uwe Schneekloth, uwe.schneekloth@desy.de

References:

http://web.mit.edu/OLYMPUS/

The mother of all beam tests.

Crucial milestone for Belle II achieved

“The mother of all beam tests” is the phrase coined by Belle II spokesperson Tom Browder from Hawaii University when he came to Europe to witness preparations for a very complex beam test at DESY. Together with seven German university groups, MPI for Physics and MPG Semiconductor Lab (MPG HLL) in Munich, DESY will contribute an important component to the vertex detector of the Belle II experiment at the SuperKEKB facility in Japan: a novel pixel detector. An integrated test of the entire system including its associated electronics and sophisticated readout concept was recently successfully completed at the DESY test beam after a long period of intensive preparations. More than 80 scientists, engineers and technicians worked over several months to achieve this very important milestone for Belle II.

In 2011, DESY joined the Belle II collaboration, which is presently upgrading the former Belle detector to fully exploit the increase of luminosity by a factor of 50 that will be provided by the upgraded SuperKEKB asymmetric electron–positron collider at KEK in Japan. This next-generation *B* factory is scheduled to start physics running in 2016; it will complement the searches for new physics beyond the Standard Model currently being carried out at the energy frontier by the experiments at the LHC at CERN in Switzerland.

The German institutes contribute to the Belle II experiment by developing and constructing a new type of pixel vertex detector (PXD), which is based on the DEPFET detector concept originally developed for the International Linear Collider (ILC). This technology combines signal detection and amplification in a single silicon pixel structure, so that the position measurement of traversing particles can be achieved with a minimum amount of material. This is particularly important since the decay products of the *B* mesons typically have rather low momenta. A four-layer double-sided silicon strip detector (SVD) that is being designed by KEK and the HEPHY institute in Vienna, Austria, will surround the two-layer PXD. Together, the two systems will form the Belle II vertex detector (VXD) (Fig. 1 left).

The close proximity of the VXD to the interaction point – the innermost PXD layer has a radius of only 1.4 cm – and the large background (which is due to the enormous increase in

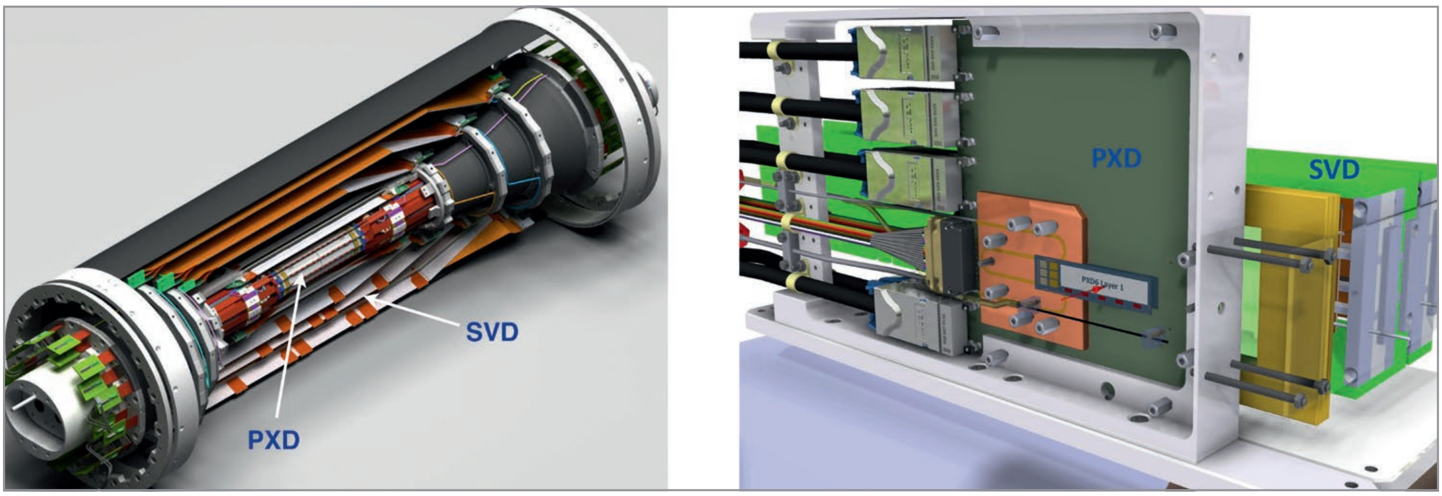

Figure 1

Schematic cut-out view of the VXD consisting of the two-layer PXD and the four-layer SVD (left). CAD drawing of the setup used for the DESY test beam with prototype sensors simulating a slice of PXD and SVD (right).

Figure 2

Participants of an international workshop held at DESY in October 2013 to prepare the test beam campaign

luminosity with respect to Belle I) pose many technological challenges in terms of radiation hardness, electronics, cooling, mechanical integration and installation. DESY has key responsibilities in several of these areas. According to the present schedule, the construction of the individual detectors has to be completed in summer 2015 such that PXD and SVD commissioning can start at KEK in autumn 2015. While prototypes of all individual elements of the entire VXD system have already been carefully tested in various laboratories in the past, a complete system test to prove that all components work together as foreseen had not yet been performed. To prepare such an integrated system test at the DESY test beam, the VXD community held two workshops in 2013 at DESY with more than 80 participants (Fig. 2).

The objective of the test was to expose prototype sensors of both PXD and SVD to electrons in the 1 T field of the superconducting PCMAG magnet in test beam area 24/1 (TB24/1) in an arrangement very much resembling the real experiment (Fig. 1 right and Fig. 3).

Besides testing the concepts for CO_2 detector cooling, slow control and detector alignment, particular emphasis was put on the verification of the complex trigger and data acquisition scheme of the VXD. Due to the high level of background at SuperKEKB, the small PXD alone is expected to produce about 20 GByte/s of data, which is too much to be handled by the Belle II event builder. Therefore, a sophisticated readout scheme has been developed, which uses track information from other subdetectors to compute “regions of interest” (ROI) in the PXD (Fig. 4 top). A data reduction by roughly a factor of 10 can be expected when only the hits in these ROIs are read out. The lower part of Fig. 4 shows an event in which hits in the four SVD layers are used to form a track that is then extrapolated into the PXD. The insert shows in red the corresponding ROI, which indeed contains the true PXD hit as indicated in yellow.

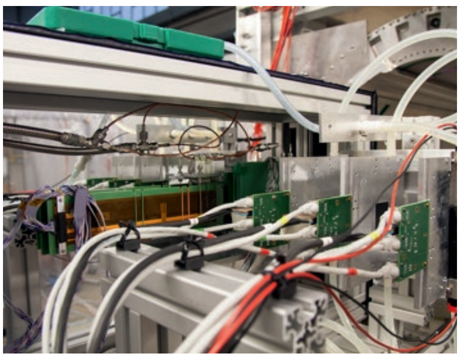

Figure 3

PXD and SVD planes together with the EUDET telescope during assembly and before moving into the PCMAG magnet in TB24/1

Following the big success of this test beam campaign, another integrated system test has been scheduled for the end of 2014 or beginning of 2015 with the goal of employing final protoype ladders of both PXD and SVD. To reduce the set-up time needed for this follow-on test, all essential ingredients of the complex data acquisition and trigger system that have been installed at DESY by the collaborating groups starting in October 2013 have been moved to the detector lab in HERA hall West, where they are kept fully operationally for further development.

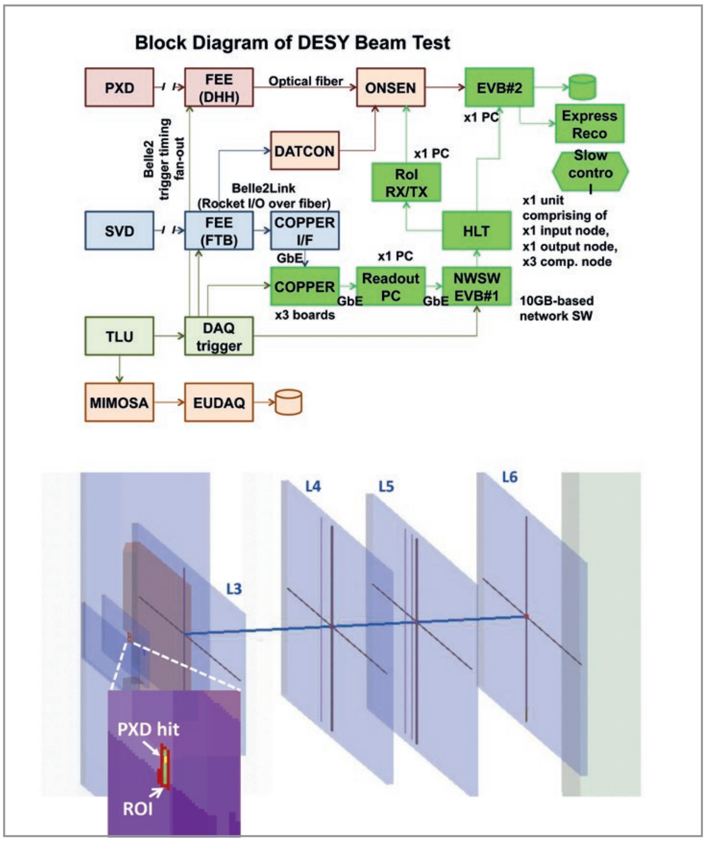

Figure 4

Schematic view of the VXD readout scheme used in the test beam (top). Event display of an event demonstrating the concept of ROI finding (bottom).

Contact:

Carsten Niebuhr, carsten.niebuhr@desy.de

Any Light Particle Search II.

Detecting single photons and straightening magnets

The ALPS II experiment at DESY is looking for very weakly interacting slim (sub-eV) particles (WISPs), such as hidden photons or axion-like particles (ALPs). These particles are well motivated theoretically, are perfect cold dark matter candidates and could explain puzzling astrophysical phenomena, such as the surprising transparency of the universe for TeV photons.

ALPS II is an experiment of the "light-shining-through-a-wall" kind, in which laser light is shone onto a wall: if WISPs exist, photons might oscillate into them before the wall and, in the form of a WISP, easily traverse the wall. Such WISPs could then oscillate back into photons behind the wall to give the impression that some of the laser light shone through the wall. Details of the planned setup with 20 HERA dipole magnets installed in one of the straight sections of HERA were given in the 2012 Annual Report.

ALPS II places extreme demands on photon detection:
> Due to constraints given by the optics and the laser system, ALPS II will be operated with 1.17 eV photons, for which charged-coupled devices (CCDs) are very inefficient.
> The expected rate of light-shining-through-a-wall photons is a meagre few per day. Hence, any detector must have an extremely low dark count rate.

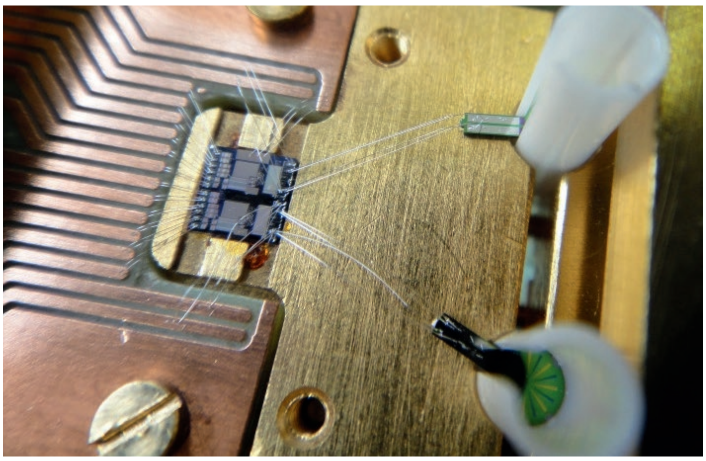

Figure 1

NIST TES sensor module

For these reasons, the ALPS II group decided to investigate a detection system based on a transition edge sensor (TES). These high-end chips take advantage of the extremely temperature-dependent resistance of a material at the transition between normal- and superconducting. At ALPS, we have successfully tested a TES provided by the US National Institute of Standards and Technology (NIST) and equipped with readout superconducting quantum interference devices (SQUIDs) by the Physikalisch-Technische Bundesanstalt (PTB) in Berlin (Fig. 1). The sensitive area consists of a 20 nm thin tungsten film with a size of 25 × 25 μm^2. The TES is cooled down to 80 mK by an adiabatic demagnetisation refrigerator. After characterisation of the sensor modules, the ALPS detector setup can now measure pulses induced by single 1.17 eV photons (Fig. 2). The pulse height corresponds to a current decrease of about 70 nA in the TES, the rise time of the pulses is of the order of 0.1 µs and the fall time about 5 µs. The energy resolution of the TES was measured to be about 8%, good enough for the TES to also be a sensitive calorimeter. Most importantly for ALPS II, the intrinsic noise of the NIST TES chips was measured to be only about 10^{-4} per second. These detailed pioneering studies have led to the conclusion that TES-based detectors are very strong candidates for use in the ALPS II experiment and beyond.

Another, quite different, challenge for the ALPS II experiment is related to the HERA dipole magnets that will be used for the final stage of the experiment. The sensitivity of ALPS II crucially depends on the magnetic length of the setup and the effective power of the laser light inside the magnetic field. The maximum length is determined by the aperture of the beam tube, because clipping losses of the laser light are to be avoided.

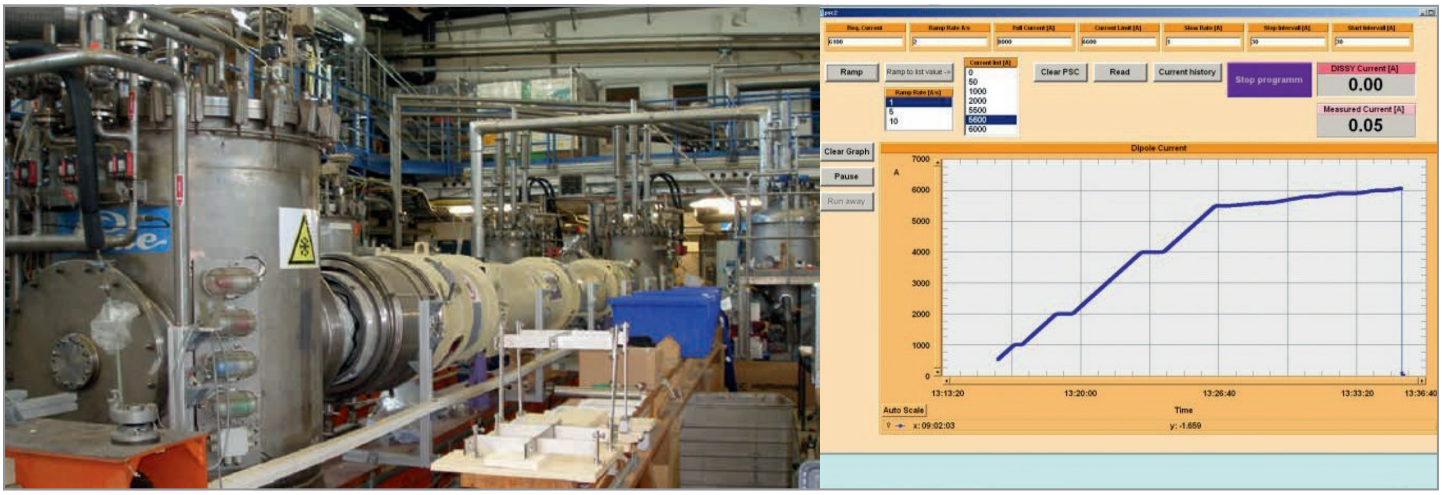

Figure 3

Test of a HERA magnet after the straightening procedure had been applied. The quench current of the straightened magnet amounted to 6072 A, while the original magnet quenched already at 5920 A.

The inner diameter of the vacuum pipe in the superconducting HERA dipole is 55 mm, which would be more than sufficient for an installation of 20 HERA dipole magnets for ALPS II. However, the HERA dipoles were designed for a storage ring application and are therefore curved. Thus, the effective straight-line horizontal aperture is only about 35 mm, which would limit ALPS II to just eight magnets. To fix the problem, a simple and very cheap method was developed for straightening the yoke and thus the beam pipe: a “brute force” is applied from the outer vacuum vessel at the three support planes of the dipole. The procedure effectively removes the bend and thereby yields an aperture of 50 mm, which is sufficient for ALPS II.

Since the deformation of the yoke is elastic, the deforming force must be maintained during operation at cryogenic temperatures. Therefore, props were designed to maintain the correct pressure while keeping the thermal flux from the vacuum vessel (which is at room temperature) to the yoke (which is at liquid-helium temperature) within acceptable limits. The props at the ends of the dipole also need to allow for length changes of the yoke during cool-down and warm-up. As a test of the concept, the HERA dipole used for the ALPS I experiment was straightened on a test bench and then operated continuously for 30 hours at the ALPS II design current of 5700 A, which corresponds to a field strength of 5.3 T (Fig. 3).

After the successful review of the ALPS II experiment by the DESY Physics Research Committee (PRC) in November 2012 and the approval of the first stages of the ALPS II experiment by the DESY Directorate in February 2013, these encouraging results mark the passing of further milestones towards the realisation of ALPS II. We are now confident that first ALPS II results on hidden photons will appear before the end of 2014.

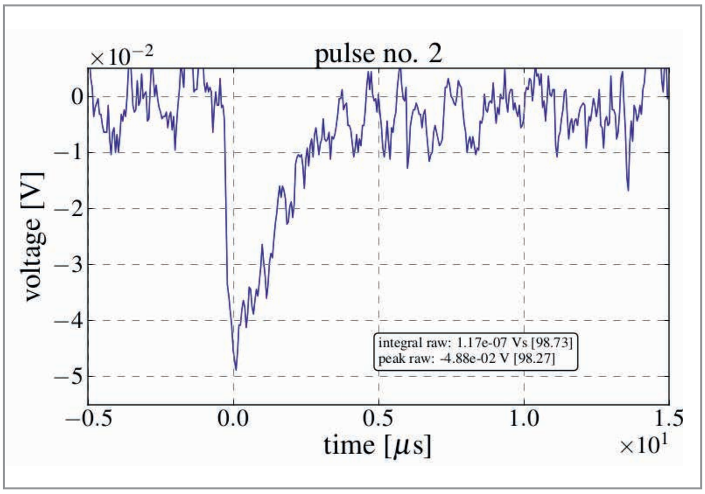

Figure 2

Photon pulse detected with the ALPS detector setup

Contact:

Axel Lindner, axel.lindner@desy.de

TES: Friederike Januschek, friederike.januschek@desy.de

Magnets: Dieter Trines, dieter.trines@desy.de

References:

http://alps.desy.de

ALPS-TDR: R Bähre et al., 2013 JINST 8 T09001

Breakthrough of the year.

Opening a new window into the universe with IceCube

2013 was a pivotal year for the IceCube neutrino telescope and high-energy astrophysics. The observations of TeV and PeV neutrinos of extraterrestrial origin in the IceCube data have opened a new window into the high-energy universe. Neutrinos have now taken their place alongside photons and cosmic rays as unique messengers that can be used to explore the nature of non-thermal processes in our universe. But IceCube is more than "just" a neutrino telescope. By exploiting the low energy threshold of IceCube's densely instrumented core and new analysis techniques, the collaboration has demonstrated another aspect of the instrument: the ability to measure fundamental neutrino properties.

For more than three decades, scientists have been searching for neutrinos arriving from the depth of the universe. For almost as long, DESY researchers have been playing an important role in shaping and advancing this undertaking, which started in Siberia's Lake Baikal and has been continuing beyond the completion of IceCube at the South Pole a few years ago up to the present.

In 2013, extraterrestrial neutrinos were found in the data recorded with IceCube. An analysis of two years of data, recorded with the (almost) completed detector between May 2010 and April 2012, found 28 events above an energy threshold of 30 TeV (Fig. 1), while only about 10 events were expected from atmospheric backgrounds. This corresponds to a 4.1σ excess of signal compared to the background expectation. Not only is the numeric excess striking, the distribution of the events across the sky, their energy spectrum and their detector signatures all point to an extraterrestrial origin [1].

Very recently, preliminary results of an updated search, based on the analysis of a third year of IceCube data (May 2012 – Apr 2013), were presented by the IceCube collaboration. The new data raised the count of extraterrestrial neutrino candidates to 37. Moreover, one of the new candidates, with a measured energy of more than 2 PeV, turned out to be the highest-energy neutrino ever observed.

An important step leading to the conclusion that the data are indeed showing an emerging extraterrestrial signal was the accurate measurement of the energy spectrum of the observed events. To achieve this, DESY researchers combined the above-mentioned data set with a number of data sets collected during the construction phase of the detector. These older data sets had already provided first hints, albeit not statistically conclusive, of extraterrestrial neutrinos. The result of the combination is the most accurate measurement of the neutrino energy spectrum so far (Fig. 2); it is now ready to be compared to predictions of the neutrino emissions from various populations of astrophysical objects both inside and outside of our galaxy.

Amid all the excitement over this breakthrough in neutrino astronomy, another important measurement performed with the IceCube detector in 2013 should not be forgotten: the first measurement of neutrino oscillation parameters with the

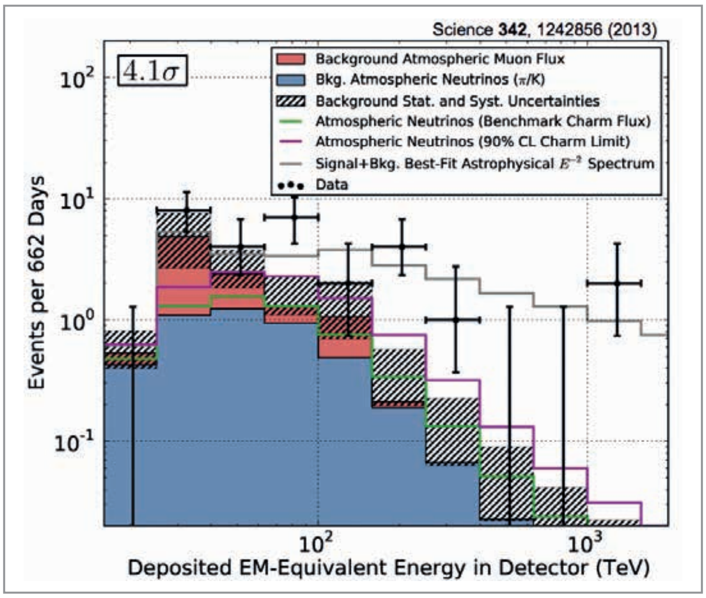

Figure 1

Energy spectrum of neutrinos with energies above 30 TeV observed in an analysis of two years of IceCube data on top of predictions of the background from atmospheric neutrinos

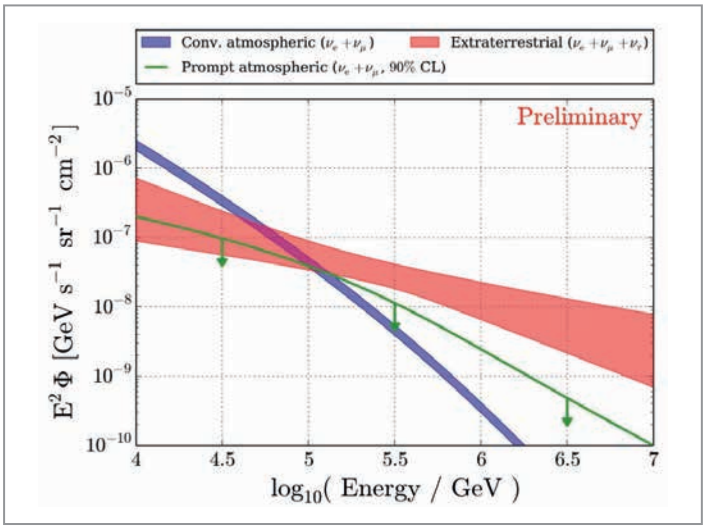

Figure 2

Energy spectrum of extraterrestrial neutrinos (red) derived from a global fit of the results of multiple searches for extraterrestrial neutrinos during the construction phase of IceCube and with the completed detector

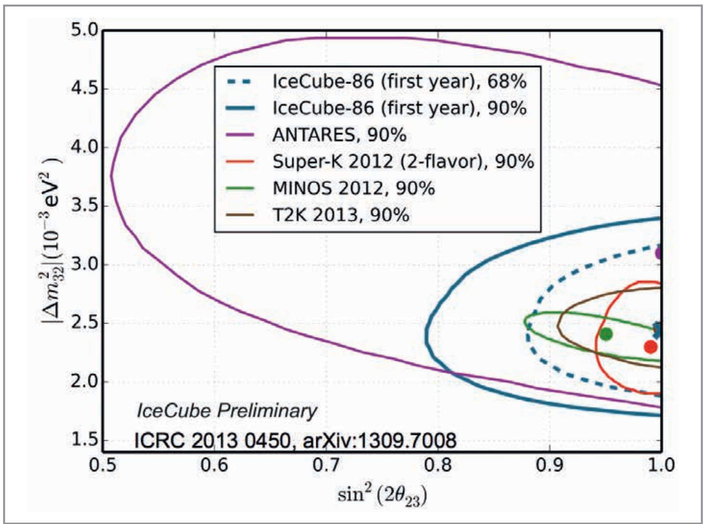

Figure 3

Constraints on the atmospheric neutrino oscillation parameters derived from one year of IceCube data taking

completed IceCube array. The oscillation parameters were derived from the observation of a disappearance of atmospheric muon neutrinos in certain directions and at certain energies with IceCube's densely instrumented inner part, called DeepCore.

The quality of this measurement was greatly improved over an earlier one that used data from the construction phase of IceCube (reported in 2012), not least due to new analysis and event reconstruction methods developed by DESY researchers. The new reconstruction methods were dedicated to extracting the energy and direction of neutrinos with energies between 10 GeV and 100 GeV. Such "low-energy" events are usually of limited use for neutrino astronomy and therefore had not received much attention. They are, however, essential for the measurement of neutrino oscillation parameters.

While the constraints on neutrino oscillation parameters with just one year of IceCube data are still weaker than constraints from other experiments (Fig. 3), their measurement is still an important milestone since it demonstrates the promise that IceCube will be making a significant impact on the measurement precision of these parameters in just two to three years.

Contact:

Markus Ackermann, markus.ackermann@desy.de

References:

[1] M.C. Aartsen et al., Science 342, 1242856 (2013)

IceCube++.

Towards a neutrino observatory for the next decade

The largest particle detector in the world, the IceCube neutrino telescope in Antarctica, comprises an instrumented volume of one cubic kilometre, which monitors a mass of about one gigatonne of ice at the South Pole. The first results in both astroparticle and particle physics have now been extracted from more than three years of data taken with the full detector. The IceCube collaboration is working to further improve the physics capabilities of the observatory by substantially increasing the detector volume and lowering its energy threshold. A broad R&D programme has recently been launched to work out the details and prepare for transforming IceCube into an even more powerful neutrino observatory in the next decade.

The IceCube detector was originally designed for the detection of neutrino interactions in the TeV to PeV energy range. The original programme was extended by the addition of a densely instrumented inner part, DeepCore, in which the detection threshold is of the order of 10 GeV, considerably lower than in the rest of the detector, to allow the parameters of neutrino oscillations to be measured. A further reduction of the threshold by several GeV would facilitate the measurement of the effects of matter on neutrino oscillations and thereby the determination of their mass hierarchy – one of today's fundamental questions in particle physics. Preconditions for such a measurement are sufficiently precise energy and direction measurements at low energies.

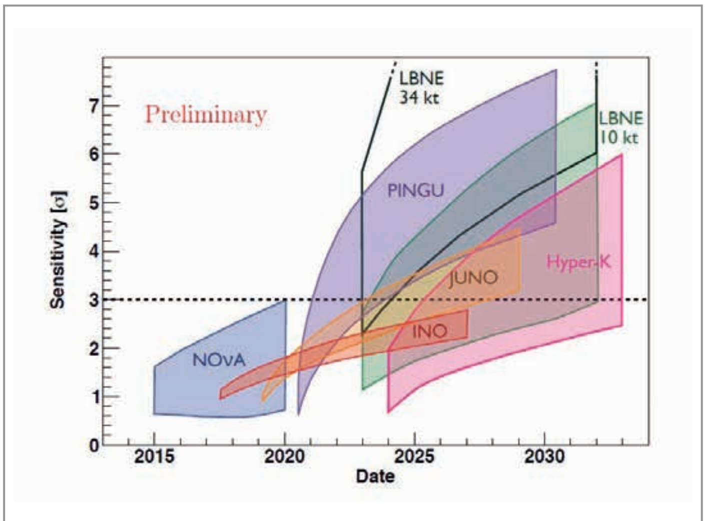

Figure 1

Comparison of the sensitivity range to determine the neutrino mass hierarchy for different experiments planned or under construction

This extension towards low energy is being pursued by the Precision IceCube Next Generation Upgrade (PINGU) project, which was initiated in 2011 by the IceCube collaboration together with new international partners. The first version of the PINGU letter of intent was recently released [1].

The present PINGU design foresees an additional 40 strings of detectors in the centre of IceCube, packed even more densely than the already dense DeepCore. Depending on analysis cuts, this extension will lead to a fiducial target volume of several megatonnes. The sensitivity for the neutrino mass hierarchy determination with such a design is shown in Fig. 1. In addition to the mass hierarchy measurement, PINGU would yield improved results on oscillation parameters, extend the lower mass limit of the WIMP dark-matter search and enable the neutrino-based tomography of the Earth.

Plans are also being formulated to extend IceCube's capabilities to detect the highest-energy cosmic neutrinos. IceCube is the first experiment to have recorded neutrinos from cosmic sources at energies in the PeV range. However, discovering their sources will require event sample sizes well beyond the handful that could be achieved by just running the currently configured detector longer. Thus, unravelling the mystery of the origin of these neutrinos will require a substantial increase of the detector's sensitivity, which could only be accomplished by a significant upgrade of the detector.

Two approaches are being considered. The first is to increase the detector volume by deploying more detector strings over

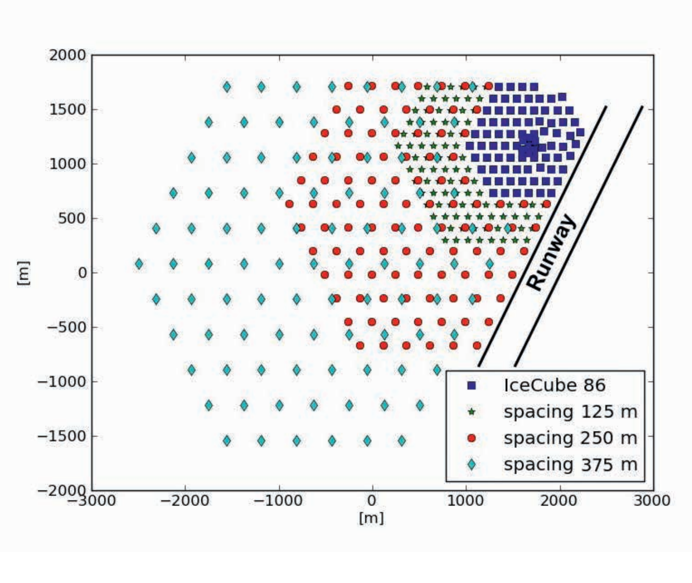

Figure 2

Three example detector geometries

a larger area. A design that would add 100 additional strings distributed over an area of 5–10 km^2 is being evaluated. Examples of three possible configurations are sketched in Fig. 2. This solution is expensive, however, and would require solving complex technical issues, particularly in the areas of drilling and deployment. Long-term R&D aimed towards developing the required cost-effective, highly efficient light sensors and alternative drilling technologies are under way at DESY.

The other approach to increasing sensitivity relies on a completely different strategy: rather than increase the detector volume, extend the angular range over which cosmic neutrinos can be separated from background processes. This approach would be less expensive and could be realised on a shorter time scale. The basic idea is to extend the present IceTop array, which suppresses backgrounds from terrestrial neutrinos, to cover a much larger area and thus increase the angular aperture of IceCube that is suitable for detecting cosmic neutrinos. The deployment of 1000 simple particle detectors distributed in a circular area of 7 km radius would provide IceCube with a neutrino aperture for zenith angles from 0 to 75°.

Several issues must be resolved before such a large detector array could be built and efficiently operated, particularly in the areas of power distribution, communication and detector synchronisation. To address these issues, DESY researchers, acting within the Helmholtz Alliance for Astroparticle Physics and together with colleagues from KIT in Karlsruhe, Germany, have developed the Transportable Array for eXtremely large area Instrumentation studies (TAXI). A single TAXI array consists of four clusters of three background detectors and one signal sensor. The clusters can be distributed over a circle of 100 m to study large-array design problems as well as environmental parameters. The whole setup can be packed into a single container for easy transport and quickly readied for measurements at any chosen location. The first TAXI cluster has been operating at DESY in Zeuthen since July 2013.

Contact:

Rolf Nahnhauer, rolf.nahnhauer@desy.de

References:

[1] M. C. Aartsen et al., arXiv 1401.2046

Hunting pulsar outflows.

Making the most of a giant in the desert

The H.E.S.S. group at DESY in Zeuthen is investigating the cosmic accelerators that reside in our own galaxy, the Milky Way, the centre of which is best viewed from the southern hemisphere. From its location in Namibia, the giant H.E.S.S. II telescope has a unique view of the galaxy's centre, with superb viewing conditions that permit the group to study the large plasma clouds created by pulsar winds and the gamma-ray pulsars that have their place among the most fascinating objects of the southern sky. DESY researchers are strongly involved in the commissioning of H.E.S.S. II and in the development of the tools needed for its full exploitation. In addition, DESY engineers in Zeuthen are hard at work on the refurbishment of the four H.E.S.S. I cameras. Together, these activities will help to ensure a full science return of the mixed-size H.E.S.S. system in its final years of operation before it yields the floor to the planned Cherenkov Telescope Array (CTA) gamma-ray observatory.

The H.E.S.S. II telescope (Fig. 1), the largest Cherenkov telescope ever built, was inaugurated in 2012. By placing this huge 600-tonne telescope with its 28-metre diameter mirror into the middle of the four existing 12-metre H.E.S.S. I telescopes, the first mixed-size array of Cherenkov telescopes was born. The mixing of the telescope sizes has enabled the coverage of an exceptionally wide energy range with unprecedented stereoscopic resolution for cosmic gamma-ray showers. The low energy threshold of H.E.S.S. II and its optimal view of the Milky Way are giving researchers the opportunity to search the southern sky for pulsars and to observe the galactic centre along with diffuse galactic emission. The H.E.S.S. collaboration is now pushing to produce the first results of the newly commissioned telescope. Scientists at DESY are contributing by developing tools for the low-energy, monoscopic analysis of H.E.S.S. II and also by preparing software for the spectral analysis of pulsars.

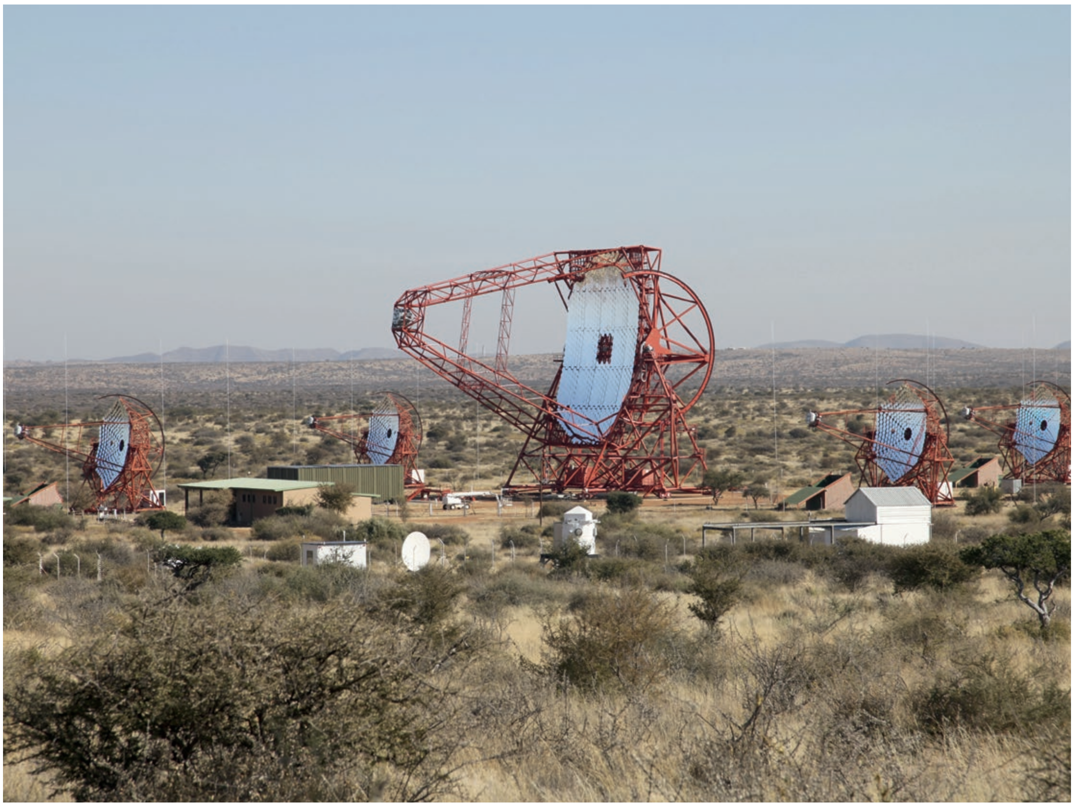

Figure 1

The five-telescope H.E.S.S. experiment in Namibia, comprising four 12-metre and one 28-metre telescope

Pulsars and pulsar winds

A big surprise happened in March 2013: the second-biggest flare ever observed occurred in the standard candle of gamma-ray astronomy, the Crab Nebula. The Crab Nebula is a pulsar wind nebula and is many light years across; it is not expected to show variability at time scales of less than a few days. The flare was first spotted by the satellite-borne Fermi-LAT telescope at GeV energies. In a stroke of good luck, both H.E.S.S. and VERITAS were in a position to look for the flare in the TeV energy range. In all previous attempts at simultaneous observation of such flares, either the moon or the weather had rendered data taking impossible at just the moment of the GeV eruptions. The data taken during the four nights of flare activity showed, however, that neither H.E.S.S. nor VERITAS could observe a corresponding TeV flare (Abramowski et al. 2014, Aliu et al. 2014). The fact that the flares appear to be unnoticeable at all wavelengths other than that of GeV gamma rays adds to their mysterious nature.

In another development, the ongoing efforts to produce a major data release of the 10-year H.E.S.S. galactic-plane scan were first presented for discussion at international conferences in 2013. According to the plan, wide-scale TeV gamma-ray sky maps of the entire inner galaxy, along with a unified list of sources, are, for the first time, to be made available to the public. DESY is a very active participant in a parallel study that is seeking to systematically analyse the whole population of 20–30 pulsar wind nebulae found in the data set. This study will help to test theoretical ideas of pulsar wind nebulae evolution with time, and their interactions with their surroundings.

H.E.S.S. I camera upgrade

Two problems involving the mixed-size H.E.S.S. II array are being addressed by engineers at DESY in Zeuthen: The 10-year old electronics of H.E.S.S. I are having a hard time keeping up with the higher trigger rates of H.E.S.S. II. Also, the number of technical failures of the H.E.S.S. I readout system is increasing due to its advanced age. These two problems are conspiring to produce a well-understood but large detection dead time of up to 45%. To fully exploit the high potential of the five-telescope H.E.S.S. array, the electronics of the H.E.S.S. I photomultiplier cameras must be renewed and a modern and low-maintenance readout system must be implemented. Ten years after the inauguration of the experiment, faster readout chips and network technology are available, and a more versatile architecture of the data flow can be realised at reasonable cost and effort.

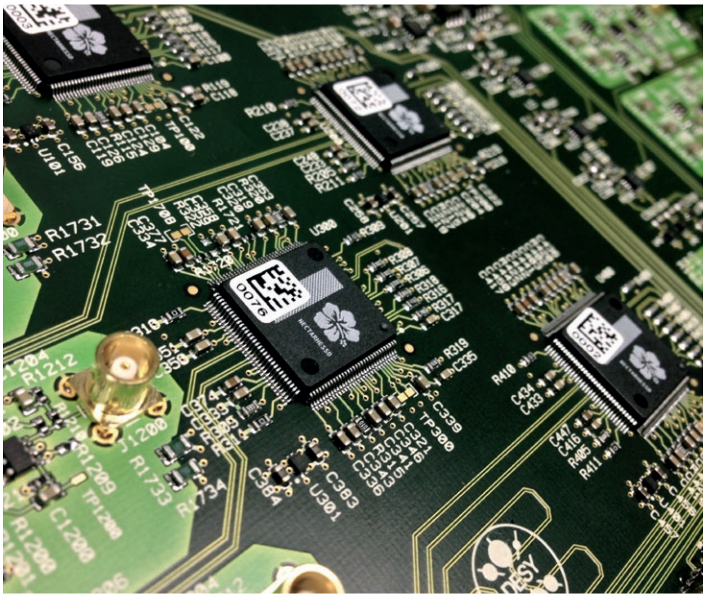

Figure 2

Analogue board prototype for the H.E.S.S. camera upgrade. The black chip with the flower logo is a NECTAR chip, a prototype analogue readout chip for CTA.

To benefit from synergies with the planned CTA gamma-ray observatory, the Zeuthen engineers are using CTA technology in the redesign effort wherever possible. For example, the new, fast analogue readout chip developed for CTA, NECTAR, is being integrated into the new readout boards (Fig. 2). Communication paths for the new camera infrastructure are based on standard Ethernet technology for flexibility and ease of maintenance. Each 16-channel module will run its own CPU with a Linux kernel to enable optimal remote monitoring of the camera's processes and status. The new system will also include improved power supply and ventilation systems, which will help to reduce the penetration of sand and dust into the camera. A major activity of the upgrade preparation effort is the testing of new components at DESY. Tested components for the first camera will be shipped to Namibia in early 2015, and the project will be completed in 2016.

Contact:

Stefan Klepser, stefan.klepser@desy.de

References:

Holler et al. 2013, Proc. 33rd ICRC, arXiv:1307.6003

Abramowski et al. (H.E.S.S. Collaboration) 2014, A&A 562, L4

Aliu et al. (VERITAS Collaboration) 2014, ApJ, 781, L11

The flaring gamma-ray sky.

As viewed by the Fermi Large Area Telescope

The Large Area Telescope (LAT) onboard the Fermi Gamma-Ray Space Telescope is the most sensitive telescope available for observing photons with energies between 20 MeV and 100 GeV (Fig. 1). In 2013, DESY scientists used the LAT to develop the first catalogue of flaring gamma-ray sources [1]. The catalogue contains 215 sources, mostly associated to active galactic nuclei. Seven flaring gamma-ray sources in our galaxy have been identified.

Figure 1

Artist's impression of the Fermi satellite with a variety of sources seen in gamma rays. The universe is home to numerous exotic and beautiful phenomena, some of which can generate almost inconceivable amounts of energy. Supermassive black holes, merging neutron stars and streams of hot gas moving close to the speed of light are but a few of the marvels that generate gamma-ray radiation – the most energetic form of radiation, billions of times more energetic than the light visible to our eyes. With the Fermi space telescope, astronomers at long last have a superior tool to study these phenomena.

DESY researchers also looked into one particular flaring source: the Crab Nebula. This historical supernova remnant had previously been thought to be constant in flux on a time scale of years; it was therefore used to cross-calibrate instruments in the X-ray and gamma-ray domain. However, strong flares have been detected in the energy range observed by the LAT. Analysis of LAT data on the second-brightest of these flares, which occurred in March 2013, and in particular of its rapidity and spectral energy distribution allowed us to infer that explosive magnetic-reconnection events inside the nebula are likely to be responsible for the gamma-ray outbursts [2]. The LAT observation of this event was accompanied by observations of the world's most sensitive instruments at lower frequencies, such as the Hubble Space Telescope or the Chandra X-ray Observatory. A simultaneous analysis of all relevant data is in progress.

Last but not least, we studied the possibility, predicted by some models, that bow shocks of runaway stars in our galaxy are emitters of gamma rays. However, our analysis of 27 of them turned up no evidence of any gamma-ray emission. The upper limits on radiation intensity are, in some cases, below the predictions of the models and thus put important constraints on emission models [3].

Contact:

Rolf Bühler, rolf.buehler@desy.de

References:

[1] Ackermann et al., ApJ 771 1, 2013
[2] Mayer et al., ApJL 775 2, 2013
[3] Schulz et al., accepted for publication in A&A

The VERITAS observatory.

When active galactic nuclei go wild

From its location in southern Arizona (Fig. 1), the VERITAS Cherenkov telescope array observes the very high-energy (VHE) gamma-ray sky in an energy range extending from 85 GeV up to 30 TeV. In 2012, the VERITAS cameras were outfitted with high quantum efficiency photomultiplier tubes, which enabled a significant reduction of the energy detection threshold. The benefits of the camera upgrade showed up in the past viewing season, particularly for the science of extragalactic sources. Active galactic nuclei (AGN) make up the great majority of known extragalactic VHE sources. VERITAS dedicates 40% of its observing time to AGN, and the collected wealth of information is advancing our understanding of these formidable cosmic accelerators and their extreme environments.

The VERITAS group at DESY studies AGN. These objects, which are among the most powerful in the universe, are capable of accelerating charged particles to very high energies. The supermassive black holes in their centres accrete matter from their surroundings and, in the process, sometimes launch collimated highly relativistic plasma outflows (jets). When these jets are observed head-on, their emission lines are "boosted", or shifted towards higher energies, due to relativistic effects. The resulting objects, called blazars, constitute the large majority of AGN detected through observations of VHE gamma rays.
Photon emission from blazars covers the whole electromagnetic spectrum from radio waves to gamma rays. A more complete understanding of blazars thus requires multi-wavelength observations. Blazars are also highly variable. This characteristic can be exploited to provide crucial clues on the processes taking place in the vicinity of black holes, their evolution and their interaction with their environment.

Major cosmic explosion in 2013

In April 2013, VERITAS detected one of the brightest outbursts ever seen in the sky. It came from the famous blazar Mrk 421 and produced an observed flux of up to one photon per second, about 50 times brighter than the usual flux from this source. It is by studying such flaring episodes that big steps in our understanding of AGN phenomena can be made.
Thanks to a multi-wavelength campaign underway at the time of the flare, precise measurements of the source in radio, optical, X-ray and high-energy gamma-ray wavelengths (100 MeV–100 GeV) are now available. Furthermore, the large number of VHE photons measured during the outburst allows us to perform fine spatial, temporal and spectral studies.
The hunt for the precise spot, within the blazar, at which the particles are accelerated is a central focus of the study. The resolution of current Cherenkov telescopes is insufficient to pinpoint the exact site. Rather, a multi-wavelength approach using instruments with finer angular resolution is employed. Additional information on the acceleration site can be obtained by analysing the fastest flux variations: the size of the emission region can be inferred from the shortest measured time scales (less than a minute) using causality arguments. A small emission region, of the order of the Schwarzschild radius, is usually assumed to indicate a site near to the central black hole.
In cases in which rapid variability is also associated with extreme brightness, fundamental questions can be addressed. For example, the violation of Lorentz invariance, predicted by some models of quantum gravity, can be tested. If the emission from contiguous energy bands is assumed to be simultaneous and to originate from the same region, a limit on the energy dependence of the speed of light can be derived by comparing the arrival time of well-identified emission peaks in different energy bands. Assuming that the anomalous energy dependence has at most a linear dependence, the quantum gravity energy scale cannot be less than 10^{17} GeV.

Figure 1
The VERITAS observatory in southern Arizona, USA

Contact:
Gernot Maier, gernot.maier@desy.de

MAGIC eyes.

Low-energy cosmic rays as cosmic messengers

The MAGIC observatory, consisting of twin Cherenkov telescopes located in a remote, mountainous region of the island of La Palma, Spain, is contributing observations of cosmic rays in the lowest energy range to a broad range of astroparticle topics, such as the search for the origin of cosmic rays, the study of ultrarelativistic processes in active galactic nuclei (AGN), the measurement of the diffuse electron (and positron) spectrum, and the search for telltale signs of dark matter. The underlying strategy of the work described here is the so-called multimessenger approach, in which information from a variety of cosmic messengers, e.g. radio-frequency waves, visible light, cosmic rays and neutrinos, is combined to achieve a comprehensive picture of astrophysical phenomena.

Study of AGN emission models

Recently, the spectral analysis of AGN has been attracting increasing interest. AGN are a diverse class of objects, many of which have been observed with the MAGIC telescopes. As is the case with photons of other wavelengths, gamma rays from AGN can be emitted by relativistic electrons and positrons or from collisions of hadrons with ambient photons. A characteristic feature of many AGN is variability: they display low-flux, quiescent states alternating with flares of high fluxes and varying duration.

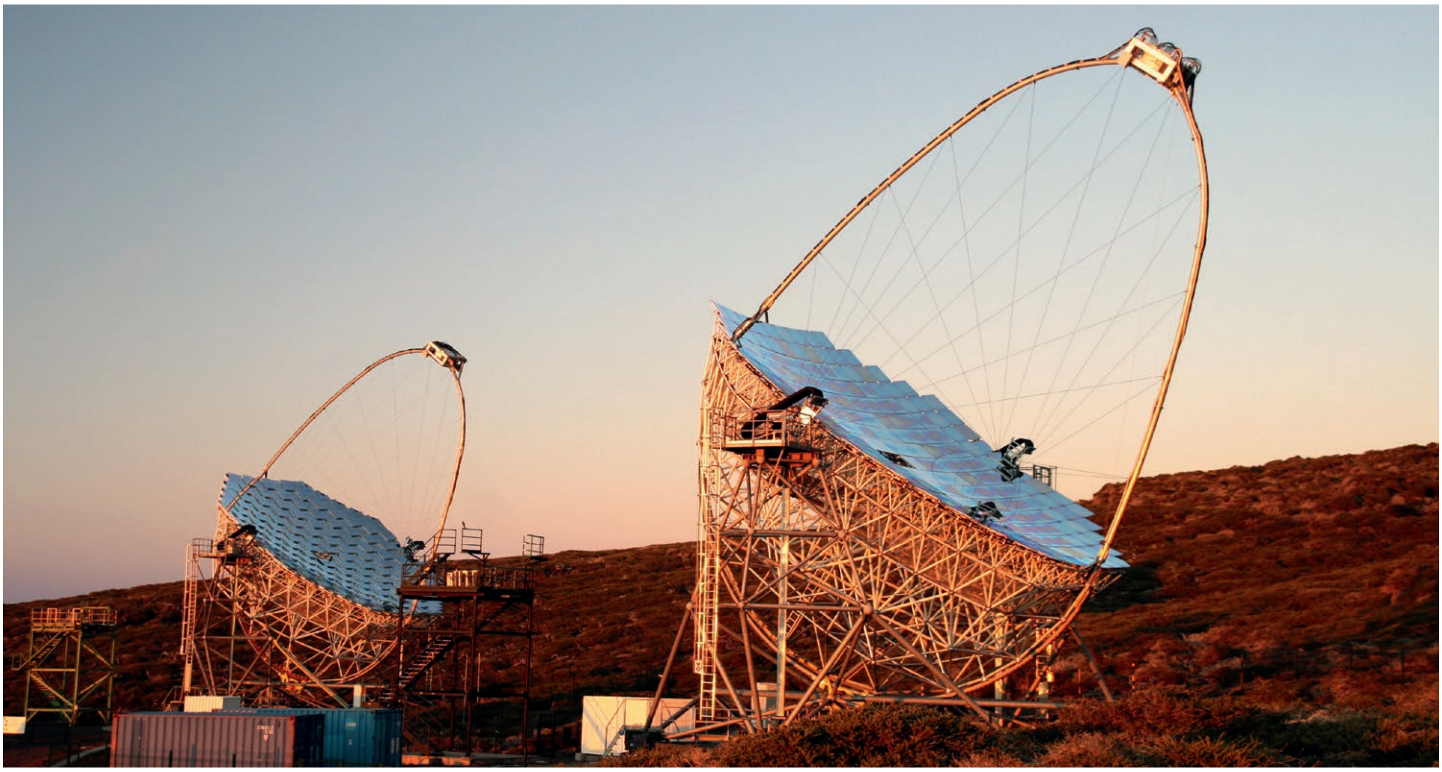

Figure 1

The two MAGIC telescopes at the Roque de los Muchachos observatory on the Canary island of La Palma, Spain, observe very high-energy gamma rays reaching the Earth from the distant universe.

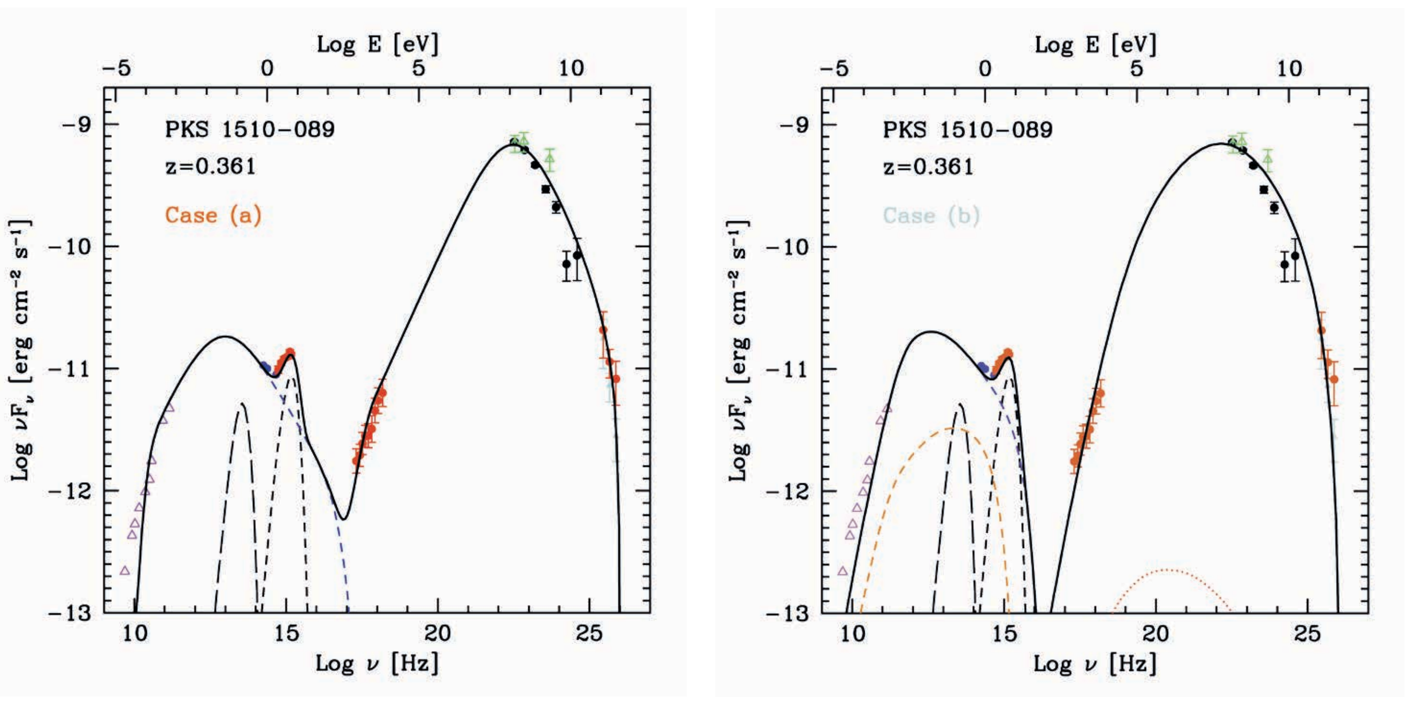

Figure 2

Spectral energy distribution of flat-spectrum radio quasar PKS 1510-089 in February–April 2012 [3]. The solid black curve shows the overall emission model. The high-energy bump is dominated by the external Compton mechanism, which is modelled by using as seed, photons either from the infrared torus (Case (a)) or from a slow sheath surrounding the jet (Case (b)).

DESY scientists are developing a general tool for determining the spectral energy distribution of AGN and for comparing the energy dependence of their light output during flaring episodes and quiescent states. To do so, the modelling must be time-dependent in order to incorporate the dynamics (cooling, interaction and transport) of all processes contributing to the production of gamma rays. The modelling problem can be reduced to a system of coupled differential equations spanning a large range in time and particle energy.

Starting towards solving these differential equations from a simplified approach containing a limited number of contributing processes, we were able to obtain results that largely match known analytical solutions.

We are currently working towards a full picture including all (leptonic and hadronic) processes.

Data analysis

In 2013, the DESY MAGIC group focused on three AGN: the BL Lac object 1ES 1727+502 discovered by MAGIC, and 3C 279 and PKS 1510-089, two flat-spectrum radio quasars (Figure 2). The results of MAGIC were complemented with multi-wavelength observations at lower energies. Different emission scenarios (see discussion above), consistent with both the multi-wavelength light curves and the broadband spectral energy distribution could be proposed. The results have been presented at different international conferences and are now submitted for publication [1, 2, 3].

Contact:

Elisa Bernardini, elisa.bernardini@desy.de

References:

[1] J. Aleksić et al., submitted to A&A, arXiv:1302.6140

[2] J. Aleksić et al., submitted to A&A, arXiv:1311.2833

[3] J. Aleksić et al., submitted to A&A, arXiv:1401.5646

The Cherenkov Telescope Array.

Choosing a site for the next-generation gamma-ray observatory

The next-generation ground-based gamma-ray observatory, the Cherenkov Telescope Array (CTA), will provide an order-of-magnitude increase in sensitivity compared to the current generation of instruments. It will thus give unprecedented and deep insights into the non-thermal processes of the universe. The CTA will observe cosmic-ray particle acceleration in astrophysical objects such as supernova remnants, pulsars and active galactic nuclei with exceptionally high spatial, spectral and temporal resolution. The CTA will consist of two observatories, one in each of the Earth's hemispheres. The choice of site is crucial for the performance of the instrument, since the Earth's atmosphere itself is a part of the detector. DESY groups are deeply involved in essential aspects of the site characterisation process, including studies of the atmospheric conditions at the various sites and Monte Carlo simulations of the sensitivities of sample arrays for each site.

Astrophysical photons with energies above 30 GeV can be measured with ground-based imaging atmospheric Cherenkov telescopes. An incoming gamma ray produces a shower of particles – mainly electrons, positions and photons – in the atmosphere. The measurement of the Cherenkov light produced by the secondary charged particles of the shower can be used to determine the direction and energy of the initial gamma ray. The CTA is currently in the preparatory phase, and when finished, will consist of approximately 80 imaging atmospheric Cherenkov telescopes of different sizes with an effective overall sensitive area of a few square kilometres. Construction will begin in 2016, and the first scientific data will be acquired after 2017.

CTA site search

Where should the CTA be built? The sensitivity of imaging Cherenkov telescopes depends on the amount of Cherenkov light collected and on the quality of the imaging of the extensive air showers. These factors, in turn, depend on the height of the observatory (typically at locations between 1500 and 3500 m above sea level), the quality of the atmosphere (e.g. aerosol content) and the strength of the geomagnetic field. Anthropogenic light pollution and unfavourable weather conditions, such as cloudy periods or high winds, further limit the available observing time and thus the sensitivity. From the civil-engineering point of view, the large arrays of the CTA require a rather flat area of a few square kilometres.

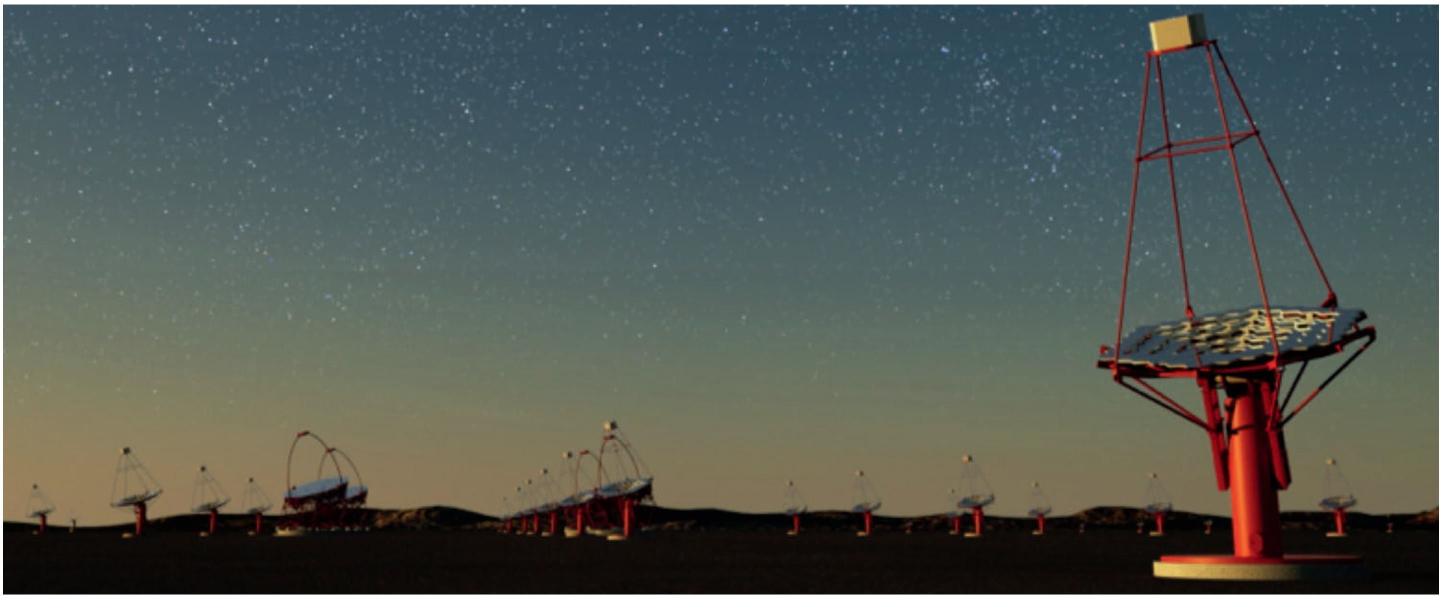

Figure 1

Artist's view of the CTA array with telescopes of three different sizes

Site candidates and characterisation

The CTA consortium has compiled a list of suitable candidate sites: five candidate sites in the southern hemisphere, located in Argentina, Chile and Namibia, and four candidate sites in the northern hemisphere, located on Tenerife (Spain), in Mexico and in the USA. The consortium evaluated all sites and, in 2013, provided a ranking based on expected sensitivity, available observing time and site development costs. The quality of the atmosphere at the different locations was evaluated by on-site instruments that measured cloud cover, temperature, external light levels and humidity. These data were complemented by satellite-based data and atmospheric modelling to provide a long-term picture of the quality of the atmospheric conditions. The best sites provide an average annual observation time of almost 1300 h with differences ranging up to 300 h.

Sensitivity

The geographic location of a site, i.e. its altitude above sea level and the strength of the local geomagnetic field, affects the obtainable sensitivity. In general, high sites achieve lower energy thresholds, but lower sites provide better sensitivities at energies above 80 GeV. Higher geomagnetic fields lead to a reduction in sensitivity at all energies. The precise estimation of the impact of the geographic location on the sensitivity of the CTA requires detailed Monte Carlo simulations of the shower development and the measurement process, since the sensitivity of an array of telescopes depends in a non-trivial way on its response to gamma-ray showers and its ability to distinguish gamma rays from hadronic background events.

DESY used local and Grid-based resources for the large-scale production of Monte Carlo simulations and developed analysis tools to calculate the sensitivity of different possible versions of the CTA at the various candidate sites. The results of this study show differences in the performance of CTA configurations at the various sites of up to 45% (in effective observing time). For the southern hemisphere, sites at altitudes of 1600 to 2000 m are now favoured. The northern candidate sites are found to be nearly equivalent with each other, but somewhat worse than the best southern sites.

Schedule

The site decision process will be finished in 2014 after political and financial boundary conditions have also been factored in. The site development process and construction phase will start immediately afterwards. The CTA consortium will be able to start the early scientific phase already during the construction period, and the CTA will become the most sensitive instrument to high-energy gamma rays by 2018. Completion of construction and full sensitivity are expected for 2019.

Contact:
Stefan Schlenstedt, stefan.schlenstedt@desy.de

MSTs and array control: the backbone of the CTA.

Developing crucial components of the CTA observatory

DESY has assumed responsibility for the design and project management of the mid-sized telescopes (MST) as well as for the development of the array control software, the design and test of digital trigger electronics and the provision of massive computing resources.

The mid-sized telescopes

The structure and the drive and safety systems of the MST have been designed by DESY, which is also providing system engineering and project management, including quality management and the use of the DESY engineering data management system (EDMS) for documentation for the MST, both in the current phase and extending into the production phase.

A full-size mechanical prototype of an MST has been installed at a site close to DESY in Berlin (Fig. 1). A structural survey of the prototype has proven that the actual structural performance meets all design specifications. The prototype has a complete drive system for both azimuthal and elevation movements, which can steer the telescope to any point in the sky in less than 90 s and also follow any object with high precision. Currently, tests are being performed under load conditions (such as winds of 36 km/h) to investigate the performance and smoothness of the drive mechanism. Sensors mounted on the device are measuring the acceleration and inclination, thereby providing valuable input for analysis of correlations between mechanical movements, drive operation and weather conditions.

The MST prototype carries 84 mirrors; currently, 25 mirrors are real mirror prototypes from different international providers. The procedure to adjust the mirrors so as to minimise the point-spread function of the telescope is being optimised, and the pointing accuracy of the telescope is being assessed and improved. The DESY group is also performing tests of mirror prototypes, both when mounted on the MST prototype and in the DESY climate chamber for long-term evaluation.

Array control

The array control and data acquisition system (ACTL) is a multi-institutional effort of European and US research centres and universities. DESY has accepted to lead the ACTL project and, together with Humboldt University Berlin, is coordinating two ACTL subprojects: the development of the global operation infrastructure and the definition and implementation of the CTA on-site computing and networking infrastructure.

The ACTL project encompasses all aspects of central control, monitoring and operation as well as data acquisition and the central scheduling of either the entire array or of selected sub-arrays for parallel operation. In comparison to existing imaging atmospheric Cherenkov telescope projects (such as H.E.S.S., MAGIC and VERITAS), the CTA is far more complex and requires that the individual telescopes of the array operate with far higher autonomy and reliability. This in turn creates new demands for many aspects of array control, operation, particularly given the stringent overall CTA performance requirements. In addition, the CTA's data rates will be at least one order of magnitude larger than those of current arrays and will thus require higher bandwidth, the ability to cope with longer networking latencies, and a more complex synchronisation scheme. The handling of sub-arrays of different types of telescopes by a central control system is a further complication, which demands a more flexible control system and advanced algorithms for observation scheduling.

The principles guiding the hardware development are the limitation of the number of different hardware components (bus systems, CPUs etc.) and the use of off-the-shelf computing and networking components that can be easily upgraded whenever

Figure 1

Prototype of the CTA mid-sized telescopes near DESY in Berlin

newer and more powerful versions become available. Similarly, the principles guiding the software development are the use of a well-defined software framework for all processes and the standardisation of the software interface for the control and readout of the various hardware components in the system. The selection of appropriate tools is based on the principle of re-using technologies and (if possible) codes that have already been successfully employed in observatories with requirements similar to those of the CTA. Based on these principles, the ACTL group has identified possible hardware and software solutions. Software technologies for dedicated purposes (database storage, high-bandwidth data acquisition) have also been evaluated, and work has started on the design of software subsystems and on the definition of software interfaces (e.g. to different telescopes and cameras).

Software developed for the MST, the first operational CTA prototype and other CTA prototypes is giving the ACTL group the opportunity to evaluate the ALMA common software (ACS) as a possible common ACTL software framework and the OPC unified architecture (OPC UA) as a possible common ACTL device interface. The control software for components of the MST, such as the drive system, the CCD monitoring cameras, the telescope weather station and the active mirror controls, has already been developed within the ACS and OPC UA frameworks and is already providing valuable test results.

Contact:
Stefan Schlenstedt, stefan.schlenstedt@desy.de

Explosions in the universe.

Theoretical astroparticle physics enters violent environments

Supernova explosions and gamma-ray bursts are the most energetic, explosive events in the universe. A significant fraction of the released energy is channelled into very energetic particles, which we observe either directly as cosmic rays or indirectly through their gamma-ray or neutrino emissions. Elucidating the processes responsible for the acceleration of these energetic particles is a major area of theoretical research.

The year 2012 marked the hundredth anniversary of the detection of cosmic rays. Can we finally solve the mystery of their origin? Understanding where and how these ubiquitous particles are accelerated would have profound implications for many other areas of research and is thus one of the most important goals of modern physics.

Relativistic electrons from supernova remnants were indirectly detected through their synchrotron radiation more than 50 years ago, but unequivocal evidence for the acceleration of hadrons, which make up 99% of cosmic rays, was still missing. The recent discovery of a characteristic signature of neutral-pion decay in the shells of supernova remnants was a very big step forward since it confirmed that hadronic cosmic rays are also accelerated in supernova remnants. This discovery also demonstrated the unprecedented sensitivity of today's detectors. With these new experimental achievements, theorists can now develop and test detailed and realistic scenarios of particle acceleration in supernova remnants.

Modelling particle acceleration in supernova remnants is a multiscale endeavour. Globally, the expansion of the remnants, their internal structure and their impact on the environment can be described with hydrodynamics. On the other hand, energetic particles rarely collide, so their interactions with the ambient plasma must be treated kinetically in terms of self-excited collective electromagnetic fields. It is also imperative that the growth and transport of magnetic turbulence be modelled in parallel since it determines the coupling between energetic particles and a quasi-thermal plasma. To address these issues, we constructed a model that combines hydrodynamical simulations with a code describing the acceleration and transport of energetic particles in a fully time-dependent fashion.

A new insight emerging from our studies is that the structure of the medium into which the supernova remnant expands has an important influence. The progenitor stars of supernovae have strong winds that carve cavities into the environment. Type Ia supernovae arise from thermonuclear explosions of white dwarfs and evolve in a quasi-homogeneous environment. Two other supernova types involve core collapses of massive stars: type IIP supernovae explode into a wind zone of very high gas density, whereas type Ic progenitors produce a large wind zone of low gas density. Consequently, the remnants of supernovae of type Ia, type Ic, or type IIP accelerate particles with different efficiencies and appear distinct in their gamma-ray emission.

In Fig. 1, we compare the expected emission spectra from supernova remnants of these three different supernova types at various points in time with sensitivity curves of the satellite-borne Fermi-LAT telescope and with the forthcoming Cherenkov Telescope Array (CTA) observatory. Figure 1 shows that not only the normalisations but also the shapes of the energy spectra are affected by the different environments of the supernova.

The emissions of gamma-ray bursts (GRBs) in the GeV energy range indicate that particles are being accelerated to very high energies. Such emissions can potentially be used to address the question of whether GRBs are powerful

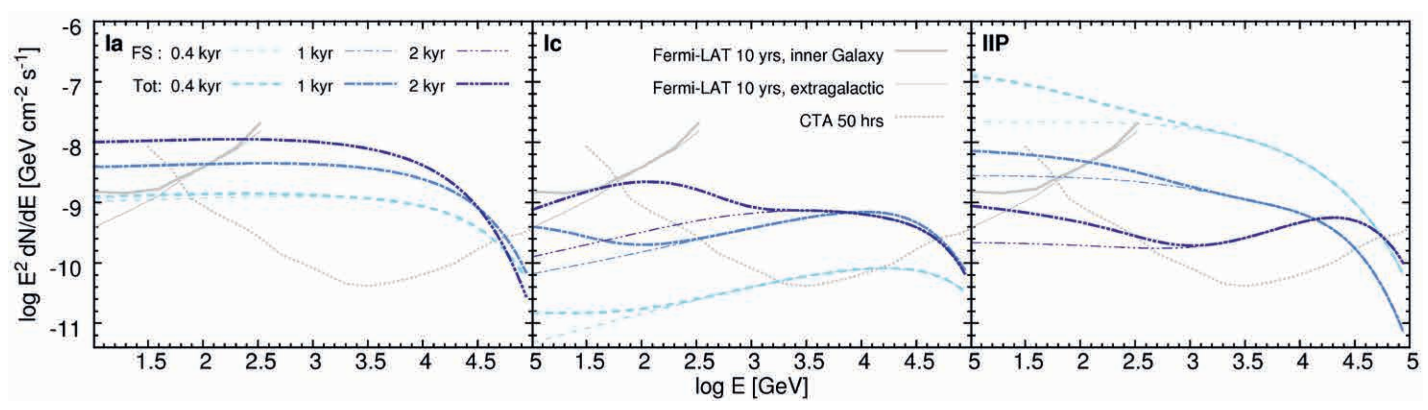

Figure 1

Theoretical gamma-ray emission spectra due to pion decay and inverse Compton emission for various supernova remnant types, ages of 400, 1000 and 2000 years, and a distance of 4500 light-years. “FS” denotes spectra due to acceleration in the forward shock only, and “Tot” denotes the total emission spectra due to particle acceleration at both forward and reverse shock.

enough to provide a significant fraction of the observed ultrahigh-energy cosmic-ray flux. Recently, the GeV-band energy output of GRBs was estimated on the basis of the handful of GRBs that were detected individually with Fermi-LAT. The energy output was found to be less than the amount needed to account for the cosmic-ray flux at very high energies, above the so-called “ankle” in the cosmic-ray energy spectrum, at $10^{18.6}$ eV. However, this estimate is highly uncertain since the flux of high-energy photons from the many GRBs that are too dim to be detected individually by Fermi-LAT is unknown. We therefore re-analysed the Fermi-LAT data with the goal of inferring the average GeV-band emission from the full range of GRBs. Surprisingly, the GeV-band emission episodes were found to last considerably longer than those of the keV/MeV energy range.

Figure 2 shows the gamma-ray flux plotted as a function of T_{90}, i.e. the time during which 90% of the total signal is observed, and demonstrates that altogether only (12 ± 7)% of the total photon fluence in the range from 300 MeV to 30 GeV is emitted during T_{90}. With this new knowledge, we find that the average all-sky energy flux from GRBs in the GeV band is still only about 4% of the energy flux of cosmic rays above the ankle at $10^{18.6}$ eV, which renders the idea that GRBs provide the bulk of ultrahigh-energy cosmic rays very improbable. The search for the origin of cosmic rays goes on!

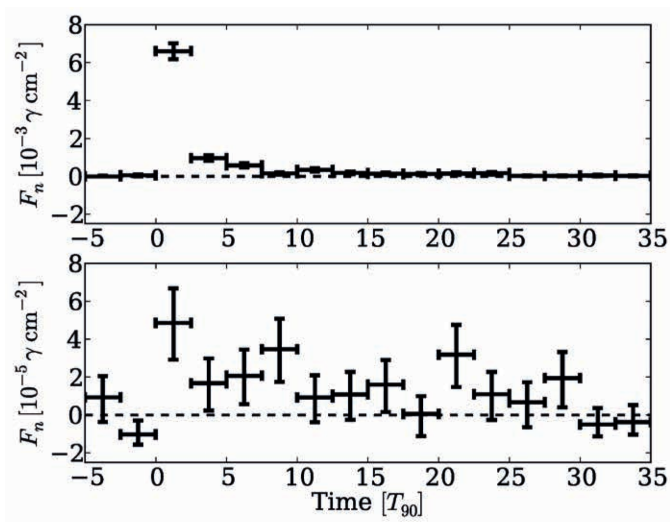

Figure 2

Time-resolved GeV-band gamma-ray flux from GRBs. The top panel is for bright GRBs that were detected individually, while the bottom panel shows the average emission from 85 GRBs that were in the field of view of the gamma-ray detector but not resolved individually. The time unit is the time period during which 90% of the keV/MeV-band emission was observed. Surprisingly, the GeV-band emission from weak bursts is very long-lasting compared with the quasi-thermal emission in the keV/MeV band.

Contact:

Martin Pohl, martin.pohl@desy.de

References:

Telezhinsky, I., Dwarkadas, V.V. & Pohl, M. (2013), A&A 552, A102
Lange, J., Pohl, M. (2013), A&A 551, A89

Watching the big bang.

From microwaves in the sky to inflation in string theory

Observational cosmology suggests that a very early phase of cosmological inflation took place prior to the hot big bang. Future observations in line with those made by the Planck satellite in 2013 might produce evidence for the primordial gravitational waves that would be generated during inflation. If such evidence is found, it would imply that the energy scale of inflation is so high that string theory, as a candidate quantum gravity theory, would alter inflationary predictions and thus become testable.

Recent years have seen the emergence of what has come to be known as the concordance model of cosmology. This model results from a general consensus of cosmologists that was nurtured by high-precision measurements of distant supernovae and cosmic microwave background (CMB) radiation from several sources, notably the recent seven-year data of the Wilkinson Microwave Anisotropy Probe (WMAP) collaboration. According to the concordance model, the universe is spatially flat and composed of 4% ordinary matter, 22% dark matter and 74% dark energy. The initial conditions of the hot big bang match beautifully with the predictions of a very early phase of cosmological inflation.

By “inflation”, we mean a form of quasi-exponential expansion of the very early universe driven by the potential energy density of a slowly rolling scalar field. In addition to the primordial density fluctuations responsible for all of the visible structure of the universe today, inflation should also have produced a spectrum of primordial gravitational waves. Their intensity relative to the intensity of density fluctuations depends on the energy scale of inflation. If such primordial gravitational waves do indeed exist, they would have imprinted a particular pattern in the polarisation of the electromagnetic radiation of the CMB, the so-called B-mode or curl pattern. Future or current observations of polarisation, such as those already made by the Planck satellite (but not yet published), might detect this pattern. Observations of such patterns would imply that the energy scale of inflation is sufficiently high that string theory could modify the inflationary predictions and might thus be testable.

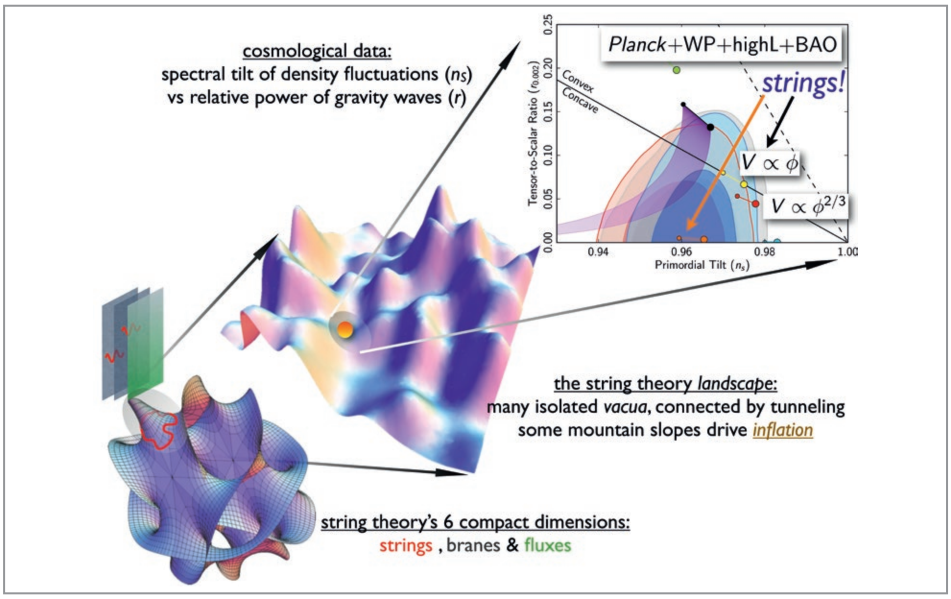

Figure 1

String theory produces a landscape of vacua, some containing inflationary slopes. High enough slopes generate gravitational waves detectable by the Planck satellite. Their stringy origin “deforms” the shape of the slopes and their inflationary predictions compared to naive field theory.

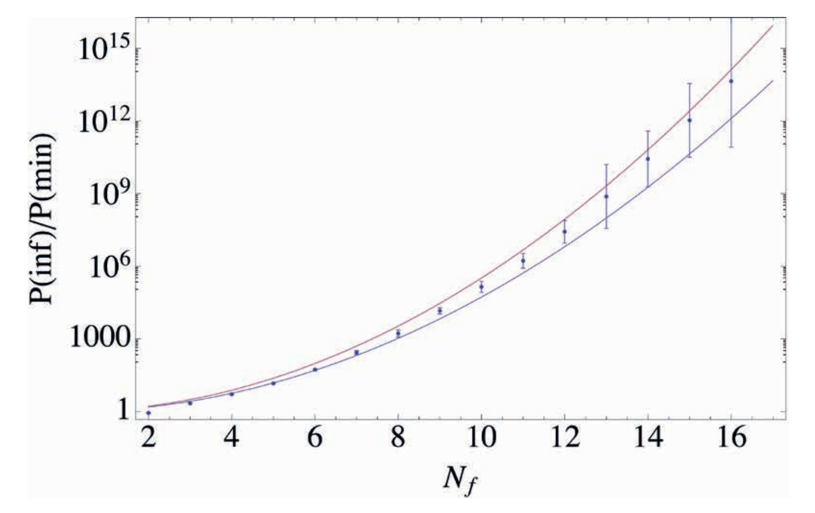

Figure 2

Frequency of low-scale inflation “valleys” relative to local vacua (“minima” of the scalar potential) in a large random landscape approximating the actual string landscape. The number of vacua is itself exponentially large in the number of scalar fields, N_f. This seems to exponentially favour low-scale inflation – however, other factors remain to be explored [6].

String theorists have constructed [1] stabilised four-dimensional string vacua that are cosmologically viable and free of unwanted additional light scalar fields, a prerequisite for inflation. This has led to the realisation that string theory generates a whole “landscape” of vacua, that is, (meta-)stable solutions of string theory (Fig. 1) [2]. Recently, the DESY cosmology group has constructed controlled models of inflation in string theory [3] in which the energy scale of inflation predicts primordial gravitational waves that might be visible to Planck. The study has shown, moreover, that there seems to be a generic tendency in the string landscape to “flatten” away the properties of gravitational waves from the naive field theory expectation of those string inflation models that generate detectable intensities of gravitational waves [4].

The extremely large number of string vacua (10^{500}) expected in the landscape provides a way for theory to accommodate the observed extremely small amount of dark energy in the universe, 10^{-122} in units of the string/Planck scale, as was pointed out by Weinberg [5]. The argument goes as follows: The formation of the numerous large galaxies observed in our universe would not tolerate dark energy more than 10 times larger than the observed value. Thus, if an extremely large number of universes that take on all possible values of dark energy exists, then the existence of large galaxies in our universe necessarily implies that it be among the few having low dark-energy content. String theory made this idea into a working theoretical construction by providing an extremely large set of vacua with a varying amount of dark energy, which can all be realised in different universes by the process of eternal inflation, as first spelled out clearly in string theory by Susskind in 2003 [2]. Since a statistical argument from the string landscape successfully explains the observed present-day value of dark energy in our universe, we may expect that a similar statistical argument will provide a prediction for the inflationary scale of dark energy.

Recently, members of our group [6,7] applied such a statistical idea to the question of the frequency of low-scale and high-scale inflation among the very large set of string vacua. Preliminary results indicate a trend towards inflation models with energy scales significantly below the energy scale of grand unification. If this is true, then consistency with string theory would demand that primordial gravitational waves not be observed by any foreseeable CMB experiment. Thus, the theory could potentially be tested. We are now working to extend the idea by imposing the requirement that a successful theory of inflation must produce a consistent exit from the early inflationary epoch of our universe to the stable vacuum with the very small amount of dark energy observed in our present universe. To include the restriction that this condition places on the counting statistics, a more comprehensive prediction for the expected scale of inflation in string theory must be provided. Once in place, these developments will hopefully allow us to confront string theory with observational data at energy scales farbeyond those reached at particle accelerators.

In March 2014, after the editorial deadline of this brochure, the BICEP2 collaboration announced that it had indeed found B-modes in the CMB polarisation. This exciting result – if confirmed by other results, e.g. from the Planck satellite – will help to significantly advance the theory, including the work presented here.

Contact:

Alexander Westphal, alexander.westphal@desy.de

References:

[1] S. Kachru et al., Phys. Rev. D68, 046005 (2003)
S. Kachru et al., arXiv:hep-th-0308055
[2] L. Susskind, arXiv:hep-th/0302219
[3] E. Silverstein and A. Westphal, Phys. Rev. D78, 106003 (2008)
L. McAllister et al., arXiv:0808.0706
[4] X. Dong et al., Phys. Rev. D84, 026011 (2011)
[5] S. Weinberg, Rev. Mod. Phys. 61 1 (1989)
[6] F. Pedro and A. Westphal, arXiv:1303.3224
[7] A. Westphal, arXiv:1206.4034

The top–antitop threshold.

Precision physics at a future lepton collider

Measuring the top–antitop resonance line shape is a major goal at the planned International Linear Collider (ILC). It will allow for a precise determination of the properties of the top quark and reveal details about its interactions. In particular, the mass of the top quark may be extracted with unprecedented precision from the expected experimental data on electron–positron collisions at the ILC. On the theory side, this requires a very precise prediction of the top–antitop production cross section in the threshold region, i.e. at collision energies of around twice the top mass. The field-theoretical calculations for this process can be performed in a non-relativistic framework (NRQCD), exploiting the fact that the relative velocity of the top pair produced near threshold is small.

Among the six quarks of the Standard Model (SM) of particle physics, the top quark plays a prominent role. The reason is its very large mass of about 174 GeV – roughly 40 times the mass of the next-to-heaviest matter particle, the bottom quark. Not only the mass, but also the decay width (~1.5 GeV) of the top is much larger than that of the other quarks. This translates into an extremely short lifetime of the order of 10^{-24} s. In fact, once a top quark is produced in a collision it decays, unlike the other quarks, before it hadronises, i.e. before it forms a colourless bound state (hadron) with other coloured particles from the surroundings or the vacuum. Hence, top quark production offers the unique opportunity to study the properties of a strongly interacting particle directly, without the uncontrolled non-perturbative effects related to confinement.

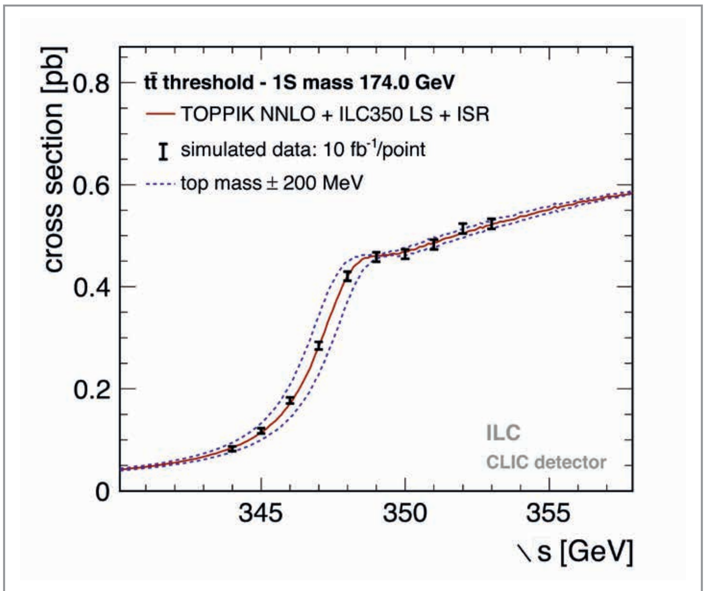

Figure 1

Simulated experimental ILC data (black error bars) for top–antitop production near threshold. The red line represents a (NNLO) theory prediction convoluted with the expected ILC luminosity spectrum and accounts for initial-state radiation. Figure taken from [1].

A precise measurement of the top mass is crucial for precision tests of the SM, vacuum stability studies and analyses of many models for physics beyond the SM. Experimental studies [1] have shown that, at the ILC, an experimental uncertainty of the top mass below 100 MeV is feasible (Fig. 1). This precision is an order of magnitude better than what is possible at the LHC and, relative to the mass, far better than what is known for all other quarks. The strong coupling constant, the top decay width and the top Yukawa coupling can also be extracted from the height and the shape of the resonance cross section with small statistical uncertainties.

The expected accuracy of the experimental data imposes high requirements on the precision of the theoretical prediction for the total cross section near threshold, which can in principle be met by high-order perturbative calculations using effective field theories based on NRQCD. Although the top–antitop pair actually does not have the time to form a bound state, its dynamics near the threshold is still bound-state-like and resembles, to some extent, that of positronium. This is reflected in a steep rise of the cross section at the energy of the would-be toponium ground state, i.e. roughly twice the top mass. One can therefore almost directly read off the top mass from the position at which the cross section rises in future ILC data. The precise value, however, must be determined by a fit of the theoretical prediction to the measured threshold cross section.

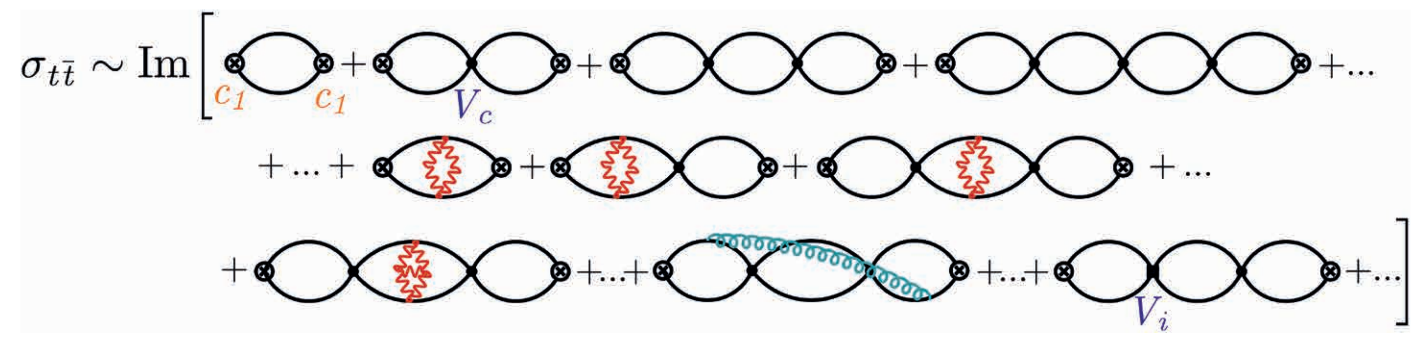

Figure 2

Sketch of the NRQCD calculation for the total top–antitop threshold cross section. The relevant modes in the effective theory are the non-relativistic (anti)top quark (black line), the soft gluon (red zigzag line) and the ultrasoft gluon (green spiral line). The black dot represents the interaction due to the Coulomb potential (V_c), whereas the black square represents interactions due to v-suppressed potentials (V_i). The effective top pair production (annihilation) current is depicted as crossed vertex (c_1) to the left (right) of each diagram.

The typical (relative) velocity (v) of the top quarks in the resonance region is parametrically of the same order as the strong coupling constant (α_s) that is $v \sim \alpha_s \sim 0.1$. As a consequence, conventional perturbation theory, which is based on an expansion in α_s to a given (finite) order, fails to give a reliable prediction for the production process at threshold. This is due to terms that scale as $(\alpha_s/v)^n \sim 1$ at any order in the perturbation series of the cross section. They originate from the binding (colour) Coulomb force between the top and the antitop quark. Furthermore, higher-order quantum corrections typically involve large logarithms of the velocity $\sim(\alpha_s \ln v)^n$, which can deteriorate the convergence of the perturbative expansion.

Both issues can be addressed in the NRQCD framework, where a systematic expansion in the small velocity v is established in addition to the usual perturbative expansion in α_s. The calculation of the cross section is then carried out in terms of NRQCD Feynman diagrams, each of which contributes to a specific order in α_s and v. In practice, the total cross section is related to the imaginary part of top pair production–annihilation diagrams by the optical theorem, as pictorially sketched in Fig. 2.

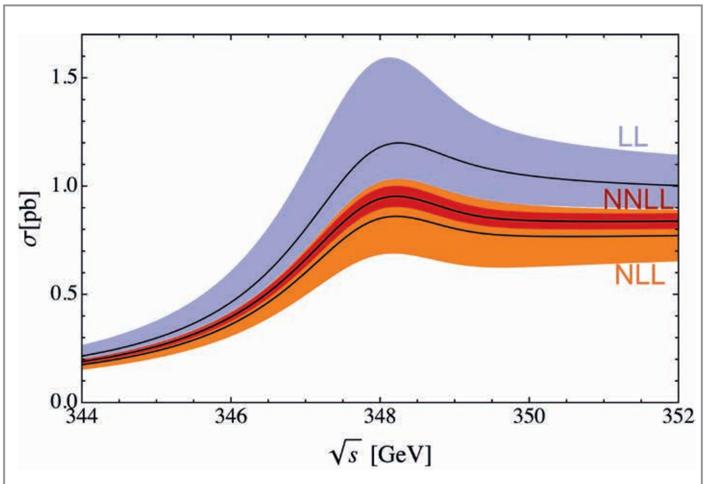

Figure 3

Theory prediction for the total top pair production cross section in the threshold region with increasing precision. The (overlapping) coloured bands represent estimates of the theoretical uncertainty for the respective cross sections (black curves). For this plot, we used a top mass of 174 GeV and a top decay width of 1.5 GeV as input.

The first line in Fig. 2 represents the infinite series of Coulomb interaction diagrams that all contribute to the leading approximation, since $v \sim \alpha_s$. In NRQCD, they can be resummed using a Schrödinger equation. This resummation is crucial for the correct description of the behaviour of the cross section at threshold. Higher-order corrections (in α_s and v) to the cross section involve soft and ultrasoft gluon exchange as well as subleading potential interactions. Extended versions of NRQCD, in addition, allow for a consistent resummation of the large velocity logarithms to all orders in α_s. The outcome of the non-relativistic calculation for the normalised cross section, the so-called R-ratio, then schematically takes the form

$$R = \frac{\sigma_{t\bar{t}}}{\sigma_{\mu^+\mu^-}} = v \sum_k \left(\frac{\alpha_s}{v}\right)^k \sum_i (\alpha_s \ln v)^i \times \left\{1\,(\mathrm{LL});\ \alpha_s, v\,(\mathrm{NLL});\ \alpha_s^2,\ \alpha_s v,\ v^2\,(\mathrm{NNLL}); \ldots\right\},$$

where the terms belonging to leading logarithmic (LL) order, next-to-leading logarithmic (NLL) order etc. are indicated.

Recently, the NRQCD prediction of the total cross section reached NNLL precision [2]. The result is shown in Fig. 3 together with the LL and NLL approximations (black curves) as well as the respective estimates for the theoretical uncertainties (coloured bands). The theory error analysis at NNLL order yields an uncertainty of about 5% for the height of the cross section at the peak. This closely approaches the 3% aim required to match the expected experimental uncertainties. The stable peak position of the cross section suggests that a top quark mass determination with an uncertainty well below 100 MeV may indeed be possible at the ILC.

Contact:

Maximilian Stahlhofen, maximilian.stahlhofen@desy.de

References:

[1] K. Seidel, F. Simon, M. Tesar and S. Poss, Eur. Phys. J. C 73, 2530 (2013)
[2] A. Hoang and M. Stahlhofen, arXiv:1309.6323 [hep-ph]

The lepton anomalous magnetic moment.

A QED precision observable

As was already shown by Schwinger in 1947, the lepton anomalous magnetic moment, a_e, (i.e. the deviation of the lepton's magnetic moment from 2) is, at leading order in perturbation theory, given by $\alpha/2\pi$, where α is the fine-structure constant. On the experimental side, the anomalous magnetic moment of both the electron and the muon are among the best-measured physical quantities. The experimental precision has reached 0.24 parts per billion for the electron and 0.54 parts per million for the muon. The experimental precision alone is already astonishing, but would be of little use if the corresponding theoretical predictions were of lower quality. Matching the experimental precision theoretically involves going well beyond Schwinger's leading-order calculation.

The theoretical calculation of the anomalous magnetic moment of the electron is one of the benchmarks of perturbative quantum electrodynamics (QED). Because of the smallness of the electron mass, all contributions due to additional leptons or stemming from quantum chromodynamics (QCD) are suppressed by m_e^2/M^2, where m_e is the electron mass and M the mass of the additional lepton or pion. The anomalous magnetic moment of the electron is thus essentially insensitive to new physics that involves large masses. After considerable effort, the precision of the theoretical prediction has reached "five-loop accuracy" and matches that of the experimental measurement. The experimental and theoretical results are: $a_e^{\text{exp}} = 1\,159\,652\,180.73\,(0.28) \cdot 10^{-12}$ [0.24 ppb] and $a_e^{\text{theo}} = 1\,159\,652\,181.78\,(6)(4)(3)(77) \cdot 10^{-12}$ [0.67 ppb] [1], respectively. The uncertainties on the theoretical value, shown in parentheses, originate from the eighth- and tenth-order QED contributions, the hadronic contribution and the uncertainty of the fine-structure constant. As can be seen, the uncertainty is dominated by that of the fine-structure constant α. Since experiment and theory agree well with each other, the measurement of the anomalous moment of the electron can be reliably used to obtain the most precise value of the fine-structure constant now available: $\alpha^{-1} = 137.035\,999\,1736\,(68)(46)(26)(331)$ [0.25 ppb].

Due to the larger mass of the muon, its environment is less clean: a sizable hadronic contribution is present and contributions from electrons also play an important role. The current status can be summarised by comparing the best experimental measurement with the theoretical prediction: $a_\mu^{\text{exp}} = 116\,592\,089\,(63) \cdot 10^{-11}$ [0.54 ppm] and $a_\mu^{\text{theo}} = 116\,591\,840\,(59) \cdot 10^{-11}$ [2]. The values differ by about three standard deviations. This gives rise to speculations about a possible influence of new physics. Improvement on the precision of these two numbers would be welcome, although, since the uncertainty on a_μ^{theo} is dominated by contributions from both hadronic vacuum polarisation insertions and light-by-light scattering, which are estimated from experimental data, a further reduction might prove difficult. A possible approach would be to replace the input from experiment by lattice calculations, although this is not presently feasible. On the experimental side, the precision of the measurement of the muon's anomalous magnetic moment is expected to be improved by a factor of 4 by a future experiment at Fermilab.

For the muon, the difference between the experimental value and the theoretical prediction appears to be of the same size as the four-loop QED contribution. However, since the calculation of this contribution was made by only a single collaboration, confirmation is still needed. The first steps towards a new calculation have recently been published [3]. The many QED contributions are conventionally divided into three different categories: the universal contribution, A_1, which is the same for electron and muon; a mass-dependent contribution, A_2, which either depends on m_e/m_μ, where m_μ is the mass of the muon, or m_μ/m_τ, where m_τ is the mass of the tau lepton; and a part A_3 that depends on both m_e/m_μ and m_μ/m_τ. While in the case of the universal contributions no further simplifications are possible and genuine four-loop propagator-type integrals have to be calculated, we can, in the case of $A_2(m_\mu/m_\tau)$, make use of the strong hierarchy $m_\mu \ll m_\tau$ to perform an expansion in m_μ/m_τ. This expansion simplifies the problem since at most four-loop vacuum diagrams, which are well understood, have to be calculated. The method is illustrated for the two-loop case in Fig. 1.

In the expansion, the calculation of a propagator-type, two-loop diagram can be substituted by the calculation of a two-loop

Set	$A_2(m_\mu/m_\tau)\cdot 10^2$ New result [3]	$A_2(m_\mu/m_\tau)\cdot 10^2$ Old result [2]
I(a)	0.00324281(2)	0.0032(0)
I(b) + I(c) + II(b) + II(c)	−0.6292808(6)	−0.6293(1)
I(d)	0.0367796(4)	0.0368(0)
III	4.5208986(6)	4.504(14)
II(a) + IV(d)	−2.316756(5)	−2.3197(37)
IV(a)	3.851967(3)	3.8513(11)
IV(b)	0.612661(5)	0.6106(31)
IV(c)	−1.83010(1)	−1.823(11)

Table 1

Comparison of results of the contributions of the gauge-invariant sets of diagrams to $A_2(m_\mu/m_\tau)$. See Ref. [2] for more details and an explanation of the set naming scheme.

vacuum diagram and the product of two one-loop diagrams. At next-to-next-to-next-to-leading order, i.e. at four loops, we have shown that this method leads to an improved prediction for $A_2(m_\mu/m_\tau)$. In Table 1, we compare the results of our calculations of various sets of gauge-invariant diagrams contributing to $A_2(m_\mu/m_\tau)$ (cf. Ref. [2]) with those obtained by Kinoshita. As can be seen, the uncertainties are substantially reduced and the results are in agreement with the previous results of Kinoshita et al.

Contributions from the hadronic vacuum polarisation can be calculated by integrating a kernel function with the so-called *R*-ratio, which is measured experimentally. At leading order, the analysis is limited by the uncertainty on the *R*-ratio measurement, which is the source of the dominant uncertainty on a_μ^{theo} mentioned earlier. We therefore analysed this contribution using a higher-order calculation, i.e. up to next-to-next-to-leading order. The result of the new calculation of the hadronic vacuum polarisation contribution [4], $a_\mu^{\text{had,NNLO}} = 1.24\ 10^{-10}$, is surprisingly large and leads to a decrease of the discrepancy between the experimental and theoretical values by 0.2 standard deviations, thus reducing the overall deviation from 2.9σ to 2.7σ.

Calculations for the universal part and contributions from diagrams with closed electron loops are on the way and will soon allow a complete check of the available results by an independent method.

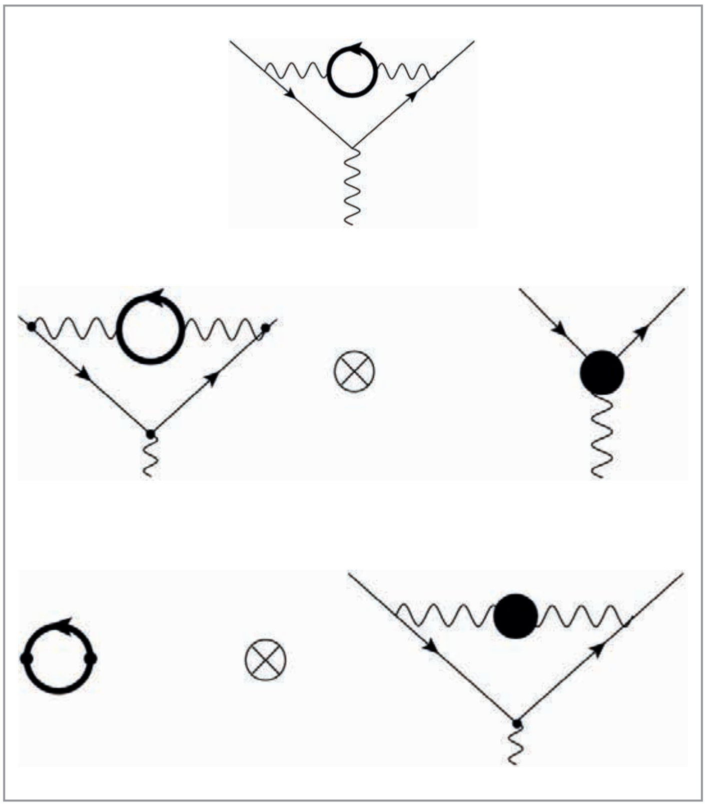

Figure 1

Asymptotic expansion. The diagram at the top receives contributions from two different regions illustrated by the two bottom lines.

Contact:
Peter Marquard, peter.marquard@desy.de

References:

[1] T. Aoyama, M. Hayakawa, T. Kinoshita, M. Nio, Phys. Rev. Lett. 109 (2012) 111807
[2] T. Aoyama, M. Hayakawa, T. Kinoshita, M. Nio, Phys. Rev. Lett. 109 (2012) 111808
[3] A. Kurz, T. Liu, P. Marquard, M. Steinhauser, Nucl. Phys. B879 (2014) 1-18
[4] A. Kurz, T. Liu, P. Marquard, M.Steinhauser, arXiv:1403.6400

Simulation accelerators.

Progress in algorithms for lattice QCD

Lattice QCD simulations on fine lattices and with quark masses set near to their physical values have recently become possible due to rapid progress in algorithm development and advances in computing hardware. In particular, the algorithms used to solve the Dirac equation have improved drastically and a setup has been found in which the topological charge no longer freezes in the continuum limit. These advances are making it possible to simulate QCD on fine lattices in which the dynamical effect of up, down and strange quarks is taken into account.

For lattice QCD computations to be precise, two essential requirements must be fulfilled: the quark masses must be set close to their natural values and the computation has to be repeated on a series of finer and finer lattices so that the extrapolation to zero lattice spacing, i.e. the "continuum limit", can be performed.

A decade ago, such precise computations in QCD seemed unfeasible. For a computation to be completed in a reasonable amount of time, up and down quarks had to be assigned masses more than ten times their physical values and lattices had to be kept coarse. The scaling properties of algorithms were such that even with the most powerful computer resources that we have available today, there would have been little hope to reach high precision. Since then, the situation has improved significantly, in part due to progress in algorithm development. We will discuss two important examples: the tackling of the problems associated with the topological structure of the QCD vacuum, and progress made in solver algorithms. Within the elementary particle physics research group of the John von Neumann Institute for Computing (NIC) at DESY, the simulations are being pursued in the framework of two large European efforts: the European Twisted Mass (ETM) collaboration and the newly formed Coordinated Lattice Simulations (CLS) group.

Taking the continuum limit requires repeating a computation in a fixed physical volume at several values of the lattice spacing. This is computationally expensive. Not only does the number of points on the four-dimensional lattice scale as the fourth power of the inverse lattice spacing, but the phenomenon of critical slowing down, namely the tendency of algorithms to become less efficient as the continuum limit is approached, is encountered. The computation time typically scales with lattice spacing as a power law with a dynamical critical exponent, z, so that if a is the lattice spacing, the computing time grows as a^{-4-z}. For the standard algorithm used for full QCD simulations, $z = 2$ [1]; halving the lattice spacing increases the cost by a factor of 64. However, this is not what had been actually observed in lattice simulations. In particular, the topological charge of gauge configurations moved very slowly during the simulation; for example, we found $z \gtrsim 5$ in pure gauge theory, i.e. in a theory with only gluons [2]. The origin of the behaviour lies in the continuum physics of QCD. Here, the field space is disconnected and therefore separates into sectors characterised by the integer topological charge of the field configurations. Since the Hybrid Monte Carlo – the standard algorithm used in these simulations – is based on quasi-continuous deformation of fields, it has problems with changing between sectors.

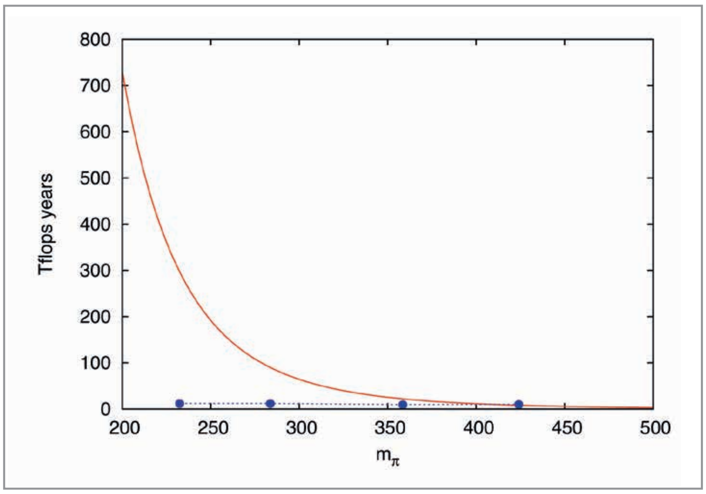

Figure 1

Cost of a simulation. The solid line is Ukawa's 2001 estimate, the dots represent the cost of current simulations based on the algorithm discussed in this text.

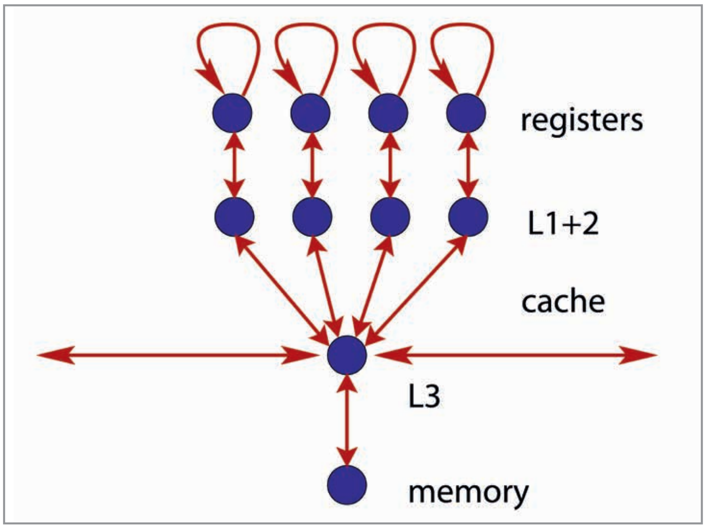

Figure 2

Simplified model of a current processor architecture with several levels of memory hierarchy (blue) and related data transport paths (red)

In our current work, we are exploring a possible solution in which the continuum gauge fields are connected: when open boundary conditions are imposed in the temporal directions, the field space is connected, and therefore a catastrophic slowing down can be avoided. After having already demonstrated that this works in pure gauge theory, we are now investigating what happens when fermions are included into the calculation.

One particularly interesting development has recently taken place in the area of the algorithms used for the solution of the Dirac equation. On the lattice, the Dirac equation is formulated as a huge, sparse system of linear equations. A recently proposed algorithm (the “deflated solver” proposed by Martin Lüscher [3]) made it possible to simulate lighter quark masses without incurring a significant increase in the time needed to solve the linear system. This is due to a new method for incorporating information about the infrared properties of QCD in a way that can be efficiently implemented on current computer architectures. The scaling of the computation time with the quark mass is in stark contrast to previously used methods, where the computational cost increased drastically with decreasing quark masses, as can be seen in Fig. 1.

Computer architectures are also quickly evolving. The current trend has changed from increasing the power of individual computing cores towards increasing the number of computing cores. To efficiently exploit this distributed computing power, algorithmic developments are needed. To this end, simplified models of the hardware architectures (Fig. 2) are being used to aid the analysis of the algorithms in terms of their data flow.

We have described two major algorithmic innovations of recent years. These innovations enable simulations that will lead to precision results in many areas of phenomenology, and in particular in areas of interest to the NIC group at DESY: the fundamental parameters of QCD, such as the strong coupling constant, observables in flavour physics, *g*-2, and hadron structure. Despite these advances in algorithms, the simulations still require very significant computing resources, and generating the gauge configurations used in the simulation is by far the computationally most expensive part of lattice calculations. As a consequence, it is natural to use such configurations in as many projects as possible. Therefore, the NIC group has become involved in two efforts: the ETM collaboration and the CLS group. In both collaborations, computational power and manpower are joined to generate such a set of field configurations.

The newly formed CLS group includes researchers from Denmark, Germany, Ireland, Italy, Spain and Switzerland and has obtained access to substantial computer resources via the European PRACE programme. Simulations currently under way by CLS are taking into account the dynamical effects of up, down and strange quarks. Furthermore, the use of open boundaries is allowing us to simulate at three different, small values of the lattice spacing. With the deflated solver, quark masses close to the physical values can be reached. Thus, the algorithmic work of the recent years is paying off, and we are looking forward to many physics results in diverse areas, from hadron spectroscopy and hadron structure to flavour physics.

Contact:

NIC group (http://nic.desy.de)
Karl Jansen, karl.jansen@desy.de
Stefan Schaefer, stefan.schaefer@desy.de
Hubert Simma, hubert.simma@desy.de
Rainer Sommer, rainer.sommer@desy.de

References:

[1] M. Lüscher, S. Schaefer, JHEP 1104 (2011) 104
[2] S. Schaefer, R. Sommer, F. Virotta, Nucl. Phys. B (2011) 93-119
[3] M Lüscher, JHEP 0707 (2007) 081

A colourful duality.

Towards a renormalisable theory of quantum gravity

In our current understanding of nature, forces are carried by particles. For the forces within the Standard Model of particle physics, these particles have one unit of spin. However, the model is known to be incomplete as a theory of nature, as it does not incorporate one of nature's forces: gravity. The gravitational force should be transmitted by a spin-two particle, the graviton. The standard description of spin-two particles is, however, extremely complicated – or at least it was before the advent of a new idea dubbed colour-kinematic duality. This idea relates scattering amplitudes in gravity to a certain "square" of amplitudes with spin-one force particles. Intense ongoing investigations focus on proving and exploring this unexpected colour-kinematic duality.

Scattering experiments form the backbone of particle physics. The key to describing their outcome is the accurate computation of so-called scattering amplitudes, which measure the likelihood of particular scattering processes. The ability to reliably compute scattering amplitudes is therefore usually a basic requirement for any would-be theory of nature. Another basic requirement is that theories of nature should be predictive. After measuring a finite number of constants, such as the charges and masses of the particles, the theory should be completely fixed: all further computations should yield falsifiable predictions. This requirement is harder to satisfy than you might think: it is the core reason why it is hard to arrive at a sensible theory of quantum gravity!

This problem follows from the main tenet of quantum mechanics, "anything that can happen will happen", and the most famous formula in physics, $E = mc^2$. A basic scattering experiment features incoming particles (such as hadrons in the LHC at CERN) and measures what comes out. What happens before the collision products reach the detector remains unobserved. Quantum mechanics tells us that we have to take into account everything that could happen with the prescribed ingoing and outgoing particles. Albert Einstein told us that energy and mass are equivalent, apart from a multiplicative constant (the speed of light squared), which is needed to make up for different units. As a consequence of both, within the detector, particles can split and join, turning energy into mass and vice-versa (Fig. 1). The unobserved particles could have arbitrarily high energies, far beyond what we can measure. This should not matter for a physical theory: only predictions for the energies we can measure are required. However, can those very high-energy intermediate particles safely be ignored?

For the Standard Model of particle physics, it has been shown that you can indeed safely ignore them – provided that you are very careful to define the constants of the theory in terms of

$$\left.\begin{aligned} E &= mc^2 \\ i\hbar\frac{\partial}{\partial t}\psi &= \hat{H}\psi \end{aligned}\right\}$$

Figure 1

As a consequence of quantum mechanics and the equivalence of energy and mass postulated by Albert Einstein, particles in scattering processes can split and join, turning energy into mass and vice-versa.

Figure 2

Towards a renormalisable theory of gravity

the outcome of measurements. All would-be problems in the theory of the very high-energy intermediate particles can be absorbed into a finite number of these constants. Technically, this process is known as “renormalisation”. A theory that is completely fixed by a finite number of measurements is known as a “renormalisable” theory. This property is so important that Nobel Prizes have been awarded for showing the renormalisablity of the Standard Model of particle physics.

The Standard Model of particle physics, however, does not include the gravitational force. The reason is that, as a quantum theory, general relativity does not seem to be renormalisable: an infinite number of measurements seem to be needed to fix the theory. This would render it completely incapable of predicting anything, and therefore unphysical. This is the famous problem of defining a theory of “quantum gravity”. Many solutions, such as string theory, have been proposed, but none have been completely satisfactory.

As an attentive reader, you will have noticed the word “seem” in the previous paragraph. This word is used because of the unfortunate fact that a theory that describes spin-two particles is fantastically complicated, especially compared to the much simpler theories that describe spin-one particles as they appear in the Standard Model of particle physics. For this reason, investigating the renormalisability properties of quantum gravity theories traditionally relies on estimating certain properties of the computation of scattering amplitudes, typically properties of large sums of different terms. It could be that unexpected cancellations are hidden in the sums, but such cancellations long seemed to be an impossible dream.

However, this dream has recently come a big step closer to reality with a conjecture dubbed “colour-kinematic duality”. There are two sides to this conjecture. The first states that many spin-one theories can be rewritten in such a way that a new and unexpected symmetry emerges for the kinematic parts of the computation. What is more, with this particular rewriting, amplitudes with gravitons are simply obtained by taking two spin-one theories and “squaring” them together in a certain prescribed way. Excitingly, the enormous simplification suggested by colour-kinematic duality makes true quantum computations in gravity feasible. Currently, the duality is being studied to understand the extent to which it holds. In addition, the conjecture alone is already being used to investigate the renormalisability properties of quantum gravity theories. Intriguingly, these theories seem to be generically much better behaved than was naively expected. It will be interesting to further explore how much better they are exactly. Perhaps the old intuition that gravity theory is inherently non-renormalisable might require rethinking.

Contact:

Rutger Boels, rutger.boels@desy.de

References:

A technical introduction can be found e.g. in Reinke Sven Isermann’s thesis http://inspirehep.net/record/1239990/files/desy-thesis-13-020.pdf

Putting new detectors into the beam.

A record year for the DESY II test beam facility

DESY operates the DESY II test beam facility for detector R&D projects from a wide range of communities. In 2013, users from the LHC detector upgrade community, the linear collider detector R&D community and many others made extensive use of the facility. Because of its user-friendliness and its unique infrastructure, it is a highly popular facility for testing detector prototypes: usage in 2013 exceeded all expectations.

At its Hamburg site, DESY provides detector developers with a most welcome test beam facility. The beams are delivered by the DESY II synchrotron, which, in addition to being the injector for the PETRA III synchrotron radiation facility, delivers electron and positron beams from 1 GeV up to 6 GeV to three test beamlines via a secondary target. The energy spread of the beams is less than 5%, and the flux can be as high as 5000 particles/cm^2/s, depending on the choice of target. Each test beamline is fully controllable by the user and outfitted with additional infrastructure to facilitate detector tests. The facility's ease of use makes it very popular for testing detector prototypes.

Unique infrastructure

All test areas offer basic infrastructure such as *XY*-stages for remotely moving devices under test and patch panels for cabling and network connectivity. A high-precision pixel beam telescope, built at DESY, can be made available in any of the areas to provide accurate tracking of beam particles and thereby facilitate studies of the tracking efficiency and resolution of detectors under test. One test area is also equipped with a large-bore superconducting solenoid magnet with a field of up to 1 T, a unique facility worldwide. In the last two years, the magnet was upgraded with a new cooling system to facilitate user operation. The initial funding for both the pixel telescope and the magnet was provided by the EU-FP6 EUDET project. The EU-FP7 project AIDA, DESY and KEK jointly supported the further upgrade of the telescope and magnet infrastructures.

DESY II test beam facility in 2013

DESY is one of the few sites worldwide where tests of particle detectors with high-energy beams can be performed. In 2013 alone, over 400 users from 24 countries came to test their detectors. 75% of the users came from abroad – 43% from the EU and 32% from non-EU countries. 55% of these users came for the first time. In total, 123 weeks were allocated to the user groups and the facility was completely booked out for the entire period. The remarkably reliable operation of DESY II (>99% availability) meant that the test beam was constantly available for users – the facility achieved an up-time of 69% over the year.

The largest fraction of the user groups, nearly 50%, came from the LHC experiments, followed by a total linear collider fraction of about 30% (groups such as LCTPC, CALICE and FCAL). Among the remaining 20% were groups from Belle II, Mu3e, the experiments at FAIR, RHIC and Jefferson Lab, and European XFEL. This user distribution underlines the central role of the facility for worldwide detector R&D carried out by groups working at the LHC, on a future linear collider and at many other facilities throughout the world. In the following, we give a few examples of the tests performed during the year.

ATLAS diamond beam monitor

The ATLAS diamond beam monitor (DBM) will replace the experiment's present beam monitor for measurements of LHC luminosity and beam background. The monitor's novel polycrystalline diamond sensors are extremely radiation-hard and instrumented with a highly granular readout to improve the dynamic range of the luminosity measurement. The prototype sensors were tested in particle beams to measure their hit and charge collection efficiency. For these studies, the high-resolution pixel telescope was indispensable.

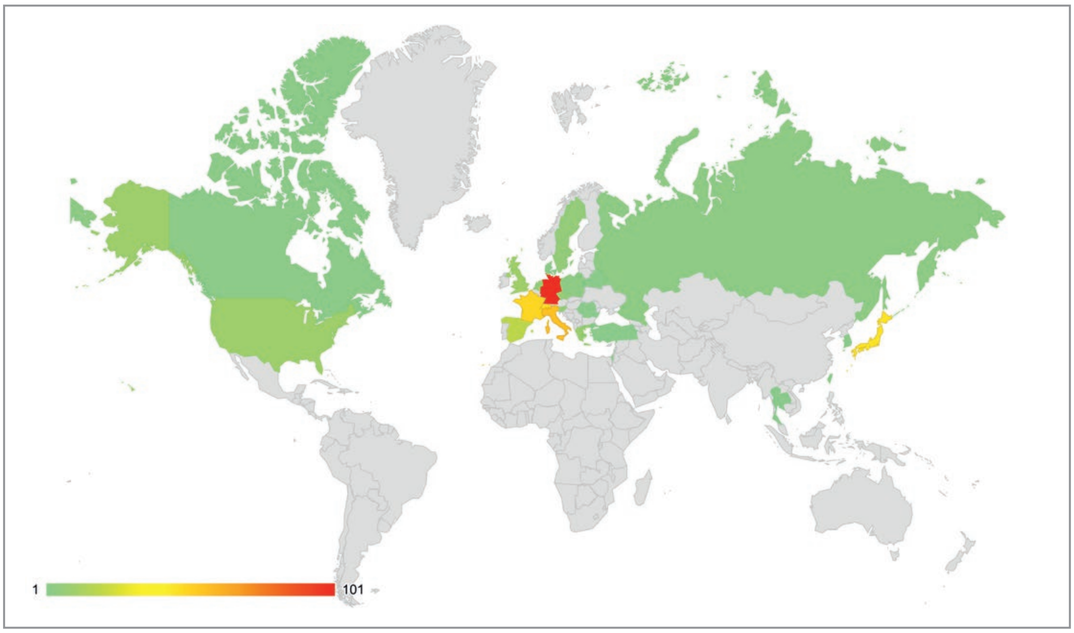

Figure 1

Countries of origin of DESY II test beam users in 2013

Belle II vertex detector system test

The Belle II collaboration performed an integrated system test of their vertex detector. The vertex detector is a key element of the Belle II physics programme, which focuses on precision measurements of *B* meson decays. The detector is due to be installed in 2016.

Prototypes of all subsystems, including their support systems, were tested at DESY (Fig. 2). All of them performed as expected. The large-bore superconducting solenoid proved to be key to the success of the test. Given the significance of the beam test for Belle II, the current spokesperson, Tom Browder from Hawaii University, came to DESY where he expressed his satisfaction: “This mother of all beam tests has been a great success. The conditions, the support and the infrastructure at DESY were perfectly suited to our needs for such a complex test.”

GEM-based front tracker

A new large-area (150 x 40 cm^2) lightweight tracker based on gas electron multiplier (GEM) technology is required for experiments planned for Jefferson Lab in the USA. During their test campaign at DESY, the Jefferson Lab group took advantage of the large-bore solenoid to characterise the performance of a single module in a magnetic field.

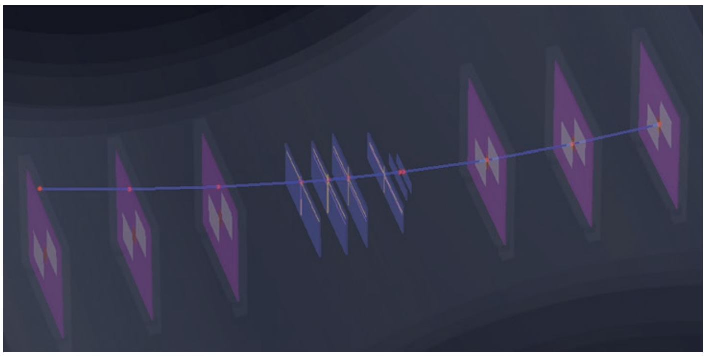

Figure 2

Event display of a track in the Belle II vertex detector prototype

ILC polarimetry

Beam polarisation is a key feature of the International Linear Collider (ILC). To measure it, Compton polarimeters based on Cherenkov detectors are positioned on either side of the ILC collision point. The possibility of building a polarimeter that uses quartz instead of the usual gaseous Cherenkov radiator is being investigated. The use of quartz should dramatically boost the photon yield of the detector. A four-channel prototype of a quartz-based detector was recently exposed to the beam at the DESY test facility.

LCTPC

The LCTPC group is developing a time projection chamber (TPC) as the main tracker of an ILC detector. The current focus of the group is on studies of a large prototype that can house up to seven large readout modules. The prototype was especially designed to fit into the superconducting solenoid of the DESY II test beam facility. In 2013, many system aspects, including the performance of a new two-phase CO_2 cooling system, were successfully tested.

Outlook

The DESY II test beam facility had an extremely successful year 2013, which saw over 400 users perform tests of new detectors. With the start of the shutdown in March 2014, activities will shift to the preparation for another successful run when DESY II resumes operation towards the end of the year.

Contact:

testbeam-coor@desy.de

Ralf Diener, Norbert Meyners, Marcel Stanitzki

References:

http://testbeam.desy.de

Tracking particles worldwide.

EUDET/AIDA pixel beam telescopes for detector development

Thanks to its excellent resolution, high readout rate and its ability to integrate easily with other devices, the high-resolution test beam telescope developed by the DESY-led EUDET project has become an essential test beam tool for many detector development groups. As a result, several copies manufactured by DESY are now in operation at test beams around the world. Within the EU-funded AIDA project, a next-generation pixel beam telescope offering LHC-speed response and even higher readout rates is currently being developed.

New instruments pave the way to future scientific breakthroughs. In particle physics, tracking detectors play an essential role, and their development is crucial for advances in the field. As for any detector, tracking detectors must be tested under realistic operating conditions during the development cycle. Typically, this is done at facilities that provide energetic beams of charged particles. To make effective use of the beam, however, the point of impact of beam particles with the device under test (DUT) must be measured with a precision that exceeds the expected resolution of the DUT. This is normally done with a beam telescope. Traditionally, users would bring such telescopes with them along with the detector to be tested. The EUDET project sought to change this by developing a precise, user-friendly and robust telescope that is sufficiently configurable to serve as a general purpose, well-trusted device usable by any test beam user.

Figure 1

Setting up a device to be tested in the beam telescope at DESY. The two arms of the beam telescope, each consisting of three detector planes housed in aluminium supports, can be seen near the top left of the photo.

The EUDET beam telescope was originally built at DESY within the EUDET project specifically for detector R&D towards the International Linear Collider (ILC). As can be seen in Fig. 1, the EUDET telescope features two arms, each consisting of three sensor planes, mounted on high-precision mechanical frames. A translation-and-rotation stage, on which a DUT can be mounted to allow remotely controlled precise positioning, is available for installation between the two arms. The Mimosa26 CMOS pixel sensor was chosen as the sensitive element since, of all the available detectors, it best fulfills the design requirements. The Mimosa26 sensor consists of a 14 mm by 21 mm silicon chip divided into 576 by 1152 individual detector elements (pixels) and circuitry to support fast readout. With this setup, a point-of-impact resolution of ~ 2 µm has been achieved at the DESY II electron beams.

The EUDET research infrastructure development went well beyond the construction of the telescope itself. The main goal of one of the joint research activities of the project was the creation of a test beam environment, equipped in a unified way such that the time needed for test beam preparation and the subsequent data analysis would be significantly reduced. To this end, a system capable of providing a signal (a trigger) to the readout electronics of the telescope as well as the DUT whenever a charged particle traverses the telescope was needed. The dedicated trigger logic unit (TLU) was built to play this central role. Together with the EUDAQ software package, it offers a simple interface for the seamless integration of arbitrary data acquisition systems with the telescope readout. Last, but by far not least, the EUTelescope software library was developed for the purpose of reconstructing the recorded particle tracks and providing a framework for the analysis of the acquired data.

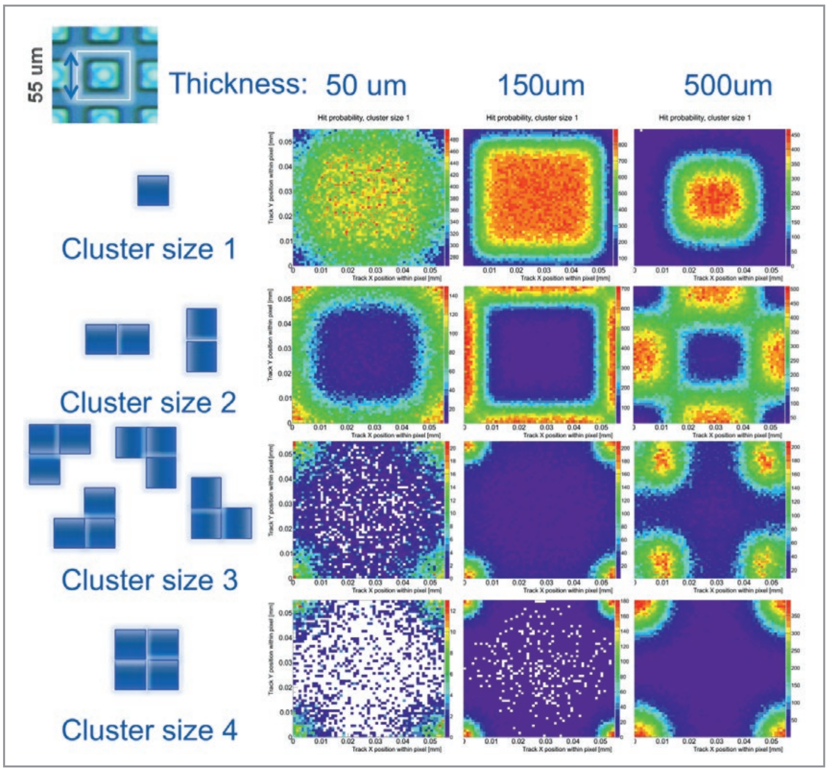

Figure 2

The high-precision tracks from the telescope at DESY provide the input needed to make the study of charge sharing inside a pixel cell over a variety of cluster sizes and thicknesses a reality. (CLICpix collaboration, 9th "Trento" Workshop, 2014)

High popularity and exciting results

Since the conclusion of the EUDET programme in 2010, DESY has blossomed into a telescope manufacturer: already the fifth telescope of the EUDET family was commissioned in June 2013 at Carleton University, Canada, and more copies are being requested. In 2013, three of the telescopes were made available to the users of the DESY II test beam facility. Over 40 high-energy physics R&D groups from various collaborations requested their use for a total of 93 weeks of beam time from January 2013 to the shutdown of DESY II in March 2014.

The beam tests are crucial for the different R&D groups to establish technology choices, for example for the future ATLAS and CMS pixel detectors. Moreover, the high precision of the beam telescopes enables the study of even sub-pixel properties of devices, as demonstrated by the CLICpix collaboration (Fig. 2).

Next-generation beam telescopes

To provide a system that is better suited to the disparate and evolving requirements of the user community, significant effort is going into developing a common cooling and powering of the DUT systems, increasing the detector coverage, upgrading the triggering scheme, improving the selectivity of the trigger and providing the precise timing of beam particle traversals. This development is being done within the European AIDA project.

In addition, a new dead-time-free TLU has been developed, which provides the sub-nanosecond resolution needed for some LHC applications and a synchronous clock for all connected devices. To support such high-speed triggering and the resultant high data rates, a new underlying data model that allows asynchronous data streams, decentralised data handling and a revised online monitoring scheme has been specified for the EUDAQ framework and is currently being implemented at DESY.

Serving the user community

The EUDET/AIDA telescopes have proven to be indispensable to the detector R&D community. An important factor in their success is the strong support offered by DESY. In addition to technical and routine user support work, DESY sponsored a two-day EUTelescope workshop in March 2013, which brought together over 60 participants from many different collaborations for an active exchange of test beam and telescope knowledge between experts as well as for the initiation of new users. Because of the great interest of the user community, a similar event is being planned for 2014.

Contact:
eutelescope-coordinators@desy.de
Hanno Perrey
Igor Rubinskiy

References:
http://beam-telescopes.desy.de

Versatile digital readout electronics for pixel array detectors.

One common digital readout concept for three different detectors

Three pixel array detectors intended for use at different X-ray light source facilities are currently being developed at DESY and will benefit from a common digital readout concept: all three will use an identical digital data acquisition and control board positioned behind the sensor and a readout ASIC.

Readout concept

The signal paths for the three detectors are very similar: for individual pixel areas, the digital output signals of an ASIC or a successive ADC stage are sent in parallel to the input of the readout electronics, to be buffered, preprocessed and finally transmitted to standard computing hardware. All of the resources needed for these generic fast-readout tasks are being integrated onto a common mezzanine card (8 x 25 cm^2), which is plugged into a detector-specific carrier board by way of two high-speed / high-density connectors (900 pins altogether). The carrier boards hold the complete application-specific infrastructure and can be rather simple, providing only the necessary system voltages for the mezzanine card and a connection to the digitised detector output signals. Depending on the detector, more sophisticated features, such as A/D conversion of the analogue detector signals or a slow control system for operating a particular detector could be added. This concept of separating generic data acquisition electronics from those specific to a particular detector allows for an easy and efficient adaption of the complex digital readout circuits to a variety of applications.

Mezzanine board

The design of the mezzanine board is based on a Xilinx Virtex5 FPGA, which is able to handle peak data rates of more than 100 Gbit/s through 146 LVDS input pairs working in parallel at speeds of up to 800 Mbit/s each. The maximum sustained data throughput of the module is limited to 40 Gbit/s by four 10G Ethernet links to external processing devices. For applications in which the full data throughput is not needed, one of the links can be operated as a standard 1 GBit TCP/IP connection. Two SO-DIMM slots can be equipped with 8 GBytes of DDR2 memory to provide high bandwidth (80 Gbit/s) storage for internal data sorting and processing. The board configuration is managed by a CPLD to allow the booting of the FPGA from multiple local (Platform Flash RAM, 8 GBit CompactFlash Card) and external sources such as JTAG or a microcontroller interface. Several firmware versions with different functionalities and data processing algorithms can be kept locally on the board. Multiple boards can be used in a network to build scalable and online-reconfigurable systems. A flexible clocking interface as well as several general-purpose IOs and buses like I2C, SPI, etc. simplify the integration of the board into various

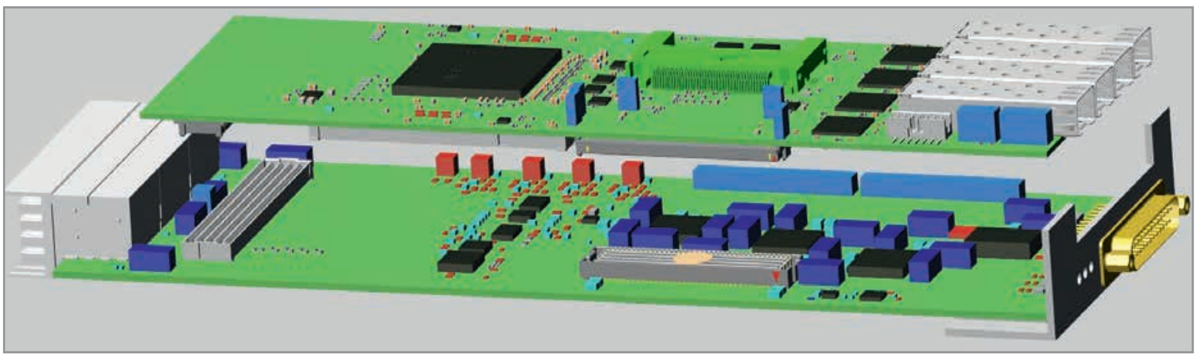

Figure 1

A mezzanine card holding generic readout electronics is shown above a detector-specific carrier.

applications. The two FPGA-internal PowerPC processors can also be used for additional control and monitoring tasks.

FPGA framework

Keeping in mind that the data flow and requirements of these detector systems are similar, but that they will be applied to different experiments, we have created a common FPGA framework to simplify the development of application- and experiment-specific firmware. This framework provides generic access to the board's peripherals such as Input/Output, DDR2 memory access and on-board flash memory. For fast data transfer via the four 10G Ethernet links, a UDP stack is implemented in VHDL to enable the communication with standard PC hardware. The two FPGA-internal PowerPC processors allow for the efficient implementation of control, monitoring and debugging applications in high-level languages even with an operating system as well as for remote firmware updates and data flow management tasks.

This approach has the great advantage that it allows users to apply and reuse the generic functions and therefore to fully concentrate on their core activities, such as detector-specific readout sequences, data processing or calibration algorithms. It is obvious that this approach will reduce the FPGA firmware development time substantially.

Applications

The digital readout is part of the three detector prototypes shown in Figs. 2–4, which are currently being tested. For the final detector systems, 200 mezzanine cards are currently being manufactured.

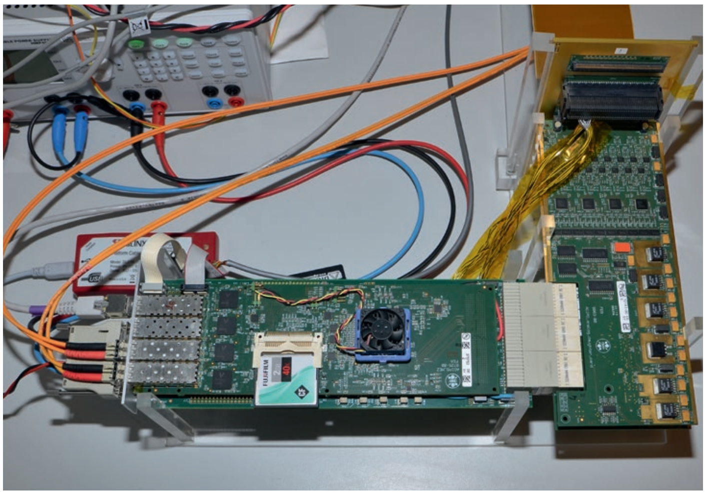

Figure 2

AGIPD (Adaptive Gain Integrating Pixel Detector) is a high-speed X-ray camera for the European XFEL designed for single-pulse imaging at 4.5 MHz frame rate. The dynamic range allows detection of single photons or up to more than 10 000 12.4 keV photons in the same pixel and image.

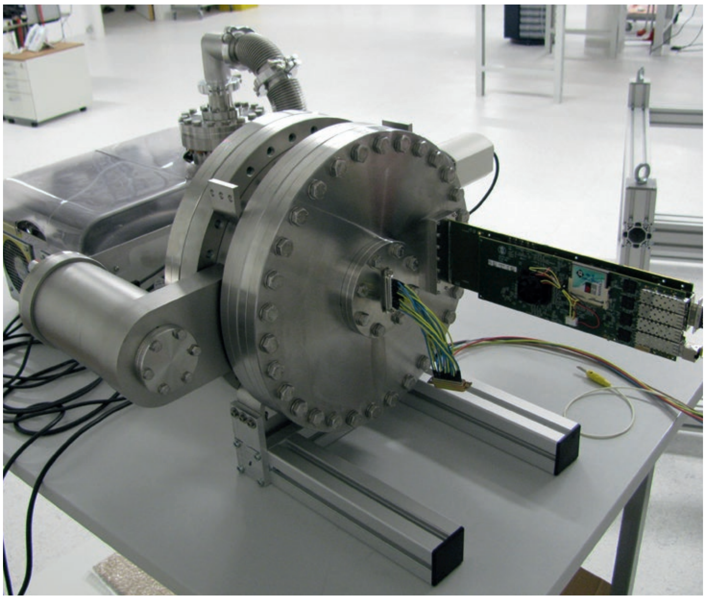

Figure 3

PERCIVAL (Pixelated Energy Resolving CMOS Imager, Versatile and Large) is a multimegapixel monolithic active pixel sensor (MAPS) for the soft X-ray regime (0.25–1 keV), based on CMOS technology.

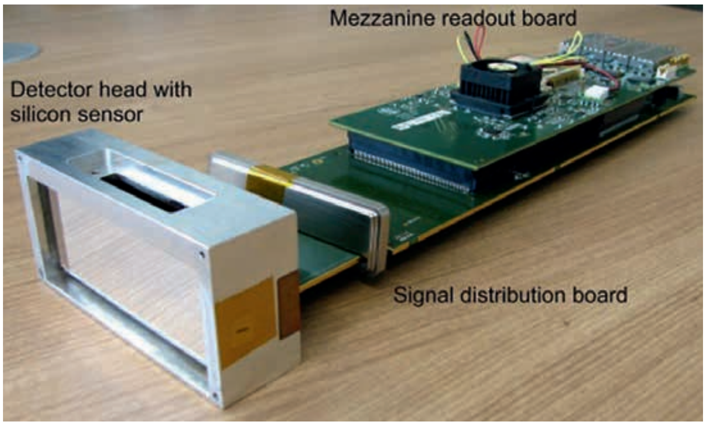

Figure 4

LAMBDA (Large-area Medipix-Based Detector Array) is a photon-counting pixel detector system based on the Medipix3 readout chip. It is the basis of the so-called Helmholtz cube, which will serve as a development platform for new sensor materials, readout ASICs and interconnect technology, as well as a prototype system for photon science experiments.

Contact:
Manfred Zimmer, manfred.zimmer@desy.de

Streamlining electronics development.

New enterprise resource planning system for electronics service centre

Many R&D groups at DESY are designing and building printed-circuit board (PCB) assemblies and electronic devices intended for use in the development, production and operation of particle accelerators, new detectors, data acquisition systems, signal processing and data storage. They rely heavily on the DESY Service Centre Electronics to provide them with infrastructure and expertise.

The DESY Service Centre Electronics offers several services to DESY's numerous R&D groups:
> construction of PCB assemblies and electronic devices, including development of PCB layouts,
> in-house production of prototypes and small runs of PCB assemblies and electronic equipment,
> handling of orders for external production of large series,
> wire bonding,
> repair and test of PCB assemblies and electronic equipment,
> advising of DESY staff regarding equipment, safety and technology for the production of PCBs and electronic devices.

To accomplish these tasks, the service centre possesses extensive infrastructure, including
> a production line for surface-mounted devices comprising a stencil printer, an automated pick-and-place machine, a reflow oven, an automated optical inspection system and a repair workstation for ball grid arrays and other parts,
> a through-hole soldering workshop equipped with a wave soldering machine, lead-free solder workstations, press-in tools and a cable stripping machine,
> a wire bond laboratory, equipped with an automated ultrasonic wire bonding machine and optical inspection systems,
> a test laboratory, equipped with a flying-probe tester, a boundary scan testing system and electromagnetic compatibility testing devices.

The coordination of all work tasks and of the material flow for more than 400 orders per year is conducted by staff members of the service centre's job preparation section. To improve the steering and workflow control of the process, an enterprise resource planning (ERP) system has been implemented. In a first implementation step, only the time-tracking part of the new ERP system was deployed. This gave the group members the opportunity to familiarise themselves with the user interface and to test its stability without having to cope with the full scope of its services. By July 2013, all tests of the new system had been successfully passed, and the system had reached a sufficient level of acceptance by the group members to allow the entire workflow of the service centre to be switched to the new system.

The core of the system is a powerful database that stores all relevant information and the complete process logic on a dedicated server machine maintained by the IT department. Through its use, the workflow at the service centre has become completely article-oriented. Step by step, all components as well as PCB assemblies and electronic devices are being stored as unique articles in the article database to allow the identification, traceability and assignment of all component articles.

Each article representing a PCB assembly or electronic device is also associated with a work schedule, likewise stored in the database, which forms the basis for the scheduling of all work tasks (e.g. the assignment to machines and staff members). The work schedule tracks all associated activities, including parts delivery and the actual production. It also improves the ability to share work tasks between staff members; this is especially important for complex electronic devices comprising large numbers of components and sub-assemblies. Furthermore, new productions of previously produced PCBs and electronic devices are tremendously simplified, require

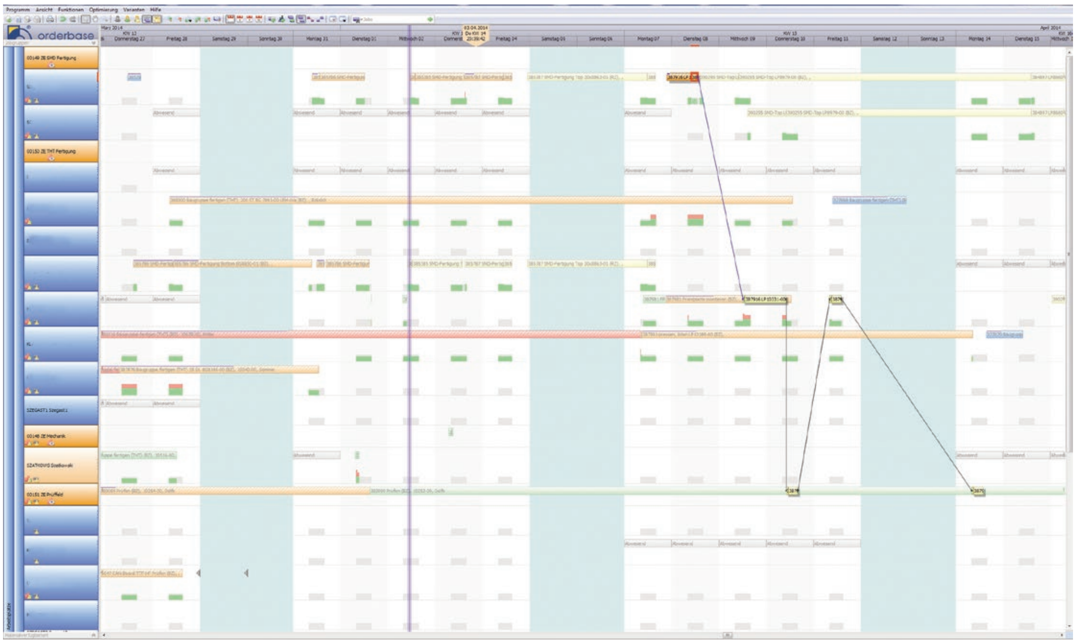

Figure 1

Example of a resource planning chart for work orders

less effort and are less subject to any errors encountered during the earlier production runs.

The documentation task will also be greatly simplified: each article and work task is linked to a corresponding document folder, which contains all associated documents. As a result, the collaboration between the job preparation step, the processing in the workshop and the testing in the laboratory as well as the preparation of the final product documentation for the customer will be significantly simplified.

Last but not least, the various DESY R&D groups employ different CAD systems for schematic design and PCB layout. To avoid the time-consuming and error-prone manual importation of data into the production parts list and to simplify the ordering of parts themselves, the service centre has recently started to work with its client groups to synchronise all parts databases with the central article database of the ERP system.

Contact:
desy-ze@desy.de

Author:
Otto-Christian Zeides, otto-christian.zeides@desy.de

The Grid and NAF at DESY.

Computing resources for local, national and global communities

After having demonstrated the power of its Grid Centre and National Analysis Facility (NAF), through their prominent role in the discovery of the Higgs boson by the Large Hadron Collider (LHC) communities, DESY is concentrating on integrating new communities into the Grid and NAF infrastructure. An evolved NAF setup was put into operation to meet the requirements of new communities such as Belle II, Herafitter and ILC in addition to serving its regular users.

In line with its role as a large national laboratory, DESY is offering the computing resources of its Grid sites in Hamburg (DESY-HH) and Zeuthen (DESY-ZN) [1] not only to local user groups but also to national and global communities. In addition, the DESY Grid is serving as a Tier-2 centre of the Worldwide LHC Computing Grid (WLCG) [2] for the LHC experiments ATLAS, CMS and LHCb. The second important computing facility at DESY, the NAF [3], continues to serve the German physics communities and to complement the Grid services with its optimised general analysis infrastructure.

The analysis work of all communities at DESY requires a close collaboration between the Grid and NAF infrastructures. Although they are separate, many external components are used by both systems. For example, data are delivered to computing nodes by a common storage infrastructure. Software is provided by way of a shared network file system (CVMFS) that is optimised to deliver experiment-specific software in a fast, scalable and reliable way.

Both the DESY Grid Centre and the NAF have also recently become an important computing resource for the upcoming electron–positron experiments at the SuperKEKB facility in Japan (Belle II) and at the planned International Linear Collider (ILC). In 2013, these two communities carried out massive Monte Carlo production campaigns with significant contributions by DESY. The computing needs of the astroparticle physics groups of the CTA gamma-ray observatory and the IceCube neutrino telescope are being supported by DESY in Zeuthen.

The Grid

DESY operates a common Grid infrastructure, which federates resources among 20 virtual organisations (VOs) – experimental groups with a share of available Grid computing resources – and allows for opportunistic allocation of free resources. Moreover, DESY plays the role of "home" for a number of global VOs, e.g. ILC and IceCube, and provides all essential Grid services for them. Since 2013, DESY has been operating a CVMFS server for the central software repository of the ILC and is preparing to serve as a main CVMFS hub for the ATLAS, CMS, and LHCb VOs. To better serve this expanding user community, DESY made a modest upgrade of computing and storage resources of the Grid Centre in 2013; the current values are listed in Table 1.

Site	Job slots	kHS06	Disk space (PB)
DESY-HH	10 000	90	8.3 (dCache, without HERA)
DESY-ZN	1600	23	2.3 (dCache)
NAF	4500	52	0.8 (Sonas)

Table 1

Overview of resources at both DESY sites

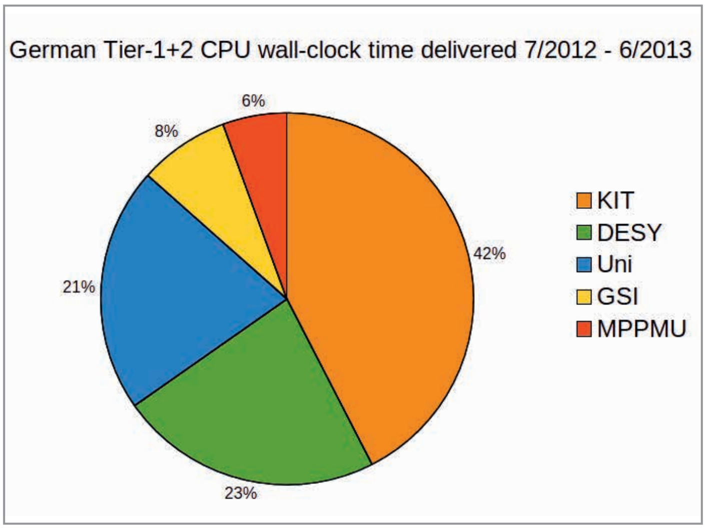

Figure 1

Delivered resources in terms of wall-clock time of the Tier-1/2 sites in Germany. At DESY, roughly 20% of the computing resources are used by non-LHC experiments.

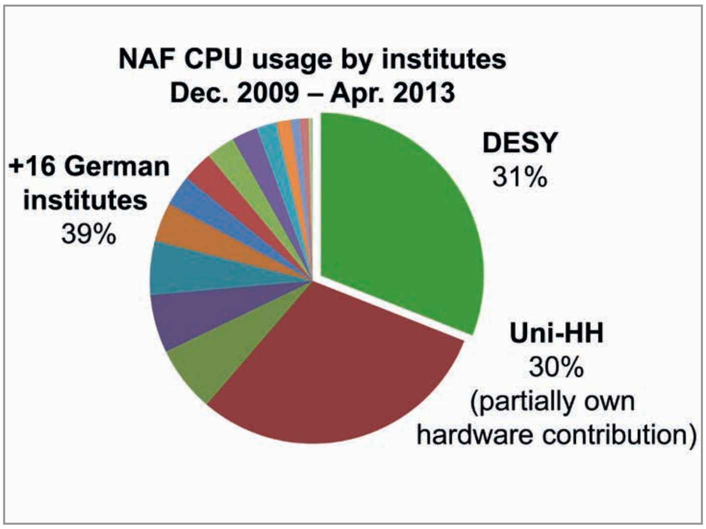

Figure 2

NAF usage by institutes from December 2009 to April 2013. Many institutes profit from the NAF, making it truly a facility for the whole German LHC and ILC community.

The NAF

The NAF has been in operation at DESY since 2007 and is well used, both by local groups and throughout Germany, as illustrated in Fig. 2. It was initially designed to serve the German LHC and ILC communities but is now being adapted to meet new challenges and respond to the evolving needs of the experiments, e.g. by providing more graphical tools and other software packages, including commercial products, as well as better remote access capabilities. Furthermore, new user communities, including the Belle collaboration and the HeraFitter project, have joined and legacy support for the HERA communities has been added.

After a thorough study, it was concluded that NAF usage and administration could be better optimised by integrating it into the other, standard DESY infrastructure and by concentrating the NAF at a single site. Therefore, in 2013, a new independent NAF facility was set up under the project name “NAF 2.0”, while the old NAF continues to operate. To a large extent, the building blocks of the NAF have been integrated into already existing infrastructures:

> The DESY registry is used for account and access right management. The accounts are regular DESY accounts with username/password authentication.

> The workgroup server setup is similar to the standard DESY workgroup server.

> The batch farm is integrated into the DESY BIRD facility, a general-purpose batch facility used by many DESY groups.

> The AFS cell used for home and group directories is the common desy.de cell.

In addition, to better address remote access needs, several “NAF remote desktops” were installed. These are server systems running a desktop installation that offers high-performing graphics access remotely. Finally, we note that the mass storage system dCache, which is central to all HEP data analysis at DESY, is accessible by all computing resources, including NAF 2.0.

The migration of users from the old NAF to NAF 2.0 has been under way since late 2013. This includes the migration, with support from IT, of the user data residing on the SONAS storage system. The ATLAS and LHCb users have refocused their NAF-related activities to the DESY Hamburg site, while DESY in Zeuthen remains a Tier-2 centre for ATLAS and will serve the needs of the astroparticle physics community. By the end of 2013, most of the NAF resources were migrated to NAF 2.0. The old NAF will be turned off in spring 2014, according to present planning.

Contact:

Andreas Gellrich, andreas.gellrich@desy.de
Andreas Haupt, andreas.haupt@desy.de
Yves Kemp, yves.kemp@desy.de
Peter Wegner, peter.wegner@desy.de

References:

[1] http://grid.desy.de/
[2] http://wlcg.web.cern.ch/
[3] http://naf.desy.de/

Enabling global computing.

LSDMA initiative and dCache big data cloud

2013 was a busy year in global computing, in particular for the dCache collaboration and the Large Scale Data Management and Analysis (LSDMA) initiative: dCache.org further consolidated its leadership role in the worldwide management of scientific data by offering extended outreach and support activities as well as by providing financial support for the LSDMA initiative, a portfolio extension of the Helmholtz Association. In addition, LSDMA and dCache.org are working together to promote the increased sharing of national and European computing resources by organising meetings, by collaborating with other European infrastructure projects and by providing prototypes. Finally, in collaboration with the University of Applied Sciences (HTW) in Berlin, dCache.org and LSDMA are investing in the education of students and young scientists in the area of big data and cloud computing.

LSDMA

The LSDMA initiative is an extension of the Helmholtz portfolio, which was launched in 2012 with the ultimate goal of deploying a German national scientific infrastructure that enables a wide range of communities to analyse an ever-increasing quantity of scientific data. The collaboration is composed of four Helmholtz centres and seven associated universities and has a total five-year budget of over 13 million euro, of which DESY will receive slightly under 2.5 million euro.

Building on its on-going engagements in the Data Lifecycle Labs (DLCL) and Data Service Integration Teams (DSIT), DESY is preparing a Germany-wide authentication and identity management infrastructure. Since this infrastructure must also be compatible with other European efforts, DESY is also leading a similar activity in the context of the Federated Cloud Initiative of the European Grid Infrastructure (EGI). In another LSDMA-related activity, DESY collected requirements from the various photon science communities on how they envisage the design of their data lifecycle processes and, based on the results, has been designing a prototype, which will be implemented in 2014.

LSDMA, dCache.org and international networking activities

dCache.org started in 2000 as a collaboration of computer scientists from Fermilab, the Nordic Data Grid Facility (NDGF) and DESY. In 2012, the already established loose connection between dCache.org and HTW Berlin was tightened, essentially through the LSMDA project, since HTW became a subcontractor of DESY. In this context, DESY is supporting HTW students working on their Bachelor's or Master's degrees by providing direct access to dCache.org storage experts as well as financial support through LSDMA.

LSDMA and dCache.org share the common high-level objective of simplifying the procedure used by scientists to gain access to distributed storage resources, both within Europe and elsewhere, by requesting that users identify themselves only by supplying their home institute credentials (e.g. home institute login credentials) or nationally issued X509 certificates. To work on the political issues involved, dCache.org also joined the EGI Federated Cloud Initiative and is closely connected with the US Open Science Grid (OSG) community through dCache.org colleagues at Fermilab.

Figure 1

Poster of the 2nd Asian Pacific dCache Workshop, organised by the DESY dCache.org team with great support from RWTH Aachen, Germany, and Academia Sinica, Taipei, Taiwan

As part of the Worldwide LHC Computing Grid (WLCG), dCache.org is working with CERN to improve the integration of heterogeneous data storage systems by switching from the proprietary WLCG software stack to open protocols and software. This effort was triggered by the European Middleware Initiative (EMI) and is being continued as a private collaboration between CERN, dCache.org and other interested groups.

dCache.org and the big data cloud

Historically, dCache has been used as a scientific storage management system that provides access to the data storage frameworks of individual experiments through either community-specific protocols or standards such as the Storage Resource Manager (SRM) protocol, GridFTP or NFSv4.1. More recently, given the growing importance of cloud and big data computing, dCache has been extending its services to also include cloud protocols like WebDAV and the Cloud Data Management Interface (CDMI), overseen by the Storage Networking Industry Association (SNIA).

Its ten years of experience in managing huge amounts of data, its collection of community-specific access protocols, its commitment to open standards and now its integration of cloud semantics make dCache a unique tool for solving the big-data requirements of medium to large scientific laboratories. As a test of its usability, dCache.org and HTW Berlin are operating a dCache cloud system that is used by HTW students and other selected interested customers.

dCache deployment and outreach activities

In addition to offering storage-specific workshops, such as the dCache tutorials during the annual “GridKa School of Computing”, the 7th International dCache Workshop in Berlin and the 1st Asian Pacific Workshop in Taipei, dCache.org organised two generic computing workshops, which served to keep DESY in the focus of scientific computing: a data federation workshop in collaboration with SLAC, CERN and the University of Chicago, and the LSDMA Identity workshop with presentations from European experts in that field.

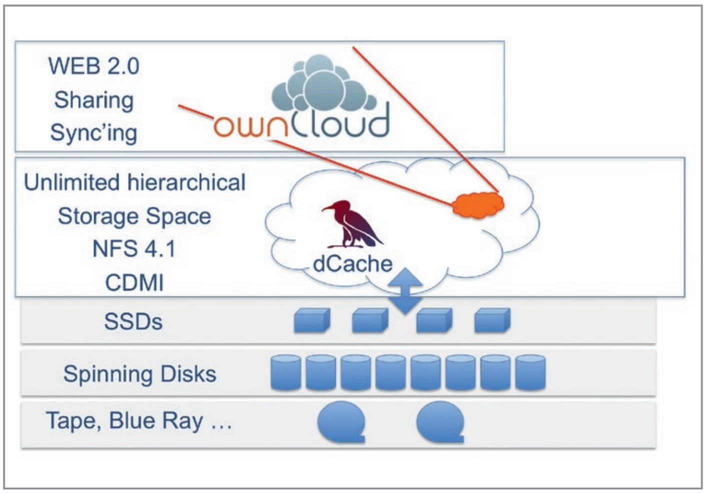

Figure 2

By combining ownCloud, a well-established open-source cloud system, with dCache, DESY will provide a unique big data cloud solution.

The continuous, dedicated software support of dCache.org and its extended outreach activities have certainly been prime factors in the decision of the Fermilab Extensity Frontier project to base their storage system on dCache and in the decision of the Fermilab CMS Tier-1 to extend their tape-based dCache system to a disk-only one.

dCache at DESY

The dCache Operations Team (DOT) at DESY in Hamburg is operating five dCache instances. Three are Grid-enabled storage elements, two of which are dedicated to LHC experiments and their virtual organisations (ATLAS, CMS), the third one mainly serving ILC and Belle. The two remaining storage elements are used by the local HERA experiments and the various DESY photon science groups. Not being part of the global Grid file exchange infrastructure, both are using professional transfer services, e.g. Globus-Online, for exchanging large amounts of data between DESY and laboratories around the world. In total, DESY in Hamburg is serving about 11 PB of data on disk and roughly 12 PB on tape, both managed by the dCache technology. DESY in Zeuthen is operating about 2.5 PB on disks and 1.8 PB on tape, supporting the ATLAS, IceCube, CTA, PITZ and NIC experiments.

Summary

In 2013, DESY has continued to play a leading role in distributed worldwide computing through its many activities within dCache.org and LSDMA, with the goal of extending the reach of global computing by refining and unifying protocols, simplifying procedures for gaining access to resources, providing technical and user support for dCache and supporting efforts to educate the next generation of global computing professionals and users.

Contact:
Patrick Fuhrmann, patrick.fuhrmann@desy.de
Martin Gasthuber, martin.gasthuber@desy.de

SCOAP³.

Sponsoring Consortium for Open Access Publishing in Particle Physics

Thanks to SCOAP³, a large fraction of particle physics publications have, since 1 January 2014, been published under the open access paradigm. The consortium brings together 24 countries and 11 publishers, with obvious benefits for the readers as well as the authors who will retain their copyrights.

Figure 1

Representatives of the SCOAP³ initiative at CERN during the meeting at which the SCOAP³ memorandum was signed

Since 1 January 2014, a large fraction of the publications appearing in particle physics journals have been freely available as open access publications. This is the result of the successful launch of the SCOAP³ consortium in December 2013, after several years of intense preparation involving thousands of libraries and key funding agencies from 24 countries. The DESY library and documentation group has been an active participant from the beginning and has both represented the Helmholtz Association and served as one of three German national contact points. The DESY group was also actively involved in the preparation of the SCOAP³ tendering process and provided the figures that formed the basis for the distribution of membership fees for all partners within Germany.

With SCOAP³, 11 publishers have transformed some of their journals either completely or at least partially (the particle physics-related sections) into open access journals. Among them are well-known companies such as Springer, Elsevier or IOP Publishing. Thus, the largest fraction of worldwide publications in particle physics will be published free of charge to the authors and the readers. The copyrights for the publications will remain with the authors, which will allow maximum use and reuse while respecting the rights of the publishers. The costs of the publishers and of the review process are redirected from the previous subscription fees of the institutions involved in SCOAP³ to the SCOAP³ fund at CERN.

Contact:
Martin Köhler, martin.koehler@desy.de

INSPIRE.

Developing new services

In 2013, the DESY library and documentation group continued to improve the INSPIRE database. The main changes were to the back end, particularly to the way data are ingested into the system. At the same time, many new features were introduced into the front end. The new author profile page is well used, and information from the HepData project at Durham, UK, has also been integrated. The DESY group plays an active role in the coordination and planning of future developments, daily operations and handling of user requests. It concentrates on content selection and classification, the ingestion of journal articles as well as the maintenance and improvement of the corresponding workflow. Another important focus of the DESY group is data preservation.

Until February 2013, INSPIRE was just another front end to the SPIRES database. Since then, curation of records has been handled by INSPIRE in order to allow access to a richer set of metadata organized in a new structure. Journal records are now ingested before the final curation, which leads to information being made available more quickly. Tools for the matching of journal articles to preprints and for helping with the selection of articles have been ported into the new system and improved, and a complete clean-up of the institution database is under way. The migration of the back end from SPIRES tools to an integrated INSPIRE workflow is expected to be finished by the end of 2014.

Many developments that affect the user interface are in progress, including the following.

The user feedback system, which handles general questions and suggestions and allows for additions and corrections to the database, is being improved. Guided forms will allow for faster processing of the requests.

The identification of authors is continuously being improved; it has also been integrated with the global ORCID system and other author IDs. A new author profile page has been set up, which summarises the old HEPNames information about a person (contact information and history) as well as the author's publications (literature list, citations, co-authors, frequent keywords etc.). This very concise overview has turned out to be extremely useful.

Another big step is the integration of research data, mainly from the Durham HepData group, into the database, which is now being presented to the user along with the publication itself. DOIs are assigned to single plots or tables to improve the precision of citations. Questions on how to count citations of data with respect to citations of the publication are under discussion.

The archival of collaboration notes is part of data preservation. Several collaborations (H1, ZEUS, HERMES, D0, CDF and BaBar) store their internal notes in private collections to guarantee the availability of supporting information for future use of the research data. The data preservation project was started and organised by the DESY group.

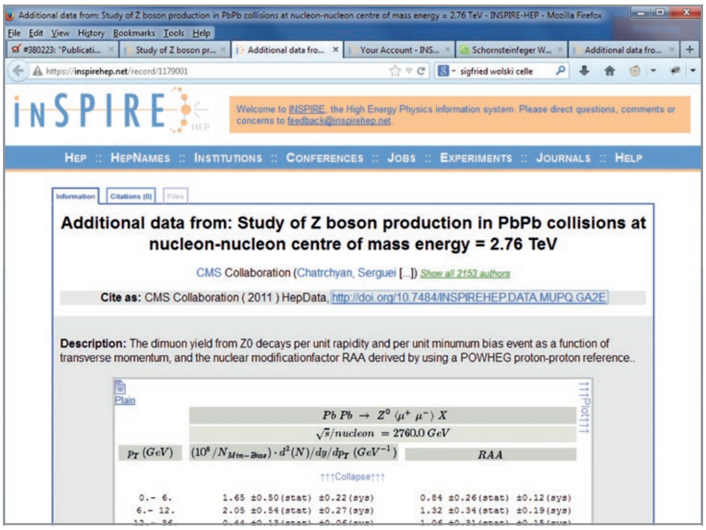

Figure 1

Data from the Durham HepData project integrated in INSPIRE and citable via DOI

Contact:

Kirsten Sachs, kirsten.sachs@desy.de

References:

http://inspirehep.net

References

Committees.

DESY Administrative Council

Representatives of the Federal Republic of Germany:

VLR I **M. Häusler**
(Federal Foreign Office)

MinR'in **O. Keppler**
(Federal Ministry of Education and Research)

Dr.-Ing. **B. Vierkorn-Rudolph** (Chair)
(Federal Ministry of Education and Research)

Representatives of the Free and Hanseatic City of Hamburg:

LRD Dr. **R. Greve**
(Ministry of Education and Research)

J. Dühring (interim)
(Ministry of Finance)

Representatives of the Federal State of Brandenburg

Dr. **C. Menzel**
(Ministry of Finance)

H. Topel
(Ministry of Science, Research and Culture)

Representatives from science and industry

Prof. Dr. **U. Beisiegel**
(President, Georg-August-Universität Göttingen)

Dr. **M. Kraas**
(Olympus Surgical Technologies)

Dr. **G. Mecke**
(AIRBUS)

Dr. **C. Quitmann**
(Lund University)

DESY Board of Directors

Dr. **R. Brinkmann**
(Accelerator Division)

Prof. Dr. **H. Dosch**
(Chairman of the DESY Board of Directors)

Prof. Dr. **J. Mnich**
(Particle Physics and Astroparticle Physics Division)

C. Scherf
(Administrative Division)

Prof. Dr. **E. Weckert**
(Photon Science Division)

Prof. Dr. **C. Stegmann**
(Representative of the Directorate in Zeuthen)

DESY Scientific Council

Prof. Dr. **J. Daillant**
Synchrotron Soleil (FR)

Prof. Dr. **M. Danilov**
ITEP, Moscow (RU)

Prof. Dr. **P. Drell** (Chair)
SLAC National Accelerator Laboratory (USA)

Dr. **F. Gianotti**
CERN, Geneva (CH)

Prof. Dr. **K. Hämäläinen**
University of Helsinki (FIN)

Prof. Dr. **J. Hastings**
SLAC National Accelerator Laboratory (USA)

Dr. **N. Holtkamp**
SLAC National Accelerator Laboratory (USA)

Prof. Dr. **S. Larsen**
MAX IV Laboratory (SE)

Dr. **L. Merminga**
TRIUMF (CA)

Prof. Dr. **S. Ritz**
University of California (USA)

Dr. **E. Shaposhnikova**
CERN (CH)

Prof. Dr. **G. Wormser**
LAL, Orsay (FR)

Prof. Dr. **L. Young**
Argonne National Laboratory (USA)

and the chairs of

ECFA: Dr. **M. Krammer**
Institut für Hochenergiephysik, Wien (AU)

DESY MAC: Prof. Dr. **A. Jankowiak**
HZB

DESY PRC: Prof. Dr. **A. White**
U Texas (USA)

DESY PSC: Prof. Dr. **M. Drescher**
U Hamburg

DESY Scientific Board: Dr. **M. Kasemann**
DESY

European XFEL: Prof. Dr. **M. Altarelli**
European XFEL

DESY Scientific Board

M. Ackermann (DESY)
R. Balewski (DESY)
T. Behnke (DESY)
F. Beckmann (HZG)
M. Bieler (DESY)
K. Borras (DESY)
F. Brinker (DESY)
K. Büßer (DESY)
W. Buchmüller (DESY)
H. Chapman (DESY)
W. Drube (DESY)
G. Eckerlin (DESY)
H. J. Eckold (DESY)
E. Elsen (DESY)
K. Flöttmann (DESY)
B. Foster (DESY)
H. Franz (DESY)
H. Graafsma (DESY)
G. Grübel (DESY)
V. Gülzow (DESY)
T. Finnern (DESY)
I.-M. Gregor (DESY)
J. Haller (U Hamburg)
A. Kappes (DESY)
M. Kasemann (DESY, Chair)
F. Kärtner (DESY)
O. Kind (HU Berlin)
A. Meyer (DESY)
V. Miltchev (U Hamburg)
K. Mönig (DESY)
T. Naumann (DESY)
C. Niebuhr (DESY)
D. Nölle (DESY)
E. Plönjes-Palm (DESY)
M. Pohl (DESY)
B. Racky (DESY)
K. Rehlich (DESY)
A. Ringwald (DESY)
R. Röhlsberger (DESY)
R. Santra (DESY)
O. Seeck (DESY)
S. Schlenstedt (DESY)
J. Schmid (EMBL)
M. Schmitz (DESY)
T. Schörner-Sadenius (DESY)
V. Schomerus (DESY)
S. Schreiber (DESY)
C. Schrör (TU Dresden)
H. Schulte-Schrepping (DESY)
H. C. Schulz-Coulon (U Heidelberg)
A. Schwarz (DESY)
G. Sigl (U Hamburg)
J. Spengler (DESY)
A. Stierle (DESY)
M. Tischer (DESY)
T. Tschentscher (XFEL)
J. Viefhaus (DESY)
M. Vogt (DESY)
P. Wegner (DESY)
G. Weiglein (DESY)
H. Weise (DESY)
M. Wieland (U Hamburg)

Machine Advisory Committee (MAC)

Dr. **M. Borland** (ANL, USA)
Dr. **H. Braun** (PSI, CH)
Dr. **Massimo Ferrario** (INFN, IT)
Dr. **Zhirong Huang** (SLAC, USA)
Prof. Dr. **A. Jankowiak** (HZB, DE, Chair)
Dr. **K. Oide** (KEK, JP)
Dr. **Pantaleo Raimondi** (ESRF, FR)
Dr. **R. Schmidt** (CERN, CH)

Physics Research Committee (PRC)

Dr. **E. Aschenauer** (BNL, USA)
Prof. Dr. **M. Beneke** (RWTH Aachen)
Dr. **M. Carena** (Fermilab, USA)
Dr. **J. Haba** (KEK, JP)
Prof. Dr. **M. Kobel** (TU Dresden)
Prof. Dr. **L. Köpke** (U Mainz)
Prof. Dr. **R. Ong** (UCLA, USA)
Prof. Dr. **L. Rosenberg** (U Washington, USA)
Prof. Dr. **R. Wallny** (ETH Zürich, CH)
Prof. Dr. **A. White** (U Texas, Chair)
Dr. **R. Yoshida** (ANL, USA)

Ex-officio members:
Prof. Dr. **H. Dosch** (DESY)
Prof. Dr. **J. Mnich** (DESY)
Prof. Dr. **E. Weckert** (DESY)
Dr. **R. Brinkmann** (DESY)
Prof. Dr. **C. Stegmann** (DESY)

Helmholtz Alliance International Advisory Board

Prof. Dr. **J. Brau** (U Oregon, USA)
Dr. **N. Geddes** (RAL, UK)
Dr. **P. Jenni** (CERN, CH)
Dr. **D. Schlatter** (CERN, CH)
Prof. Dr. **B. Spaan** (U Dortmund)
Prof. Dr. **T. Virdee** (Imperial College London, UK)
Prof. Dr. **S. Yamada** (U Tokyo, JP)

German Committee for Particle Physics (KET)

Prof. Dr. **S. Bethke** (MPP München)
Dr. **K. Borras** (DESY)
Prof. Dr. **I. Brock** (U Bonn)
Prof. Dr. **S. Dittmaier** (U Freiburg)
Prof. Dr. **T. Hebbeker** (RWTH Aachen)
Prof. Dr. **W. Hollik** (MPP München)
Dr. **H. Kroha** (MPP München)
Prof. Dr. **T. Mannel** (U Siegen)
Prof. Dr. **J. Mnich** (DESY)
Prof. Dr. **T. Müller** (KIT)
Prof. Dr. **G. Quast** (KIT)
Prof. Dr. **P. Schleper** (U Hamburg, Chair)
Dr. **C. Rembser** (CERN, CH)
Prof. Dr. **R. Rückl** (U Regensburg)
Prof. Dr. **C. Zeitnitz** (U Wuppertal)

German Committee for Astroparticle Physics (KAT)

Prof. Dr. **J. Bluemer** (KIT)
Prof. Dr. **K Danzmann** (U Hannover)
Prof. Dr. **R. Diehl** (MPE Garching)
Prof. Dr. **D. Horns** (U Hamburg)
Prof. Dr. **J. Jochum** (U Tübingen)
Prof. Dr. **K. Kampert** (U Wuppertal)
Prof. Dr. **M. Lindner** (MPP München)
Prof. Dr. **L. Oberauer** (TU München)
Prof. Dr. **E. Resconi** (TU München)
Prof. Dr. **G. Sigl** (U Hamburg)
Prof. Dr. **C. Stegmann** (DESY)
Prof. Dr. **C. Weinheimer** (U Münster)

Memberships.

ACOT-Advisory Committee for TRIUMF (Canada)
Kerstin Borras

Advisory Committee of the Max-Planck-Institut für Gravitationsphysik, Potsdam
Wilfried Buchmüller

AIDA Management Board / Steering Committee
Ties Behnke, Ingrid-Maria Gregor

Akademie der Wissenschaften Hamburg
Wilfried Buchmüller

ATLAS-Canada Review Committee of NSERC, Canada
Eckhard Elsen

ATLAS Executive Board
Klaus Mönig

ATLAS UK Upgrade Oversight Committee (UK)
Marcel Stanitzki

AUGER Scientific Advisory Committee
Christian Spiering

BMBF, Gutachterausschuss Hadronen und Kernphysik
Hans Weise

BMBF, Gutachterausschuss Teilchenphysik
Eckard Elsen, Joachim Mnich

CALICE Steering Board
Felix Sefkow (Chair)

CERN Machine Advisory Committee
Reinhard Brinkmann

CERN Science Policy Committee
Christian Spiering

CERN SPS Committee
Markus Diehl

CLIC Steering Committee
Brian Foster

Cluster of Excellence for Fundamental Physics, Munich: Scientific Advisory Committee
Wilfried Buchmüller (Chair)

CMS Collaboration Board and Authorship Board
Matthias Kasemann (Chair)

CMS Collaboration Board, Conference Board, Finance Board and Management Board
Kerstin Borras

CMS Tracker Institution Board
Günter Eckerlin

Computer Applications in Nuclear and Plasma Sciences (CANPS), Technical Committee
Günter Eckerlin

Computing Resource Review Board, CERN
Volker Gülzow

CTA Scientific and Technical Advisory Committee
Christian Spiering

Data Preservation and Long Term Analysis in High Energy Physics (DPHEP) International Steering Committee
Zaven Akopov, Achim Geiser, Volker Gülzow, David South

Deutsches Forschungsnetz DFN Verwaltungsrat / Betriebsausschuss
Joachim Mnich / Volker Gülzow

DKE Deutsche Kommission Elektrotechnik, Elektronik und Informationstechnik im DIN und VDE, Kommission K967
Peter Göttlicher

DPG Vorstandsrat
Thomas Naumann

DPG, Beirat der Sektion Teilchenphysik
Ties Behnke

DPG, Wissenschaftlicher Beirat des Physikzentrums
Georg Weiglein

DPG, Fachverband Teilchenphysik
Christian Spiering (deputy chair)

EMI Project Technical Board and Collaboration Board
Patrick Fuhrmann

European Committee for Future Accelerators (ECFA)
Joachim Mnich

European Strategy Group for Accelerator R&D (ESGARD)
Eckhard Elsen

FAIR, Machine Advisory Committee
Kay Wittenburg

Gauss Allianz, Mitgliederversammlung und Grid-Koordinationsausschuss
Volker Gülzow

German Executive LHC Outreach Group (GELOG)
Ulrike Behrens, Klaus Ehret, Gerrit Hörentrup, Matthias Kasemann, Christian Mrotzek, Thomas Naumann, Thomas Zoufal

Global Design Effort (GDE)
Wilhelm Bialowons, Brian Foster (European Director), Nicholas John Walker (Project Manager)

GridKa, Technical Advisory Board
Martin Gasthuber, Birgit Lewendel

GridKa, Overview Board
Volker Gülzow

Helmholtz Alliance, Institute Assembly
Ingrid-Maria Gregor

Helmholtz Alliance, Management Board
Ties Behnke (Scientific Coordinator), Karsten Buesser, Eckhard Elsen, Matthias Kasemann, Joachim Mnich, Klaus Mönig, Thomas Schörner-Sadenius (Scientific Manager)

Helmholtz Alliance, Project Boards
Doris Eckstein, Eckhard Elsen, Volker Gülzow, Matthias Kasemann, Katja Krüger, Klaus Mönig, Thomas Schörner-Sadenius, Felix Sefkow, Georg Weiglein

Helmholtz Arbeitskreis Bibliotheks- und Informationsmanagement
Martin Köhler

Helmholtz Lenkungsausschuss Struktur der Materie
Ties Behnke, Reinhard Brinkmann, Helmut Dosch, Volker Gülzow, Joachim Mnich, Edgar Weckert

Helmholtz Programmsprecher für Elementarteilchenphysik
Joachim Mnich

Helmholtz Versammlung der wissenschaftlich-technischen Räte
Matthias Kasemann

Helsinki Physics Institute, Scientific Advisory Board
Wilfried Buchmüller

Humboldt Universität CCSA
Karl Jansen

IAC EINN 2013
Karl Jansen

IEEE Radiation Instrumentation Steering Committee
Ingrid-Maria Gregor

ILC MDI Common Task Group
Karsten Buesser (Chair)

ILC Physics and Experiment Board
Ties Behnke, Karsten Buesser

ILC Programme Advisory Committee
Hans Weise

ILC Steering Committee (ILCSC)
Joachim Mnich

ILD Executive Board
Ties Behnke, Karsten Buesser, Wolfgang Lohmann, Felix Sefkow

ILD Joint Steering Board
Ties Behnke

INFN International Evaluation Committee (IT)
Christian Spiering

INSPIRE Steuerungsgremium
Jürgen Reuter, Kirsten Sachs

Institut Pluridisciplinaire Hubert Curien, Advisory Board
Joachim Mnich

International Committee for Future Accelerators (ICFA)
Joachim Mnich

International Committee for Future Accelerators (ICFA), Panel on Advanced and Novel Accelerators
Siegfried Schreiber

International Committee for Future Accelerators (ICFA), Beam Dynamics Panel
Rainer Wanzenberg

International Lattice Data Grid
Karl Jansen

International Linear Collider and High Gradient Superconducting RF-Cavities
Eckhard Elsen (coordinator)

IUPAP, Chair of Commission C4 (Astroparticle Physics)
Johannes Knapp

John von Neumann Institute for Computing (NIC), Director
Joachim Mnich

John von Neumann Institute for Computing (NIC), Scientific Council
Hubert Simma

Joint Institute of Nuclear Research JINR, Physics Advisory Committee and Scientific Council
Joachim Mnich

KIT Center Elementary Particle and Astroparticle Physics (KCETA), Advisory Board
Joachim Mnich

KM3NeT Scientific and Technical Advisory Committee
Christian Spiering

Koordinierungsausschuss Datenverarbeitung der Helmholtz-Gemeinschaft (KODA)
Volker Gülzow

Komitee für Astroteilchenphysik (KAT)
Christian Spiering (Chair), Christian Stegmann

Komitee für Beschleunigerphysik
Hans Weise

Komitee für Elementarteilchenphysik (KET)
Kerstin Borras, Joachim Mnich

Laboratoire Souterraine Modane, Scientific Committee
Christian Spiering

L'Agence d'Evaluation de la Recherche et de l'Enseignement Superieur (AERES)
Eckhard Elsen

LHC Experiments Committee (LHCC)
Eckhard Elsen (Chair)

LHC Resources Review Boards (LHC-RRB)
Manfred Fleischer

LHC-RRB, Computing Resource Scrutiny Group
Martin Gasthuber

LHC-RRB, Scrutiny Group
Carsten Niebuhr

LHC Review Committee Japan (JP)
Eckhard Elsen

LHC-US Accelerator Research Program Advisory Committee
Kay Wittenburg

Linear Collider Board LCB
Joachim Mnich

Linear Collider Collaboration, European Director
Brian Foster

Linear Collider Collaboration, Physics and Detector Executive Board
Ties Behnke, Karsten Buesser, Marcel Stanitzki

MAGIC Collaboration Board and Executive Board
Markus Garczarczyk

MAGIC Time Allocation Committee
Elisa Bernardini

Main Panel B, Research Excellence Framework, Higher Education Funding Council for England (UK)
Brian Foster

MPI-München, Scientific Advisory Board
Joachim Mnich (Chair)

NIKHEF Scientific Committee (NL)
Christian Spiering

Particle Data Group
Klaus Mönig, Georg Weiglein

Peta QCD Scientific Advisor
Karl Jansen

PHIL Scientific Committee
Markus Garczarczyk, Frank Stephan

Plenary European Committee for Accelerators (P-ECFA)
Kerstin Borras

Rat Deutscher Sternwarten
Martin Pohl

Romanian CERN Project Funding Program of the Romanian Ministry of Education and Research, Scientific Advisory Board
Eckard Elsen

Steering Group of the European Network for Novel Accelerators (EuroNNAc)
Jens Osterhoff

SwissFEL Beam Diagnostic Review Committee (CH)
Bernhard Schmidt

Sectional Committee 2, Royal Society (UK)
Brian Foster

SiD Co-spokesperson
Marcel Stanitzki

STFC Oversight Committee Dark Matter (UK)
Johannes Knapp

STFC Oversight Committee for ATLAS UK
Bernd Löhr

Wolfgang Pauli Centre
Wilfried Buchmüller (Spokesperson)

ZKI
Volker Gülzow

Collaborations.

H1

I. Physikalisches Institut, RWTH Aachen

Universiteit Antwerpen (BE)

VINCA Institute of Nuclear Sciences, Belgrade (CS)

School of Physics and Space Research, University of Birmingham (GB)

Inter-University Institute for High Energies ULB-VUB, Brussels (BE)

National Institute for Physics and Nuclear Engineering, Bucharest (RO)

Rutherford Appleton Laboratory, Chilton, Didcot (GB)

Henryk Niewodniczaski Institute of Nuclear Physics, Cracow (PL)

Institut für Physik, Technische Universität Dortmund

Joint Institute for Nuclear Research (JINR), Dubna (RU)

CEA, DSM-DAPNIA, CE Saclay, Gif-sur-Yvette (FR)

Deutsches Elektronen-Synchrotron DESY

Institut für Experimentalphysik, Universität Hamburg

Max-Planck-Institut für Kernphysik, Heidelberg

Kirchhoff Institut für Physik, Universität Heidelberg

Physikalisches Institut, Universität Heidelberg

Institute of Experimental Physics, Slovak Academy of Sciences, Košice (SK)

School of Physics and Chemistry, University of Lancaster (GB)

Oliver Lodge Laboratory, University of Liverpool (GB)

Queen Mary and Westfield College, London (GB)

Physics Department, University of Lund (SE)

Physics Department, University of Manchester (GB)

CPPM, Université de la Méditerranée, IN2P3-CNRS, Marseille (FR)

Departamento de Fisica Aplicada, CINVESTAV, Mérida (MX)

Departamento de Fisica, CINVESTAV, México (MX)

Institute for Theoretical and Experimental Physics (ITEP), Moscow (RU)

Russian Academy of Sciences, Lebedev Physical Institute, Moscow (RU)

Max-Planck-Institut für Physik, Werner-Heisenberg-Institut, München

LAL, Université Paris-Sud, IN2P3-CNRS, Orsay (FR)

Laboratoire Louis Leprince Ringuet, LLR, IN2P3-CNRS, Palaiseau (FR)

LPNHE, Université Paris VI et VII, IN2P3-CNRS, Paris (FR)

Faculty of Natural Sciences and Mathematics, University of Montenegro, Podgorica (YU)

Institute of Physics, Academy of Sciences of the Czech Republic, Prague (CZ)

Institute of Particle and Nuclear Physics, Charles University, Prague (CZ)

Dipartimento di Fisica, Università Roma 3 and INFN Roma 3, Rome (IT)

Institute for Nuclear Research and Nuclear Energy, Sofia (BG)

Institute of Physics and Technology, Mongolian Academy of Sciences, Ulaanbaatar (MN)

Paul Scherrer Institut, Villigen (CH)

Fachbereich Physik, Bergische Universität-GH Wuppertal

Yerevan Physics Institute, Yerevan (AM)

Institut für Teilchenphysik, ETH Zürich (CH)

Physik Institut, Universität Zürich (CH)

ZEUS

Department of Engineering in Management and Finance, University of the Aegean (GR)

Institute of Physics and Technology, Ministry of Education and Science of Kazakhstan, Almaty (KZ)

National Institute for Nuclear and High Energy Physics (NIKHEF), Amsterdam (NL)

Argonne National Laboratory (ANL), Argonne IL (USA)

Andrews University, Berrien Springs MI (USA)

University and INFN, Bologna (IT)

Physikalisches Institut, Universität Bonn

H.H. Wills Physics Laboratory, University of Bristol (GB)

Panjab University, Chandigarh (IN)

Rutherford Appleton Laboratory, Chilton, Didcot (GB)

Physics Department, Ohio State University, Columbus OH (USA)

Physics Department, Calabria University and INFN, Cosenza (IT)

The Henryk Niewodniczaski Institute of Nuclear Physics, Cracow (PL)

Department of Physics, Jagellonian University, Cracow (PL)

Faculty of Physics and Nuclear Techniques, AGH-University of Science and Technology, Cracow (PL)

University and INFN, Florence (IT)

Fakultät für Physik, Universität Freiburg

Department of Physics and Astronomy, University of Glasgow (GB)

Deutsches Elektronen-Synchrotron DESY

Institut für Experimentalphysik, Universität Hamburg

Nevis Laboratories, Columbia University, Irvington on Hudson NY (USA)

Institute for Nuclear Research, National Academy of Science and Kiew National University, Kiew (UA)

Department of Physics, Malaya University, Kuala Lumpur (MY)

Department of Physics, Chonnam National University, Kwangju (KR)

High Energy Nuclear Physics Group, Imperial College London (GB)

Physics and Astronomy Department, University College, London (GB)

Institute de Physique Nucléaire, Université Catholique de Louvain, Louvain-la-Neuve (BE)

Department of Physics, University of Wisconsin, Madison WI (USA)

Departamento de Fisica Teórica, Universidad Autónoma Madrid (ES)

Department of Physics, McGill University, Montreal (CA)

Moscow Engineering und Physics Institute, Moscow (RU)

Institute of Nuclear Physics, Moscow State University, Moscow (RU)

Max-Planck-Institut für Physik, München

Department of Physics, York University, North York (CA)

Department of Physics, University of Oxford (GB)

Dipartimento di Fisica, University and INFN, Padova (IT)

Department of Particle Physics, Weizmann Institute, Rehovot (IL)

Dipartimento di Fisica, Università La Sapienza and INFN, Roma (IT)

Polytechnic University, Sagamihara (JP)

Kyungpook National University, Taegu (KR)

School of Physics, University of Tel Aviv (IL)

Department of Physics, Tokyo Institute of Technology, Tokyo (JP)

Department of Physics, Tokyo Metropolitan University, Tokyo (JP)

Department of Physics, University of Tokyo (JP)

Università degli Studi di Torino and INFN, Torino (IT)

Università del Piemonte Orientale, Novara and INFN, Torino (IT)

Department of Physics, University of Toronto (CA)

Institute for Particle and Nuclear Study, KEK, Tsukuba (JP)

Department of Physics, Pennsylvania State University, University Park PA (USA)

Institute for Nuclear Studies, Warsaw (PL)

Institut of Experimental Physics, University of Warsaw (PL)

Faculty of General Education, Meiji Gakuin University, Yokohama (JP)

HERMES

National Institute for Subatomic Physics (NIKHEF), Amsterdam (NL)

Department of Physics and Astronomy, Vrije Universiteit, Amsterdam (NL)

Randall Laboratory of Physics, University of Michigan, Ann Arbor MI (USA)

Physics Division, Argonne National Laboratory, Argonne IL (USA)

Dipartimento di Fisica dell'Università and INFN, Bari (IT)

School of Physics, Peking University, Beijing (CN)

Nuclear Physics Laboratory, University of Colorado, Boulder CO (USA)

Joint Institute for Nuclear Research (JINR), Dubna (RU)

Physikalisches Institut, Universität Erlangen-Nürnberg

Dipartimento di Fisica dell'Università and INFN, Ferrara (IT)

Laboratori Nazionali di Frascati, INFN, Frascati (IT)

Petersburg Nuclear Physics Institute (PNPI), Gatchina (RU)

Department of Subatomic and Radiation Physics, University of Gent (BE)

Physikalisches Institut, Universität Gießen

School of Physics and Astronomy (SUPA), University of Glasgow (GB)

Deutsches Elektronen-Synchrotron DESY

P. N. Lebedev Physical Institute, Moscow (RU)

Institute for High Energy Physics (IHEP), Protvino (RU)

Institut für Theoretische Physik, Universität Regensburg

Gruppo Sanità, INFN and Physics Laboratory, Istituto Superiore di Sanità, Rome (IT)

Department of Physics, Tokyo Institute of Technology, Tokyo (JP)

Department of Physics, University of Illinois, Urbana IL (USA)

TRIUMF, Vancouver (CA)

Andrzeij Soltan Institute for Nuclear Studies, Warsaw (PL)

Yerevan Physics Institute, Yerevan (AM)

OLYMPUS

INFN, Bari (IT)

Rheinische Friedrich-Wilhelms-Universität Bonn

Massachusetts Institute of Technology, Cambridge (USA)

University of New Hampshire, Durham (USA)

INFN, Ferrara (IT)

Petersburg Nuclear Physics Institute, Gatchina (RU)

University of Glasgow (UK)

Deutsches Elektronen-Synchrotron DESY

Hampton University, Hampton (USA)

Johannes Gutenberg-Universität Mainz

MIT-Bates Linear Accelerator Center, Middleton (USA)

INFN, Rome (IT)

Arizona State University, Tempe (USA)

Yerevan Physics Institute, Yerevan (AM)

TESLA Technology Collaboration

Argonne National Laboratory (ANL), Argonne IL (USA)

Fermi National Accelerator Laboratory (Fermilab), Batavia IL (USA)

Peking University, Beijing (CN)

Institute for High Energy Physics (IHEP), Academia Sinica, Beijing (CN)

Tsinghua University, Beijing (CN)

Lawrence Berkeley National Laboratory, Berkeley (USA)

Helmholtz-Zentrum Berlin für Materialien und Energie

AGH-University of Science and Technology, Cracow (PL)

Henryk Niewodnizaski Institute of Nuclear Physics, Polish Academy of Science, Cracow (PL)

Technische Universität Darmstadt

CCLRC, Daresbury & Rutherford Appleton Laboratory, Chilton, Didcot (GB)

Helmholtz-Zentrum Dresden-Rossendorf

Joint Institute for Nuclear Research (JINR), Dubna (RU)

Universität Frankfurt/Main

Laboratori Nazionali di Frascati, INFN, Frascati (IT)

Helmholtz-Zentrum Geesthacht

CERN, Geneva (CH)

CEA/DSM DAPNIA, CE-Saclay, Gif-sur-Yvette (FR)

Deutsches Elektronen-Synchrotron DESY

Universität Hamburg

Raja Ramanna Centre of Advanced Technology (RRCAT), Indore (IN)

Cornell University, Ithaca NY (USA)

Variable Energy Cyclotron Centre VECC, Kolkata (IN)

Istituto Nazionale di Fisica Nucleare (INFN), Legnaro (IT)

Technical University of Lodz (PL)

Royal Holloway University of London (RHUL/JAI), London (GB)

University College London (UCL), London (GB)

SLAC National Accelerator Laboratory (SLAC), Menlo Park CA (USA)

Istituto Nazionale di Fisica Nucleare (INFN), Milan (IT)

Institute for Nuclear Research (INR), Moscow (RU)

Moscow Engineering and Physics Institute (MEPhI), Moscow (RU)

Bhabha Atomic Research Centre (BARC), Mumbai (IN)

Jefferson Lab, Newport News VA (USA)

Budker Institute for Nuclear Physics (BINP), Novosibirsk (RU)

LAL, Université Paris-Sud, IN2P3-CNRS, Orsay (FR)

Andrzej Soltan Institute for Nuclear Studies, Otwock-wierk (PL)

University of Oxford (JAI), Oxford (GB)

Institute for High Energy Physics (IHEP), Protvino (RU)

Istituto Nazionale di Fisica Nucleare (INFN), Rome II (IT)

Universität Rostock

Sincrotrone Trieste (IT)

Institute for Particle and Nuclear Study, KEK, Tsukuba (JP)

Canada's National Laboratory for Particle and Nuclear Physics (TRIUMF), Vancouver (CA)

Institute of High Pressure Physics, Polish Academy of Sciences, Warsaw (PL)

Warsaw University of Technology (WUT), Warsaw (PL)

Warsaw University, Department of Physics, Warsaw (PL)

Bergische Universität-GH Wuppertal

CANDLE, Yerevan (AM)

Yerevan Physics Institute, Yerevan (AM)

Physics at the Terascale, Helmholtz Alliance

Rheinisch-Westfälische Technische Hochschule Aachen
Humboldt-Universität zu Berlin
Rheinische Friedrich-Wilhelms-Universität Bonn
Deutsches Elektronen-Synchrotron DESY
Technische Universität Dortmund
Technische Universität Dresden
Albert-Ludwigs-Universität Freiburg
Justus-Liebig-Universität Gießen
Georg-August-Universität Göttingen
Universität Hamburg
Ruprecht-Karls-Universität Heidelberg
Karlsruher Institut für Technologie – Großforschungsbereich
Karlsruher Institut für Technologie – Universitätsbereich
Johannes Gutenberg-Universität Mainz
Ludwig-Maximilians-Universität München
Max-Planck-Institut für Physik München
Universität Rostock
Universität Siegen
Julius-Maximilians-Universität Würzburg
Bergische Universität Wuppertal

Adjunct Partner
Universität Regensburg

ALPS

Deutsches Elektronen-Synchrotron DESY
Universität Hamburg
Albert-Einstein-Institut Hannover
Johannes Gutenberg-Universität Mainz

Large Collaborations with DESY Participation

ATLAS Collaboration
Belle/Belle II Collaboration
CMS Collaboration
CALICE Collaboration
LCTPC Collaboration
John von Neumann Institute for Computing (NIC)

Amanda/IceCube Collaboration
CTA Collaboration
H.E.S.S. Collaboration
MAGIC Collaboration

Publications.

H1

Published

C. Alexa et al.
Measurement of Charged Particle Spectra in Deep-Inelastic ep Scattering at HERA.
The European physical journal / C, C73(4):2406, and DESY-2013-00234, DESY 13-012.
http://dx.doi.org/10.1140/epjc/s10052-013-2406-x

C. Alexa et al.
Elastic and Proton-Dissociative Photoproduction of J/ψ Mesons at HERA; 1st ed..
The European physical journal / C, 73(6):2466, and DESY-2013-00874, DESY-13-058.
http://dx.doi.org/10.1140/epjc/s10052-013-2466-y

V. Chekelian.
Proton Structure Measurements from HERA to LHC.
Nuclear physics / B / Proceedings supplements, volume 234, pages 62 – 65, Amsterdam, 07/02/2012 - 07/07/2012 2013. 16th International Conference in Quantum Chromo Dymamics, Montpellier(France), Elsevier.
http://dx.doi.org/10.1016/j.nuclphysbps.2012.11.015

H1 and ZEUS Collaborations.
Combination and QCD analysis of charm production cross section measurements in deep-inelastic ep scattering at HERA.
The European physical journal / C, 73:2311, and PHPPUBDB-26530, DESY-12-172; arXiv:1211.1182.
http://dx.doi.org/10.1140/epjc/s10052-013-2311-3

Ph.D. Thesis

P. Belov.
Combination of the H1 and ZEUS Inclusive Cross-Section Measurements at Proton Beam Energies of 460 and 575 GeV and Tests of Low Bjorken-x Phenomenological Models.
University of Hamburg, Hamburg, 2013.

A. Dossanov.
High Transverse Momentum Dijet Cross Section Measurements in Photoproduction at HERA.
University of Hamburg, 2013.

F. Huber.
Elastic and Proton Dissociative J/ψ Photoproduction at low $W_{\gamma p}$ with the H1 Detector at HERA.
Ruperto-Carola Univ. of Heidelberg, 2013.

H. Pirumov.
QCD Analysis of Neutral and Charged Current Cross Sections and Search for Contact Interactions at HERA.
Univ. Heidelberg, 2013.

HERMES

Published

A. Airapetian et al.
Azimuthal distributions of charged hadrons, pions, and kaons produced in deep-inelastic scattering off unpolarized protons and deuterons.
Physical review / D, 87:012010, and PHPPUBDB-25566, DESY 12-060; arXiv:1204.4161.
http://dx.doi.org/10.1103/PhysRevD.87.012010

A. Airapetian et al.
Multiplicities of charged pions and kaons from semi-inclusive deep-inelastic scattering by the proton and the deuteron.
Physical review / D, 87:074029, and PHPPUBDB-26476, DESY 12-157; arXiv:1212.5407.
http://dx.doi.org/10.1103/PhysRevD.87.074029

A. Airapetian et al.
The HERMES Recoil Detector.
Journal of Instrumentation, 8(05):49, and DESY-2013-00184, arXiv:1302.6092; DESY 13-034.
http://dx.doi.org/10.1088/1748-0221/8/05/P05012

Augustyniak, W. and HERMES Collaboration.
Exclusive electroproduction of vector mesons in lepton nucleon scattering at the HERMES experiment.
Nuclear physics / B / Proceedings supplements, volume 245, pages 207 – 214, Amsterdam, 06/30/2013 - 07/04/2013 2013. 7th Joint International Hadron Structure Conference, Tatranská Štrba(Slovak Republic), Elsevier.
http://dx.doi.org/10.1016/j.nuclphysbps.2013.10.041

Karyan, Gevorg and HERMES Collaboration.
Charged hadron multiplicities at the HERMES experiment.
In *3rd Workshop on the QCD Structure of the Nucleons - QCD-N'12, Il nuovo cimento / C*, volume 2013, pages 139–142, [S.l.], 10/22/2012 - 10/26/2012 2013. 3rd Workshop on the QCD Structure of the Nucleons, Bilbao(Spain), Italian Physical Society.
http://dx.doi.org/10.1393/ncc/i2013-11608-1

Marukyan, Hrachya and HERMES Collaboration.
Exclusive reactions at HERMES.
In *3rd Workshop on the QCD Structure of the Nucleons - QCD-N'12, Il nuovo cimento / C*, volume 2013, pages 55–60, [S.l.], 10/22/2012 - 10/26/2012 2013. 3rd Workshop on the QCD Structure of the Nucleons, Bilbao(Spain), Italian Physical Society.
http://dx.doi.org/10.1393/ncc/i2013-11586-2

G. Schnell.
Overview of recent results from the HERMES experiment.
Physics of particles and nuclei, volume 44, pages 954 – 958, Moskva, 09/17/2012 - 09/22/2012 2013. The 20th International Symposium on Spin Physics, Dubna(Russia), MAIK Nauka/Interperiodica.
http://dx.doi.org/10.1134/S1063779613060208

Ph.D. Thesis

S. J. Joosten.
Fragmentation and nucleon structure in semi-inclusive deep-inelastic scattering at the HERMES experiment.
University of Illinois at Urbana-Champaign, 2013.

G. A. Karyan.
A study of charged hadron yields and the multidimensional nuclear attenuation effect at the HERMES experiment.
A.I. Alikhanyan National Science Laboratory, 2013.

Master Thesis

E. Etzelmüller.
Measurement of asymmetries in associated DVCS using the HERMES Recoil detector.
Justus-Liebig-Universität Gießen, 2013.

M. Stahl.
Analysis of Resonant Structures in the pK_S0-channel at HERMES.
Justus-Liebig-Universität Gießen, 2013.

ZEUS

Published

D. Eichler, R. Kumar, and M. Pohl.
IS THE GALACTIC COSMIC-RAY SPECTRUM CONSTANT IN TIME?.
The astrophysical journal, 769(2):138, and DESY-2014-00178.
http://dx.doi.org/10.1088/0004-637X/769/2/138

M. Garny, A. Ibarra, M. Pato, and S. Vogl.
Internal bremsstrahlung signatures in light of direct dark matter searches.
Journal of cosmology and astroparticle physics, 2013(12):046 – 046, and DESY-2014-00192, DESY 13-115.
http://dx.doi.org/10.1088/1475-7516/2013/12/046

A. Gizhko.
HERAFitter - an open source QCD fit framework.
Nuclear physics / B / Proceedings supplements, volume 245, pages 161 – 163, Amsterdam, 06/30/2013 - 07/04/2013 2013. 7th Joint International Hadron Structure'13 Conference, Tatranské Matliare(Slovakia), Elsevier.
http://dx.doi.org/10.1016/j.nuclphysbps.2013.10.031

R. Klanner, E. Fretwurst, I. Pintilie, J. Schwandt, and J. Zhang.
Study of high-dose X-ray radiation damage of silicon sensors.
Nuclear instruments & methods in physics research / A, 732:117 – 121, and DESY-2014-01975.
http://dx.doi.org/10.1016/j.nima.2013.05.131

H. Kowalski, L. N. Lipatov, and D. A. Ross.
BFKL Evolution as a Communicator Between Small and Large Energy Scales.
Physics of particles and nuclei, 44(3):547 – 567, and DESY-2014-01652.
http://dx.doi.org/10.1134/S1063779613030052

O. Kuprash.
Isolated Photons + Jets in DIS and Photoproduction at ZEUS.
Nuclear physics / B / Proceedings supplements, volume 245, pages 141 – 144, Amsterdam, 06/30/2013 - 07/04/2013 2013. 7th Joint International Hadron Structure'13 Conference, Tatranské Matliare(Slovakia), Elsevier.
http://dx.doi.org/10.1016/j.nuclphysbps.2013.10.026

A. V. Lipatov.
Isolated prompt photon pair production at hadron colliders with kt-factorization.
Journal of high energy physics, 2013:009, and PHPPUBDB-26277, DESY 12-169; arXiv:1210.0823.
http://dx.doi.org/10.1007/JHEP02(2013)009

M. Lisovyi.
Particle Production at HERA.
In *Proceedings of 5th Workshop on Excited QCD 2013*, *Acta physica Polonica / B*, volume 6, pages 815–820, Cracow, 02/03/2013 - 02/09/2013 2013. 5th Workshop on Excited QCD 2013, Sarajevo(Bosnia-Herzegovina), Inst. of Physics, Jagellonian Univ.
http://dx.doi.org/10.5506/APhysPolBSupp.6.815

T. Poehlsen et al.
Study of the accumulation layer and charge losses at the $Si–SiO_2$ interface in p+n-silicon strip sensors.
Nuclear instruments & methods in physics research / A, 721:26 – 34, and DESY-2014-01946.
http://dx.doi.org/10.1016/j.nima.2013.04.026

M. Pohl and D. Eichler.
UNDERSTANDING TeV-BAND COSMIC-RAY ANISOTROPY.
The astrophysical journal, 766(1):4, and DESY-2014-00179.
http://dx.doi.org/10.1088/0004-637X/766/1/4

I. Telezhinsky, V. V. Dwarkadas, and M. Pohl.
Acceleration of cosmic rays by young core-collapse supernova remnants.
Astronomy and astrophysics, 552:A102 –, and DESY-2014-00195.
http://dx.doi.org/10.1051/0004-6361/201220740

K. Wichmann.
Deep inelastic scattering at HERA.
Acta physica Polonica / B, volume 6, pages 709–714, Cracow, 09/17/2012 - 09/21/2012 2013. International Symposium on Multiparticle Dynamics, Kielce(Poland), Inst. of Physics, Jagellonian Univ.
http://dx.doi.org/10.5506/APhysPolBSupp.6.709

ZEUS Collaboration.
Measurement of charm fragmentation fractions in photoproduction at HERA.
Journal of high energy physics, 2013(09):058, and DESY-2013-01068, DESY-13-106; ISSN:1029-8479.
http://dx.doi.org/10.1007/JHEP09(2013)058

ZEUS Collaboration.
Measurement of $D^{\pm}$ production in deep inelastic ep scattering with the ZEUS detector at HERA.
Journal of high energy physics, 2013(5):23, and DESY-2013-00365, DESY 13-028; arXiv: 1302.5058.
http://dx.doi.org/10.1007/JHEP05(2013)023

ZEUS Collaboration.
Measurement of $D^{*\pm}$ production in deep inelastic scattering at HERA.
Journal of high energy physics, 2013(5):97, and DESY-2013-00366, DESY 13-054; arXiv:1303.6578.
http://dx.doi.org/10.1007/JHEP05(2013)097

ZEUS Collaboration.
Measurement of $high-Q^2$ neutral current deep inelastic e^+p scattering cross sections with a longitudinally polarized positron beam at HERA.
Physical review / D, 87(5):052014, and DESY-2014-00266, DESY 12-145.
http://dx.doi.org/10.1103/PhysRevD.87.052014

ZEUS Collaboration.
Measurement of Inelastic J/ψ and ψ' Photoproduction at HERA.
Journal of high energy physics, 2013:071, and PHPPUBDB-25948, DESY 12-226; arXiv:1211.6946.
http://dx.doi.org/10.1007/JHEP02(2013)071

ZEUS Collaboration.
Production of the excited charm mesons D_1 and D_2^* at HERA.
Nuclear physics / B, 866:229–254, and PHPPUBDB-22400, DESY 12-144; arXiv:1208.4468.
http://dx.doi.org/10.1016/j.nuclphysb.2012.09.007

ZEUS Collaboration.
Production of Z^0 bosons in elastic and quasi-elastic ep collisions at HERA.
Physics letters / B, 718:915–921, and PHPPUBDB-24154, DESY 12-168; arXiv 1210.5511.
http://dx.doi.org/10.1016/j.physletb.2012.11.051

Ph.D. Thesis

V. Libov.
Measurement of Charm and Beauty Production in Deep Inelastic Scattering at HERA and Test Beam Studies of ATLAS Pixel Sensors.
Hamburg University, Hamburg, 2013.

A. Verbytskyi.
Production of the Excited Charm Mesons D_1 and $D*_2$ at HERA.
University of Hamburg, 2013.

ATLAS

Published

T. Aaltonen et al.
Operational experience, improvements, and performance of the CDF Run II silicon vertex detector.
Nuclear instruments & methods in physics research / A, 729:153 – 181, and DESY-2014-02193.
http://dx.doi.org/10.1016/j.nima.2013.07.015

M. Aliev et al.
A forward silicon strip system for the ATLAS HL-LHC upgrade.
Nuclear instruments & methods in physics research / A, 730:210 – 214, and DESY-2014-01944.
http://dx.doi.org/10.1016/j.nima.2013.05.155

ATLAS Collaboration.
ATLAS search for new phenomena in dijet mass and angular distributions using pp collisions at $\sqrt{s} = 7$ TeV.
Journal of high energy physics, 2013:29, and DESY-2013-00468, CERN-PH-EP-2012-257; arXiv:1210.1718.
http://dx.doi.org/10.1007/JHEP01(2013)029

ATLAS Collaboration.
Characterisation and mitigation of beam-induced backgrounds observed in the ATLAS detector during the 2011 proton-proton run.
Journal of Instrumentation, 8(7):P07004, and DESY-2013-00401, CERN-PH-EP-2012-313; arXiv:1303.0223.
http://dx.doi.org/10.1088/1748-0221/8/07/P07004

ATLAS Collaboration.
Dynamics of isolated-photon plus jet production in pp collisions at $\sqrt{s} = 7$ TeV with the ATLAS detector.
Nuclear physics / B, 875:483–535, and DESY-2013-00709, CERN-PH-EP-2013-092.
http://dx.doi.org/10.1016/j.nuclphysb.2013.07.025

ATLAS Collaboration.
Evidence for the spin-0 nature of the Higgs boson using ATLAS data.
Physics letters / B, 726(1-3):120 – 144, and DESY-2013-00383, CERN-PH-EP-2013-102.
http://dx.doi.org/10.1016/j.physletb.2013.08.026

ATLAS Collaboration.
Improved luminosity determination in pp collisions at $\sqrt{s} = 7$ TeV using the ATLAS detector at the LHC.
The European physical journal / C, 73(8):2518, and DESY-2013-00814, CERN-PH-EP-2013-026.
http://dx.doi.org/10.1140/epjc/s10052-013-2518-3

ATLAS Collaboration.
Jet energy measurement with the ATLAS detector in proton-proton collisions at $\sqrt{s} = 7$ TeV.
The European physical journal / C, 73:2304, and DESY-2013-00701, CERN-PH-EP-2011-191.
http://dx.doi.org/10.1140/epjc/s10052-013-2304-2

ATLAS Collaboration.
Jet energy resolution in proton-proton collisions at $\sqrt{s} = 7$ TeV recorded in 2010 with the ATLAS detector.
The European physical journal / C, 73(3):2306, and DESY-2013-00445, CERN-PH-EP-2012-191.
http://dx.doi.org/10.1140/epjc/s10052-013-2306-0

ATLAS Collaboration.
Measurement of angular correlations in Drell–Yan lepton pairs to probe Z/γ^* boson transverse momentum at $\sqrt{s} = 7$ TeV with the ATLAS detector.
Physics letters / B, 720(1-3):32 – 51, and DESY-2013-00451, CERN-PH-EP-2012-325.
http://dx.doi.org/10.1016/j.physletb.2013.01.054

ATLAS Collaboration.
Measurement of charged-particle event shape variables in inclusive $\sqrt{s} = 7$ TeV proton-proton interactions with the ATLAS detector.
Physical review / D, 88(3):032004, and DESY-2013-00549, CERN-PH-EP-2012-178.
http://dx.doi.org/10.1103/PhysRevD.88.032004

ATLAS Collaboration.
Measurement of hard double-parton interactions in $W(\rightarrow \ell\nu)$ + 2-jet events at $\sqrt{s}=7$ TeV with the ATLAS detector.
New journal of physics, 15(3):033038, and DESY-2013-00418, CERN-PH-EP-2012-355.
http://dx.doi.org/10.1088/1367-2630/15/3/033038

ATLAS Collaboration.
Measurement of isolated-photon pair production in pp collisions at $\sqrt{s}=7$ TeV with the ATLAS detector.
Journal of high energy physics, 2013(1):86, and DESY-2013-00435, CERN-PH-EP-2012-300.
http://dx.doi.org/10.1007/JHEP01(2013)086

ATLAS Collaboration.
Measurement of κ_T splitting scales in $W\rightarrow \ell\nu$ events at $\sqrt{s}=7$ TeV with the ATLAS detector.
The European physical journal / C, 73(5):2432, and DESY-2013-00412, CERN-PH-EP-2013-003.
http://dx.doi.org/10.1140/epjc/s10052-013-2432-8

ATLAS Collaboration.
Measurement of Z Boson Production in Pb-Pb Collisions at $\sqrt{s_{NN}}=2.76$TeV with the ATLAS Detector.
Physical review letters, 110(2):022301, and DESY-2013-00444, CERN-PH-EP-2012-223.
http://dx.doi.org/10.1103/PhysRevLett.110.022301

ATLAS Collaboration.
Measurement of ZZ production in pp collisions at $\sqrt{s}=7$ TeV and limits on anomalous ZZZ and $ZZ\gamma$ couplings with the ATLAS detector.
Journal of high energy physics, 2013(3):128, and DESY-2013-00427, CERN-PH-EP-2012-318.
http://dx.doi.org/10.1007/JHEP03(2013)128

ATLAS Collaboration.
Measurement of jet shapes in top-quark pair events at $\sqrt{s}=7$ TeV using the ATLAS detector.
The European physical journal / C, 73(12):2676, and DESY-2014-00164, CERN-PH-EP-2013-067.
http://dx.doi.org/10.1140/epjc/s10052-013-2676-3

ATLAS Collaboration.
Measurement of the Azimuthal Angle Dependence of Inclusive Jet Yields in Pb+Pb Collisions at $\sqrt{s_{NN}}=2.76$TeV with the ATLAS Detector.
Physical review letters, 111(15):152301, and DESY-2014-00070.
http://dx.doi.org/10.1103/PhysRevLett.111.152301

ATLAS Collaboration.
Measurement of the cross-section for W boson production in association with b-jets in pp collisions at $\sqrt{s}=7$ TeV with the ATLAS detector.
Journal of high energy physics, 2013(6):84, and DESY-2013-00411, CERN-PH-EP-2012-357.
http://dx.doi.org/10.1007/JHEP06(2013)084

ATLAS Collaboration.
Measurement of the differential cross-section of B^+ meson production in pp collisions at $\sqrt{s}=7$ TeV at ATLAS.
Journal of high energy physics, 2013:42, and DESY-2013-01518, CERN-PH-EP-2013-089; arXiv:1307.0126v2.
http://dx.doi.org/10.1007/JHEP10(2013)042

ATLAS Collaboration.
Measurement of the distributions of event-by-event flow harmonics in lead-lead collisions at $\sqrt{s_{NN}}$ = 2.76 TeV with the ATLAS detector at the LHC.
Journal of high energy physics, 2013:183, and DESY-2014-00085, CERN-PH-EP-2013-04.
http://dx.doi.org/10.1007/JHEP11(2013)183

ATLAS Collaboration.
Measurement of the flavour composition of dijet events in pp collisions at $\sqrt{s}=7$ TeV with the ATLAS Detector.
The European physical journal / C, 73:2301, and DESY-2013-00677, CERN-PH-EP-2012-255.
http://dx.doi.org/10.1140/epjc/s10052-013-2301-5

ATLAS Collaboration.
Measurement of the high-mass Drell–Yan differential cross-section in pp collisions at $\sqrt{s}=7$ TeV with the ATLAS detector.
Physics letters / B, 725(4-5):223 – 242, and DESY-2013-00829, CERN-PH-EP-2013-064.
http://dx.doi.org/10.1016/j.physletb.2013.07.049

ATLAS Collaboration.
Measurement of the inclusive jet cross-section in pp collisions at $\sqrt{s}=2.76$ TeV and comparison to the inclusive jet cross-section at $\sqrt{s}=7$ TeV using the ATLAS detector.
The European physical journal / C, 73:2509, and DESY-2013-00594, CERN-PH-EP-2013-036.
http://dx.doi.org/10.1140/epjc/s10052-013-2509-4

ATLAS Collaboration.
Measurement of the $t\bar{t}$ production cross section in the tau + jets channel using the ATLAS detector.
The European physical journal / C, 73(3):2328, and DESY-2013-00425, CERN-PH-EP-2012-328.
http://dx.doi.org/10.1140/epjc/s10052-013-2328-7

ATLAS Collaboration.
Measurement of the jet radius and transverse momentum dependence of inclusive jet suppression in lead–lead collisions at $\sqrt{s_{NN}}=2.76$ TeV with the ATLAS detector.
Physics letters / B, 719(4-5):220 – 241, and DESY-2013-00686, CERN-PH-EP-2012-134.
http://dx.doi.org/10.1016/j.physletb.2013.01.024

ATLAS Collaboration.
Measurement of the Λ_b^0 lifetime and mass in the ATLAS experiment.
Physical review / D, 87(3):032002, and DESY-2013-00699, CERN-PH-EP-2012-163.
http://dx.doi.org/10.1103/PhysRevD.87.032002

ATLAS Collaboration.
Measurement of the mass difference between top and anti-top quarks in pp collisions at $\sqrt{s}=7$ TeV using the ATLAS detector.
Physics letters / B, page S0370269313009854, and DESY-2013-01427, CERN-PH-EP-2013-171; arXiv:1310.6527.
http://dx.doi.org/10.1016/j.physletb.2013.12.010

ATLAS Collaboration.
Measurement of the production cross section of jets in association with a Z boson in pp collisions at $\sqrt{s}=7$ TeV with the ATLAS detector.
Journal of high energy physics, 2013(7):32, and
DESY-2013-00397, CERN-PH-EP-2013-023.
http://dx.doi.org/10.1007/JHEP07(2013)032

ATLAS Collaboration.
Measurement of the top quark charge in pp collisions at $\sqrt{s}=7$ TeV with the ATLAS detector.
Journal of high energy physics, 2013:31, and
DESY-2014-00081, CERN-PH-EP-2013-056.
http://dx.doi.org/10.1007/JHEP11(2013)031

ATLAS Collaboration.
Measurement of Top Quark Polarization in Top-Antitop Events from Proton-Proton Collisions at $\sqrt{s}=7$ TeV Using the ATLAS Detector.
Physical review letters, 111(23):232002, and
DESY-2014-00158, CERN-PH-EP-2013-101.
http://dx.doi.org/10.1103/PhysRevLett.111.232002

ATLAS Collaboration.
Measurement of Upsilon production in 7 TeV pp collisions at ATLAS.
Physical review / D, 87(5):052004, and DESY-2013-00424,
CERN-PH-EP-2012-295.
http://dx.doi.org/10.1103/PhysRevD.87.052004

ATLAS Collaboration.
Measurement of W^+W^- production in pp collisions at $\sqrt{s}=7$TeV with the ATLAS detector and limits on anomalous WWZ and WW_γ couplings.
Physical review / D, 87(11):112001, and DESY-2013-00369,
CERN-PH-EP-2012-242.
http://dx.doi.org/10.1103/PhysRevD.87.112001

ATLAS Collaboration.
Measurement with the ATLAS detector of multi-particle azimuthal correlations in $_p$+Pb collisions at $\sqrt{s_{NN}}$=5.02 TeV.
Physics letters / B, 725(1-3):60 – 78, and DESY-2013-00379,
CERN-PH-EP-2013-029.
http://dx.doi.org/10.1016/j.physletb.2013.06.057

ATLAS Collaboration.
Measurements of Higgs boson production and couplings in diboson final states with the ATLAS detector at the LHC.
Physics letters / B, 726(1-3):88 – 119, and
DESY-2013-00862, CERN-PH-EP-2013-103.
http://dx.doi.org/10.1016/j.physletb.2013.08.010

ATLAS Collaboration.
Measurements of $W\gamma$ and $Z\gamma$ production in pp collisions at $\sqrt{s}=7$TeV with the ATLAS detector at the LHC.
Physical review / D, 87(11):112003, and DESY-2013-00413,
CERN-PH-EP-2012-345.
http://dx.doi.org/10.1103/PhysRevD.87.112003

ATLAS Collaboration.
Measurements of top quark pair relative differential cross-sections with ATLAS in pp collisions at $\sqrt{s}=7$ TeV.
The European physical journal / C, 73:2261, and
DESY-2013-00689, CERN-PH-EP-2012-165.
http://dx.doi.org/10.1140/epjc/s10052-012-2261-1

ATLAS Collaboration.
Multi-channel search for squarks and gluinos in $\sqrt{s}=7TeV$ pp collisions with the ATLAS detector at the LHC.
The European physical journal / C, 73:2362, and
PHPPUBDB-26436, CERN-PH-EP-2012-330.
http://dx.doi.org/10.1140/epjc/s10052-013-2362-5

ATLAS Collaboration.
Observation of Associated Near-Side and Away-Side Long-Range Correlations in $\sqrt{s_{NN}}=5.02$ TeV Proton-Lead Collisions with the ATLAS Detector.
Physical review letters, 110(18):182302, and
DESY-2013-00422, CERN-PH-EP-2012-366.
http://dx.doi.org/10.1103/PhysRevLett.110.182302

ATLAS Collaboration.
Performance of jet substructure techniques for large-R jets in proton-proton collisions at $\sqrt{s}=7$ TeV using the ATLAS detector.
Journal of high energy physics, 2013(9):76, and
DESY-2013-00830, CERN-PH-EP-2013-069.
http://dx.doi.org/10.1007/JHEP09(2013)076

ATLAS Collaboration.
Search for a heavy narrow resonance decaying to $e\mu$, $e\tau$, or $\mu\tau$ with the ATLAS detector in $\sqrt{s}=7$ TeV pp collisions at the LHC.
Physics letters / B, 723(1-3):15 – 32, and DESY-2013-00373,
CERN-PH-EP-2012-326.
http://dx.doi.org/10.1016/j.physletb.2013.04.035

ATLAS Collaboration.
Search for a light charged Higgs boson in the decay channel $H^+ \to c\bar{s}$ in $t\bar{t}$ events using pp collisions at $\sqrt{s}=7$ TeV with the ATLAS detector.
The European physical journal / C, 73(6):2465, and
DESY-2013-00410, CERN-PH-EP-2012-338.
http://dx.doi.org/10.1140/epjc/s10052-013-2465-z

ATLAS Collaboration.
Search for charged Higgs bosons through the violation of lepton universality in $t\bar{t}$ events using pp collision data at $\sqrt{s}=7$ TeV with the ATLAS experiment.
Journal of high energy physics, 2013(3):76, and
DESY-2013-00423, CERN-PH-EP-2012-347.
http://dx.doi.org/10.1007/JHEP03(2013)076

ATLAS Collaboration.
Search for charginos nearly mass degenerate with the lightest neutralino based on a disappearing-track signature in pp collisions at $\sqrt{s}=8$ TeV with the ATLAS detector.
Physical review / D, 88(11):112006, and DESY-2014-00161,
CERN-PH-EP-2013-155.
http://dx.doi.org/10.1103/PhysRevD.88.112006

ATLAS Collaboration.
Search for contact interactions and large extra dimensions in dilepton events from pp collisions at $\sqrt{s}=7$TeV with the ATLAS detector.
Physical review / D, 87(1):015010, and DESY-2013-00439,
CERN-PH-EP-2012-279.
http://dx.doi.org/10.1103/PhysRevD.87.015010

ATLAS Collaboration.
Search for dark matter candidates and large extra dimensions in events with a jet and missing transverse momentum with the ATLAS detector.
Journal of high energy physics, 2013:75, and DESY-2013-00467, CERN-PH-EP-2012-210.
http://dx.doi.org/10.1007/JHEP04(2013)075

ATLAS Collaboration.
Search for Dark Matter Candidates and Large Extra Dimensions in Events with a Photon and Missing Transverse Momentum in pp Collision Data at $\sqrt{s} = 7$TeV with the ATLAS Detector.
Physical review / D, 110(1):011802, and DESY-2013-00469, CERN-PH-EP-2012-209.
http://dx.doi.org/10.1103/PhysRevLett.110.011802

ATLAS Collaboration.
Search for direct chargino production in anomaly-mediated supersymmetry breaking models based on a disappearing-track signature in pp collisions at $\sqrt{s} = 7TeV$ with the ATLAS detector.
Journal of high energy physics, 2013:131, and PHPPUBDB-25582, CERN-PH-EP-2012-243.
http://dx.doi.org/10.1007/JHEP01(2013)131

ATLAS Collaboration.
Search for direct production of charginos and neutralinos in events with three leptons and missing transverse momentum in $\sqrt{s} = 7$ TeV pp collisions with the ATLAS detector.
Physics letters / B, 718(3):841 – 859, and DESY-2013-00678, CERN-PH-EP-2012-217.
http://dx.doi.org/10.1016/j.physletb.2012.11.039

ATLAS Collaboration.
Search for direct slepton and gaugino production in final states with two leptons and missing transverse momentum with the ATLAS detector in pp collisions at $\sqrt{s} = 7$ TeV.
Physics letters / B, 718(3):879 – 901, and DESY-2013-00683, CERN-PH-EP-2012-216.
http://dx.doi.org/10.1016/j.physletb.2012.11.058

ATLAS Collaboration.
Search for direct third-generation squark pair production in final states with missing transverse momentum and two b-jets in $\sqrt{s} = 8$ TeV pp collisions with the ATLAS detector.
Journal of high energy physics, 2013:189, and DESY-2014-00079, CERN-PH-EP-2013-119.
http://dx.doi.org/10.1007/JHEP10(2013)189

ATLAS Collaboration.
Search for displaced muonic lepton jets from light Higgs boson decay in proton–proton collisions at $\sqrt{s} = 7$ TeV with the ATLAS detector.
Physics letters / B, 721(1-3):32 – 50, and DESY-2013-00685, CERN-PH-EP-2012-241.
http://dx.doi.org/10.1016/j.physletb.2013.02.058

ATLAS Collaboration.
Search for excited electrons and muons in $\sqrt{s} = 8$ TeV proton–proton collisions with the ATLAS detector.
New journal of physics, 15(9):093011, and DESY-2013-00782, CERN-PH-EP-2013-131.
http://dx.doi.org/10.1088/1367-2630/15/9/093011

ATLAS Collaboration.
Search for extra dimensions in diphoton events from proton–proton collisions at $\sqrt{s} = 7$ TeV in the ATLAS detector at the LHC.
New journal of physics, 15(4):043007, and DESY-2013-00441, CERN-PH-EP-2012-289.
http://dx.doi.org/10.1088/1367-2630/15/4/043007

ATLAS Collaboration.
A search for high-mass resonances decaying to $\tau^+\tau^-$ in pp collisions at $\sqrt{s} = 7$ TeV with the ATLAS detector.
Physics letters / B, 719(4-5):242 – 260, and DESY-2013-00443, CERN-PH-EP-2012-280.
http://dx.doi.org/10.1016/j.physletb.2013.01.040

ATLAS Collaboration.
Search for $t\bar{t}$ resonances in the lepton plus jets final state with ATLAS using 4.7fb^{-1} of pp collisions at $\sqrt{s} = 7$TeV.
Physical review / D, 88(1):012004, and DESY-2013-00394, CERN-PH-EP-2013-032.
http://dx.doi.org/10.1103/PhysRevD.88.012004

ATLAS Collaboration.
Search for WH production with a light Higgs boson decaying to prompt electron-jets in proton–proton collisions at $\sqrt{s} = 7$ TeV with the ATLAS detector.
New journal of physics, 15(4):043009, and DESY-2013-00409, CERN-PH-EP-2012-365.
http://dx.doi.org/10.1088/1367-2630/15/4/043009

ATLAS Collaboration.
Search for light top squark pair production in final states with leptons and b-jets with the ATLAS detector in $\sqrt{s} = 7$ TeV proton–proton collisions.
Physics letters / B, 720(1-3):13 – 31, and DESY-2013-00470, CERN-PH-EP-2012-207.
http://dx.doi.org/10.1016/j.physletb.2013.01.049

ATLAS Collaboration.
Search for long-lived, heavy particles in final states with a muon and multi-track displaced vertex in proton–proton collisions at $\sqrt{s} = 7$ TeV with the ATLAS detector.
Physics letters / B, 719(4-5):280 – 298, and DESY-2013-00442, CERN-PH-EP-2012-259.
http://dx.doi.org/10.1016/j.physletb.2013.01.042

ATLAS Collaboration.
Search for long-lived, multi-charged particles in pp collisions at $\sqrt{s} = 7$ TeV using the ATLAS detector.
Physics letters / B, 722(4-5):305 – 323, and DESY-2013-00419, CERN-PH-EP-2012-360; arXiv:1301.5272.
http://dx.doi.org/10.1016/j.physletb.2013.04.036

ATLAS Collaboration.
Search for long-lived stopped R-hadrons decaying out-of-time with pp collisions using the ATLAS detector.
Physical review / D, 88(11):112003, and DESY-2014-00086, CERN-PH-EP-2013-161.
http://dx.doi.org/10.1103/PhysRevD.88.112003

ATLAS Collaboration.
Search for microscopic black holes in a like-sign dimuon final state using large track multiplicity with the ATLAS detector.
Physical review / D, 88(7):072001, and DESY-2013-01517.
http://dx.doi.org/10.1103/PhysRevD.88.072001

ATLAS Collaboration.
Search for new phenomena in events with three charged leptons at $\sqrt{s} = 7$TeV with the ATLAS detector.
Physical review / D, 87(5):052002, and DESY-2013-00426, CERN-PH-EP-2012-310.
http://dx.doi.org/10.1103/PhysRevD.87.052002

ATLAS Collaboration.
Search for new phenomena in final states with large jet multiplicities and missing transverse momentum at $\sqrt{s} = 8$ TeV proton-proton collisions using the ATLAS experiment.
Journal of high energy physics, 2013(10):130, and DESY-2014-00075, CERN-PH-EP-2013-110.
http://dx.doi.org/10.1007/JHEP10(2013)130

ATLAS Collaboration.
Search for new phenomena in photon+jet events collected in proton-proton collisions at $\sqrt{s} = 8$ TeV with the ATLAS detector.
Physics letters / B, 728:562–578, and DESY-2014-00170, CERN-PH-EP-2013-126; CERN-PH-EP-2013-126.
http://dx.doi.org/10.1016/j.physletb.2013.12.029

ATLAS Collaboration.
Search for new phenomena in the $WW \rightarrow \ell\nu\ell'\nu'$ final state in pp collisions at $\sqrt{s} = 7$ TeV with the ATLAS detector.
Physics letters / B, 718(3):860 – 878, and DESY-2013-00684, CERN-PH-EP-2012-197; ATLAS-EXOT-2012-11-003.
http://dx.doi.org/10.1016/j.physletb.2012.11.040

ATLAS Collaboration.
Search for nonpointing photons in the diphoton and E_T^{miss} final state in $\sqrt{s} = 7$TeV proton-proton collisions using the ATLAS detector.
Physical review / D, 88(1):012001, and DESY-2013-00405, CERN-PH-EP-2013-049.
http://dx.doi.org/10.1103/PhysRevD.88.012001

ATLAS Collaboration.
Search for pair-produced massive coloured scalars in four-jet final states with the ATLAS detector in proton–proton collisions at $\sqrt{s} = 7$ TeV.
The European physical journal / C, 73:2263, and DESY-2013-00458, CERN-PH-EP-2012-256.
http://dx.doi.org/10.1140/epjc/s10052-012-2263-z

ATLAS Collaboration.
Search for pair production of heavy top-like quarks decaying to a high-p_T W boson and a b quark in the lepton plus jets final state at $\sqrt{s} = 7$ TeV with the ATLAS detector.
Physics letters / B, 718(4-5):1284 – 1302, and DESY-2013-00454, CERN-PH-EP-2012-258.
http://dx.doi.org/10.1016/j.physletb.2012.11.071

ATLAS Collaboration.
A search for prompt lepton-jets in pp collisions at $\sqrt{s} = 7$ TeV with the ATLAS detector.
Physics letters / B, 719(4-5):299 – 317, and DESY-2013-00421, CERN-PH-EP-2012-319.
http://dx.doi.org/10.1016/j.physletb.2013.01.034

ATLAS Collaboration.
Search for resonances decaying into top-quark pairs using fully hadronic decays in pp collisions with ATLAS at $\sqrt{s} = 7$ TeV.
Journal of high energy physics, 2013(1):116, and DESY-2013-00428, CERN-PH-EP-2012-291.
http://dx.doi.org/10.1007/JHEP01(2013)116

ATLAS Collaboration.
Search for resonant diboson production in the $WW/WZ \rightarrow \ell\nu jj$ decay channels with the ATLAS detector at $\sqrt{s} = 7$ TeV.
Physical review / D, 87(11):112006, and DESY-2013-00356, CERN-PH-EP-2012-296.
http://dx.doi.org/10.1103/PhysRevD.87.112006

ATLAS Collaboration.
Search for single b^*-quark production with the ATLAS detector at $\sqrt{s} = 7$ TeV.
Physics letters / B, 721(4-5):171 – 189, and DESY-2013-00420, CERN-PH-EP-2012-344; arXiv:1301.1583.
http://dx.doi.org/10.1016/j.physletb.2013.03.016

ATLAS Collaboration.
Search for squarks and gluinos with the ATLAS detector in final states with jets and missing transverse momentum using 4.7fb^{-1} of $\sqrt{s} = 7$TeV proton-proton collision data.
Physical review / D, 87(1):012008, and DESY-2013-00688, CERN-PH-EP-2012-195.
http://dx.doi.org/10.1103/PhysRevD.87.012008

ATLAS Collaboration.
Search for supersymmetry in events with photons, bottom quarks, and missing transverse momentum in proton-proton collisions at a centre-of-mass energy of 7 TeV with the ATLAS detector.
Physics letters / B, 719:261–279, and PHPPUBDB-25909, CERN-PH-EP-2012-308.
http://dx.doi.org/10.1016/j.physletb.2013.01.041

ATLAS Collaboration.
Search for the neutral Higgs bosons of the Minimal Supersymmetric Standard Model in pp collisions at $\sqrt{s} = 7$ TeV with the ATLAS detector.
Journal of high energy physics, 2013(2):95, and DESY-2013-00452, CERN-PH-EP-2012-323.
http://dx.doi.org/10.1007/JHEP02(2013)095

ATLAS Collaboration.
Search for third generation scalar leptoquarks in pp collisions at $\sqrt{s} = 7$ TeV with the ATLAS detector.
Journal of high energy physics, 2013(6):33, and DESY-2013-00406, CERN-PH-EP-2012-317.
http://dx.doi.org/10.1007/JHEP06(2013)033

ATLAS Collaboration.
Searches for heavy long-lived sleptons and R-hadrons with the ATLAS detector in pp collisions at $\sqrt{s} = 7$ TeV.
Physics letters / B, 720(4-5):277 – 308, and DESY-2013-00438, CERN-PH-EP-2012-236.
http://dx.doi.org/10.1016/j.physletb.2013.02.015

ATLAS Collaboration.
Single hadron response measurement and calorimeter jet energy scale uncertainty with the ATLAS detector at the LHC.
The European physical journal / C, 73:2305, and DESY-2013-00700, CERN-PH-EP-2012-005.
http://dx.doi.org/10.1140/epjc/s10052-013-2305-1

ATLAS Collaboration.
Triggers for displaced decays of long-lived neutral particles in the ATLAS detector.
Journal of Instrumentation, 8(07):P07015, and DESY-2013-00450, CERN-PH-EP-2013-047.
http://dx.doi.org/10.1088/1748-0221/8/07/P07015

R. Bates et al.
A combined ultrasonic flow meter and binary vapour mixture analyzer for the ATLAS silicon tracker.
Journal of Instrumentation, 8(02):P02006, and DESY-2014-01960, arXiv:1210.4835.
http://dx.doi.org/10.1088/1748-0221/8/02/P02006

R. Bruce et al.
Sources of machine-induced background in the ATLAS and CMS detectors at the CERN Large Hadron Collider.
Nuclear instruments & methods in physics research / A, 729:825 – 840, and DESY-2014-02192.
http://dx.doi.org/10.1016/j.nima.2013.08.058

C. Deterre and A. Grohsjean.
Measurement of the combined rapidity and p_T dependence of dijet azimuthal decorrelations in $p\bar{p}$ collisions at $\sqrt{s} = 1.96$TeV.
Physics letters / B, 721(4-5):212 – 219, and DESY-2014-02196.
http://dx.doi.org/10.1016/j.physletb.2013.03.029

R. Nagai et al.
Evaluation of novel KEK/HPK n-in-p pixel sensors for ATLAS upgrade with testbeam.
Nuclear instruments & methods in physics research / A, volume 699, pages 78 – 83, Amsterdam, 12/05/2011 - 12/08/2011 2013. The 8th International “Hiroshima” Symposium on the Development and Application of Semiconductor Tracking Detectors — Academia Sinica, Taipei, Taiwan, December 5 – 8, 2011, Taipei(Taiwan), North-Holland Publ. Co. *http://dx.doi.org/10.1016/j.nima.2012.04.081*

T. Perez Cavalcanti.
Neural network based cluster reconstruction in the ATLAS silicon Pixel Detector.
Journal of Instrumentation, volume 8, page C04003, London, 2012-07-01 - 2012-07-05 2013. 14th International Workshop on Radiation Imaging Detectors, Figueira da Foz(Portugal), Inst. of Physics.
http://dx.doi.org/10.1088/1748-0221/8/04/C04003

I. Rubinskiy.
Irradiation and beam tests qualification for ATLAS IBL Pixel Modules.
Nuclear instruments & methods in physics research / A, volume 699, pages 67 – 71, Amsterdam, 12/05/2011 - 12/08/2011 2013. the 8th International “Hiroshima” Symposium on the Development and Application of Semiconductor Tracking Detectors — Academia Sinica, Taipei(Taiwan), North-Holland Publ. Co.
http://dx.doi.org/10.1016/j.nima.2012.04.078

CMS

Published

G. Bauer et al.
10 Gbps TCP/IP streams from the FPGA for the CMS DAQ eventbuilder network.
Journal of Instrumentation, volume 8, pages C12039 – C12039, London, 09/23/2013 - 09/27/2013 2013. Topical Workshop on Electronics for Particle Physics , Perugia(Italy), Inst. of Physics.
http://dx.doi.org/10.1088/1748-0221/8/12/C12039

G. Bauer et al.
A Comprehensive Zero-Copy Architecture for High Performance Distributed Data Acquisition Over Advanced Network Technologies for the CMS Experiment.
IEEE transactions on nuclear science, 60(6):4595 – 4602, and DESY-2014-01903.
http://dx.doi.org/10.1109/TNS.2013.2282340

P. Cipriano et al.
Higgs boson as a gluon trigger.
Physical review / D, 88(9):097501, and DESY-2014-01913.
http://dx.doi.org/10.1103/PhysRevD.88.097501

CMS Collaboration.
Angular analysis and branching fraction measurement of the decay $B^0 \to K^{*0}\mu^+\mu^-$.
Physics letters / B, B727(1-3):77 – 100, and DESY-2014-00059, arXiv:1308.3409; CMS-BPH-11-009; CERN-PH-EP-2013-152.
http://dx.doi.org/10.1016/j.physletb.2013.10.017

CMS Collaboration.
Energy calibration and resolution of the CMS electromagnetic calorimeter in pp collisions at √s = 7 TeV.
Journal of Instrumentation, 8(09):P09009, and DESY-2014-00054, arXiv:1306.2016; CMS-EGM-11-001; CERN-PH-EP-2013-097.
http://dx.doi.org/10.1088/1748-0221/8/09/P09009

CMS Collaboration.
Erratum: search for new physics in events with same-sign dileptons and b jets in pp collisions at $\sqrt{s} = 8$ TeV.
Journal of high energy physics, 2013:41, and DESY-2014-01139, arXiv:1212.6194; CMS-SUS-12-017; CERN-PH-EP-2012-361.
http://dx.doi.org/doi:10.1007/JHEP07(2013)041

CMS Collaboration.
Event shapes and azimuthal correlations in events in pp collisions at $\sqrt{s} = 7$ TeV.
Physics letters / B, 722(4-5):238 – 261, and DESY-2013-00360, arXiv:1301.1646 ; CMS-EWK-11-021 ; CERN-PH-EP-2013-001.
http://dx.doi.org/10.1016/j.physletb.2013.04.025

CMS Collaboration.
Evidence for associated production of a single top quark and W boson in pp collisions at $\sqrt{s}$ = 7 TeV.
Physical review letters, 110(2):022003, and DESY-2014-01294, arXiv:1209.3489; CMS-TOP-11-022; CERN-PH-EP-2012-266.
http://dx.doi.org/10.1103/PhysRevLett.110.022003

CMS Collaboration.
Forward-backward asymmetry of Drell-Yan lepton pairs in pp collisions at $\sqrt{s} = 7$ TeV.
Physics letters / B, 718(3):752 – 772, and DESY-2014-01310, arXiv:1207.3973; CMS-EWK-11-004; CERN-PH-EP-2012-187.
http://dx.doi.org/10.1016/j.physletb.2012.10.082

CMS Collaboration.
Identification of b-quark jets with the CMS experiment.
Journal of Instrumentation, 8(04):P04013, and DESY-2014-01200, arXiv:1211.4462; CMS-BTV-12-001; CERN-PH-EP-2012-262.
http://dx.doi.org/10.1088/1748-0221/8/04/P04013

CMS Collaboration.
Inclusive search for supersymmetry using the razor variables in pp collisions at $\sqrt{s} = 7$ TeV.
Physical review letters, 111(8):081802, and DESY-2013-00896, arXiv:1212.6961; CMS-SUS-11-024; CERN-PH-EP-2012-332.
http://dx.doi.org/10.1103/PhysRevLett.111.081802

CMS Collaboration.
Interpretation of searches for supersymmetry with simplified models.
Physical review / D, D88(5):052017, and DESY-2014-00045, arXiv:1301.2175; CMS-SUS-11-016; CERN-PH-EP-2012-351.
http://dx.doi.org/10.1103/PhysRevD.88.052017

CMS Collaboration.
Jet and underlying event properties as a function of charged-particle multiplicity in proton–proton collisions at $\sqrt{s}$ = 7 TeV.
The European physical journal / C, 73(12):2674, and DESY-2014-00062, arXiv:1310.4554; CMS-FSQ-12-022; CERN-PH-EP-2013-195.
http://dx.doi.org/10.1140/epjc/s10052-013-2674-5

CMS Collaboration.
Measurement of associated production of vector bosons and top quark-antiquark pairs in pp collisions at $\sqrt{s} = 7$ TeV.
Physical review letters, 110(17):172002, and DESY-2013-00313, arXiv:1303.3239 ; CMS-TOP-12-014 ; CERN-PH-EP-2013-033.
http://dx.doi.org/10.1103/PhysRevLett.110.172002

CMS Collaboration.
Measurement of differential top-quark pair production cross sections in pp colisions at $\sqrt{s} = 7$ TeV.
The European physical journal / C, 73:2339, and DESY-2014-01214, arXiv:1211.2220; CMS-TOP-11-013; CERN-PH-EP-2012-322.
http://dx.doi.org/10.1140/epjc/s10052-013-2339-4

CMS Collaboration.
Measurement of masses in the t t-bar system by kinematic endpoints in pp collisions at $\sqrt{s} = 7$ TeV.
The European physical journal / C, C73(7):2494, and DESY-2013-00538, arXiv:1304.5783; CMS-TOP-11-027; CERN-PH-EP-2013-059.
http://dx.doi.org/10.1140/epjc/s10052-013-2494-7

CMS Collaboration.
Measurement of neutral strange particle production in the underlying event in proton-proton collisions at sqrt(s) = 7 TeV.
Physical review / D, D88(5):052001, and DESY-2013-00959.
http://dx.doi.org/10.1103/PhysRevD.88.052001

CMS Collaboration.
Measurement of the $t\bar{t}$ production cross section in the all-jet final state in pp collisions at $\sqrt{s} = 7$ TeV.
Journal of high energy physics, 2013(5):65, and DESY-2013-00336, arXiv:1302.0508; CMS-TOP-11-007; CERN-PH-EP-2012-358.
http://dx.doi.org/10.1007/JHEP05(2013)065

CMS Collaboration.
Measurement of the azimuthal anisotropy of neutral pions in PbPb collisions at $\sqrt{s_{NN}} = 2.76$ TeV.
Physical review letters, 110(4):042301, and DESY-2014-01311, arXiv:1208.2470; CMS-HIN-11-009; CERN-PH-EP-2012-231.
http://dx.doi.org/10.1103/PhysRevLett.110.042301

CMS Collaboration.
Measurement of the $B_s^0 \to \mu^+\mu^-$ branching fraction and search for $B^0 \to \mu^+\mu^-$ with the CMS Experiment.
Physical review letters, 111(10):101804, and DESY-2013-00958, arXiv:1307.5025; CMS-BPH-13-004-003; CERN-PH-EP-2013-129.
http://dx.doi.org/10.1103/PhysRevLett.111.101804

CMS Collaboration.
Measurement of the cross section and angular correlations for associated production of a Z boson with b hadrons in pp collisions at $\sqrt{s}$ = 7 TeV.
Journal of high energy physics, 1312(12):39, and DESY-2014-00061, arXiv:1310.1349; CMS-EWK-11-015; CERN-PH-EP-2013-153.
http://dx.doi.org/10.1007/JHEP12(2013)039

CMS Collaboration.
Measurement of the differential and double-differential Drell-Yan cross sections in proton-proton collisions at $\sqrt{s} = 7$ TeV.
Journal of high energy physics, 1312(12):30, and DESY-2014-00063, arXiv:1310.7291; CMS-SMP-13-003; CERN-PH-EP-2013-168.
http://dx.doi.org/10.1007/JHEP12(2013)030

CMS Collaboration.
Measurement of the elliptic anisotropy of charged particles produced in PbPb collisions at nucleon-nucleon center-of-mass energy = 2.76 TeV.
Physical review / Special topics / Accelerators and beams, 87:014902, and PHPPUBDB-24749, CMS-HIN-10-002.

CMS Collaboration.
Measurement of the elliptic anisotropy of charged particles produced in PbPb collisions at nucleon-nucleon center-of-mass energy = 2.76 TeV.
Physical review / C, C87(1):014902, and DESY-2014-01916, CMS-HIN-10-002, CERN-PH-EP-2012-095; arXiv:1204.1409.
http://dx.doi.org/10.1103/PhysRevC.87.014902

CMS Collaboration.
Measurement of the hadronic activity in events with a Z and two jets and extraction of the cross section for the electroweak production of a Z with two jets in pp collisions at $\sqrt{s}$ = 7 TeV.
Journal of high energy physics, 1310(10):62, and DESY-2014-00052, arXiv:1305.7389; CMS-FSQ-12-019; CERN-PH-EP-2013-060.
http://dx.doi.org/10.1007/JHEP10(2013)062

CMS Collaboration.
Measurement of the inelastic proton-proton cross section at $\sqrt{s} = 7$ TeV.
Physics letters / B, 722(1-3):5 – 27, and DESY-2014-01231, arXiv:1210.6718; CMS-FWD-11-001; CERN-PH-EP-2012-293.
http://dx.doi.org/10.1016/j.physletb.2013.03.024

CMS Collaboration.
Measurement of the Λ_b^0 lifetime in pp collisions at $\sqrt{s} = 7$ TeV.
Journal of high energy physics, 07(7):163, and
DESY-2014-00049, arXiv:1304.7495; CMS-BPH-11-013;
CERN-PH-EP-2013-065.
http://dx.doi.org/10.1007/JHEP07(2013)163

CMS Collaboration.
Measurement of the production cross section for $Z\gamma \to \nu\bar{\nu}\gamma$ in pp collisions at $\sqrt{s} = 7$ TeV and limits on $ZZ\gamma$ and $Z\gamma\gamma$ triple gauge boson couplings.
Journal of high energy physics, 1310(10):164, and
DESY-2013-01292, arXiv:1309.1117; CMS-SMP-12-020;
CERN-PH-EP-2013-098.
http://dx.doi.org/10.1007/JHEP10(2013)164

CMS Collaboration.
Measurement of the prompt Jψ and ψ(2S) polarizations in pp collisions at $\sqrt{s} = 7$ TeV.
Physics letters / B, 727(4-5):381 – 402, and
DESY-2014-00058, arXiv:1307.6070; CMS-BPH-13-003-003;
CERN-PH-EP-2013-140.
http://dx.doi.org/10.1016/j.physletb.2013.10.055

CMS Collaboration.
Measurement of the ratio of the inclusive 3-jet cross section to the inclusive 2-jet cross section in pp collisions at $\sqrt{s} = 7$ TeV and first determination of the strong coupling constant in the TeV range.
The European physical journal / C, 73(10):2604, and
DESY-2014-00050, arXiv:1304.7498; CMS-QCD-11-003;
CERN-PH-EP-2013-057.
http://dx.doi.org/10.1140/epjc/s10052-013-2604-6

CMS Collaboration.
Measurement of the sum of WW and WZ production with W+dijet events in pp collisions at $\sqrt{s} = 7$ TeV.
The European physical journal / C, 73:2283, and
DESY-2014-01223, arXiv:1210.7544; CMS-SMP-12-015;
CERN-PH-EP-2012-311.
http://dx.doi.org/10.1140/epjc/s10052-013-2283-3

CMS Collaboration.
Measurement of the $t\bar{t}$ production cross section in pp collisions at $\sqrt{s} = 7$ TeV with lepton + jets final states.
Physics letters / B, 720(1-3):83 – 104, and DESY-2014-01126,
arXiv:1212.6682; CMS-TOP-11-003; CERN-PH-EP-2012-285.
http://dx.doi.org/10.1016/j.physletb.2013.02.021

CMS Collaboration.
Measurement of the tt¯ production cross section in the τ+jets channel in pp collisions at s√ = 7 TeV.
The European physical journal / C, 73(4):2386, and
DESY-2013-00340, arXiv:1301.5755; CMS-TOP-11-004;
CERN-PH-EP-2012-374.
http://dx.doi.org/10.1140/epjc/s10052-013-2386-x

CMS Collaboration.
Measurement of the $\Upsilon(1S), \Upsilon(2S)$, and $\Upsilon(3S)$ cross sections in pp collisions at $\sqrt{s} = 7$ TeV.
Physics letters / B, B727(1-3):101 – 125, and
DESY-2014-00048, arXiv:1303.5900; CMS-BPH-11-001;
CERN-PH-EP-2012-373.
http://dx.doi.org/10.1016/j.physletb.2013.10.033

CMS Collaboration.
Measurement of the W-boson helicity in top-quark decays from $t\bar{t}$ production in lepton+jets events in pp collisions at $\sqrt{s} = 7$ TeV.
Journal of high energy physics, 1310(10):167, and
DESY-2014-00060, arXiv:1308.3879; CMS-TOP-11-020;
CERN-PH-EP-2013-133.
http://dx.doi.org/10.1007/JHEP10(2013)167

CMS Collaboration.
Measurement of the W^+W^- Cross section in pp Collisions at $\sqrt{s} = 7$ TeV and Limits on Anomalous $WW\gamma$ and WWZ couplings.
The European physical journal / C, 73(10):2610, and
DESY-2014-00053, arXiv:1306.1126; CMS-SMP-12-005;
CERN-PH-EP-2013-075.
http://dx.doi.org/10.1140/epjc/s10052-013-2610-8

CMS Collaboration.
Measurement of the X(3872) production cross section via decays to J/ψπ + π − in pp collisions at $\sqrt{s} = 7$ TeV.
Journal of high energy physics, 2013(4):154, and
DESY-2013-00321, arXiv:1302.3968 ; CMS-BPH-11-011 ;
CERN-PH-EP-2013-014.
http://dx.doi.org/10.1007/JHEP04(2013)154

CMS Collaboration.
Measurement of the Y1S, Y2S and Y3S polarizations in pp collisions at $\sqrt{s} = 7$ TeV.
Physical review letters, 110(8):081802, and
DESY-2014-01296, arXiv:1209.2922; CMS-BPH-11-023;
CERN-PH-EP-2012-205.
http://dx.doi.org/10.1103/PhysRevLett.110.081802

CMS Collaboration.
Measurement of the ZZ production cross section and search for anomalous couplings in 2 l2l ' final states in pp collisions at $\sqrt{s} = 7$ TeV.
Journal of high energy physics, 2013:63, and
DESY-2014-01198, arXiv:1211.4890; CMS-SMP-12-007;
CERN-PH-EP-2012-336.
http://dx.doi.org/10.1007/JHEP01(2013)063

CMS Collaboration.
Measurement of W^+W^- and ZZ production cross sections in pp collisions at $\sqrt{s} = 8$ TeV.
Physics letters / B, 721(4-5):190 – 211, and
DESY-2013-00506, arXiv:1301.3792; CMS-SUS-12-004;
CERN-PH-EP-2012-252.
http://dx.doi.org/10.1016/j.physletb.2013.03.027

CMS Collaboration.
Measurements of differential jet cross sections in proton-proton collisions at $\sqrt{s} = 7$ TeV with the CMS detector.
Physical review / D, 87(11):112002, and DESY-2014-01128,
arXiv:1212.6660; CMS-QCD-11-004; CERN-PH-EP-2012-343.
http://dx.doi.org/10.1103/PhysRevD.87.112002

CMS Collaboration.
Multiplicity and transverse momentum dependence of two- and four-particle correlations in pPb and PbPb collisions.
Physics letters / B, B724(4-5):213 – 240, and
DESY-2013-00541, arXiv:1305.0609; CMS-HIN-13-002;
CERN-PH-EP-2013-077.
http://dx.doi.org/10.1016/j.physletb.2013.06.028

CMS Collaboration.
Observation of a diffractive contribution to dijet production in proton-proton collisions at $\sqrt{s} = 7$ TeV.
Physical review / D, D87(1):012006, and DESY-2014-01299, arXiv:1209.1805; CMS-FWD-10-004; CERN-PH-EP-2012-248.
http://dx.doi.org/10.1103/PhysRevD.87.012006

CMS Collaboration.
Observation of a new boson with mass near 125 GeV in pp collisions at $\sqrt{s} = 7$ and 8 TeV.
Journal of high energy physics, 2013(6):81, and DESY-2013-00310, arXiv:1303.4571 ; CMS-HIG-12-036 ; CERN-PH-EP-2013-035.
http://dx.doi.org/10.1007/JHEP06(2013)081

CMS Collaboration.
Observation of long-range near-side angular correlations in proton-lead collisions at the LHC.
Physics letters / B, 718:795–814, and PHPPUBDB-24901, CMS-HIN-12-005.
http://dx.doi.org/10.1016/j.physletb.2012.11.025

CMS Collaboration.
The performance of the CMS muon detector in proton-proton collisions at √ s = 7 TeV at the LHC.
Journal of Instrumentation, 8(11):P11002, and DESY-2014-00056, CMS-MUO-11-001; CERN-PH-EP-2013-072; arXiv:1306.6905.
http://dx.doi.org/10.1088/1748-0221/8/11/P11002

CMS Collaboration.
Rapidity distributions in exclusive Z + jet and γ + jet events in pp collisions at $\sqrt{s}$=7 TeV.
Physical review / D, D88(11):112009, and DESY-2014-01754, rXiv:1310.3082; CMS-SMP-12-004; CERN-PH-EP-2013-169.
http://dx.doi.org/10.1103/PhysRevD.88.112009

CMS Collaboration.
Search for a Higgs boson decaying into a b-quark pair and produced in association with b quarks in proton–proton collisions at 7 TeV.
Physics letters / B, 722(4-5):207 – 232, and DESY-2013-00323, arXiv:1302.2892; CMS-HIG-12-033; CERN-PH-EP-2012-375.
http://dx.doi.org/10.1016/j.physletb.2013.04.017

CMS Collaboration.
Search for a Higgs boson decaying into a Z and a photon in pp collisions at $\sqrt{s}$ = 7 and 8 TeV.
Physics letters / B, 726(4-5):587 – 609, and DESY-2014-00057, arXiv:1307.5515; CMS-HIG-13-006; CERN-PH-EP-2013-113.
http://dx.doi.org/10.1016/j.physletb.2013.09.057

CMS Collaboration.
Search for a narrow spin-2 resonance decaying to a pair of Z vector bosons in the semileptonic final state.
Physics letters / B, 718:1208–1228, and PHPPUBDB-24891, CMS-EXO-11-102.
http://dx.doi.org/10.1016/j.physletb.2012.11.063

CMS Collaboration.
Search for a new bottomonium state decaying to $\Upsilon(1S)\pi^+\pi^-$ in pp collisions at $\sqrt{s}$ = 8 TeV.
Physics letters / B, 727(1-3):57 – 76, and DESY-2013-01294, arXiv:1309.0250; CMS-BPH-11-016; CERN-PH-EP-2013-157.
http://dx.doi.org/10.1016/j.physletb.2013.10.016

CMS Collaboration.
Search for a non-standard-model Higgs boson decaying to a pair of new light bosons in four-muon final states.
Physics letters / B, 726(4-5):564 – 586, and DESY-2014-01228, arXiv:1210.7619; CMS-EXO-12-012; CERN-PH-EP-2012-292.
http://dx.doi.org/10.1016/j.physletb.2013.09.009

CMS Collaboration.
Search for a standard-model-like Higgs boson with a mass in the range 145 to 1000 GeV at the LHC.
The European physical journal / C, 73(6):2469, and DESY-2013-00304, arXiv:1304.0213; CMS-HIG-12-034; CERN-PH-EP-2013-050.
http://dx.doi.org/10.1140/epjc/s10052-013-2469-8

CMS Collaboration.
Search for a W ' boson decaying to a bottom quark and a top quark in pp collisions at $\sqrt{s} = 7$ TeV.
Physics letters / B, 718(4-5):1229 – 1251, and DESY-2014-01312, arXiv:1208.0956; CMS-EXO-12-001; CERN-PH-EP-2012-192.
http://dx.doi.org/10.1016/j.physletb.2012.12.008

CMS Collaboration.
Search for anomalous production of highly boosted Z bosons decaying to dimuons in pp collisions at $\sqrt{s} = 7$ TeV.
Physics letters / B, B722(1-3):28 – 47, and DESY-2014-01293, arXiv:1210.0867; CMS-EXO-11-025; CERN-PH-EP-2012-294.
http://dx.doi.org/10.1016/j.physletb.2013.03.037

CMS Collaboration.
Search for contact interactions in $\mu^+\mu^-$ events in pp collisions at $\sqrt{s} = 7$ TeV.
Physical review / D, 87(3):032001, and DESY-2014-01144, arXiv:1212.4563; CMS-EXO-11-009; CERN-PH-EP-2012-329.
http://dx.doi.org/10.1103/PhysRevD.87.032001

CMS Collaboration.
Search for contact interactions using the inclusive jet p_T spectrum in pp collisions at $\sqrt{s} = 7$ TeV.
Physical review / D, 87(5):052017, and DESY-2013-00341, arXiv:1301.5023; CMS-EXO-11-010; CERN-PH-EP-2013-002.
http://dx.doi.org/10.1103/PhysRevD.87.052017

CMS Collaboration.
Search for excited leptons in pp collisions at $\sqrt{s} = 7$ TeV.
Physics letters / B, 720(4-5):309 – 329, and DESY-2014-01286, arXiv:1210.2422; CMS-EXO-11-034; CERN-PH-EP-2012-261.
http://dx.doi.org/10.1016/j.physletb.2013.02.031

CMS Collaboration.
Search for exotic resonances decaying into WZ/ZZ in pp collisions at $\sqrt{s} = 7$ TeV.
Journal of high energy physics, 2013:36, and DESY-2014-01197, arXiv:1211.5779; CMS-EXO-12-014; CERN-PH-EP-2012-312.
http://dx.doi.org/10.1007/JHEP02(2013)036

CMS Collaboration.
Search for flavor changing neutral currents in top quark decays in pp collisions at 7 TeV.
Physics letters / B, B718(4-5):1252 – 1272, and DESY-2014-01924, CMS-TOP-11-028, CERN-PH-EP-2012-206; arXiv:1208.0957.
http://dx.doi.org/10.1016/j.physletb.2012.12.045

CMS Collaboration.
Search for fractionally charged particles in *pp* collisions at $\sqrt{s} = 7$ TeV.
Physical review / D, D87(9):092008, and DESY-2014-01808, CMS-EXO-11-074; CERN-PH-EP-2012-282; arXiv:1210.2311.
http://dx.doi.org/10.1103/PhysRevD.87.092008

CMS Collaboration.
Search for gluino mediated bottom- and top-squark production in multijet final states in pp collisions at 8 TeV.
Physics letters / B, 725(4-5):243 – 270, and DESY-2014-00051, arXiv:1305.2390; CMS-SUS-12-024; CERN-PH-EP-2013-076.
http://dx.doi.org/10.1016/j.physletb.2013.06.058

CMS Collaboration.
Search for heavy narrow dilepton resonances in *pp* collisions at $\sqrt{s} = 7$ TeV and $\sqrt{s} = 8$ TeV.
Physics letters / B, 720:63–82, and DESY-2014-01150, arXiv:1212.6175; CMS-EXO-12-015; CERN-PH-EP-2012-364.
http://dx.doi.org/10.1016/j.physletb.2013.02.003

CMS Collaboration.
Search for heavy quarks decaying into a top quark and a W or Z boson using lepton + jets events in *pp* collisions at $\sqrt{s} = 7$ TeV.
Journal of high energy physics, 2013(1):154, and DESY-2014-01226, arXiv:1210.7471; CMS-B2G-12-004; CERN-PH-EP-2012-309.
http://dx.doi.org/10.1007/JHEP01(2013)154

CMS Collaboration.
Search for heavy resonances in the W/Z-tagged dijet mass spectrum in pp collisions at 7 TeV.
Physics letters / B, 723(4-5):280 – 301, and DESY-2014-01195, arXiv:1212.1910; CMS-EXO-11-095; CERN-PH-EP-2012-356.
http://dx.doi.org/10.1016/j.physletb.2013.05.040

CMS Collaboration.
Search for long-lived particles decaying to photons and missing energy in proton-proton collisions at $\sqrt{s} = 7$ TeV.
Physics letters / B, 722(4-5):273 – 294, and DESY-2014-01196, arXiv:1212.1838; CMS-EXO-11-035; CERN-PH-EP-2012-342.
http://dx.doi.org/10.1016/j.physletb.2013.04.027

CMS Collaboration.
Search for microscopic black holes in pp collisions at $\sqrt{s} = 8$ TeV.
Journal of high energy physics, 1307(7):178, and DESY-2013-00897, arXiv:1303.5338; CMS-EXO-12-009; CERN-PH-EP-2013-043.
http://dx.doi.org/10.1007/JHEP07(2013)178

CMS Collaboration.
Search for narrow resonances and quantum black holes in inclusive and *b*-tagged dijet mass spectra from *pp* collisions at $sqrts = 7$ **TeV**.
Journal of high energy physics, 1301:013, and PHPPUBDB-24897, CMS-EXO-11-094.

CMS Collaboration.
Search for narrow resonances and quantum black holes in inclusive and *b*-tagged dijet mass spectra from *pp* collisions at $\sqrt{s} = 7$ TeV.
Journal of high energy physics, 1301(1):13, and DESY-2014-01925, CMS-EXO-11-094; CERN-PH-EP-2012-277; arXiv:1210.2387.
http://dx.doi.org/10.1007/JHEP01(2013)013

CMS Collaboration.
Search for narrow resonances using the dijet mass spectrum in pp collisions at $\sqrt{s} = 8$ TeV.
Physical review / D, D87(11):114015, and DESY-2014-00046, arXiv:1302.4794; CMS-EXO-12-016; CERN-PH-EP-2013-015.
http://dx.doi.org/10.1103/PhysRevD.87.114015

CMS Collaboration.
Search for new physics in events with opposite-sign leptons, jets, and missing transverse energy in *pp* collisions at $\sqrt{s} = 7$ TeV.
Physics letters / B, 718(3):815 – 840, and DESY-2014-01314, arXiv:1206.3949; CMS-SUS-11-011; CERN-PH-EP-2012-156.
http://dx.doi.org/10.1016/j.physletb.2012.11.036

CMS Collaboration.
Search for new physics in events with photons, jets, and missing transverse energy in *pp* collisions at $\sqrt{s} = 7$ TeV.
Journal of high energy physics, 2013:111, and DESY-2014-01199, arXiv:1211.4784; CMS-SUS-12-001; CERN-PH-EP-2012-321.
http://dx.doi.org/10.1007/JHEP03(2013)111

CMS Collaboration.
Search for new physics in events with same-sign dileptons and b jets in *pp* collisions at $\sqrt{s} = 8$ TeV.
Journal of high energy physics, 1303:037, and DESY-2014-01920, CMS-SUS-12-017; CERN-PH-EP-2012-361; arXiv:1212.6194.
http://dx.doi.org/10.1007/JHEP03(2013)037

CMS Collaboration.
Search for new physics in final states with a lepton and missing transverse energy in pp collisions at the LHC.
Physical review / D, 87(7):072005, and DESY-2013-00325, arXiv:1302.2812; CMS-EXO-12-010; CERN-PH-EP-2013-010.
http://dx.doi.org/10.1103/PhysRevD.87.072005

CMS Collaboration.
Search for pair-produced dijet resonances in four-jet final states in pp collisions at $\sqrt{s} = 7$ TeV.
Physical review letters, 110(14):141802, and DESY-2013-00339, arXiv:1302.0531; CMS-EXO-11-016; CERN-PH-EP-2013-007.
http://dx.doi.org/10.1103/PhysRevLett.110.141802

CMS Collaboration.
Search for pair production of third-generation leptoquarks and top squarks in *pp* collisions at $\sqrt{s} = 7$ TeV.
Physical review letters, 110(8):081801, and DESY-2014-01234.
http://dx.doi.org/10.1103/PhysRevLett.110.081801

CMS Collaboration.
Search for physics beyond the standard model in events with tau leptons, jets, and large transverse momentum imbalance in pp collisions at $\sqrt{s} = 7$ TeV.
The European physical journal / C, C73(7):2493, and DESY-2013-00543, arXiv:1301.3792; CMS-SUS-12-004; CERN-PH-EP-2012-252.
http://dx.doi.org/10.1140/epjc/s10052-013-2493-8

CMS Collaboration.
Search for supersymmetry in events with opposite-sign dileptons and missing transverse energy using an artificial neural network.
Physical review / D, 87(7):072001, and DESY-2013-00361, arXiv:1301.0916 ; CMS-SUS-11-018 ; CERN-PH-EP-2012-341.
http://dx.doi.org/10.1103/PhysRevD.87.072001

CMS Collaboration.
Search for supersymmetry in events with photons and low missing transverse energy in pp collisions at $\sqrt{s} = 7$ TeV.
Physics letters / B, 719(1-3):42 – 61, and DESY-2014-01288, arXiv:1210.2052; CMS-SUS-12-014; CERN-PH-EP-2012-272.
http://dx.doi.org/10.1016/j.physletb.2012.12.055

CMS Collaboration.
Search for supersymmetry in final states with a single lepton, b-quark jets, and missing transverse energy in proton-proton collisions at $\sqrt{s} = 7$ TeV.
Physical review / D, 87(5):052006, and DESY-2014-01211, arXiv:1211.3143; CMS-SUS-11-028; CERN-PH-EP-2012-316.
http://dx.doi.org/10.1103/PhysRevD.87.052006

CMS Collaboration.
Search for supersymmetry in final states with missing transverse energy and 0, 1, 2, or at least 3 b-quark jets in 7 TeV pp collisions using the variable alphaT.
Journal of high energy physics, 2013:77, and DESY-2014-01221, arXiv:1210.8115; CMS-SUS-11-022; CERN-PH-EP-2012-290.
http://dx.doi.org/10.1007/JHEP01(2013)077

CMS Collaboration.
Search for supersymmetry in pp collisions at $\sqrt{s} = 7$ TeV in events with a single lepton, jets, and missing transverse momentum.
The European physical journal / C, 73:2404, and DESY-2014-01131, arXiv:1212.6428; CMS-SUS-12-010; CERN-PH-EP-2012-348.
http://dx.doi.org/10.1140/epjc/s10052-013-2404-z

CMS Collaboration.
Search for the standard model Higgs boson produced in association with a top-quark pair in pp collisions at the LHC.
Journal of high energy physics, 2013(5):145, and DESY-2013-00317, arXiv:1303.0763; CMS-HIG-12-035; CERN-PH-EP-2013-027.
http://dx.doi.org/10.1007/JHEP05(2013)145

CMS Collaboration.
Search for top-squark pair production in the single-lepton final state in pp collisions at $\sqrt{s}$ = 8 TeV.
The European physical journal / C, 73(12):2677, and DESY-2014-01039, arXiv:1308.1586; CMS-SUS-13-011; CERN-PH-EP-2013-148.
http://dx.doi.org/10.1140/epjc/s10052-013-2677-2

CMS Collaboration.
Search for top squarks in R-parity-violating supersymmetry using three or more leptons and b-tagged jets.
Physical review letters, 111(22):221801, and DESY-2014-00055, arXiv:1306.6643; CMS-SUS-13-003; CERN-PH-EP-2013-093.
http://dx.doi.org/10.1103/PhysRevLett.111.221801

CMS Collaboration.
Search for Z ' resonances decaying to $t\bar{t}$ in dilepton+jets final states in pp collisions at $\sqrt{s} = 7$ TeV.
Physical review / D, 87(7):072002, and DESY-2014-01210, arXiv:1211.3338; CMS-TOP-11-010; CERN-PH-EP-2012-324.
http://dx.doi.org/10.1103/PhysRevD.87.072002

CMS Collaboration.
Search in leptonic channels for heavy resonances decaying to long-lived neutral particles.
Journal of high energy physics, 2013:85, and DESY-2014-01213, arXiv:1211.2472; CMS-EXO-11-101; CERN-PH-EP-2012-304.
http://dx.doi.org/10.1007/JHEP02(2013)085

CMS Collaboration.
Searches for Higgs bosons in pp collisions at in the context of four-generation and fermiophobic models.
Physics letters / B, 06:S0370269313005182, and DESY-2013-00333, arXiv:1302.1764; CMS-HIG-12-013; CERN-PH-EP-2013-011.
http://dx.doi.org/10.1016/j.physletb.2013.06.043

CMS Collaboration.
Searches for long-lived charged particles in pp collisions at $\sqrt{s}$=7 and 8 TeV.
Journal of high energy physics, 1307(7):122, and DESY-2013-00542, arXiv:1305.0491; CMS-EXO-12-026; CERN-PH-EP-2013-073.
http://dx.doi.org/10.1007/JHEP07(2013)122

CMS Collaboration.
Searches for new physics using the $t\bar{t}$ invariant mass distribution in pp collisions at $\sqrt{s}$=8 TeV.
Physical review letters, 111(21):211804, and DESY-2014-01755, arXiv:1309.2030; CMS-B2G-13-001-003; CERN-PH-EP-2013-162.
http://dx.doi.org/10.1103/PhysRevLett.111.211804

CMS Collaboration.
Studies of jet mass in dijet and W/Z + jet events.
Journal of high energy physics, 2013(5):90, and DESY-2013-00307, arXiv:1303.4811; CMS-SMP-12-019; CERN-PH-EP-2013-016.
http://dx.doi.org/10.1007/JHEP05(2013)090

CMS Collaboration.
Studies of jet quenching using isolated-photon+jet correlations in PbPb and pp collisions at $sqrts_{NN} = 2.76$ TeV.
Chemical physics letters, 718:773–794, and PHPPUBDB-24758, CMS-HIN-11-010.

CMS Collaboration.
Studies of jet quenching using isolated-photon+jet correlations in PbPb and pp collisions at $\sqrt{s_{NN}} = 2.76$ TeV.
Physics letters / B, B718(3):773 – 794, and DESY-2014-01908, CMS-HIN-11-010, CERN-PH-EP-2012-089; arXiv:1205.0206.
http://dx.doi.org/10.1016/j.physletb.2012.11.003

CMS Collaboration.
Study of exclusive two-photon production of W^+W^- in pp collisions at $\sqrt{s} = 7$ TeV and constraints on anomalous quartic gauge couplings.
Journal of high energy physics, 1307(7):116, and DESY-2013-00540, CERN-PH-EP-2013-084; CMS-FSQ-12-010; arXiv:1305.5596.
http://dx.doi.org/10.1007/JHEP07(2013)116

CMS Collaboration.
Study of the Mass and Spin-Parity of the Higgs Boson Candidate Via Its Decays to Z Boson Pairs.
Physical review letters, 110(8):081803, and DESY-2014-01121, arXiv:1212.6639; CMS-HIG-12-041; CERN-PH-EP-2012-372.
http://dx.doi.org/10.1103/PhysRevLett.110.081803

CMS Collaboration.
Study of the underlying event at forward rapidity in pp collisions at $\sqrt{s}$ = 0.9, 2.76, and 7 TeV.
Journal of high energy physics, 1304(4):72, and DESY-2014-01917, S-FWD-11-003, CERN-PH-EP-2013-012; arXiv:1302.2394.
http://dx.doi.org/10.1007/JHEP04(2013)072

S. K. Dooling, P. Gunnellini, F. Hautmann, and H. Jung.
Longitudinal momentum shifts, showering, and nonperturbative corrections in matched next-to-leading-order shower event generators.
Physical review / D, 87(9):094009, and DESY-2013-01185, DESY 12-166, OUTP-12-19P, arXiv:1212.6164.
http://dx.doi.org/10.1103/PhysRevD.87.094009

J. Gao, M. Guzzi, and P. M. Nadolsky.
Charm quark mass dependence in a global QCD analysis.
The European physical journal / C, 73:2541, and DESY-2014-00019.
http://dx.doi.org/10.1140/epjc/s10052-013-2541-4

V. Guzey, M. Guzzi, P. M. Nadolsky, M. Strikman, and B. Wang.
Massive neutral gauge boson production as a probe of nuclear modifications of parton distributions at the LHC.
The European physical journal / A, 49(3):35, and DESY-2014-01894.
http://dx.doi.org/10.1140/epja/i2013-13035-6

I. Marfin.
Search for Higgs boson production in association with b quarks at CMS in pp collisions.
Acta physica Slovaca, page 403, Bratislava, 09/12/2012 - 09/15/2012 2013. 32nd International Symposium on Physics in Collision, Strbske Pleso(Slovakia), Inst. of Physics, Slovak Acad. of Sciences.

CMS Collaboration.
Determination of the top-quark pole mass and strong coupling constant from the $t\bar{t}$ production cross section in pp collisions at $\sqrt{s}$ = 7 TeV.
Physics letters / B, 728:496 – 517, and DESY-2014-01040, arXiv:1307.1907; CMS-TOP-12-022; CERN-PH-EP-2013-121.
http://dx.doi.org/10.1016/j.physletb.2013.12.009

Ph.D. Thesis

A. Bethani.
Neutral Higgs boson searches in the $H - \tau\tau - \mu\mu$ decay channel.
University of Karlsruhe, Karslruhe, 2013.

J. Lange.
Differential Top-Quark-Pair Cross Sections in pp Collisions at $\sqrt{s} = 7$ TeV with CMS and Charge Multiplication in Highly-Irradiated Silicon Sensors.
Universität Hamburg, 2013.

H. Schettler.
The Event-Mixing Technique for Modeling the tt Background in a Search for Supersymmetry in the Di-Lepton Channel.
University of Hamburg, Hamburg, 2013.

J. Zhang.
X-ray Radiation Damage Studies and Design of a Silicon Pixel Sensor for Science at the XFEL.
University of Hamburg, Hamburg, 2013.

Master Thesis

M. Hempel.
Application of Diamond Based Beam Loss Monitors at LHC.
TU Cottbus, 2013.

C. Neubueser.
Impact of Irradiations by Protons with different Energies on Silicon Sensors.
University of Hamburg, Hamburg, 2013.

Linear Collider

Published

C. Adloff et al.
Validation of GEANT4 Monte Carlo models with a highly granular scintillator-steel hadron calorimeter.
Journal of Instrumentation, 8(07):P07005 – P07005, and DESY-2014-01910.
http://dx.doi.org/10.1088/1748-0221/8/07/P07005

C. Adloff et al.
Track segments in hadronic showers in a highly granular scintillator-steel hadron calorimeter.
Journal of Instrumentation, 8(09):1–22, and DESY-2014-00785.
http://dx.doi.org/10.1088/1748-0221/8/09/P09001

Aleph Collaboration, Delphi Collaboration, L3 Collaboration, OPAL Collaboration, and Boson, LEP working group for Higgs.
Search for Charged Higgs bosons: Combined Results Using LEP Data.
The European physical journal / C, 73:2463, and DESY-2014-00957.
http://dx.doi.org/10.1140/epjc/s10052-013-2463-1

ALEPH Collaboration, DELPHI Collaboration, L3 Collaboration, OPAL Collaboration, and LEP Electroweak Working Group.
Electroweak measurements in electron–positron collisions at W-boson-pair energies at LEP.
Physics reports, 532(4):119 – 244, and DESY-2014-00955.
http://dx.doi.org/10.1016/j.physrep.2013.07.004

N. Aubry et al.
EndoTOFPET-US: a novel multimodal tool for endoscopy and positron emission tomography.
Journal of Instrumentation, volume 8, page C04002, London, 2013. 14th INTERNATIONAL WORKSHOP ON RADIATION IMAGING DETECTORS, FIGUEIRA DA FOZ(PORTUGAL), Inst. of Physics.
http://dx.doi.org/10.1088/1748-0221/8/04/C04002

H. Baer and J. List.
Post-LHC8 supersymmetry benchmark points for ILC physics.
Physical review / D, 88(5):1–29, and DESY-2014-00605.
http://dx.doi.org/10.1103/PhysRevD.88.055004

T. Behnke, R. Diener, C. Rosemann, and L. Steder.
A Novel Self-supporting GEM-based Amplification Structure for a Time Projection Chamber at the ILC.
Journal of Instrumentation, 8(12):P12009, and DESY-2014-00973, DESY-12-212.
http://dx.doi.org/10.1088/1748-0221/8/12/P12009

T. Behnke, F. J. Mueller, A. Muennich, and K. Zenker.
GEM module design for the ILD TPC.
Journal of Instrumentation, volume 8, page C10010, London, 07/01/2013 - 07/06/2013 2013. 3rd Conference on Micro-Pattern Gaseous Detectors & RD51 Collaboration meeting, Zaragoza(Spain), Inst. of Physics.
http://dx.doi.org/10.1088/1748-0221/8/10/C10010

M. Berggren et al.
Tackling light higgsinos at the ILC.
The European physical journal / C, 73(12):1–22, and DESY-2014-00555, DESY 13-098, arXiv:1307.3566.
http://dx.doi.org/10.1140/epjc/s10052-013-2660-y

P. Goettlicher.
Simulations and Measurements for a concept of powering CALICE-AHCAL at a train-cycled accelerator.
Journal of Instrumentation, volume 8, pages C01054 – C01054, London, 09/17/2012 - 09/21/2012 2013. Topical Workshop on Electronics for Particle Physics, Oxford(Great-Britain), Inst. of Physics.
http://dx.doi.org/10.1088/1748-0221/8/01/C01054

J. Grebenyuk, A. Martinez de la Ossa, T. Mehrling, and J. Osterhoff.
Beam-driven plasma-based acceleration of electrons with density down-ramp injection at FLASHForward.
Nuclear instruments & methods in physics research / A, page S0168900213014356, Amsterdam, 06/02/2013 - 06/07/2013 2013. 1st European Advanced Accelerator Concepts Workshop, La Biodola, Isola d'Elba(Italy), North-Holland Publ. Co. *http://dx.doi.org/10.1016/j.nima.2013.10.054*

A. Martinez de la Ossa et al.
High-quality electron beams from field-induced ionization injection in the strong blow-out regime of beam-driven plasma accelerators.
Nuclear instruments & methods in physics research / A, page S016890021301334X, Amsterdam, 06/02/2013 - 06/07/2013 2013. 1st European Advanced Accelerator Concepts Workshop, La Biodola, Isola d'Elba(Italy), North-Holland Publ. Co. *http://dx.doi.org/10.1016/j.nima.2013.10.016*

A. Martinez de la Ossa, J. Grebenyuk, T. Mehrling, L. Schaper, and J. Osterhoff.
High-Quality Electron Beams from Beam-Driven Plasma Accelerators by Wakefield-Induced Ionization Injection.
Physical review letters, 111(24):245003–1 – 245003–5, and DESY-2014-00540.
http://dx.doi.org/10.1103/PhysRevLett.111.245003

R. Mitzner et al.
L-Edge X-ray Absorption Spectroscopy of Dilute Systems Relevant to Metalloproteins Using an X-ray Free-Electron Laser.
The journal of physical chemistry letters, 4(21):3641 – 3647, and DESY-2014-02037.
http://dx.doi.org/10.1021/jz401837f

G. Moortgat-Pick, P. Osland, A. A. Pankov, and A. V. Tsytrinov.
Unique heavy lepton signature at e^+e^- linear collider with polarized beams.
Physical review / D, 87(9):095017, and DESY-2014-00924.
http://dx.doi.org/10.1103/PhysRevD.87.095017

A. Navitski, S. Lagotzky, D. Reschke, X. Singer, and G. Müller.
Field emitter activation on cleaned crystalline niobium surfaces relevant for superconducting rf technology.
Physical review / Special topics / Accelerators and beams, 16(11):112001 – 112008, and DESY-2014-00549.
http://dx.doi.org/10.1103/PhysRevSTAB.16.112001

J.-P. Schwinkendorf, S. Wunderlich, L. Schaper, B. Schmidt, and J. Osterhoff.
TADPOLE for longitudinal electron-bunch diagnostics based on electro-optic upconversion.
Nuclear instruments & methods in physics research / A, page S016890021301721X, Amsterdam, 06/02/2013 - 06/07/2013 2013. 1st European Advanced Accelerator Concepts Workshop, La Biodola, Isola d'Elba(Italy), North-Holland Publ. Co. *http://dx.doi.org/10.1016/j.nima.2013.12.030*

Ph.D. Thesis

M. Beckmann.
Spin Transport at the International Linear Collider and its Impact on the Measurement of Polarization.
University of Hamburg, 2013.

M. K. Bock.
Measuring the Electron Bunch Timing with Femtosecond Resolution at FLASH..
Universität Hamburg, 2013.

F. Schlander.
Study of Quality and Field Limitation of Superconducting 1.3 GHz 9-Cell RF-Cavities at DESY.
Universität Hamburg, Hamburg, 2013.

Diploma Thesis

S. Schefer.
Aufbau und Charakterisierung eines balancierten optischen Kreuzkorrelators zur Synchronisation von Titan:Saphir-Lasersystemen mit Femtosekundenpräzision..
Universität Hamburg, 2013.

Master Thesis

L. Goldberg.
Laser-Based Discharge Ignition for Capillary Waveguides.
Universität Hamburg, Hamburg, 2013.

BELLE

Published

Belle Collaboration.
Evidence for $\bar{B}_s^0 \to \Lambda_c^+ \bar{\Lambda} \pi^-$.
Physics letters / B, 726(1-3):206 – 210, and DESY-2013-01012, Belle preprint 2013-4.
http://dx.doi.org/10.1016/j.physletb.2013.08.057

Belle Collaboration.
Evidence for the suppressed decay $B^- \to DK^-, D \to K^+\pi^-\pi^0$.
Physical review / D, 88(9):091104, and DESY-2013-01488, Belle Preprint 2013-24.
http://dx.doi.org/10.1103/PhysRevD.88.091104

Belle Collaboration.
Measurement of the Decays $B_s^0 \to J/\psi\, \phi(1020)$, $B_s^0 \to J/\psi\, f_2'(1525)$ and $B_s^0 \to J/\psi\, K^+K^-$ at Belle.
Physical review / D, 88:114006, and DESY-2013-01479, Belle Preprint 2013-21; arXiv:1309.0704.
http://dx.doi.org/10.1103/PhysRevD.88.114006

Belle Collaboration.
Measurement of the CP Violation Parameters in $B^0 - \pi^+\pi^-$ Decays.
Physical review / D, 88(9):092003, and DESY-2013-01387, Belle Preprint 2013-11.
http://dx.doi.org/10.1103/PhysRevD.88.092003

V. Bhardwaj et al.
Evidence of a New Narrow Resonance Decaying to $\chi_{c1}\gamma$ in $B \to \chi_{c1}\gamma K$.
Physical review letters, 111(3):032001, and DESY-2013-00448, Belle Preprint 2013-7.
http://dx.doi.org/10.1103/PhysRevLett.111.032001

K. Chilikin et al.
Experimental constraints on the spin and parity of the $Z(4430)^+$.
Physical review / D, 88(7):074026, and DESY-2013-01013, Belle preprint 2013-12.
http://dx.doi.org/10.1103/PhysRevD.88.074026

R. Chistov et al.
First observation of Cabibbo-suppressed Ξ_c^0 decays.
Physical review / D, 88(7):071103, and DESY-2013-01014, Belle preprint 2013-13.
http://dx.doi.org/10.1103/PhysRevD.88.071103

M. Friedl et al.
The Belle II Silicon Vertex Detector.
Nuclear instruments & methods in physics research / A, 732:83 – 86, and DESY-2014-01897.
http://dx.doi.org/10.1016/j.nima.2013.05.171

V. Gaur et al.
Evidence for the decay $B^0 \to K^+K^-\pi^0$.
Physical review / D, 87(9):091101, and DESY-2013-00160, Belle-Preprint-2013-5.
http://dx.doi.org/10.1103/PhysRevD.87.091101

P. Krokovny et al.
First observation of the Z_b^0(10610) in a Dalitz analysis of $\Upsilon(10860) \to (nS)\pi^0\pi^0$.
Physical review / D, 88(5):052016, and DESY-2013-00857, Belle preprint 2013-20.
http://dx.doi.org/10.1103/PhysRevD.88.052016

O. Kuprash.
Power pulsing of the CMOS sensor Mimosa 26.
Nuclear instruments & methods in physics research / A, volume A732, pages 519 – 522, Amsterdam, 02/11/2013 - 02/15/2013 2013. 13th Vienna Conference on Instrumentation, Vienna(Austria), North-Holland Publ. Co.
http://dx.doi.org/10.1016/j.nima.2013.06.075

Z. Q. Liu et al.
Study of $e^+e^- \to \pi^+\pi^- J/\psi$ and Observation of a Charged Charmoniumlike State at Belle.
Physical review letters, 110(25):252002, and DESY-2013-00151.
http://dx.doi.org/10.1103/PhysRevLett.110.252002

M. Prim et al.
Angular analysis of $B^0 \to \phi K^*$ decays and search for CP violation at Belle.
Physical review / D, 88(7):072004, and DESY-2013-01016, Belle preprint 2013-16.
http://dx.doi.org/10.1103/PhysRevD.88.072004

S. Sandilya et al.
Search for bottomonium states in exclusive radiative $\Upsilon(2S)$ decays.
Physical review letters, 111(11):112001, and DESY-2013-00779, Belle preprint 2013-14.
http://dx.doi.org/10.1103/PhysRevLett.111.112001

C. P. Shen et al.
Measurement of exclusive $\Upsilon(1S)$ and $\Upsilon(2S)$ decays into vector-pseudoscalar final states.
Physical review / D, 88(1):011102, and DESY-2013-00449, Belle Preprint 2013-8.
http://dx.doi.org/10.1103/PhysRevD.88.011102

C. P. Shen et al.
Measurement of $e^+e^- \to \omega\pi^0$, $K^*(892)\bar{K}$ and $K_2^*(1430)\bar{K}$ at 10.52 GeV, 10.58 GeV, and 10.876 GeV.
Physical review / D, 88(5):052019, and DESY-2013-00882, Belle preprint 2013-19.
http://dx.doi.org/10.1103/PhysRevD.88.052019

A. Sibidanov et al.
Study of exclusive $B \to X_u \ell \nu$ decays and extraction of $|V_{ub}|$ using full reconstruction tagging at the Belle experiment.
Physical review / D, 88(3):032005, and DESY-2013-00592, Belle Preprint 2013-9.
http://dx.doi.org/10.1103/PhysRevD.88.032005

E. White et al.
Measurement of the wrong-sign decay $D^0 \to K^+\pi^-\pi^+\pi^-$.
Physical review / D, 88(5):051101, and DESY-2013-01015, Belle preprint 2013-17.
http://dx.doi.org/10.1103/PhysRevD.88.051101

A. Zupanc et al.
Measurements of branching fractions of leptonic and hadronic D_s^+ meson decays and extraction of the D_s^+ meson decay constant.
Journal of high energy physics, 2013(9):139, and DESY-2013-00881, Belle preprint 2013-15.
http://dx.doi.org/10.1007/JHEP09(2013)139

Master Thesis

K.-S. Petersen.
Event Selection and Trigger Studies for an Analysis of the Forward-Backward Asymmetry of Muon Pairs at the Belle Experiment.
University of Hamburg, 2013.

ALPS

Published

K. Baker et al.
The quest for axions and other new light particles.
Annalen der Physik, 525(6):A93–A99, and DESY-2013-00123, DESY 13-089. *http://dx.doi.org/10.1002/andp.201300727*

R. Bähre et al.
Any light particle search II — Technical Design Report.
Journal of Instrumentation, 8(09):T09001, and DESY-2013-01033, DESY 13-030.
http://dx.doi.org/10.1088/1748-0221/8/09/T09001

Astroparticle physics

Published

R. Abbasi et al.
All-particle cosmic ray energy spectrum measured with 26 IceTop stations.
Astroparticle physics, 44:40 – 58, and DESY-2014-01278.
http://dx.doi.org/10.1016/j.astropartphys.2013.01.016

R. Abbasi et al.
Cosmic ray composition and energy spectrum from 1–30PeV using the 40-string configuration of IceTop and IceCube.
Astroparticle physics, 42:15 – 32, and DESY-2014-01323.
http://dx.doi.org/10.1016/j.astropartphys.2012.11.003

R. Abbasi et al.
Lateral distribution of muons in IceCube cosmic ray events.
Physical review / D, 87(1):012005, and DESY-2014-01248.
http://dx.doi.org/10.1103/PhysRevD.87.012005

R. Abbasi et al.
Search for relativistic magnetic monopoles with IceCube.
Physical review / D, 87(2):022001, and DESY-2014-01254.
http://dx.doi.org/10.1103/PhysRevD.87.022001

R. Abbasi et al.
An improved method for measuring muon energy using the truncated mean of dE/dx.
Nuclear instruments & methods in physics research / A, 703:190 – 198, and DESY-2014-01277.
http://dx.doi.org/10.1016/j.nima.2012.11.081

R. Abbasi et al.
SEARCHES FOR HIGH-ENERGY NEUTRINO EMISSION IN THE GALAXY WITH THE COMBINED ICECUBE-AMANDA DETECTOR.
The astrophysical journal, 763(1):33, and DESY-2014-01326.
http://dx.doi.org/10.1088/0004-637X/763/1/33

A. A. Abdo et al.
THE SECOND FERMI LARGE AREA TELESCOPE CATALOG OF GAMMA-RAY PULSARS.
The astrophysical journal / Supplement series, 208(2):1–59, and DESY-2014-00864.
http://dx.doi.org/10.1088/0067-0049/208/2/17

F. Acero et al.
CONSTRAINTS ON THE GALACTIC POPULATION OF TeV PULSAR WIND NEBULAE USING FERMI LARGE AREA TELESCOPE OBSERVATIONS.
The astrophysical journal, 773(77):1–27, and DESY-2014-00854.
http://dx.doi.org/10.1088/0004-637X/773/1/77

B. S. Acharya et al.
Introducing the CTA concept.
Astroparticle physics, 43:3 – 18, and DESY-2014-00190.
http://dx.doi.org/10.1016/j.astropartphys.2013.01.007

M. Ackermann et al.
THE FERMI ALL-SKY VARIABILITY ANALYSIS: A LIST OF FLARING GAMMA-RAY SOURCES AND THE SEARCH FOR TRANSIENTS IN OUR GALAXY.
The astrophysical journal, 771(57):1–12, and DESY-2014-00869.
http://dx.doi.org/10.1088/0004-637X/771/1/57

M. Ackermann et al.
Search for gamma-ray spectral lines with the Fermi Large Area Telescope and dark matter implications.
Physical review / D, 88(8):082002, and DESY-2014-01050.
http://dx.doi.org/10.1103/PhysRevD.88.082002

M. Ackermann et al.
DETERMINATION OF THE POINT-SPREAD FUNCTION FOR THE FERMI LARGE AREA TELESCOPE FROM ON-ORBIT DATA AND LIMITS ON PAIR HALOS OF ACTIVE GALACTIC NUCLEI.
The astrophysical journal, 765(1):54, and DESY-2014-01075.
http://dx.doi.org/10.1088/0004-637X/765/1/54

M. Ackermann et al.
THE FIRST FERMI -LAT CATALOG OF SOURCES ABOVE 10 GeV.
The astrophysical journal / Supplement series, 209(34):1–34, and DESY-2014-00830.
http://dx.doi.org/10.1088/0067-0049/209/2/34

M. Ackermann et al.
Detection of the Characteristic Pion-Decay Signature in Supernova Remnants.
Science, 339(6121):807 – 811, and DESY-2014-01153.
http://dx.doi.org/10.1126/science.1231160

M. Ackermann et al.
ERRATUM: "FERMI LARGE AREA TELESCOPE STUDY OF COSMIC-RAYS AND THE INTERSTELLAR MEDIUM IN NEARBY MOLECULAR CLOUDS" (2012, ApJ, 755, 22).
The astrophysical journal, 778(1):82, and DESY-2014-01041.
http://dx.doi.org/10.1088/0004-637X/778/1/82

M. Ackermann et al.
THE FIRST FERMI -LAT GAMMA-RAY BURST CATALOG.
The astrophysical journal / Supplement series, 209(1):1–90, and DESY-2014-00837.
http://dx.doi.org/10.1088/0067-0049/209/1/11

M. Ackermann et al.
MULTIWAVELENGTH OBSERVATIONS OF GRB 110731A: GeV EMISSION FROM ONSET TO AFTERGLOW.
The astrophysical journal, 763(2):71, and DESY-2014-01078.
http://dx.doi.org/10.1088/0004-637X/763/2/71

M. Ackermann et al.
ASSOCIATING LONG-TERM γ-RAY VARIABILITY WITH THE SUPERORBITAL PERIOD OF LS I +61°303.
The astrophysical journal / 2, 773(2):L35, and DESY-2014-01058.
http://dx.doi.org/10.1088/2041-8205/773/2/L35

Ackermann, Markus and IceCube collaboration.
Evidence for High-Energy Extraterrestrial Neutrinos at the IceCube Detector.
Science, 342(6161):1242856, and DESY-2014-01241.
http://dx.doi.org/10.1126/science.1242856

J. Aleksic et al.
Discovery of very high energy gamma-ray emission from the blazar 1ES 1727+502 with the MAGIC Telescopes.
Astronomy and astrophysics, in Press:0, and DESY-2014-00625, arXiv:1302.6140.
http://dx.doi.org/10.1051/0004-6361/201321360

J. Aleksić et al.
Very high energy gamma-ray observation of the peculiar transient event Swift J1644+57 with the MAGIC telescopes and AGILE.
Astronomy and astrophysics, 552(A112):1–6, and DESY-2014-00787.
http://dx.doi.org/10.1051/0004-6361/201321197

J. Aleksić et al.
The Simultaneous Low State Spectral Energy Distribution of 1ES 2344+514 from Radio to Very High Energies.
Astronomy and astrophysics, 556(A67):1–28, and DESY-2014-00828, arXiv:1211.2608.
http://dx.doi.org/10.1051/0004-6361/201220714

E. Aliu et al.
Discovery of TeV Gamma-Ray Emission Toward Supernova Remnant SNR G78.2+2.1.
The astrophysical journal, 770(2):93 –, and DESY-2014-00172.
http://dx.doi.org/10.1088/0004-637X/770/2/93

E. Aliu et al.
LONG TERM OBSERVATIONS OF B2 1215+30 WITH VERITAS.
The astrophysical journal, 779(2):92, and DESY-2014-00165.
http://dx.doi.org/10.1088/0004-637X/779/2/92

E. Aliu et al.
MULTIWAVELENGTH OBSERVATIONS AND MODELING OF 1ES 1959+650 IN A LOW FLUX STATE.
The astrophysical journal, 775(1):3, and DESY-2014-00171.
http://dx.doi.org/10.1088/0004-637X/775/1/3

E. Aliu et al.
DISCOVERY OF TeV GAMMA-RAY EMISSION FROM CTA 1 BY VERITAS.
The astrophysical journal, 764(1):38, and DESY-2014-00180.
http://dx.doi.org/10.1088/0004-637X/764/1/38

E. Aliu et al.
MULTIWAVELENGTH OBSERVATIONS OF THE TeV BINARY LS I +61° 303 WITH VERITAS, Fermi -LAT, AND Swift /XRT DURING A TeV OUTBURST.
The astrophysical journal, 779(1):88, and DESY-2014-00166.
http://dx.doi.org/10.1088/0004-637X/779/1/88

A. Allafort et al.
PSR J2021+4026 IN THE GAMMA CYGNI REGION: THE FIRST VARIABLE γ-RAY PULSAR SEEN BY THE Fermi LAT.
The astrophysical journal / 2, 777(1):L2, and DESY-2014-01043.
http://dx.doi.org/10.1088/2041-8205/777/1/L2

S. Archambault et al.
DISCOVERY OF A NEW TeV GAMMA-RAY SOURCE: VER J0521+211.
The astrophysical journal, 776(2):69, and DESY-2014-00168.
http://dx.doi.org/10.1088/0004-637X/776/2/69

S. Archambault et al.
Veritas Observations of the Microquasar Cygnus X-3.
The astrophysical journal, 779(2):10, and DESY-2014-00159.
http://dx.doi.org/10.1088/0004-637X/779/2/150

T. Arlen et al.
RAPID TeV GAMMA-RAY FLARING OF BL LACERTAE.
The astrophysical journal, 762(2):92, and DESY-2014-00181, arXiv:1211.3073.
http://dx.doi.org/10.1088/0004-637X/762/2/92

S. G. Babajanyan, E. D. Gazazyan, D. Kalantaryan, V. T. Nikoghosyan, and A. D. Ter-Poghosyan.
Possibility of Yerevan synchrotron magnet structure transformation.
Journal of contemporary physics, 48(6):253 – 258, and DESY-2014-00244.
http://dx.doi.org/10.3103/S1068337213060017

A. Baushev.
EXTRAGALACTIC DARK MATTER AND DIRECT DETECTION EXPERIMENTS.
The astrophysical journal, 771(2):117, and DESY-2014-00162.
http://dx.doi.org/10.1088/0004-637X/771/2/117

S. F. Berezhnev et al.
The Tunka – Multi-component EAS detector for high energy cosmic ray studies.
Nuclear instruments & methods in physics research / A, 732:281 – 285, and DESY-2014-00900.
http://dx.doi.org/10.1016/j.nima.2013.05.180

N. Budnev et al.
Tunka-25 Air Shower Cherenkov array: The main results.
Astroparticle physics, 50-52:18 – 25, and DESY-2014-00897.
http://dx.doi.org/10.1016/j.astropartphys.2013.09.006

A. Cianchi et al.
Challenges in plasma and laser wakefield accelerated beams diagnostic.
Nuclear instruments & methods in physics research / A, 720:153 – 156, and DESY-2014-00241.
http://dx.doi.org/10.1016/j.nima.2012.12.012

O. Gress et al.
Tunka-HiSCORE – A new array for multi-TeV astronomy and cosmic-ray physics.
Nuclear instruments & methods in physics research / A, 732:290 – 294, and DESY-2014-00902.
http://dx.doi.org/10.1016/j.nima.2013.06.034

M. Gross et al.
Preparations for a plasma wakefield acceleration (PWA) experiment at PITZ.
Nuclear instruments & methods in physics research / A, in press:S0168900213015817, and DESY-2014-00243.
http://dx.doi.org/10.1016/j.nima.2013.11.042

M. Guthoff et al.
Radiation damage in the diamond based beam condition monitors of the CMS experiment at the Large Hadron Collider (LHC) at CERN.
Nuclear instruments & methods in physics research / A, volume 730, pages 168 – 173, Amsterdam, 10/09/2012 - 10/12/2012 2013. 9th International Conference on Radiation Effects on Semicondoctor Material Detectors and Devices, Florence(Italy), North-Holland Publ. Co.
http://dx.doi.org/10.1016/j.nima.2013.05.041

D. Göring, M. A. Klatt, C. Stegmann, and K. Mecke.
Morphometric analysis in gamma-ray astronomy using Minkowski functionals.
Astronomy and astrophysics, 555:A38 –, and DESY-2014-01953.
http://dx.doi.org/10.1051/0004-6361/201321136

H.E.S.S. Collaboration.
Constraints on axionlike particles with H.E.S.S. from the irregularity of the PKS 2155-304 energy spectrum.
Physical review / D, 88(10):102003, and DESY-2014-01926.
http://dx.doi.org/10.1103/PhysRevD.88.102003

H.E.S.S. Collaboration.
Discovery of high and very high-energy emission from the BL Lacertae object SHBL J001355.9–185406.
Astronomy and astrophysics, 554(A72):1–8, and DESY-2014-00641, arXiv:1304.4023.
http://dx.doi.org/10.1051/0004-6361/201220996

H.E.S.S. Collaboration.
Discovery of very high energy γ -ray emission from the BLLacertae object PKS0301−243 with H.E.S.S..
Astronomy and astrophysics, 559(A136):1–11, and DESY-2014-00655.
http://dx.doi.org/10.1051/0004-6361/201321639

H.E.S.S. Collaboration.
HESS and Fermi-LAT discovery of -rays from the blazar 1ES 1312-423.
Monthly notices of the Royal Astronomical Society, 434(3):1889 – 1901, and DESY-2014-00648.
http://dx.doi.org/10.1093/mnras/stt1081

H.E.S.S. Collaboration.
H.E.S.S. discovery of VHE γ -rays from the quasar PKS1510−089.
Astronomy and astrophysics, 554(A107):1–7, and DESY-2014-00645, arXiv:1304.8071.
http://dx.doi.org/10.1051/0004-6361/201321135

H.E.S.S. Collaboration.
H.E.S.S. observations of the binary system PSR B1259-63/LS 2883 around the 2010/2011 periastron passage.
Astronomy and astrophysics, 551:A94 –, and DESY-2014-01956.
http://dx.doi.org/10.1051/0004-6361/201220612

H.E.S.S. Collaboration.
Search for photon line-like signatures from Dark Matter annihilations with H.E.S.S..
Physical review letters, 110:041301, and PHPPUBDB-24687, arXiv:1301.1173.
http://dx.doi.org/10.1103/PhysRevLett.110.041301

H.E.S.S.Collaboration.
Discovery of TeV γ -ray emission from PKS0447-439 and derivation of an upper limit on its redshift.
Astronomy and astrophysics, 552(118):1–14, and DESY-2014-00637, arXiv:1303.1628.
http://dx.doi.org/10.1051/0004-6361/201321108

J. Hinton.
A New Era in Gamma-Ray Astronomy with the Cherenkov Telescope Array.
Astroparticle physics, 43:1 – 2, and DESY-2014-01162.
http://dx.doi.org/10.1016/j.astropartphys.2012.12.002

IceCube Collaboration.
First Observation of PeV-Energy Neutrinos with IceCube.
Physical review letters, 111(2):021103, and DESY-2014-01302.
http://dx.doi.org/10.1103/PhysRevLett.111.021103

IceCube Collaboration.
IceCube search for dark matter annihilation in nearby galaxies and galaxy clusters.
Physical review / D, 88(12):122001, and DESY-2014-01320.
http://dx.doi.org/10.1103/PhysRevD.88.122001

IceCube Collaboration.
IceTop: The surface component of IceCube..
Nuclear instruments & methods in physics research / A, 700:188–220, and PHPPUBDB-24698, arXiv:1209.3218.
http://dx.doi.org/10.1016/j.nima.2012.10.067

IceCube Collaboration.
Measurement of Atmospheric Neutrino Oscillations with IceCube.
Physical review letters, 111(8):081801, and DESY-2014-01317.
http://dx.doi.org/10.1103/PhysRevLett.111.081801

IceCube Collaboration.
Measurement of South Pole ice transparency with the IceCube LED calibration system.
Nuclear instruments & methods in physics research / A, 711:73 – 89, and DESY-2014-01292.
http://dx.doi.org/10.1016/j.nima.2013.01.054

IceCube Collaboration.
Measurement of the Atmospheric ν_e Flux in IceCube.
Physical review letters, 110(15):151105, and DESY-2014-01290.
http://dx.doi.org/10.1103/PhysRevLett.110.151105

IceCube Collaboration.
Measurement of the cosmic ray energy spectrum with IceTop-73.
Physical review / D, 88(4):042004, and DESY-2014-01316.
http://dx.doi.org/10.1103/PhysRevD.88.042004

IceCube Collaboration.
OBSERVATION OF COSMIC-RAY ANISOTROPY WITH THE ICETOP AIR SHOWER ARRAY.
The astrophysical journal, 765(1):55, and DESY-2014-01281.
http://dx.doi.org/10.1088/0004-637X/765/1/55

IceCube Collaboration.
Probing the origin of cosmic rays with extremely high energy neutrinos using the IceCube Observatory.
Physical review / D, 88(11):112008, and DESY-2014-01923.
http://dx.doi.org/10.1103/PhysRevD.88.112008

IceCube Collaboration.
Search for Dark Matter Annihilations in the Sun with the 79-String IceCube Detector.
Physical review letters, 110(13):131302, and DESY-2014-01284.
http://dx.doi.org/10.1103/PhysRevLett.110.131302

IceCube Collaboration.
Search for Galactic PeV gamma rays with the IceCube Neutrino Observatory.
Physical review / D, 87(6):062002, and DESY-2014-01282.
http://dx.doi.org/10.1103/PhysRevD.87.062002

IceCube Collaboration.
SEARCH FOR TIME-INDEPENDENT NEUTRINO EMISSION FROM ASTROPHYSICAL SOURCES WITH 3 yr OF IceCube DATA.
The astrophysical journal, 779(2):132, and DESY-2014-01318.
http://dx.doi.org/10.1088/0004-637X/779/2/132

Icecube Collaboration.
South Pole glacial climate reconstruction from multi-borehole laser particulate stratigraphy.
Journal of glaciology, 59(218):1117 – 1128, and DESY-2014-01967.
http://dx.doi.org/10.3189/2013JoG13J068

D. Kostunin et al.
Tunka-Rex: Status and results of the first measurements.
Nuclear instruments & methods in physics research / A, in press:S0168900213014617, and DESY-2014-00906, arXiv:1310.8477.
http://dx.doi.org/10.1016/j.nima.2013.10.070

M. Kunnas et al.
Hardware and first results of TUNKA-HiSCORE.
Nuclear instruments & methods in physics research / A, volume in press, page S0168900213017087, Amsterdam, 2013. Roma International Conference on Astroparticle Physics, Rom(Italy), North-Holland Publ. Co.
http://dx.doi.org/10.1016/j.nima.2013.12.025

MAGIC Collaboration.
Observations of the magnetars 4U 0142+61 and 1E 2259+586 with the MAGIC telescopes.
Astronomy and astrophysics, 549(A23):1–4, and DESY-2014-00788.
http://dx.doi.org/10.1051/0004-6361/201220275

M. Mayer et al.
RAPID GAMMA-RAY FLUX VARIABILITY DURING THE 2013 MARCH CRAB NEBULA FLARE.
The astrophysical journal / 2, 775(2):L37, and DESY-2014-00874.
http://dx.doi.org/10.1088/2041-8205/775/2/L37

D. Mazin et al.
Potential of EBL and cosmology studies with the Cherenkov Telescope Array.
Astroparticle physics, 43:241 – 251, and DESY-2014-01955.
http://dx.doi.org/10.1016/j.astropartphys.2012.09.002

N. Milke et al.
Solving inverse problems with the unfolding program TRUEE: Examples in astroparticle physics.
Nuclear instruments & methods in physics research / A, 697:133–147, and PHPPUBDB-24695, arXiv:1209.3218.
http://dx.doi.org/10.1016/j.nima.2012.08.105

T. Poehlsen et al.
Charge losses in segmented silicon sensors at the Si-SiO_2 interface.
Nuclear instruments & methods in physics research / A, 700:22, and PHPPUBDB-24287, arXiv:1207.6538.
http://dx.doi.org/10.1016/j.nima.2012.10.063

V. V. Prosin et al.
Tunka-133: Results of 3 year operation.
Nuclear instruments & methods in physics research / A, in press:S0168900213012527, and DESY-2014-00904.
http://dx.doi.org/10.1016/j.nima.2013.09.018

A. C. Rovero et al.
Design of a 7m Davies-Cotton Cherenkov telescope mount for the high energy section of the Cherenkov Telescope Array.
Experimental astronomy, 36(1-2):223 – 234, and DESY-2014-01940.
http://dx.doi.org/10.1007/s10686-013-9333-6

M. C. Weisskopf et al.
CHANDRA , KECK, AND VLA OBSERVATIONS OF THE CRAB NEBULA DURING THE 2011-APRIL GAMMA-RAY FLARE.
The astrophysical journal, 765(1):56, and DESY-2014-01069.
http://dx.doi.org/10.1088/0004-637X/765/1/56

Ph.D. Thesis

A. Hasselhuhn.
3-Loop Contributions to Heavy Flavor Wilson Coefficients of Neutral and Charged Current DIS.
Technische Universität Dortmund, 2013.

O. Novgorodova.
Characterisation and Application of Radiation Hard Sensors for LHC and ILC.
BTU Cottbus, 2013.

G. Vashchenko.
Transverse phase space studies with the new CDS booster cavity at PITZ.
University of Hamburg, Hamburg, 2013.

Master Thesis

R. Martin.
Characterization of the transverse profile of the PITZ photocathode laser.
Humboldt-University of Berlin, 2013.

Theory

Published

J. Ablinger, J. Blümlein, and C. Schneider.
Analytic and algorithmic aspects of generalized harmonic sums and polylogarithms.
Journal of mathematical physics, 54:082301, and DESY-2014-00205. *http://dx.doi.org/10.1063/1.4811117*

S. Alekhin, J. Blümlein, K. Daum, K. Lipka, and S. Moch.
Precise charm-quark mass from deep-inelastic scattering.
Physics letters / B, 720:172–176, and PHPPUBDB-26499, DESY 12-233; DO-TH-12-35; LPN-12-132; SFB-CPP-12-96; arXiv:1212.2355.
http://dx.doi.org/10.1016/j.physletb.2013.02.010

S. ALEKHIN, J. BLÜMLEIN, and S.-O. MOCH.
DETERMINATION OF α s AND m c IN DEEP-INELASTIC SCATTERING.
Modern physics letters / A, volume 28, page 1360018, Singapur, 2013. International Workshop on Determination of the Fundamental Parameters of QCD: Part III, Singapore(Singapore), World Scientific Publ.
http://dx.doi.org/10.1142/S0217732313600183

C. Alexandrou et al.
Nucleon form factors and moments of generalized parton distributions using $N_f = 2+1+1$ twisted mass fermions.
Physical review / D, 88(1):1–22, and DESY-2014-00624, DESY-13-053, SFB-CPP-13-23, arXiv:1303.5979.
http://dx.doi.org/10.1103/PhysRevD.88.014509

C. Alexandrou et al.
Nucleon Structure using lattice QCD.
Il nuovo cimento / C, number 5, pages 111–120, [S.l.], 2013. 3rd Workshop on the QCD Structure of the Nucleons, Bilbao(Spain), Italian Physical Society.
http://dx.doi.org/10.1393/ncc/i2013-11560-0

A. Ali, C. Hambrock, A. Y. Parkhomenko, and W. Wang.
Light-Cone distribution amplitudes of the ground state bottom baryons in HQET.
The European physical journal / C, 73:4, and PHPPUBDB-26310, DESY 12-225; arXiv:1212.3280.
http://dx.doi.org/10.1140/epjc/s10052-013-2302-4

A. Ali, C. Hambrock, and W. Wang.
Hadroproduction of Y(nS) above the BB[over ‾] thresholds and implications for $Y_b(10890)$.
Physical review / D, 88(5):054026, and DESY-2013-01076, DESY 13-107.
http://dx.doi.org/10.1103/PhysRevD.88.054026

S. Alioli et al.
A new observable to measure the top-quark mass at hadron colliders.
The European physical journal / C, 73(5):2438, and DESY-2014-01939.
http://dx.doi.org/10.1140/epjc/s10052-013-2438-2

S. Alioli et al.
Combining higher-order resummation with multiple NLO calculations and parton showers in GENEVA.
Journal of high energy physics, 2013(9):120, and DESY-2013-01005, DESY 12-221.
http://dx.doi.org/10.1007/JHEP09(2013)120

A. Almasy, I. Dubovyk, J. Gluza, and T. Riemann.
Reductions and Contractions of 1-loop Tensor Feynman Integrals.
Acta physica Polonica / B, volume 44, pages 2241–2247, Cracow, 09/01/2013 - 09/06/2013 2013. 37th International Conference of Theoretical Physics : Matter to the Deepest: Recent Developments in Physics of Fundamental Interactions, Ustron(Poland), Inst. of Physics, Jagellonian Univ.
http://dx.doi.org/10.5506/APhysPolB.44.2241

P. Anastasopoulos, M. Cvetic, R. Richter, and P. K. S. Vaudrevange.
String constraints on discrete symmetries in MSSM type II quivers.
Journal of high energy physics, 2013:011, and PHPPUBDB-26091, DESY 12-182.
http://dx.doi.org/10.1007/JHEP03(2013)011

S. Andreas, M. Goodsell, and A. Ringwald.
Dark matter and dark forces from a supersymmetric hidden sector.
Physical review / D, 87:24, and PHPPUBDB-24329, DESY 11-159. *http://dx.doi.org/10.1103/PhysRevD.87.025007*

M. Asano, K. Rolbiecki, and K. Sakurai.
Can R-parity violation hide vanilla supersymmetry at the LHC?.
Journal of high energy physics, 1301:14, and PHPPUBDB-25569, DESY 12-158.

M. Badziak, S. Krippendorf, H. P. Nilles, and M. W. Winkler.
The heterotic MiniLandscape and the 126 GeV Higgs boson.
Journal of high energy physics, 2013:22, and PHPPUBDB-26080, DESY 12-230; arXiv:1212.0854.
http://dx.doi.org/10.1007/JHEP03(2013)094

P. A. Baikov, A. Maier, and P. Marquard.
Progress in Analytical Calculations for the Anomalous Magnetic Moment of the Muon.
Acta physica Polonica / B, volume 44, page 2267, Cracow, 09/01/2013 - 09/06/2013 2013. Matter To The Deepest, Warsaw(Poland), Inst. of Physics, Jagellonian Univ.
http://dx.doi.org/10.5506/APhysPolB.44.2267

P. A. Baikov, A. Maier, and P. Marquard.
The QED vacuum polarization function at four loops and the anomalous magnetic moment at five loops.
Nuclear physics / B, 877(3):647 – 661, and DESY-2013-01416, arXiv:1307.6105; DESY-13-130.
http://dx.doi.org/10.1016/j.nuclphysb.2013.10.020

G. S. Bali et al.
Nucleon mass and sigma term from lattice QCD with two light fermion flavors.
Nuclear physics / B, 866:1–25, and PHPPUBDB-22730, DESY 12-105.
http://dx.doi.org/10.1016/j.nuclphysb.2012.08.009

R. D. Ball, S. Forte, S. Marzani, G. Ridolfi, and M. Bonvini.
Higgs production in gluon fusion beyond NNLO.
Nuclear physics / B, 874(3):746 – 772, and DESY-2013-00647, DESY 13-001.
http://dx.doi.org/10.1016/j.nuclphysb.2013.06.012

M. C. Bañuls, K. Cichy, J. I. Cirac, and K. Jansen.
The mass spectrum of the Schwinger model with matrix product states.
Journal of high energy physics, 2013(11):158, and DESY-2013-01411, arXiv:1305.3765; DESY-13-084; SFB-CPP-13-31.
http://dx.doi.org/10.1007/JHEP11(2013)158

P. Bechtle et al.
MSSM interpretations of the LHC discovery: light or heavy Higgs?.
The European physical journal / C, 73(4):2354, and DESY-2013-00478.
http://dx.doi.org/10.1140/epjc/s10052-013-2354-5

W. Beenakker et al.
Towards NNLL resummation: hard matching coefficients for squark and gluino hadroproduction.
Journal of high energy physics, 2013(10):120, and DESY-2013-01062, DESY 13-072.
http://dx.doi.org/10.1007/JHEP10(2013)120

M. Benayoun, P. David, L. DelBuono, and F. Jegerlehner.
An update of the HLS estimate of the muon g−2.
The European physical journal / C, 73(6):2453, and DESY-2014-01837, LPNHE-2012-01; HU-EP-12-40; DESY-12-190.
http://dx.doi.org/10.1140/epjc/s10052-013-2453-3

G. Bergner, I. Montvay, G. Muenster, U. Oezugurel, and D. Sandbrink.
Towards the spectrum of low-lying particles in supersymmetric Yang-Mills theory.
Journal of high energy physics, 1311:61, and DESY-2013-01142, DESY-13-065.
http://dx.doi.org/10.1007/JHEP11(2013)061

A. Bharucha, J. Kalinowski, G. Moortgat-Pick, K. Rolbiecki, and G. Weiglein.
One-loop effects on MSSM parameter determination via chargino production at the LC.
The European physical journal / C, 73(6):2446, and DESY-2013-01030, DESY 12-207.
http://dx.doi.org/10.1140/epjc/s10052-013-2446-2

K. Bielas, I. Dubovyk, J. Gluza, and T. Riemann.
Some Remarks on Non-planar Feynman Diagrams.
Acta physica Polonica / B, volume 44, page 2249, Cracow, 09/01/2013 - 09/06/2013 2013. 37th International Conference of Theoretical Physics : Matter to the Deepest: Recent Developments in Physics of Fundamental Interactions, Ustron(Poland), Inst. of Physics, Jagellonian Univ.
http://dx.doi.org/10.5506/APhysPolB.44.2249

L. Biferale et al.
An optimized D2Q37 Lattice Boltzmann code on GP-GPUs.
Computers & fluids, 80:55 – 62, and DESY-2014-01952.
http://dx.doi.org/10.1016/j.compfluid.2012.06.003

D. Blas, M. Garny, and T. Konstandin.
On the non-linear scale of cosmological perturbation theory.
Journal of cosmology and astroparticle physics, 2013(09):024, and DESY-2013-01039, DESY 13-060.
http://dx.doi.org/10.1088/1475-7516/2013/09/024

J. Blümlein.
The Theory of Deeply Inelastic Scattering.
Progress in particle and nuclear physics, 69:28–84, and PHPPUBDB-25097, DESY 12-096.
http://dx.doi.org/10.1016/j.ppnp.2012.09.006

J. Blümlein, A. Hasselhuhn, S. Klein, and C. Schneider.
The $O(\alpha_s^3 n_f T_F^2 C_{A,F})$ contributions to the gluonic massive operator matrix elements.
Nuclear physics / B, 866:196–211, and PHPPUBDB-23253, DESY 12-055; DO-TH-12/13; SFB/CPP-12-28; LPN 12-052.
http://dx.doi.org/10.1016/j.nuclphysb.2012.09.001

S. Bobrovskyi, J. Hajer, and S. Rydbeck.
Long-lived higgsinos as probes of gravitino dark matter at the LHC.
Journal of high energy physics, 2013:34, and PHPPUBDB-26034, DESY 12-175.
http://dx.doi.org/10.1007/JHEP02(2013)133

M. Bonvini, F. Caola, S. Forte, K. Melnikov, and G. Ridolfi.
Signal-background interference effects for $gg \to H \to W^+W^-$ beyond leading order.
Physical review / D, 88(3):034032, and DESY-2013-01038, DESY 13-059.
http://dx.doi.org/10.1103/PhysRevD.88.034032

M. Bonvini, S. Forte, M. Ghezzi, and G. Ridolfi.
The scale of soft resummation in SCET vs perturbative QCD.
Nuclear physics / B / Proceedings supplements, 241-242:121 – 126, and DESY-2013-00995.
http://dx.doi.org/10.1016/j.nuclphysbps.2013.06.020

F. Brümmer, M. Ibe, and T. T. Yanagida.
Focus point gauge mediation in product group unification.
Physics letters / B, 726(1-3):364 – 369, and DESY-2013-01035, DESY 13-042.
http://dx.doi.org/10.1016/j.physletb.2013.09.012

G. Buchalla, O. Catà, R. Rahn, and M. Schlaffer.
Effective field theory analysis of new physics in e + e − → W + W − at a linear collider.
The European physical journal / C, 73(10):2589, and DESY-2013-01358, DESY 13-007.
http://dx.doi.org/10.1140/epjc/s10052-013-2589-1

W. Buchmuller, V. Domcke, and K. Kamada.
The Starobinsky model from superconformal D-term inflation.
Physics letters / B, 726(1-3):467 – 470, and DESY-2013-01075, DESY 13-102.
http://dx.doi.org/10.1016/j.physletb.2013.08.042

W. Buchmuller.
Leptogenesis: Theory and Neutrino Masses.
Nuclear physics / B / Proceedings supplements, volume 235, page 7, Amsterdam, 2013. 25th Int. Conf. on Neutrino Physics, Kyoto(Japan), Elsevier.

W. Buchmuller, V. Domcke, K. Kamada, and K. Schmitz.
The gravitational wave spectrum from cosmological B - L breaking.
Journal of cosmology and astroparticle physics, 2013(10):003, and DESY-2013-01037, DESY 13-050.
http://dx.doi.org/10.1088/1475-7516/2013/10/003

J. Bulava, K. Jansen, and A. Nagy.
Constraining a fourth generation of quarks: Non-perturbative Higgs boson mass bounds.
Physics letters / B, 723(1-3):95 – 99, and DESY-2014-00588, arXiv:1301.3416.
http://dx.doi.org/10.1016/j.physletb.2013.04.041

F. Campanario, T. M. Figy, S. Plätzer, and M. Sjödahl.
Electroweak Higgs Boson Plus Three Jet Production at Next-to-Leading-Order QCD.
Physical review letters, 111(21):211802, and DESY-2013-01217, DESY 13-144.
http://dx.doi.org/10.1103/PhysRevLett.111.211802

C. Candu, V. Mitev, and V. Schomerus.
Anomalous dimensions in deformed WZW models on supergroups.
Journal of high energy physics, 2013:27, and PHPPUBDB-26033, DESY 12-186.
http://dx.doi.org/10.1007/JHEP03(2013)003

C. Candu, V. Mitev, and V. Schomerus.
Spectra of coset sigma models.
Nuclear physics / B, 877(3):900 – 935, and DESY-2013-01401, DESY 13-148.
http://dx.doi.org/10.1016/j.nuclphysb.2013.10.026

M. Carena, S. Heinemeyer, O. Stål, C. E. M. Wagner, and G. Weiglein.
MSSM Higgs boson searches at the LHC: benchmark scenarios after the discovery of a Higgs-like particle.
The European physical journal / C, 73(9):2552, and DESY-2013-01032, DESY 13-024.
http://dx.doi.org/10.1140/epjc/s10052-013-2552-1

M. C. Chen, M. Ratz, C. Staudt, and P. K. S. Vaudrevange.
The mu term and neutrino masses.
Nuclear physics / B, 866:157–176, and PHPPUBDB-22394, DESY 12-108.
http://dx.doi.org/10.1016/j.nuclphysb.2012.08.018

S. Y. Choi, C. Englert, and P. Zerwas.
Multiple Higgs-portal and gauge-kinetic mixings.
The European physical journal / C, 73(12):2643, and DESY-2014-01851.
http://dx.doi.org/10.1140/epjc/s10052-013-2643-z

S. Y. Choi, M. M. Muhlleitner, and P. Zerwas.
Theoretical basis of Higgs-spin analysis in and Zγ decays.
Physics letters / B, 718(3):1031 – 1035, and DESY-2014-01854.
http://dx.doi.org/10.1016/j.physletb.2012.11.050

K. Cichy, E. Garcia-Ramos, and K. Jansen.
Chiral condensate from the twisted mass Dirac operator spectrum.
Journal of high energy physics, 175(10):1–24, and DESY-2014-00621, DESY-13-038, HU-EP-13-08, SFB-CPP-13-17 , arXiv:1303.1954.
http://dx.doi.org/10.1007/JHEP10(2013)175

K. Cichy, A. Kujawa-Cichy, and M. Szyniszewski.
Lattice Hamiltonian approach to the massless Schwinger model: Precise extraction of the mass gap.
Computer physics communications, 184(7):1666 – 1672, and DESY-2014-01832.
http://dx.doi.org/10.1016/j.cpc.2013.02.010

M. Cicoli, S. d. Alwis, and A. Westphal.
Heterotic moduli stabilisation.
Journal of high energy physics, 2013:199, and DESY-2013-01395, DESY-13-066.
http://dx.doi.org/10.1007/JHEP10(2013)199

M. Constantinou et al.
Perturbatively improving regularization-invariant momentum scheme renormalization constants.
Physical review / D, 87(9):096019, and DESY-2014-00011, DESY 13-127; Edinburgh 2013/03; Liverpool LTH 972; arXiv:1303.6776.
http://dx.doi.org/10.1103/PhysRevD.87.096019

G. Cullen et al.
Next-to-Leading-Order QCD Corrections to Higgs Boson Production Plus Three Jets in Gluon Fusion.
Physical review letters, 111(13):131801, and DESY-2013-01412, arXiv:1307.4737; DESY-13-119; DF-06-2013; LPN-13-042; MPP-2013-193; SFB-CPP-13-46.
http://dx.doi.org/10.1103/PhysRevLett.111.131801

G. Cullen, N. Greiner, and G. Heinrich.
SUSY-QCD corrections to neutralino pair production in association with a jet.
The European physical journal / C, 73(4):2388, and DESY-2014-01833.
http://dx.doi.org/10.1140/epjc/s10052-013-2388-8

M. E. Dieckmann et al.
Parametric study of non-relativistic electrostatic shocks and the structure of their transition layer.
Physics of plasmas, 20(4):042111 –, and DESY-2014-00187.
http://dx.doi.org/10.1063/1.4801447

M. E. Dieckmann, G. Sarri, D. Doria, M. Pohl, and M. Borghesi.
Modification of the formation of high-Mach number electrostatic shock-like structures by the ion acoustic instability.
Physics of plasmas, 20:102112, and DESY-2014-00183.
http://dx.doi.org/10.1063/1.4825339

M. Diehl and T. Kasemets.
Positivity bounds on double parton distributions.
Journal of high energy physics, 2013(5):150, and DESY-2013-00169, DESY-13-037.
http://dx.doi.org/10.1007/JHEP05(2013)150

M. Diehl and P. Kroll.
Nucleon form factors, generalized parton distributions and quark angular momentum.
The European physical journal / C, 73(4):2397, and DESY-2013-00168, DESY-13-025.
http://dx.doi.org/10.1140/epjc/s10052-013-2397-7

F. Domingo, O. Lebedev, Y. Mambrini, J. Quevillon, and A. Ringwald.
More on the hypercharge portal into the dark sector.
Journal of high energy physics, 2013(9):20, and DESY-2013-01069, DESY 13-090.
http://dx.doi.org/10.1007/JHEP09(2013)020

C. Englert, A. Freitas, M. Spira, and P. Zerwas.
Constraining the intrinsic structure of top-quarks.
Physics letters / B, 721(4-5):261 – 268, and DESY-2014-01857.
http://dx.doi.org/10.1016/j.physletb.2013.03.017

M. Eto et al.
Cosmic R-string, R-tube and Vacuum Instability.
Journal of high energy physics, 3:28, and PHPPUBDB-26268, DESY 12-219.

P. Falgari, A. Papanastasiou, and A. Signer.
Finite-width effects in unstable-particle production at hadron colliders.
Journal of high energy physics, 2013:156, and DESY-2013-00765, DESY 13-049.
http://dx.doi.org/10.1007/JHEP05(2013)156

X. Feng et al.
Computing the hadronic vacuum polarization function by analytic continuation.
Physical review / D, 88(3):034505, and DESY-2013-01414, arXiv:1305.5878; KEK-CP-286; DESY-13-085; JLAB-THY-13-1736; SFB-CPP-13-30; HU-EP-13-24.
http://dx.doi.org/10.1103/PhysRevD.88.034505

L. Ferro, T. Łukowski, C. Meneghelli, J. Plefka, and M. Staudacher.
Harmonic R Matrices for Scattering Amplitudes and Spectral Regularization.
Physical review letters, 110(12):121602, and DESY-2013-00480.
http://dx.doi.org/10.1103/PhysRevLett.110.121602

M. Fischer, M. Ratz, J. Torrado, and P. K. S. Vaudrevange.
Classification of symmetric toroidal orbifolds.
Journal of high energy physics, 1301:51, and PHPPUBDB-24886, DESY 12-147.

M. Fischer, S. Ramos-Sánchez, and P. Vaudrevange.
Heterotic non-abelian orbifolds.
Journal of high energy physics, 2013(7):80, and DESY-2014-00191, DESY 13-075.
http://dx.doi.org/10.1007/JHEP07(2013)080

M. Frank et al.
Charged Higgs boson mass of the MSSM in the Feynman diagrammatic approach.
Physical review / D, 88(5):055013, and DESY-2013-01074, DESY 13-100.
http://dx.doi.org/10.1103/PhysRevD.88.055013

R. Frassek and C. Meneghelli.
From Baxter Q-operators to local charges.
Journal of South American earth sciences, 2013:P02019, and PHPPUBDB-25911, DESY 12-127.
http://dx.doi.org/10.1088/1742-5468/2013/02/P02019

P. Fritzsch and A. Ramos.
The gradient flow coupling in the Schrödinger functional.
Journal of high energy physics, 2013(10):1–30, and DESY-2014-00589, DESY-12-241, HU-EP-12-53, SFB-CPP-13-05, arXiv:1301.4388.
http://dx.doi.org/10.1007/JHEP10(2013)008

T. Frossard, M. Garny, A. Hohenegger, A. Kartavtsev, and D. Mitrouskas.
Systematic approach to thermal leptogenesis.
Physical review / D, 87:39, and PHPPUBDB-26311, DESY 12-202. *http://dx.doi.org/10.1103/PhysRevD.87.085009*

I. Gahramanov and G. Vartanov.
Extended global symmetries for 4D $\mathcal{N} = 1$ SQCD theories.
Journal of physics / A, 46(28):10, and DESY-2013-00649, DESY 13-041.
http://dx.doi.org/10.1088/1751-8113/46/28/285403

S. Gangal and F. Tackmann.
Next-to-leading-order uncertainties in Higgs+2 jets from gluon fusion.
Physical review / D, 87(9):093008, and DESY-2013-00120, DESY 13-029.
http://dx.doi.org/10.1103/PhysRevD.87.093008

M. Garny, A. Ibarra, M. Pato, and S. Vogl.
On the spin-dependent sensitivity of XENON100.
Physical review / D, 87:7, and PHPPUBDB-26094, DESY 12-174.

M. Garny, A. Kartavtsev, and A. Hohenegger.
Leptogenesis from first principles in the resonant regime.
Annals of physics, 328:26–63, and PHPPUBDB-24459, DESY-11-264; arXiv:1112.6428.
http://dx.doi.org/10.1016/j.aop.2012.10.007

M. Gasperini, G. Marozzi, F. Nugier, G. Veneziano, and I. Ben-Dayan.
Average and dispersion of the luminosity-redshift relation in the concordance model.
Journal of cosmology and astroparticle physics, 2013(06):002 – 002, and DESY-2013-00648, DESY 13-011.
http://dx.doi.org/10.1088/1475-7516/2013/06/002

J. Gaunt.
Single perturbative splitting diagrams in double parton scattering.
Journal of high energy physics, 01:042, and PHPPUBDB-23656.

J. González López, K. Jansen, D. B. Renner, and A. Shindler.
A quenched study of the Schrödinger functional with chirally rotated boundary conditions: Applications.
Nuclear physics / B, 867(3):609 – 635, and DESY-2014-01836, DESY-12-137, HU-EP-12-24, JLAB-THY-12-1606, SFB-CPP-12-55, arXiv:1208.4661.
http://dx.doi.org/10.1016/j.nuclphysb.2012.10.006

J. González López, K. Jansen, D. B. Renner, and A. Shindler.
A quenched study of the Schrödinger functional with chirally rotated boundary conditions: Non-perturbative tuning.
Nuclear physics / B, 867(3):567 – 608, and DESY-2014-01838, DESY-12-136, HU-EP-12-23, JLAB-THY-12-1605, SFB-CPP-12-54, arXiv:1208.4591.
http://dx.doi.org/10.1016/j.nuclphysb.2012.10.015

B. Gripaios, K. Nagao, M. Nojiri, K. Sakurai, and B. Webber.
Reconstruction of Higgs bosons in the di-tau channel via 3-prong decay.
Journal of high energy physics, 2013:18, and PHPPUBDB-26093, DESY 12-163.
http://dx.doi.org/10.1007/JHEP03(2013)106

R. Gwyn, M. Rummel, and A. Westphal.
Relations between canonical and non-canonical inflation.
Journal of cosmology and astroparticle physics, 2013(12):010, and DESY-2013-01485, DESY 12-245.
http://dx.doi.org/10.1088/1475-7516/2013/12/010

R. Gwyn, M. Rummel, and A. Westphal.
Resonant non-Gaussianity with equilateral properties.
Journal of cosmology and astroparticle physics, 1304:040, and DESY-2013-00143, DESY-12-216.
http://dx.doi.org/10.1088/1475-7516/2013/04/040

Y. Hamada, K. Kamada, T. Kobayashi, and Y. Ookouchi.
Cosmological constraints on spontaneous R-symmetry breaking models.
Journal of cosmology and astroparticle physics, 04:29, and DESY-2013-00479.
http://dx.doi.org/doi:10.1088/1475-7516/2013/04/043

J. Harz, B. Herrmann, M. Klasen, K. Kovarik, and Q. L. Boulc'h.
Neutralino-stop co-annihilation into electroweak gauge and Higgs bosons at one loop.
Physical review / D, 87:20, and PHPPUBDB-26267, DESY-12-205; arXiv:1212.5241.
http://dx.doi.org/10.1103/PhysRevD.87.054031

J. Hasenkamp and M. Winkler.
NMSSM with gravitino dark matter to be tested at LHC.
Nuclear physics / B, 877(2):419 – 440, and DESY-2013-01400, DESY 13-142.
http://dx.doi.org/10.1016/j.nuclphysb.2013.10.017

Y. Hatsuda, K. Ito, and Y. Satoh.
Null-polygonal minimal surfaces in AdS4 from perturbed W minimal models.
Journal of high energy physics, 2013:43, and PHPPUBDB-25960, DESY-12-197.
http://dx.doi.org/10.1007/JHEP02(2013)067

Y. Hatsuda, S. Moriyama, and K. Okuyama.
Instanton Effects in ABJM Theory from Fermi Gas Approach.
Journal of high energy physics, 1301:42, and PHPPUBDB-25635, DESY 12-196.

Y. Hatsuda, M. Honda, S. Moriyama, and K. Okuyama.
ABJM Wilson Loops in Arbitrary Representations.
Journal of high energy physics, 1310:168, and DESY-2013-01100, DESY-13-097.
http://dx.doi.org/10.1007/JHEP10(2013)168

Y. Hatsuda, S. Moriyama, and K. Okuyama.
Instanton Bound States in ABJM Theory.
Journal of high energy physics, 1305(5):54, and DESY-2013-00171, DESY 13-010.
http://dx.doi.org/10.1007/JHEP05(2013)054

A. Hebecker, S. C. Kraus, and A. Westphal.
Evading the Lyth bound in hybrid natural inflation.
Physical review / D, 88(12):123506, and DESY-2013-01396, DESY 13-076.
http://dx.doi.org/10.1103/PhysRevD.88.123506

S. Heinemeyer, W. Hollik, G. Weiglein, and L. Zeune.
Implications of LHC search results on the W boson mass prediction in the MSSM.
Journal of high energy physics, 2013(12):84, and DESY-2014-00185, DESY 13-015.
http://dx.doi.org/10.1007/JHEP12(2013)084

G. Herdoíza, K. Jansen, C. Michael, K. Ottnad, and C. Urbach.
Determination of low-energy constants of Wilson chiral perturbation theory.
Journal of high energy physics, 2013(5):1–23, and DESY-2014-00622, DESY-13-043, FTUAM-13-127, IFT-UAM-CSIC-13-015, MITP-13-015, –SFB-CPP-13-18 ,arXiv:1303.3516.
http://dx.doi.org/10.1007/JHEP05(2013)038

D. Hesse and R. Sommer.
A one-loop study of matching conditions for static-light flavor currents.
Journal of high energy physics, 2013:115, and PHPPUBDB-25972, DESY 12-187; SFB-CPP-12-81; arXiv:1211.0866.
http://dx.doi.org/10.1007/JHEP02(2013)115

D. Hwang, F. Pedro, and D. Yeom.
Moduli destabilization via gravitational collapse.
Journal of high energy physics, JHEP 1309:159, and DESY-2013-01426, DESY 13-105.
http://dx.doi.org/10.1007/JHEP09(2013)159

F. Jegerlehner.
Application of Chiral Resonance Lagrangian Theories to the Muon $g-2$.
Acta physica Polonica / B, 44(11):2257, and DESY-2014-01450, DESY-13-239, HU-EP-13-76.
http://dx.doi.org/10.5506/APhysPolB.44.2257

T. T. Jouttenus, I. W. Stewart, F. J. Tackmann, and W. J. Waalewijn.
Jet mass spectra in Higgs boson plus one jet at next-to-next-to-leading logarithmic order.
Physical review / D, 88(5):054031, and DESY-2013-01006, DESY 12-222.
http://dx.doi.org/10.1103/PhysRevD.88.054031

T. Kalaydzhyan.
Chiral superfluidity of the quark–gluon plasma.
Nuclear physics / A, 916:243–263, and DESY-2013-00255, DESY 12-126.
http://dx.doi.org/10.1016/j.nuclphysa.2013.06.009

K. Kamada, T. Kobayashi, K. Ohashi, and Y. Ookouchi.
Cosmic R-string in thermal history.
Journal of high energy physics, 2013:28, and PHPPUBDB-26604, DESY 13-033.
http://dx.doi.org/10.1007/JHEP05(2013)091

K. Kamada, T. Kobayashi, T. Kunimitsu, M. Yamaguchi, and J. Yokoyama.
Graceful exit from Higgs G inflation.
Physical review / D, 88(12):123518, and DESY-2013-01475, DESY 13-169.
http://dx.doi.org/10.1103/PhysRevD.88.123518

A. Kaminska, G. G. Ross, and K. Schmidt-Hoberg.
Non-universal gaugino masses and fine tuning implications for SUSY searches in the MSSM and the GNMSSM.
Journal of high energy physics, 2013(11):209, and DESY-2013-01399, DESY 13-140.
http://dx.doi.org/10.1007/JHEP11(2013)209

T. Kasemets and M. Diehl.
Angular correlations in the double Drell-Yan process.
Journal of high energy physics, 1301:23, and PHPPUBDB-25571, DESY 12-176.

I. Kirsch and P. Kucharski.
Spin-k/2-spin-k/2 SU(2) two-point functions on the torus.
Nuclear physics / B, 869:315–328, and PHPPUBDB-25573, DESY 12-189.
http://dx.doi.org/10.1016/j.nuclphysb.2012.12.013

T. Konstandin.
Quantum transport and electroweak baryogenesis.
Physics / Uspekhi, 56(8):747, and DESY-2013-01034, DESY 13-036.
http://dx.doi.org/10.3367/UFNe.0183.201308a.0785

P. Korcyl, M. Koreń, and J. Wosiek.
On Non-trivial Spectra of Trivial Gauge Theories.
Acta physica Polonica / B, 44(4):713 –, and DESY-2014-01834, DESY-12-185.
http://dx.doi.org/10.5506/APhysPolB.44.713

S. Krippendorf, H. P. Nilles, M. Ratz, and M. Winkler.
Hidden SUSY from precision gauge unification.
Physical review / D, 88(3):035022, and DESY-2013-01071, DESY 13-099.
http://dx.doi.org/10.1103/PhysRevD.88.035022

J. Lange and M. Pohl.
The average GeV-band emission from gamma-ray bursts.
Astronomy and astrophysics, 551:A89 –, and DESY-2014-00196.
http://dx.doi.org/10.1051/0004-6361/201220652

O. Lebedev and A. Westphal.
Metastable Electroweak Vacuum: Implications for Inflation.
Physics letters / B, 719:415–418, and PHPPUBDB-25958, DESY-12-179.
http://dx.doi.org/10.1016/j.physletb.2012.12.069

R. Mahbubani, M. Papucci, G. Perez, J. T. Ruderman, and A. Weiler.
Light Nondegenerate Squarks at the LHC.
Physical review letters, 110(15):5, and DESY-2013-00136, DESY 12-231.
http://dx.doi.org/10.1103/PhysRevLett.110.151804

D. Martínez-Pedrera, D. Mehta, M. Rummel, and A. Westphal.
Finding all flux vacua in an explicit example.
Journal of high energy physics, 2013(6):110, and DESY-2013-00481, DESY 12-246.
http://dx.doi.org/10.1007/JHEP06(2013)110

M. Mcgarrie.
General resonance mediation.
Journal of high energy physics, 2013:32, and PHPPUBDB-26081, DESY 12-128.
http://dx.doi.org/10.1007/JHEP03(2013)093

M. Mcgarrie.
Holography for general gauge mediation.
Journal of high energy physics, 2013:40, and PHPPUBDB-26032, DESY 12-171.
http://dx.doi.org/10.1007/JHEP02(2013)132

M. McGarrie.
5D maximally supersymmetric Yang-Mills in 4D superspace: applications.
Journal of high energy physics, 2013:21, and PHPPUBDB-26608, DESY 13-048.
http://dx.doi.org/10.1007/JHEP04(2013)161

S. G. Nibbelink and P. K. S. Vaudrevange.
Schoen manifold with line bundles as resolved magnetized orbifolds.
Journal of high energy physics, 3:27, and PHPPUBDB-26269, DESY 12-242.

H. P. Nilles, S. Ramos–Sánchez, M. Ratz, and P. Vaudrevange.
A note on discrete R symmetries in Z6-II orbifolds with Wilson lines.
Physics letters / B, 726(4-5):876 – 881, and DESY-2014-01852, DESY 13-143.
http://dx.doi.org/10.1016/j.physletb.2013.09.041

H. P. Nilles, P. Vaudrevange, and M. Ratz.
Origin of family symmetries.
Fortschritte der Physik, 61:493–506, and DESY-2013-00548, DESY-12-047. *http://dx.doi.org/10.1002/prop.201200120*

A. S. Papanastasiou, R. Frederix, S. Frixione, V. Hirschi, and F. Maltoni.
Single-top t-channel production with off-shell and non-resonant effects.
Physics letters / B, 726(1-3):223 – 227, and DESY-2013-01064, DESY 13-088.
http://dx.doi.org/10.1016/j.physletb.2013.07.062

T. Pfoh.
Phenomenology of QCD threshold resummation for gluino pair production at NNLL.
Journal of high energy physics, 2013(5):44, and DESY-2014-00206, arXiv:1302.7202; DESY-13-035; LPN-13-021; SFB-CPP-13-16.
http://dx.doi.org/10.1007/JHEP05(2013)044

S. Plaetzer.
Controlling inclusive cross sections in parton shower + matrix element merging.
Journal of high energy physics, 2013(8):114, and DESY-2013-01004, DESY 12-215.
http://dx.doi.org/10.1007/JHEP08(2013)114

T. Quella and V. Schomerus.
Superspace conformal field theory.
Journal of physics / A, 46(49):494010, and DESY-2013-01397, DESY 13-082.
http://dx.doi.org/10.1088/1751-8113/46/49/494010

M. Redi, V. Sanz, M. Vries, and A. Weiler.
Strong signatures of right-handed compositeness.
Journal of high energy physics, 2013(8):8, and
DESY-2013-00696, DESY 13-080.
http://dx.doi.org/10.1007/JHEP08(2013)008

J. Reuter and M. Tonini.
Can the 125 GeV Higgs be the Little Higgs?.
Journal of high energy physics, 2013:40, and
PHPPUBDB-25959, DESY-12-177.
http://dx.doi.org/10.1007/JHEP02(2013)077

J. Reuter and D. Wiesler.
A Fat Gluino in Disguise.
The European physical journal / C, 73:27, and
PHPPUBDB-26096, DESY 12-178.

K. Rolbiecki and K. Sakurai.
Light stops emerging in WW cross section measurements?.
Journal of high energy physics, 2013(9):4, and
DESY-2013-01061, DESY 13-052.
http://dx.doi.org/10.1007/JHEP09(2013)004

K. Schmidt-hoberg, F. Staub, and M. Winkler.
Enhanced diphoton rates at Fermi and the LHC.
Journal of high energy physics, 1301:23, and
PHPPUBDB-25572, DESY 12-203.

K. Schmidt-Hoberg, F. Staub, and M. Winkler.
Constraints on light mediators: confronting dark matter searches with B physics.
Physics letters / B, page S037026931300909X, and
DESY-2013-01189, DESY 13-192; arXiv:1310.6752.
http://dx.doi.org/10.1016/j.physletb.2013.11.015

A. Westphal.
Tensor modes on the string theory landscape.
Journal of high energy physics, 2013:55, and
PHPPUBDB-26408, DESY 12-106.
http://dx.doi.org/10.1007/JHEP04(2013)054

K. Jansen, H. Leovey, A. Ammon, A. Griewank, and
M. Müller-Preussker.
Quasi-Monte Carlo methods for lattice systems: A first look.
Computer physics communications, 185(3):948–959, and
DESY-2014-00620, DESY-13-022, HU-EP-13-05,
SFB-CPP-13-13 ,arXiv:1302.6419.
http://dx.doi.org/10.1016/j.cpc.2013.10.011

Ph.D. Thesis

S. Andreas.
Light Weakly Interacting Particles: Constraints and Connection to Dark Matter.
Universität Hamburg, 2013.

V. Domcke.
Matter, Dark Matter and Gravitational Waves from a GUT-scale U(1) Phase Transition.
University of Hamburg, 2013.

J. Hajer.
Long-lived neutralinos as probes of gravitino dark matter.
University of Hamburg, Hamburg, 2013.

J. Harz.
Supersymmetric QCD Corrections and Phenomenological Studies in Relation to Coannihilation of Dark Matter.
University of Hamburg, 2013.

T. Kalaydzhyan.
Quark-gluon plasma in strong magnetic fields.
University of Hamburg (DESY), 2013.

T. Kasemets.
Double parton scattering - a tale of two partons.
Hamburg University, 2013.

Diploma Thesis

L. Sagunski.
Gravitational Waves as Cosmological Probes for New Physics between the Electroweak and the Grand-Unification Scale.
Univ. Hamburg, Hamburg, 2013.

Electronics Development

Published

J. Becker et al.
High speed cameras for X-rays: AGIPD and others.
Journal of Instrumentation, volume 8, pages C01042 – C01042, London, 09/17/2012 - 09/21/2012 2013. Topical Workshop on Electronics for Particle Physics 2012, Oxford(United Kingdom), Inst. of Physics.
http://dx.doi.org/10.1088/1748-0221/8/01/C01042

D. Greiffenberg et al.
Optimization of the noise performance of the AGIPD prototype chips.
Journal of Instrumentation, 8(10):P10022 – P10022, and
DESY-2014-01951.
http://dx.doi.org/10.1088/1748-0221/8/10/P10022

K. Hansen, C. Reckleben, P. Kalavakuru, J. Szymanski, and I. Diehl.
8-bit 5-MS/s Analog-to-Digital Converter for Pixel-Level Integration.
IEEE transactions on nuclear science, 60(5):3843–3851, and
DESY-2013-01233.
http://dx.doi.org/10.1109/TNS.2013.2280660

Photographs and graphics
CERN
DESY
Lars Berg, Münster
Heiner Müller-Elsner, Hamburg
Reimo Schaaf, Hamburg
The figures were reproduced by permission of authors or journals.

Acknowledgement
We would like to thank all authors and everyone who helped in the creation of this annual report.

Imprint

Publishing and contact
Deutsches Elektronen-Synchrotron DESY
A Research Centre of the Helmholtz Association

Hamburg location:
Notkestr. 85, 22607 Hamburg, Germany
Tel.: +49 40 8998-0, Fax: +49 40 8998-3282
desyinfo@desy.de

Zeuthen location:
Platanenallee 6, 15738 Zeuthen, Germany
Tel.: +49 33762 7-70, Fax: +49 33762 7-7413
desyinfo.zeuthen@desy.de

www.desy.de
ISBN: 978-3-935702-87-4
doi: 10.3204/DESY_AR_ET2013

Editing
Ilka Flegel, Manfred Fleischer, Michael Medinnis,
Thomas Schörner-Sadenius

Layout
Diana Schröder

Production
Monika Illenseer

Printing
Hartung Druck + Medien GmbH, Hamburg

Editorial deadline
28 February 2014

Editorial note
The authors of the individual scientific contributions published in this report are fully responsible for the contents.

HELMHOLTZ
| ASSOCIATION

Deutsches Elektronen-Synchrotron
A Research Centre of the Helmholtz Association

The Helmholtz Association is a community of 18 scientific-technical and biological-medical research centres. These centres have been commissioned with pursuing long-term research goals on behalf of the state and society. The Association strives to gain insights and knowledge so that it can help to preserve and improve the foundations of human life. It does this by identifying and working on the grand challenges faced by society, science and industry. Helmholtz Centres perform top-class research in strategic programmes in six core fields: Energy, Earth and Environment, Health, Key Technologies, Structure of Matter, Aeronautics, Space and Transport.

www.helmholtz.de